MINERAL CARBONATION IN SOILS

ENGINEERING THE SOIL CARBON SINK

By Phil Renforth

Thesis submitted in accordance with the requirements of Newcastle University for the degree of Doctor of Philosophy

School of Civil Engineering and Geosciences, Faculty of Science Agriculture and Engineering, Newcastle University, Newcastle upon Tyne, United Kingdom

2011

Contents

List of Tables

Appendix A. Analytical Methods

Appendix B. Results Tables

List of Figures

Chapter 1. Introduction

Chapter 2. Mineral carbonation in the context of global systems

Chapter 3. Sources of calcium rich minerals

Chapter 4. Carbonate precipitation in soils

List of Photographic Plates

Appendix D. Organic acid speciation

Declaration

Except where acknowledgement is given, this thesis is the unaided work of the author. The material presented has not previously been submitted to any higher education establishment for the purpose of obtaining a higher degree.

Signed Date

Acknowledgements

The author would like to express his sincere gratitude towards supervisors Prof. David Manning and Dr Annie Borland, for their guidance and support throughout this project. The technical assistance provided Phil Green and Clive Barr during geochemistry laboratory work, and growth trials at Moorbank botantical gardens respectively were greatly appreciated. Carla-Leanne Washbourne is thanked for her support, especially her help during collection and processing of Science Central soil samples. The botany expertise provided by Dr Simon Peacock for plant identification at the IRD site and Barrasford quarry was inspiring for an engineer and very much appreciated. Undergraduate and high school students Edward Wright, Demi Champney, and Joe Taylder are thanked for sacrificing their summer vacations in the name of science, and contributing to sample collection at Rugley Farm, Consett steelworks, and Dunstanbugh Castle (EW), modelling transport distances (DC) and silicate production estimates (JT). Dr Elisa Lopez-Capel is thanked for her help collecting samples from the IRD site, Consett Steelworks and Dunstanbugh Castle. Maggie White is thanked for her support throughout the PhD and expertise in X-ray diffraction analysis. Dr Jason DeJong, Assoc. Prof. of geotechnical engineering at the University of California at Davis and colleague Brian Martinez are thanked for hosting fieldwork in California. Prof. Ulla Lundström, Dr Dan Bylund and Sara Norström at Mid Sweden University are thanked for hosting a visit and assistance during liquid chromatography mass spectrometry analysis. Prof. Tony Fallick at the Scottish Universities Environmental Research Centre is thanked for hosting a short visit in which stable isotope mass spectrometry analysis was conducted on carbonate in soil samples. Finally, the author expresses his gratitude to family and friends who have put up with him over the last three years.

Abstract

Rapid anthropogenic climate change is one of the greatest challenges that human civilisation will face in the 21st century. A 25-180 % increase in atmospheric carbon dioxide content since the early 1800's and a predicted increase of 2-3% each year will lead to a 2-6°C rise in tropospheric temperatures. The consequences of increased atmospheric temperatures are profound and would put unsustainable strain on human infrastructure, which was conservatively estimated in the Stern Review (2006) to cost approximately 20% of GDP. Given the political, technical, economic and social barriers preventing the transition to a low carbon economy, there is an unequivocal need to research 'geoengineering' technologies that can bridge the gap between carbon emission reduction targets and actual emissions. Soil mineral carbonation is one such technology.

The atmosphere is one of the smallest carbon pools at the Earth's Surface (depending on how each pool is demarcated). Soils turn over the quantity of carbon in the atmosphere in under a decade and collectively form one of the largest carbon pools (3-4 times the quantity of carbon in the atmosphere). Land use change since the agricultural revolution has released 256 GtC (40 % of anthropogenic emissions). Research investigating the potential for carbon accumulation in soils is primarily focused on restoring organic carbon concentration to pre-agricultural values through modification of farming practices. The research presented in this thesis is the first that explores the potential of increasing the inorganic carbon pool as an emissions mitigation technology.

Inorganic carbon accumulation is promoted by introducing divalent cation rich (predominantly calcium and magnesium) silicate and hydroxide minerals into the soil, which weather and supersaturate the soil solution with respect to carbonate minerals (predominantly calcite, aragonite, magnesite and dolomite). The carbon in the resultant precipitate is derived from the atmosphere. This is analogous to mineral carbonation technologies which induce carbonate precipitation from silicate weathering in industrial scale reactors at elevated temperatures and pressures. However, carbonation in soil exploits natural weathering processes to the same effect with minimal energy and infrastructure input.

The research presented in this thesis broadly investigates soil mineral carbonation by contributing work towards the fundamental issues associated with application of soil mineral carbonation technology. Research activity described herein covers a range of laboratory batch weathering experiments, field work, geochemical modelling, plant growth trials, soil microcosm experiments and literature reviews. While eclectic, all work packages contribute to the same goal of describing the efficacy, effectiveness and potential impacts of soil mineral carbonation.

The efficacy of mineral carbonation technology is primarily limited by the availability of appropriate silicate bearing material. A literature search suggests that approximately 15-16 Gt a^{-1} of silicate rich 'waste' materials are produced as a consequence of human activity. This has a carbon capture potential between 190 and 332 MtC a^{-1}, which is equivalent to other emissions mitigation strategies. Quarrying silicate specifically for carbonation is a suggested strategy that may be able to store on the order of 10^2 GtC a^{-1} (based on two sites in the US). Therefore, mineral carbonation may form part of global mitigation strategies collectively equivalent to 14 GtC a^{-1} to stabilise the CO_2 concentration of the atmosphere at 500 parts per million by volume.

Considering that the potential capacity of soil mineral carbonation is sufficient to act as a substantial emissions mitigation strategy it was appropriate to investigate issues associated with the application of such a technology. In the first instance, sites known to contain silicates were investigated. These include soils developed on natural silicates (on the Whin Sill in Northumberland), construction and demolition waste (at a brownfield site and waste transfer stations) and slag (at a former steelworks). Interpretation of fieldwork results suggests that inorganic carbon accumulation is rapid (up to 38 gC kg^{-1}(soil) a^{-1}), and is orders of magnitude

greater than organic carbon accumulation in natural soils. The average concentration of inorganic carbon (20-30 Kg m^{-3}) is equivalent to organic carbon in natural soils. The unusually light carbon and oxygen isotope ratios of the carbonate (-3.1 ‰ and -27.5 ‰ for $\delta_{13}C$ and -3.9 ‰ and -20.9 ‰ for $\delta^{18}O$) were used to determine that up to 55% of the carbon was derived from the atmosphere.

The rate of carbon capture, which is the same as the precipitation rate of carbonate, is a function of solution chemistry. The more supersaturated a solution is with respect to a carbonate mineral, the more rapid the precipitation rate. Saturation of a solution is a function of divalent cation and carbonate anion concentration. Therefore, the supply of each of these components was investigated in laboratory experiments.

Batch weathering experiments were used to investigate the supply of calcium from artificial silicates (hydrated cement gel). Up to 70-80 % of the calcium contained in the mineral was removed, which is consistent with efficiencies reported for conventional mineral carbonation. The log rate of weathering was between -10.66 and -6.86 mol Ca cm^{-2} sec^{-1}, which is several orders of magnitude greater than that usually reported for natural silicates.

Microcosm experiments were conducted to investigate the rate of supply of carbonate from the organic carbon mineralisation in high pH solutions. The research clearly demonstrates that high pH solutions inhibit the breakdown of organic carbon as a function of nutrient supply. Where organic carbon was successfully mineralised the log rates (-3.4 mmol g^{-1}(field moist soil) sec^{-1}) were equivalent to that found in previous studies.

While the influx of dissolved carbonate mineral components into the soil solution is the primary controlling step in the rate of carbon accumulation, there is a complex relationship between soil physical properties and geochemistry. This was highlighted in a numerical model that was constructed for this thesis, which suggests that soil pore volume and particle size distribution are important variables. An additional numerical model was constructed to investigate the transportation of silicate material to the application site. This model suggests that an economics of soil mineral carbonation is a function of transport costs, the value of the silicate material and the price of carbon.

Field observations, growth trials, microcosm experiments and previous research suggest a complex interaction between biology, weathering and carbonate precipitation. Additional work is required to investigate carbonate precipitation mediated by plant and microorganism activity and the degree to which soil mixed with silicates impact on ecosystem functioning.

This research has demonstrated that mineral carbonation in soils could form a substantial emissions mitigation strategy, but additional work is required in a number of areas to which this thesis provides a suitable foundation.

Chapter 1

Chapter 1. Introduction

1.1 Context of the research

The research presented in this thesis was conducted between 2007 and 2010 at a time of unprecedented interest in global environmental systems. The growing body of evidence accumulated by the Intergovernmental Panel on Climate Change (IPCC; see Parry et al., 2007; Solomon et al., 2007) demonstrates the influence of human activity on the climate, where the energy required to maintain a developed quality of life is derived from fossil fuel combustion. Humans contribute 40 Gt of carbon dioxide (equivalent) as 'greenhouse' gas emissions into the atmosphere per year derived primarily from the combustion of fossil fuels. The current and future emission of greenhouse gases will increase the global atmospheric carbon dioxide concentration from a pre industrial level of ~350 parts per million by volume to 400-800 ppmv by 2100 and contribute to a 2-6°C increase in tropospheric temperatures. The resultant climate change is likely to place substantial pressure on human infrastructure and the ecosystems services. The Stern Review, an evaluation of the economic impact of climate change, highlights the need for wide spread immediate mitigation (costing 1% of GDP) which may be substantially more expensive (costing up to 20% of GDP, although potentially impossible to quantify) if it were delayed (Stern, 2006). Human promoted depletion of ecological resources (Wilson, 2000) and the unsustainable anthropogenic impact on planetary life support systems are collectively and evocatively referred to as Disseminated Primatemaia or a 'plague of people' (Lovelock, 2006).

There is unequivocal need for humanity to find equilibrium with other planetary biogeochemical cycles, which is reflected in recent sentiments from engineers (DeJong et al., in press; Beck et al., 2009; Head, 2008). That withstanding, modifying the physical and social fabric of civilisations is something that takes decades to centuries. Therefore, there is an imperative to generate technologies to bridge the gap between climate change risk, and the implementation of sustainable human infrastructure. These technologies are referred to as 'geoengineering' to which this thesis is a component.

Geoengineering, introduced in greater detail in Chapter 2, is the intentional modification of the Earth's climate. There is a broad range of technologies within this umbrella term (including injection of aerosols into the stratosphere, afforestation, ocean fertilisation, carbon capture and storage in underground saline aquifers etc.), generally categorised by those that mitigate incoming solar radiation or those that remove carbon from the atmosphere (mitigating absorbed radiation).

Geoengineering may play an important role over the current century as one of a portfolio of mitigation measures. Pacala and Socolow (2004) describe these as 'stabilisation wedges', each mitigating 1 GtC a^{-1} by 2050. The portfolio includes increased energy and transport efficiency, decreased transport use, a fuel shift from coal to gas, nuclear and renewables, the use of underground carbon capture and storage, afforestation, and conservation tillage on agricultural land (Table 1.1). Describing climate change mitigation in this way highlights the need to develop numerous strategies and technologies, and the substantial scale at which these need to be implemented.

Table 1.1 - Summary of mitigation activity to reduce global emissions by 1 GtC a^{-1} by 2050

Sector	Example activity
Transport	• Doubling fuel efficiency of 2 billion vehicles • Half car use for 2 billion cars
Buildings	• Reduce carbon emissions from buildings and appliances by 25%
Fossil fuel energy supply	• Double the efficiency of all coal fired power stations (and those yet to be constructed to double current capacity) • Replace coal fired power stations with gas fired (4 x current gas production) • Introduce CCS at coal, gas and synfuel power plants (requiring 3500 Sleipner sized facilities)
Alternative energy supply	• Double the current capacity of nuclear power plants • 50x current capacity of wind energy (equivalent to 2 million turbines) • 700x current capacity of photovoltaics • Use 1/6 of the global cropland to produce biofuel (100x current production in USA)
Land use	• Apply conservation tillage across all crop land • Inverse current trends in deforestation

The geoengineering technology investigated as part of this thesis is referred to as mineral carbonation or enhanced weathering, which has received increasing attention since the mid 1990s. Mineral carbonation occurs as the product of silicate mineral weathering (typically in geological time scales 10^4 a). For example the weathering of calcium plagioclase feldspar in the presence of carbon dioxide is expressed in Equation 1.1 where CO_2 is removed from the atmosphere and 'stored' as a solid carbonate mineral. Recent interest in mineral carbonation is concerned with accelerating this process for relevance on human time scales to mitigate anthropogenic emissions.

Equation 1.1: $$\underset{\textit{(anorthite)}}{CaAl_2Si_2O_8} + CO_2 + 2H_2O \rightarrow \underset{\textit{(calcite)}}{CaCO_3} + \underset{\textit{(kaolinite)}}{Al_2Si_2O_5(OH)_4}$$

Conventional mineral carbonation technologies use industrial scale reactors at elevated temperatures and carbon dioxide partial pressures to accelerate the carbonation of silicate minerals. The research described in this thesis builds on the suggestion that the enhanced weathering processes in soils can be used to the same effect (Manning, 2008). In this respect, the research here is the first of its kind in a potentially new field of study.

The outcomes have been communicated to geoscientists (Renforth et al., 2009; Manning, 2008) and will be disseminated to engineers and planners (Renforth et al., 2011a). The quantification of artificial silicates has been disseminated to the international scientific community (Renforth et al., 2011b), and the cement weathering experiments (Chapter 5) have been submitted for publication.

1.2 Scope, aims and objectives

1.2.1 Overarching approach

This thesis, while broadly categorised in the field of mineral carbonation, is the first of its kind to investigate this process in soils. The general scope of the research is presented in Figure 1.1. Although this diagram is not exhaustive, it demonstrates the interconnected relationship between various stages in the life cycle of soil mineral carbonation. Therefore, given the novelty of the research topic and the considerable body of research from a number of disciplines that are drawn together, it was imperative to maintain a sufficiently wide scope as to

map the potential lines of enquiry and identify potential limitations of soil mineral carbonation feasibility (which would otherwise be lost if this research focused on only one discipline). Complimentary integrative use of engineering (material production, transport, site preparation), geosciences (mineral weathering, mineralogy, geochemical modelling) and biology (plant sciences, microbial mineralisation of organic compounds) was used to identify the key processes in soil mineral carbonation, and to deliver research outputs in important knowledge gaps. This thesis can be viewed as a scoping study for additional research which builds on the results presented here (this is reflected in the discussion and conclusions in Chapters 8 and 9).

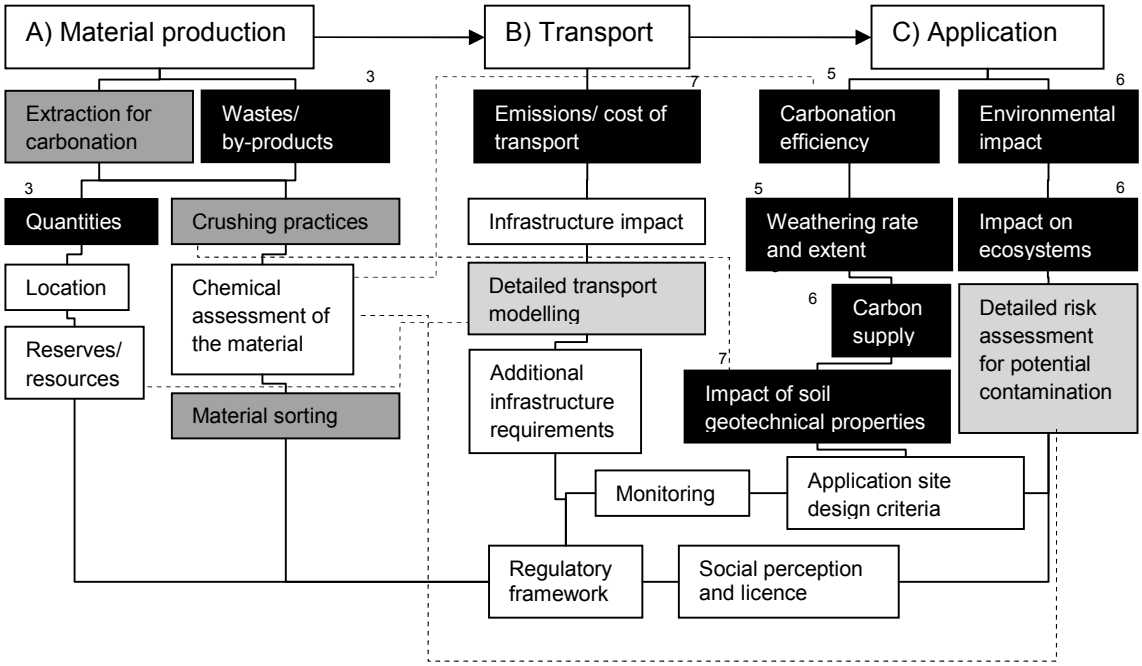

Figure 1.1 - Scope of soil mineral carbonation research. Box colour represents research in which this thesis contributes (black; chapter numbers are shown), existing research in the field of mineral carbonation (dark grey), and existing research in other fields that could be adapted for soil mineral carbonation (light grey).

1.2.2 Aims and objectives

The principal aim of this project was to investigate mineral carbonation in soils as a geoengineering technology to reduce or stabilise levels of atmospheric CO_2 and hence mitigate anthropogenic climate change. Considering the general

approach outlined above, it is important to identify subsidiary aims that define the context of the research (Aim 1 and 2), the potential efficacy of the technology (Aim 2), existing analogues (Aim 3), the effectiveness as a geoengineering tool (Aim 4), and potential issues limiting the application (Aim 5). These aims and deliverable objectives are expanded upon below.

Aim 1: Outline the global systems in which a widely implemented mineral carbonation technology would operate and perturb (including the global carbon and mineral weathering cycles; Chapter 2).

- The key components of the global carbon cycle have been quantified through a review of literature
- The importance of the anthropogenic perturbation of the global carbon cycle has been quantified as justification for developing soil mineral carbonation.
- Mineral weathering research is described which is analogous to mineral carbonation technologies.

Aim 2: Investigate the maximum carbon capture potential of soil mineral carbonation by presenting the available information regarding the production of available materials (Chapter 3).

- The production of artificial silicates from a range of industrial sources has been quantified through a review of the literature and production statistics.

Aim 3: Investigate the prevalence of pedogenic (soil formed) carbonates in artificial soils as unintentionally formed analogues to an engineered soil mineral carbonation technology (Chapter 4).

- A review of key literature is presented that discusses broadly pedogenic (soil formed) carbonates, focusing on soils developed on silicate parent material. To distinguish pedogenic from lithogenic carbonates stable isotopes are introduced as a tool for investigating the provenance of the carbonate components (C, O, and Ca).
- Fieldwork has been undertaken to quantify the accumulation of carbon as carbonate in soils that contain a range of silicate minerals.

- The prevalence of atmospheric carbon in the carbonates was quantified through the application of an isotopic mixing line hypothesis.
- The mixing line hypothesis was substantiated through investigations of pedogenic carbonate formation across a climate gradient.

Aim 4: Investigate the rate of carbon accumulation through field work (Chapter 4), laboratory trials investigating the rate of supply of calcium (Chapters 5) and carbon (Chapter 6) to the carbonate reaction, and modelling (Chapter 7).

- The carbon accumulation rate was estimated in 3 field sites by interpolation and is presented in Chapter 4.
- A series of weathering experiments has been undertaken to quantify the rate of artificial silicate weathering expressed as a function of surface area. Experiments have been conducted using organic acids as a proxy for natural plant root exudates (Chapter 5).
- A series of microcosm experiments has been undertaken to quantify the rate of citrate mineralisation in high pH solutions (Chapter 6).
- A numerical model was constructed that simulates soil weathering/carbonation as a function of geotechnical (bulk density, particle size distribution, surface area, soil moisture content) and geochemical parameters (cation content of the solid)

Aim 5: Explore the underlying key limitations to the implementation of soil mineral carbonation including impact on the environment and economics of transporting silicate material to the application site.

- Qualitative evidence was collated from field investigations in Chapter 4 and a growth trial conducted to assess the potential impact of artificial silicates on the environment (Chapter 6).
- A numerical model was constructed that simulates the feasibility of transporting silicate minerals as a function of carbon price (Chapter 7).

1.3 Thesis outline

This thesis has 9 chapters. Chapters 2 and 3 are reviews of the literature that provide context to the new data presented in Chapters 4, 5 and 6, and the feasibility studies presented in Chapter 7. Threads of discussion concerned with

efficacy and efficiency of soil mineral carbonation that run through the research are brought together in Chapter 8 and summarised/ concluded in Chapter 9.

Chapter 2 introduces the reader to mineral carbonation in the context of global environment systems, particularly the carbon cycle and mineral weathering. By quantifying the important carbon pools and fluxes, and highlighting anthropogenic perturbation of these, the case for geoengineering is made. This is the primary justification for the research presented in this thesis. Furthermore, the reader is introduced to mineral weathering as a natural climate stabilisation mechanism, and to the concept of accelerating this on human-relevant time scales (referred to as mineral carbonation).

The feasibility of mineral carbonation is primarily dependent on the quantity of available material, the efficiency of carbonation and the value of carbon. Chapter 3 presents the available information regarding the production of potential materials, primarily focusing on anthropogenic silicates (cement, fly ash, slag etc.).

To understand if mineral carbonation is possible in soils, a range of field sites known to contain natural or artificial silicates through the profile were investigated and documented in Chapter 4. This phenomenon is discussed in the context of pedogenic carbonates (well documented minerals that form in soils naturally), particularly those formed on silicate parent material. Stable isotope ratio mass spectrometry is introduced as a tool for determining the provenance of the carbonate components to unambiguously show that carbon has been sequestered from the atmosphere, rather than remobilised lithogenic minerals.

The rate of carbon accumulation is determined at a fieldscale from the analogues sites in Chapter 4. Understanding the rate controlling mechanisms for divalent-cation and carbon supply to the carbonate reaction is investigated in the laboratory in Chapters 5 and 6.

Batch weathering trials were conducted in controlled conditions in the laboratory to investigate the rate and magnitude of calcium leaching from artificial silicates. By using a classic weathering experiment design on specially prepared cement,

the results demonstrate weathering several orders of magnitude greater than those reported for natural silicates. This is documented in Chapter 5.

In Chapter 6 the contribution of organic acids to the dissolved carbon dioxide pool is investigated using a number of microcosm experiments with particular focus on high pH environments. Finally, growth trials and field observations are collated to discuss the environmental impact of artificial silicates in soils.

To understand the key feasibility limitations to soil mineral carbonation, a number of virtual models were created. First, a virtual model was constructed to simulate carbonate precipitation quantity and rate at the field scale. This is discussed in Chapter 7 and appended to this thesis on a CD-rom. Furthermore, the transport of silicates to the application site (assumed here to be the activity with the largest cost) is simulated as a function of carbon value.

Threads of discussion that run through the thesis regarding efficacy, rate of carbon capture and impact on the environment are brought together in Chapter 8.

Appendices A, B and C contain analytical methods used in this thesis, data tables and calculations respectively. Appendix D contains the results and discussion of an experiment investigating organic carbon speciation which is supplementary to the main body of text in Chapter 6.

Chapter 2

Chapter 2. Mineral carbonation in the context of global systems

A 'geoengineering' technology, one that purposefully alters the global climate, should be investigated and presented in the context of the systems it proposes to perturb. To this end, the aim of the following chapter is to outline the global carbon cycle by quantifying the key carbon pools and their fluxes. Furthermore, the recent anthropogenic influence on the carbon cycle is discussed and highlights the justification for developing soil mineral carbonation as a 'geoengineering' technology. Finally, a summary of mineral weathering research is presented which contextualises the mineral carbonation discussion presented in Chapter 3.

Delivered objective: The key components of the global carbon cycle have been quantified through a review of literature.

Delivered objective: The importance of the anthropogenic perturbation of the global carbon cycle has been quantified as justification for developing soil mineral carbonation.

Delivered objective: Mineral weathering research is described which is analogous to mineral carbonation technologies.

2.1 The global carbon cycle

2.1.1 Geological component of the global carbon cycle

The mantle and core of Earth is the largest carbon pool on the planet ($1.8x10^9$ billion tonnes of carbon (GtC); Javoy et al., 1982), the approximate concentration of which is the subject of continuing research since the 1970s (Anders and Owen, 1977). The pool can be subdivided into the upper and lower mantle, and core. The quantity of, and flux between, pools is shown in Figure 2.1. Various techniques have been used to estimate the chemical composition of the mantle including:

- Analysis of the chemical composition of chondrites (meteorites made of agglomerated space dust, which is assumed to be characteristic of this region of space) is used as a proxy for the elemental composition of the early solar system.
- Samples collected from the upper mantle.

- Seismic data used for calculations of density.

Chondrites generally contain around 3.5 wt% C, which is larger than that of samples derived from the upper mantle (Javoy, 1999). The widely accepted explanation is that around 50% of the mantle degassed early in the Earth's history producing the nitrogen, oxygen and carbon rich atmosphere (Javoy, 1999). The elemental distribution on Earth has been compared to that of Venus and Mars to explain differences in the planets which are generally composed of the same material (Lécuyer et al., 2000; Anders and Owen, 1977). The Venusian atmosphere contains twice as much carbon as the Earth's, which is attributed to a lack of lithospheric subduction, a process that transports 0.1 GtC per annum (a^{-1}) on Earth (Lécuyer et al., 2000). Assuming that the bulk Earth carbon content is similar to that of chrondrites, the carbon content of the core is estimated to be as large as 6 wt%. However, if carbon was lost during the accretion of the Earth (to 2%) then the carbon content of the core is 0.1-0.4 wt% (Dasgupta and Walker, 2008).

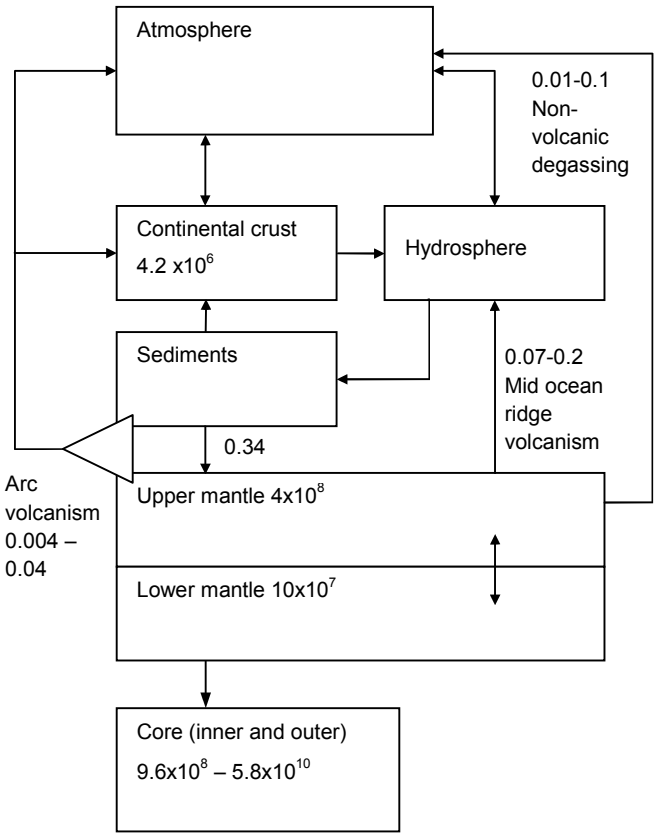

Figure 2.1 – Geological distribution of carbon in the deep Earth, (Dasgupta and Walker, 2008; Mörner and Etiope, 2002; Marty and Tolstikhin, 1998; Milliman

and Droxler, 1995; Wedepohl 1995; Javoy et al., 1982). All masses are in GtC and fluxes in GtC a^{-1}.

Quantification of the carbon flux between the mantle and the surface is important due to the relative size of the deep Earth carbon pool. It is acknowledged that methods to determine the carbon flux (either direct measurements or analysis of carbon trace gas ratios in glasses) are potentially inaccurate (Marty and Tolstikhin, 1998). However, the estimated flux ranges between 0.07-0.2 GtC a^{-1}, which is in agreement with atmospheric balancing equations and is not widely disputed (Javoy et al., 1986). Morner and Etiope (2002) estimate the degassing of the Earth's crust from non volcanic sources to be between 0.01-0.1 GtC a^{-1}.

2.1.2 Oceanic component of the global carbon cycle

The ocean is the largest reservoir of carbon on the surface of the Earth and is estimated to contain 39,800 GtC (Siegenthaler and Sarmiento, 1993). The simplest models describe the ocean in two boxes; the cold, dense and subsequently CO_2 rich deep (>1 km) ocean (38,100 GtC), and the surface ocean (1,020 GtC). Using measurements of CO_2 partial pressure in the atmosphere it is theoretically possible to estimate the quantity of CO_2 dissolved in the ocean through Henry's law, where the dissolved volatile species is directly proportional to its partial pressure in the gas phase. The reality is more complex as variation in temperature and wind modify the solubility and diffusivity of the gas. Furthermore, upwelling of deep water creates isolated areas of concentrated dissolved CO_2 at the surface (Takahashi et al., 2002). Therefore, direct measurements of oceanic carbon concentrations are made and interpolated over large (4° x 5°) areas (Takahashi et al., 2002; Archer et al., 1996). If the terrestrial carbon system was in steady state prior to human intervention, the perturbed quantities and turnover are more important to evaluate than the overall carbon content. Increased carbon storage in the ocean due to anthropogenic emissions into the atmosphere is referred to as 'carbon uptake' and is thought to have captured around half of the emitted carbon (Sabine et al., 2004). Sabine (2004) suggests that current CO_2 storage in the ocean is about one third of the maximum long term potential. The rate of uptake is proportional to the partial pressure of CO_2 in atmosphere and thought to be

between 1.58 and 2.32 GtC a^{-1} (Siegenthaler and Sarmiento, 1993), but is difficult to establish from direct measurements due to the large natural background flux. Therefore first order computational models are used which relate known, assumed or predicted differences in CO_2 partial pressure with flux and uptake (Takahashi et al., 2002).

It is estimated that around 700 Gt of dissolved organic carbon is present in the oceans (Hansell and Carlson, 1998). It is assumed that over large spatial and temporal scales that primary production (oxidation of organic matter) is equal to autotrophic respiration. However, heterotrophic organisms can consume a range of organic molecules not just those from recent photosynthesis. This leads to a decoupling of respiration and production over small spatial scales (del Giorgio and Duarte, 2002) and complicates the up scaling of organic carbon measurements. Estimation of the movement of organic carbon from the surface to the deep ocean and its subsequent mineralisation (often referred to as the 'biological pump') are generally around 5-11 GtC a^{-1} (Emerson et al., 1997; Eppley and Peterson, 1979), but may be as high as 27 GtC a^{-1} (Table 2.1; del Giorgio and Duarte, 2002).

Table 2.1 - Organic carbon production and mineralisation in the oceans (the flux between the oceanic biota and the surface waters). Source: del Giorgio and Duarte (2002).

Component	**Low estimate (GtC a^{-1})**	**High estimate (GtC a^{-1})**	**Central estimate (GtC a^{-1})**
Respiration			
Photic zone	32	42	37
Mesopelagic	21	28	24.5
Ocean interior	1.3	1.6	1.5
Mesozooplankton	1.5	4.5	3
Vertbrates			0.01
Total respiration	**55.8**	**76.1**	**66**
Organic Inputs			
Measured primary production	28	52	40
Unmeasured primary production	13.4	25	19.2
Total production	*41.4*	*77*	*59.2*
Import from coastal areas	6	6	6
Atmospheric inputs	3	3	3
Ancient organic matter	0.5	0.5	0.5
Total inputs	**50.9**	**86.5**	**68.7**

Using an estimation of calcium weathering from land and mid ocean ridges, and assumptions of alkalinity, sedimentation of inorganic carbon in the ocean is

responsible for sequestering between 0.2-0.34 GtC a^{-1} as primarily calcite, aragonite and magnesian calcite (Milliman and Droxler, 1995). Carbonate chemistry and mechanisms of precipitation are discussed in Chapter 5. A summary of the oceanic carbon cycle is presented in Figure 2.2.

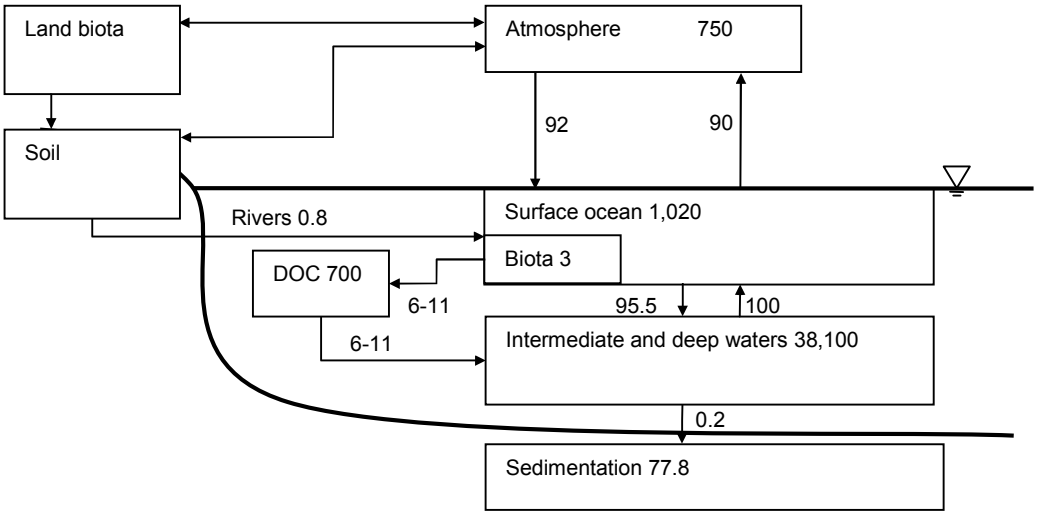

Figure 2.2 – The oceanic carbon cycle adapted from Siegenthaler (1993), Mackenzie (2004), Emerson et al. (1997). Pools are in GtC and Fluxes are in GtC a^{-1}.

2.1.3 Terrestrial component of the global carbon cycle - Soil

Soil is the largest terrestrial carbon pool and contains more carbon than the atmosphere and biosphere combined. The National Soil Characterisation Database (NSCD) and The World Inventory of Soil Emission Potential Database (WISE) contain samples from 30,000 separate locations and a have been used repeatedly in global soil carbon calculations. Collection of samples in the WISE database, which has expanded to include over 10,000 profiles, started in 1925 with the majority of samples obtained in the late 1970s (Batjes, 2008) and are geographically concentrated in South America, Europe and sub-Saharan Africa, with less concentrated sampling in North America, India and mainland South East Asia, and sparse data for areas north of 60° and desert regions (Sahara, the Arabian Peninsula and Central Australia). The NSCD is generally confined to North America with samples collected from the early 1900s to the present day (see http://ssldata.nrcs.usda.gov/ accessed 21/06/2010). Based on these data sets, authors have estimated the global soil organic carbon pool to contain

between 1456 and 1548 GtC (as soil organic carbon: SOC), when analysis is typically confined to the upper meter of the soil profile (Jobbagy and Jackson, 2000; Batjes, 1996; Schlesinger, 1977). Batjes (1996) has shown the SOC content to increase by 60% when the second and third meter were analysed, verified in a later study by Jobbagy and Jackson (2000), who estimate global soil organic carbon content to be approximately 2344 (±480) GtC (Table 2.2). It is probable that these values of organic carbon are underestimates. First, the soils were analysed years after they were collected and it is possible that highly labile organic compounds were oxidised (see Chapter 7). Furthermore, soluble organic compounds may be leached lower into the soil profile. This can be estimated in deep soils (Jobbagy and Jackson, 2000), but interpretation is more complex for thin soils where the organic carbon has leached into the joints of the parent material or groundwater (Hubbert et al., 2001).

The carbonate content of soils has not been extensively quantified, and has typically been confined to arid environments where it is the largest carbon pool (Goudie, 1996). Using a smaller component of the WISE database (1,000 samples), Batjes (1996) estimates the global pedogenic carbonate pool to contain between 695-748 GtC to a meter below the surface, primarily originating from remobilised lithogenic carbonate. However, carbonate precipitation depth is strongly linked to rainfall, and is expected to occur below 1 m in areas where the rainfall is greater than 500 mm a^{-1} (Jenny, 1941). Therefore, Batjes (1996) evaluation of the soil carbonate pool is likely to be an underestimate. Pedogenic carbonates are discussed in greater detail in Chapter 4).

*Table 2.2 – Soil organic carbon pools according to biome from Jobbagy and Jackson (2000), *from Gorham (1991).*

Biome	**Global soil organic carbon content (GtC) 0-3m**
Boreal forest	150
Cropland	248
Deserts	208
Sclerophyllous shrub	124
Temperate deciduous forest	160
Temperate evergreen forest	102
Temperate grassland	172
Tropical deciduous forest	218
Tropical evergreen forest	474
Tropical grassland/savanna	345
Tundra	144
Peatland	455*
Global soil	2344
Global soil + peat	2799

Carbon turnover is directly measured as the evolved CO_2 from an area of soil. Early experiments use potassium or sodium hydroxide traps suspended in baseless airtight containers located on a chosen area for analysis (see Schlesinger, 1977). The decrease in carbon dioxide in the chamber through absorption into the trap promotes artificially high diffusion out of the soil. Recent methods have sought to promote a slightly positive pressure in the chamber and measure the change in concentration in the effluent gas (Fang and Moncrieff, 1998). Schlesinger (1977) estimates global carbon efflux from soil to be 75 GtC a^{-1} based on data from a range of methodologies, rates which have been corroborated by a more recent study (Jenkinson et al., 1990).

Although there has been considerable debate on the definition of soil organic carbon, the general consensus is that SOC is a complex mixture of molecules with varying rates of turnover derived mainly from the chemical and microbial degradation of biological debris (Kumada, 1987). For simplicity this mixture is often modelled as two or three compartments with varying decay constants (Sohi et al., 2001; Jenkinson et al., 1990), the value of which has been questioned (Lichtfouse, 1997) suggesting that individual molecules should be modelled. Sollins et al. (1996) review degradation studies of organic molecules in soils, and a summary of their review is presented in Table 2.3.

Table 2.3 – Degradation time for organic carbon components in soils. Source: Sollins et al. (1996).

Molecule	**4 weeks wt% degradation**
Amino acids	77-86
Carbohydrates	73
-Cellulose	52
Benzoic acids	65-78
Lignin	6-12
Humic acids	1-2

Humic substances are dark coloured, acidic, predominantly aromatic, hydrophilic, chemically complex and polyelectrolytic. They are a product of chemical and biological degradation of larger organic material, and are subsequently resistant to additional degradation. As such, they are the most abundant compounds in soil organic carbon (60-70 wt%; Schnitzer and Khan, 1978). Carbohydrates, particularly cellulose, are an important component of SOC, comprising between 3-25 wt% of organic carbon (Poirier et al., 2005).

Lignin, a refractory organic material important in plant cell walls, comprises up to 4 % of soil organic carbon in agricultural soils (Poirier et al., 2005). Molecular analysis of soil organic carbon is an emergent field of investigation, and has only been applied to a small range of soil types.

2.1.4 Terrestrial component of the global carbon cycle – Biological and groundwater

Vegetation type and density is controlled by various environmental stimuli including minimum temperature, mean growing temperature and moisture requirements (Prentice et al., 1992). Based on this, Cao and Woodward (1998) suggest that global carbon storage in biotic ecosystems is 633 GtC (Table 2.4) and global net primary production (NPP – half of gross primary production) is 54 GtC a^{-1}.

Table 2.4 – Carbon storage in ecosystems. Source Cao and Woodward (1998).

	Area $10^6 km^2$	**NPP gC $m^{-2}a^{-1}$**	**Veg C kg m^{-2}**	**Veg total GtC**	**NPP GtC a^{-1}**
Polar desert Alpine Tundra	4.9	97	0.1	0.49	0.48
Wet Tundra	4.7	131	0.1	0.47	0.62
Boreal woodland	6.3	270	3.5	22.05	1.70
Boreal forest	12.1	351	4.6	55.66	4.25
Temperate coniferous	2.3	403	13.8	31.74	0.93
Desert	11.1	14	0	0	0.16
Arid shrubland	14.4	120	0.4	5.76	1.73
Short grassland	4.5	270	0.3	1.35	1.22
Tall grassland	3.5	492	0.6	2.1	1.72
Temperate savannah	6.5	318	0.6	3.9	2.07
Temperate mixed forest	4.9	586	9.7	47.53	2.87
Temperate deciduous forest	3.4	560	9.3	31.62	1.90
Temperate evergreen	3.1	698	11.6	35.96	2.16
Mediterranean shrubland	1.3	230	3	3.9	0.30
Tropical savannah	14	661	2.3	32.2	9.25
Xeromorphic forest	6.8	388	5	34	2.64
Tropical deciduous forest	4.6	759	10	46	3.49
Tropical evergreen forest	17.4	964	16	278.4	16.77
TOTAL	**125.8**			**633.13**	**54.25**

Generally, NPP estimates are between 28-75 GtC a^{-1} (Del Grosso et al., 2008; Randerson et al., 2002). Cao and Woodward (1998) estimate carbon storage in forest vegetation to be 583 GtC, whereas Dixon et al. (1994) estimate 359 GtC

is stored in forest vegetation (using direct measurements). This 40 % discrepancy highlights the potential range in values returned from different methodologies. Similarly, there is considerable variation of NPP where Litton et al. (2007) records standard deviations of NPP of 30-45 % of the mean.

The dynamics of groundwater in the global carbon cycle are poorly understood. The presence of bicarbonate in shallow ground waters has been well established (Chebotarev, 1955) and isotopic investigations suggest carbon (HCO_3 concentrations ranging from 87-270 mg l^{-1}) in equilibrium with atmospheric CO_2 (Plummer and Sprinkle, 2001). Interestingly, inorganic carbon in groundwater in a granite pluton has an organic carbon isotope signature thought to be the result of deep biological activity (Fritz et al., 1989). Dissolved organic carbon found deep within ground water systems is particularly long lived (45 ka; Murphy et al., 1989). However, global distribution and quantification of organic and inorganic carbon in groundwater is not reported.

A summary of the terrestrial carbon cycle is shown in Figure 2.3. The above-ground pools and fluxes are better understood than turnover of carbon in the soil. Generally, the quantity of carbon into the soil as decaying vegetation and organic root exudates is equivalent to the efflux of carbon as CO_2 gas. The molecular transformation and residence time of organic carbon in the soil on a global scale is poorly understood.

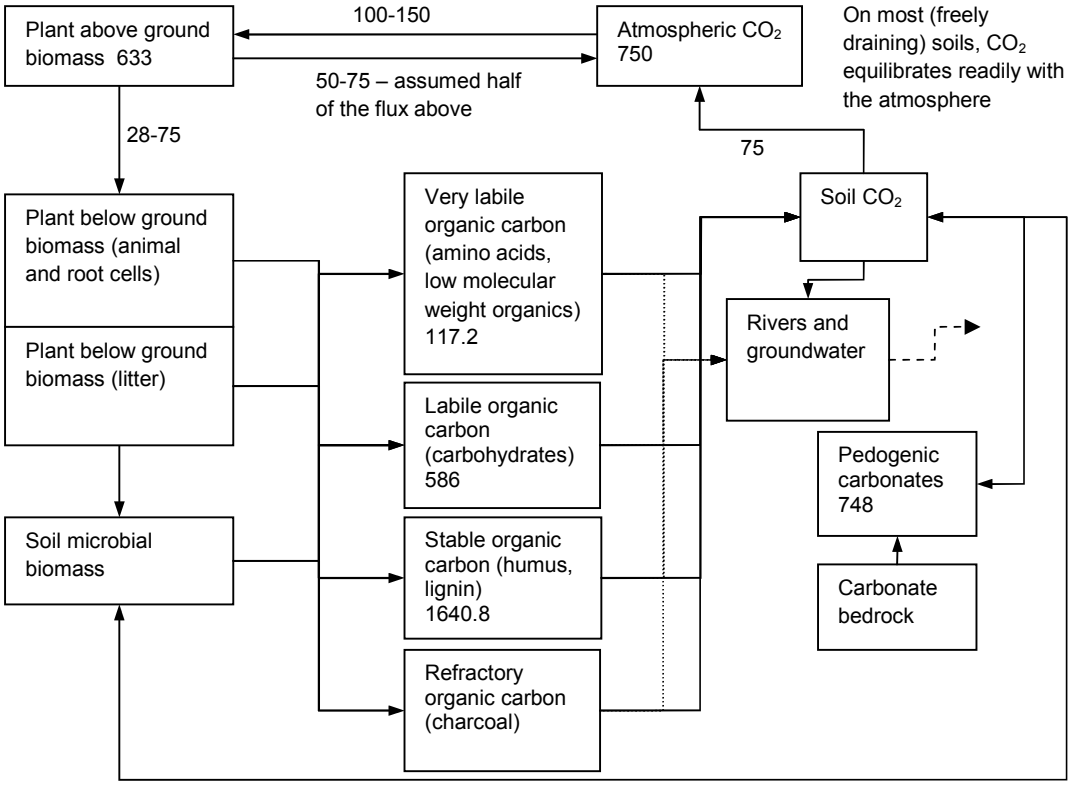

Figure 2.3 – The terrestrial carbon cycle. Fluxes in GtC a^{-1} and pools in GtC.

2.1.5 Atmospheric component of the global carbon cycle

The Earth's $5x10^6$ Gt atmosphere is composed of numerous gases (Figure 2.4). 90 wt% of the atmosphere exists within 30 km from the surface and around 50 wt% below 5.5 km. This is largely in the troposphere (0-17 km) and stratosphere (17-57 km; Wayne, 2000). The primary greenhouse gas is CO_2 (350-400 ppmv or about 750 GtC) accounting for around 60 % of the radiative forcing (Solomon et al., 2007). Methane (CH_4), nitrous oxide (N_2O) and a range of chlorofluorocarbons also contribute to the anthropogenically modified greenhouse effect.

In all global carbon cycle models the atmosphere is represented by a single pool. Heterogeneity of gas in the atmosphere is governed by residence time (Figure 2.4). Inter hemispheric mixing of the troposphere is weaker than the rotational mixing associated with the westerlies and trade winds, and occurs over a period of a year. Similarly, vertical mixing occurs over a period of days. CO_2 which is photo-chemically inert and is turned over every 7 years, has sufficient residence time to be incorporated into inter hemispheric cycles, and is thus relatively homogenous in the atmosphere (although a small 0.5 % north-

south gradient is caused by ecosystem uptake in the Northern Hemisphere; Denning et al., 1995; Tans et al., 1990), unlike water vapour with a resident time of days/weeks, which is localised in concentration (Schaeler et al., 2009).

Compound	p.p.m.v
CO_2	~350
H_2	0.53
He	5.2
H_2O	0-40000
CH_4	1.7
NH_3	<0.01
Ne	18
H_2S	10-4
N_2	780840
O_2	209460
CO	0.04-0.2
SO_2	10-4
Ar	9340
N_2O	0.3

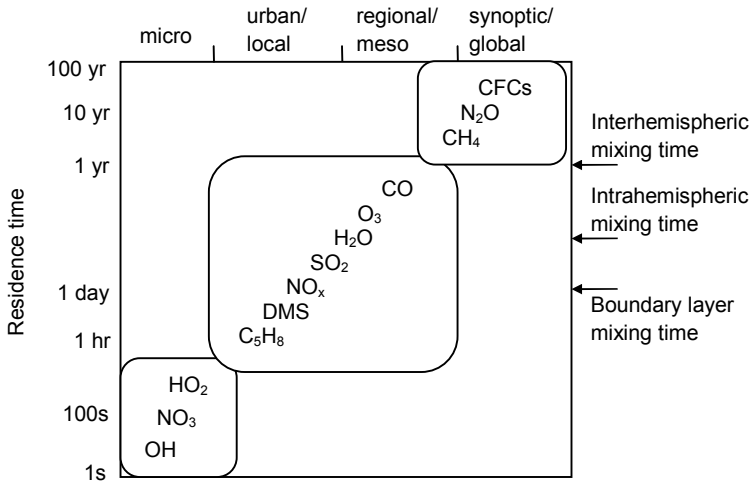

Figure 2.4 – Composition of the Earth's atmosphere and the lifetime of compounds from Wayne (2000).

2.1.6 The global carbon cycle - Summary

Summarising the information in this section in Figure 2.5 the global carbon cycle is shown to be a complex network of pools and fluxes that have been studied in varying detail and are known to varying extents. The transfer of carbon between the atmosphere, the terrestrial system and the ocean is relatively well understood. While there may be scaling errors, it is interesting to note that estimates of input of carbon into the terrestrial system (net primary production) equate with the efflux of carbon from soils (~75 GtC a^{-1}). Figure 2.5, demonstrates the importance of the terrestrial system in the global carbon cycle, which turns over the quantity of carbon in the atmosphere in under 10 years.

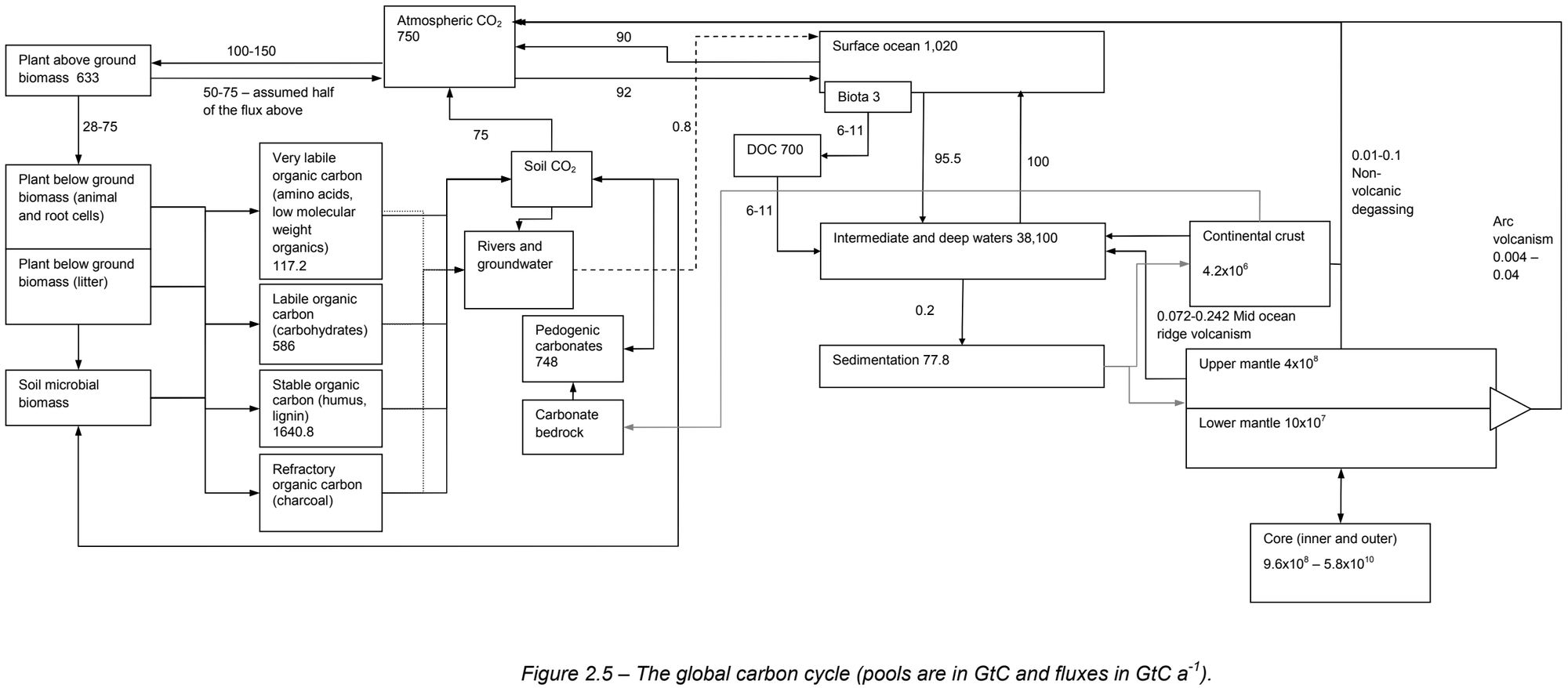

Figure 2.5 – The global carbon cycle (pools are in GtC and fluxes in GtC a^{-1}).

2.2 Anthropogenic changes in atmospheric carbon

The purpose of this section is to outline the importance of atmospheric carbon dioxide in the global climate system and the changes to carbon dioxide concentration through anthropogenic activity. A full review of the literature is beyond the scope of this thesis. The reader is directed to the IPCC's Fourth Assessment Report (Parry et al., 2007; Solomon et al., 2007) for more information.

2.2.1 Changes in atmospheric chemistry over time

The climate is primarily controlled by the energy budget in the atmosphere, which itself is a function of its chemical composition. The Earth's atmosphere is dynamic, turning over large quantities of gas, which over many (10^3-10^4) years results in 'natural' climate change (driven primarily by boundary conditions of the atmosphere energy system). This thesis is concerned with the recent and dramatic perturbation of atmospheric chemistry by human activity, namely the increase in greenhouse gas concentration from fossil fuel combustion and land use change. Table 2.5 presents the green house gas concentrations and their radiative forcing volumetrically. Carbon dioxide is the most important of these gases.

Table 2.5 – Radiative forcing of long-lived atmospheric gasses (Solomon et al., 2007 - Chapter 2).

Factor affecting the atmospheric energy balance	**Concentration**	**Radiative forcing**	
		W m^{-2}	% of total
CO_2	379 ppm	1.66	63.1
CH_4	1774 ppb	0.48	18.3
N_2O	319 ppb	0.16	6.1
Other gases including CFCs and halocarbons		0.33	12.5

The 'Greenhouse effect' can be estimated by comparing the incoming and outgoing solar radiation. Greenhouse gases absorb infrared thermal emissions over varying wavelengths and energy is re-emitted through one of the 'atmospheric windows' to compensate for this (Campbell and Norman, 1977).

The composition of the Earth's atmosphere in the late Quaternary (400,000 years to present) is determined through stratigraphic analysis of gas trapped in ice sheets (Petit et al., 1999). Not surprisingly, the gas composition has

fluctuated (Figure 2.6), which for carbon dioxide concentration is matched by a concordant change in stable oxygen isotope ratios. As stable oxygen isotope ratios are correlated to atmospheric temperature the glacial/interglacial cycles are well defined in the ice core record.

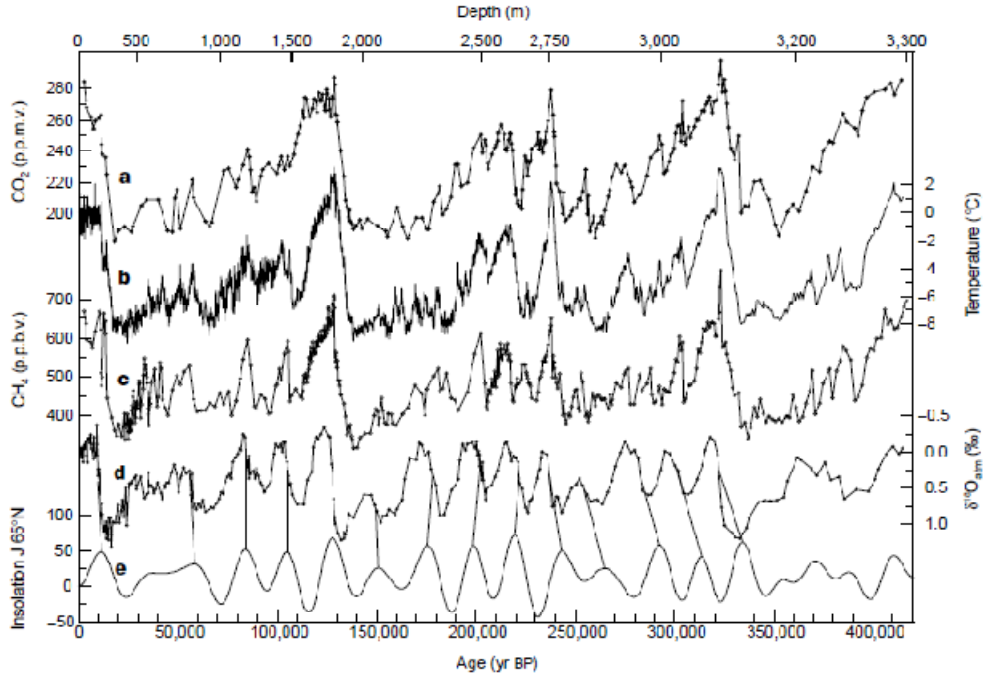

Figure 2.6 – Atmospheric composition over the past 400 ka. Source Petit et al. (1999). Lines represent (a) CO_2 concentration (b) temperature (c) methane concentration (d) δ18O isotope ratio (e) Insolation.

According to the ice core data, the Earth's Quaternary atmospheric carbon dioxide concentration has fluctuated between 200 and 280 ppmv (Petit et al., 1999). Analysis of the contemporary composition of the atmosphere (Figure 2.7) has demonstrated year on year increases in carbon dioxide concentration since 1958 (316 – 368 ppmv) thought to be the result of fossil fuel combustion and land use change (Keeling and Worf, 2004).

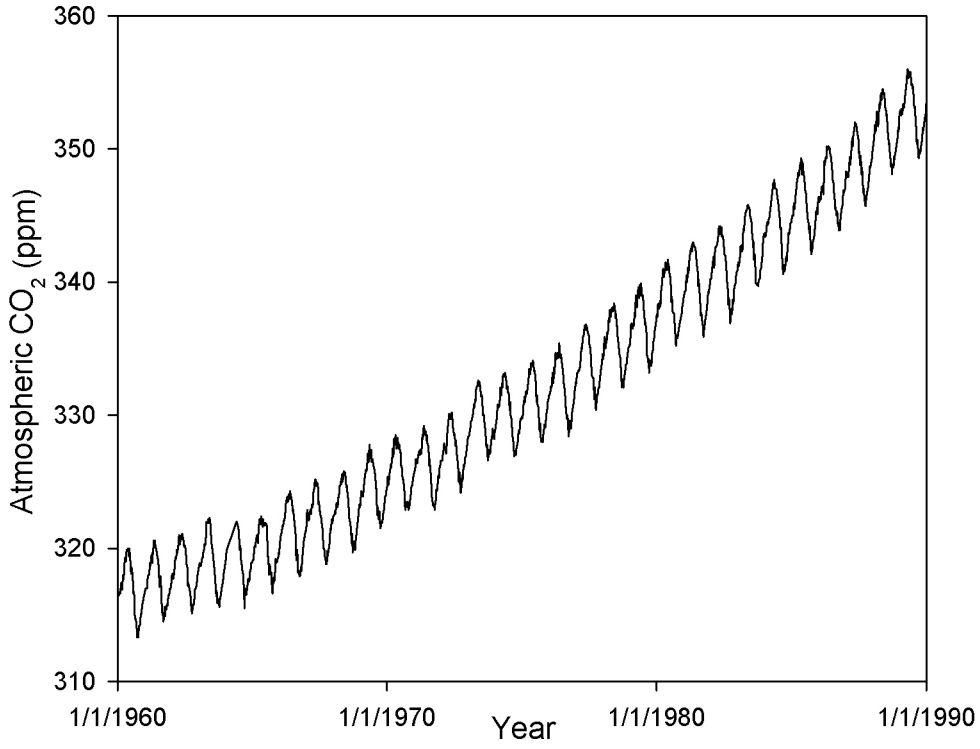

Figure 2.7 – Atmospheric CO_2 concentrations at the Mauna Loa Observatory, Hawaii, since 1960. Source: Keeling and Worf (2004).

2.2.2 Agricultural practices and land use change

The depletion of the terrestrial carbon stock through land use change since the mid 19th century is thought to have released 136 GtC into the atmosphere (Lal, 2003). Kutzbach et al. (2010) suggests that carbon emissions from early anthropogenic agricultural practices (particularly rice farming in Asia and subsequent oceanic feedback mechanisms) accounted for over 120 GtC of emissions into the atmosphere. The transformation of a soil from natural vegetation to agriculture reduces organic carbon content by approximately 30% in the top 1 m (Post and Kwon, 2000) as a result of removing influent organic carbon (through extracting above ground biomass) and oxidising and disturbing the soil matrix through tillage. Current estimates of carbon flux from land use change range between 0.6 and 2.5 GtC a^{-1} from the soil to the atmosphere (Schimel et al., 2001). However, others consider the terrestrial system a net sink for carbon (0.2 GtC a^{-1}) due to the increased atmosphere-land flux in Eurasia and North America (Janssens et al., 2003; Myneni et al., 2001), although this is disputed by others (Bellamy et al., 2005). This highlights the complex feedback mechanisms and scaling challenges for mapping terrestrial

carbon globally (Dale, 1997). For instance, lower precipitation would potentially lower crop yield and justify the conversion of woodland/forest into additional farmland. Furthermore, Janssens et al. (2003) and Mayneni et al. (2001) suggests increased carbon sequestration into European, Asian and North American forests as a result of anthropogenic emissions, a service that would be lost or reduced if land use was changed. Huston and Marland (2003) discuss the mutually exclusive benefits from land used to produce biofuel to that conserved under natural woodland. The geo-political context of landuse change is highly complex. Ecosystem services may be nationally administered, but have global consequences.

The importance of soil in the global carbon cycle has led to research on how soils may be modified to sequester atmospheric carbon. Paustian et al. (1997) and Lal (2003) present the potential of soils to mitigate anthropogenic CO_2 emissions by modification of agricultural practices through reduced tillage and the return of organic residues to the soil (often called mulch farming), which could capture between 0.4 and 0.6 GtC a^{-1}. The work published in this thesis and associated journal papers (Renforth et al., 2011; Renforth et al., 2009; Manning, 2008) is the only known research investigating the potential for increasing the inorganic carbon stock in soils. Urban development substantially modifies the soil profile (Lehmann and Stahr, 2007) through compaction, movement, chemical contamination, temperature and moisture content. Although the carbon content of urban soils is heterogeneous, they typically contain less organic carbon than the unmodified soils they replace (Renforth et al., 2011). Additional discussion is provided in Chapters 4 and 8.

2.2.3 Fossil fuel combustion

Over 337 GtC have been emitted since the 1750s as a consequence of fossil fuel combustion and cement manufacturing (Boden et al., 2010), the majority of which was released by more economically developed countries during industrialisation in the late 19th and 20th centuries.

Humans emit around 40 $GtCO_2$ equivalent (greenhouse gasses normalised against radiative forcing of CO_2) a^{-1} into the atmosphere, the majority of which is CO_2 from fossil fuel combustion and landuse change (Figure 2.8). This emissions profile is only one in a historic portfolio dating back to the start of the

agricultural revolution (see above) and is the basis for forecasting potential future scenarios.

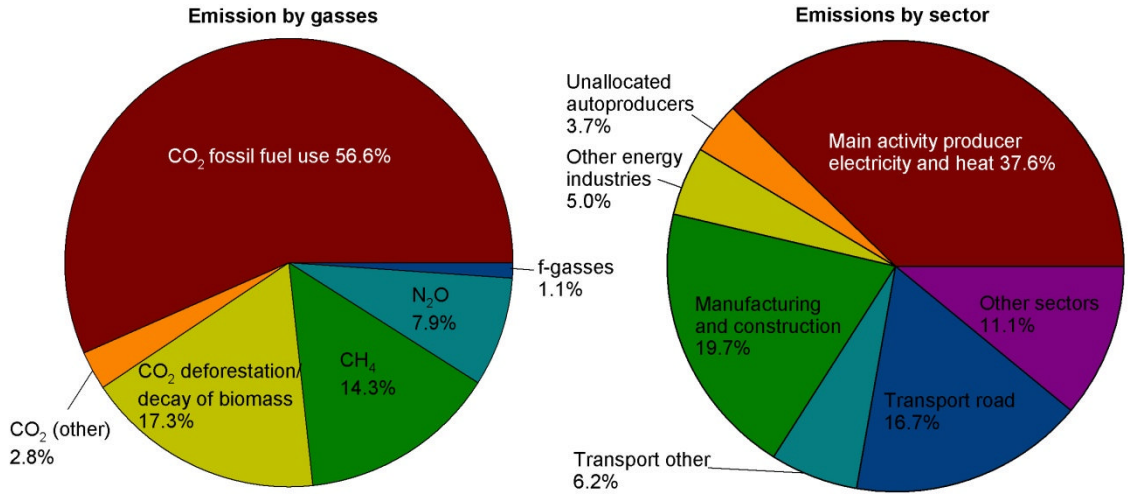

Figure 2.8 – Greenhouse gas emissions by gas and sector. Source IPCC FAR (Metz et al., 2007) and IEA (2009).

The International Energy Agency, IEA (2009), suggests that two thirds of CO_2 emissions are generated from 10 countries, China and the US accounting for around 40 % of the total. Auditing a national CO_2 footprint often omits displaced emissions due to consumerism, of which 30-40 % of a typical (developed consumer) household's footprint may be outside national boarders (Weber and Matthews, 2008). Energy generation is the largest producer of CO_2 emissions (Figure 2.7). However, industrial processes account for approximately 10 % of the global CO_2 emissions (primarily from the production of cement through the calcining of carbonate minerals).

2.2.4 Emission scenarios

The IPCC 'SRES' emissions scenarios (Figure 2.9) attempt to predict the likely change in greenhouse gas emissions over the coming century. Values for carbon emissions range from optimistic (2-4 GtC a^{-1}) to pessimistic (6-10 GtC a^{-1}). There is a wide range of possible emission scenarios highlighting the intrinsic unpredictability in forecasting. The IPCC (Metz et al., 2007) stipulates that a 35-85% reduction in greenhouse gas emissions from 2000 baseline by the mid century is required to prevent global temperature rises over 3°C, well

below the optimistic scenarios (Table 2.6). Therefore, there is an apparent discontinuity between what is likely to happen and required emissions targets.

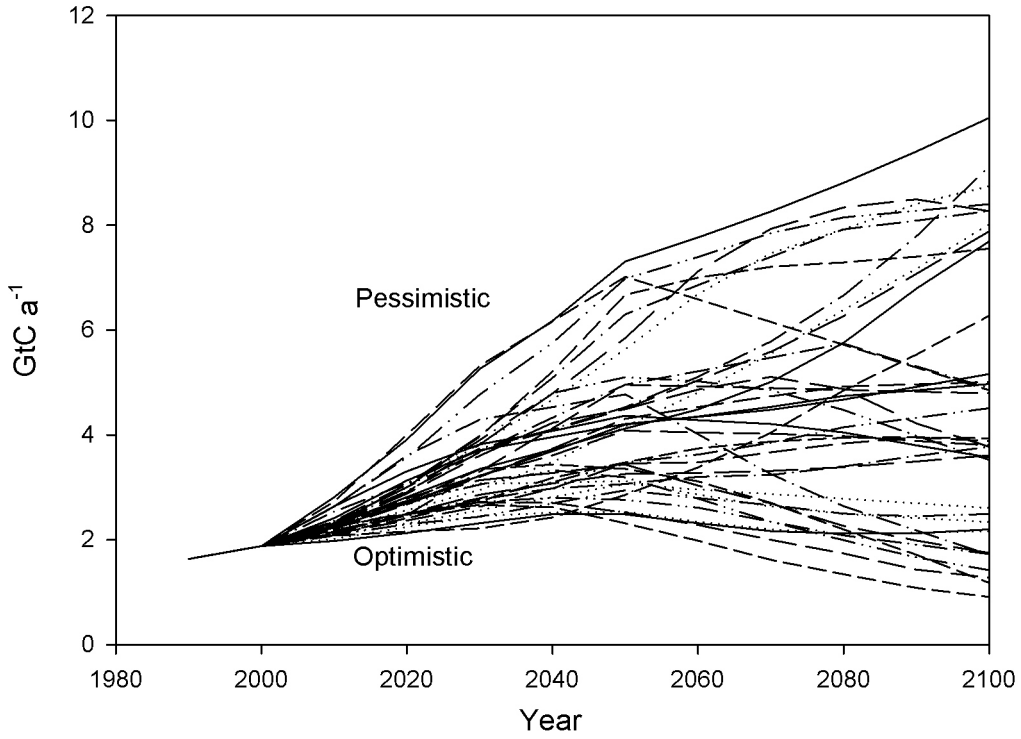

Figure 2.9 – IPCC SRES emissions scenarios. Source IPCC (2000).

Table 2.6 – Stabilisation scenarios for atmospheric CO_2. Source Metz et al. (2007).

Category	Additional radiative forcing (W/m^2)	Stabilisation CO_2 concentration (ppm)	Global temperature increase above pre-industrial (°C)	Peaking year for CO_2 emissions	% change in global CO_2 emissions from 2000 baseline
I	2.5-3.0	350-400	2.0-2.4	2000-2015	-85 to -60
II	3.0-3.5	400-440	2.4-2.8	2000-2020	-60 to -30
III	3.5-4.0	440-485	2.8-3.2	2010-2030	-30 to +5
IV	4.0-5.0	485-570	3.2-4.0	2020-2060	+10 to +60
V	5.0-6.0	570-660	4.0-4.9	2050-2080	+25 to +85
VI	6.0-7.5	660-790	4.9-6.1	2060-2090	+90 to +140

An alternative approach is to consider the emissions potential of fossil fuel reserves. Maggio and Cacciola (2009) integrate the curve in Figure 2.10 and suggests that between 2000 and 3000 equivalent billion barrels of crude oil (including poorly accessible resources) are available for fossil fuel use. Combining this in terms of CO_2 production per barrel with potential emissions from coal reserves (WCI, 2008) estimates that around 1500 GtC may be emitted if fossil fuels were exploited to their full potential. It is unlikely that all of the fossil fuel resources will be exploited in this way. The point, however, is to

highlight that the scope for perturbing the climate system is large, two orders of magnitude greater than the reduction target. The enhanced greenhouse effect is predicted to increase atmospheric temperatures and weather anomalies by the year 2100 (Meehl et al., 2005; Stott et al., 2000; Boer et al., 1992). The slow progress in renewable energy development and the potential impact of fossil fuels on the atmosphere led to the concept of geoengineering, with which the research in this thesis can be included.

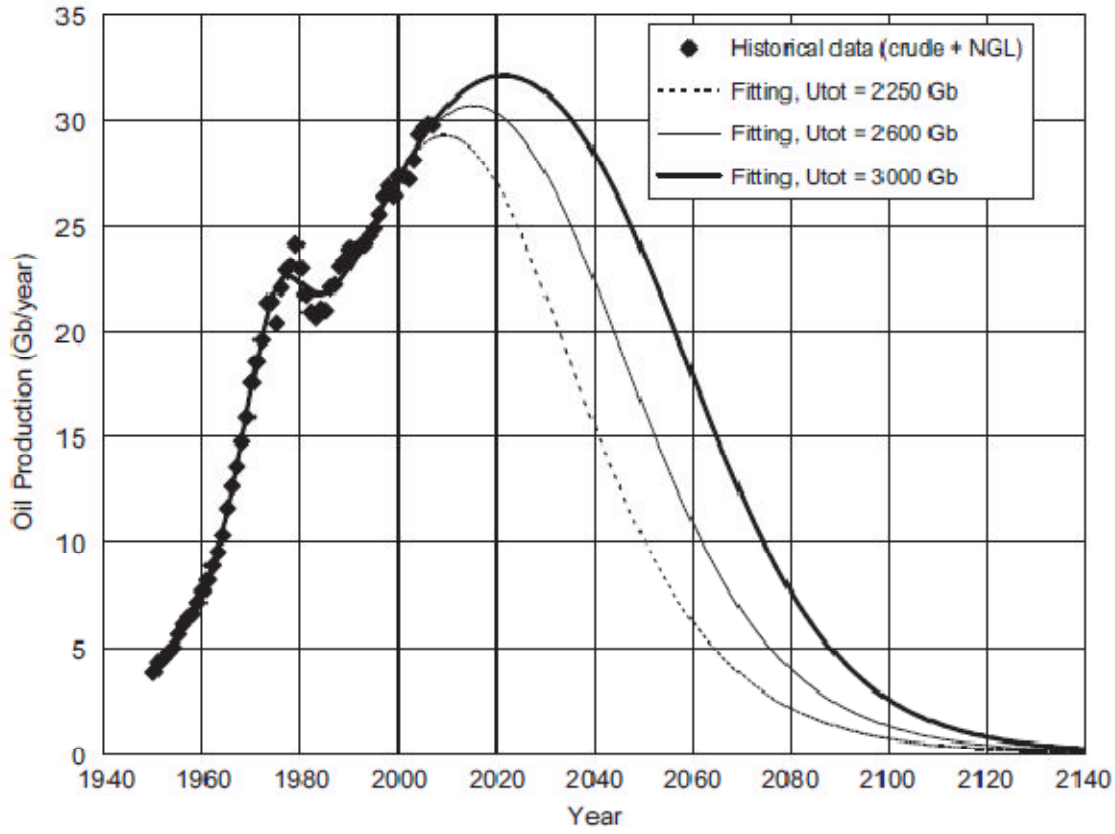

Figure 2.10 – Petroleum production forecast from Maggio and Cacciola (2009).

2.3 Geoengineering

Geoengineering is described in The Royal Society's report (The Royal Society, 2009) as 'the deliberate large-scale intervention in the Earth's climate system, in order to moderate global warming'. Suggested technologies broadly fall into two categories; those that remove carbon dioxide from the atmosphere (mineral carbonation, CO_2 air capture, biochar, ocean fertilisation etc.) and those that mediate the incoming solar radiation (stratospheric aerosols, space reflectors etc.). The Royal Society's assessment of various geoengineering technologies

(The Royal Society, 2009; Figure 2.11) highlights the relative effectiveness, affordability, timeliness (not shown here) and safety. Additional research is required on all technologies for a more accurate comparison, but no single technology predominates the analysis. The technology proposed in this thesis is similar in scope to geoengineering through enhanced weathering.

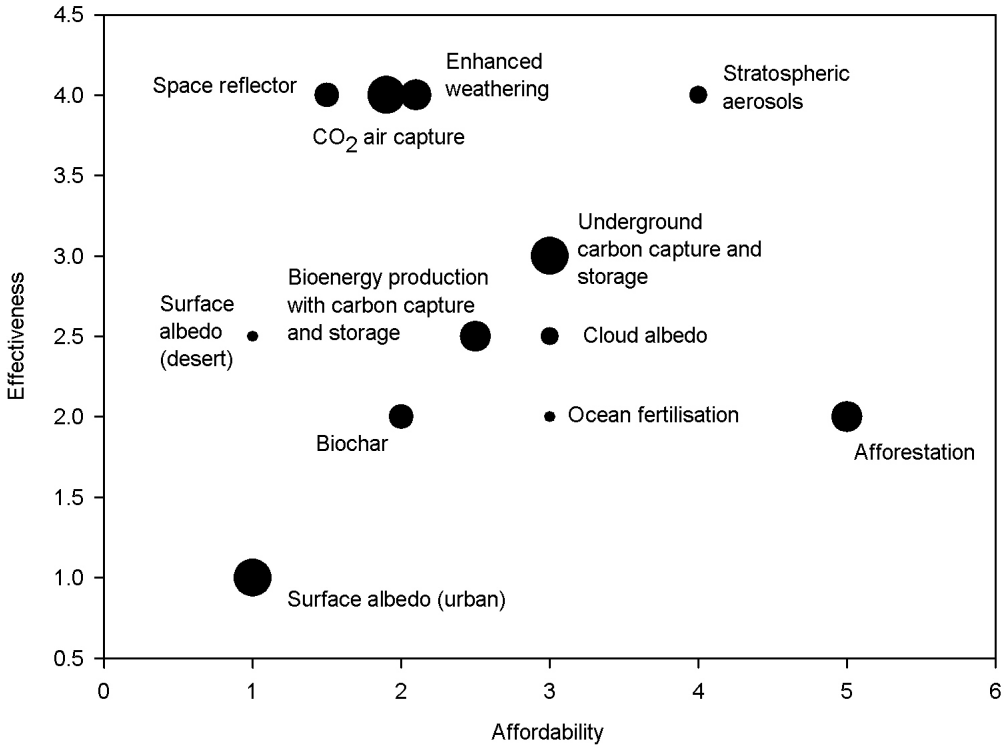

Figure 2.11 – The Royal Society's assessment of various geoengineering technologies. Note the size of the bubble is relative safety of the method (large=safe).

2.4 Mineral weathering

In the 1980s models were published which investigated the correlation between silicate weathering and paleoclimates. Walker, Hays and Kasting published a model in 1981 which described silicate weathering as a negative feedback loop to control atmospheric temperature (Walker et al., 1981). Their model suggests that weathering is controlled by surface temperature, which is controlled by partial pressure of atmospheric CO_2 .An increase in atmospheric CO_2 would result in an increase in rate of weathering, which would sequester an increased quantity of atmospheric carbon (through carbonation in the ocean), hence buffering the CO_2 rise. They speculate that this mechanism would act to partially stabilise temperatures over geological time scales. Two years later in

1983, Berner, Lasaga and Garrels published their classic (BLAG) model relating the geochemical cycle to atmospheric carbon dioxide (Berner et al., 1983). The model describes the surface water fluxes and correlates atmospheric CO_2 with continental spreading. The authors conclude that the results from the model closely match palaeontological, palaeobotanical and geographic evidence. Kasting (1984) and Berner and Barron (1984) published comments regarding the BLAG model, effectively updating and refining the initial concept. Kasting (1984) argued that the models' predicted values for dissolved calcium and biocarbonate in the Cretaceous period conflict with the occurrence of evaporite deposits from the same time period. Berner and Barron (1984) update the model with new findings regarding sea floor spreading rates and organic carbon burial.

Recent work by Berner has refined the earlier work in the BLAG model into the GEOCARB model, and the most recent version, GEOCARB III, is presented in Berner and Kothavala (2001). The model is based on similar principles as the BLAG model, but introduces several new features, including temperature responses to changes in solar radiation, increased weathering due to continental uplift, the evolution of vascular plants and the decay of organic carbon. An extensive critique of the models produced by Berner is presented by Boucot and Gray (2001). They question the fundamental assumptions made by palaeoclimatic modellers, particularly the over simplification of their models for use as an indicator for past atmospheric CO_2 levels.

Dupre et al. (2003) attempt to clarify the role of basaltic weathering in the global carbon cycle. The model, similar to BLAG and GEOCARB, equates consumption of atmospheric CO_2 to the product of surface runoff and temperature. The model produces results with the same order of magnitude as that expressed as the total cation flow in rivers ($x10^{12}$) detailed in BLAG. Lenton and Britton (2006) speculate about the potential future scenarios of atmospheric carbon against long term emission scenarios. The results suggest that over 100 years are required after fossil fuel perturbation for the atmospheric CO_2 system to stabilise itself.

There is general consensus that the methodology adopted by Berner and other paleoclimatic modellers is correct and is a useful indicator for ancient

atmospheric CO_2 levels. However, the work completed by Boucot and Gray (2001) would suggest that there is additional research required to understand the carbon cycle, the role of organisms within the cycle and the collection of data to verify the models.

The discussion of mineral weathering-climate interaction is important when considering recent attempts to accelerate mineral weathering to timescales applicable to humans for use as a geoengineering technology (Seifritz, 1990). Early work (Lackner et al., 1997; Lackner et al., 1995) investigated the carbonation of olivine and serpentine at high pressure and temperature. This 'reactor' method for accelerating carbonation has been applied to numerous artificial materials including slag (Lekakh et al., 2008; Huijgen et al., 2005), cements (Huntzinger et al., 2009; Fernandez Bertos et al., 2004) and ashes (Montes-Hernandez et al., 2009; Fléhoc et al., 2006; Rendek et al., 2006). Subsurface carbonation is possible through CO_2 gas injection into silicate rock formations, complementing conventional injection into saline aquifers (Kelemen and Matter, 2009; Matter and Keleman, 2009; Abanades et al., 2005). However, unlike saline aquifers, the carbon dioxide in silicate rock formations is intended to react chemically to immobilise the carbon (see Chapter 3). Using the enhanced mineral weathering processes in soils Manning (2008), Renforth et al. (2009), Renforth et al. (2011) and work herein suggests pedogenic carbonate formation as an alternative and complimentary strategy of carbon sequestration to those discussed above.

2.5 Chapter summary

The carbon cycle transports on the order of $10^2 – 10^3$ GtC a^{-1} through a range of pools. Carbon quantities in the mantle and core are several orders of magnitude greater than those at the surface, but the flux between the deep and outer Earth is relatively small (<0.5 GtC). Atmospheric carbon, through large transfer rates, is primarily linked to dynamics within the terrestrial and oceanic systems. From ice core records of recent geological time it can be seen that this ocean-land-atmosphere carbon cycle has been in sufficient equilibrium to stabilise temperature by ± 5 °C in the Northern Hemisphere. Recent anthropogenic perturbation of atmospheric carbon through fossil fuel combustion and land use change is predicted to cause substantial climate change over the next century. The potential impact of fossil fuel reserves and the slow progress in renewable

energy provision has led to a need to consider geoengineering technologies (in which mineral carbonation in the soil is subsidiary).

Chapter 3

Chapter 3. Sources of calcium rich minerals

The feasibility of a mineral carbonation technology is primarily dependent on the quantity of available material, the efficiency of carbonation and the value of carbon. The aim of this chapter is to investigate the maximum carbon capture potential of soil mineral carbonation by presenting the available information regarding the production of potential materials available for carbonation particularly focusing on waste production (construction and demolition waste, fuel ash etc), or materials which are considered by-products of producing a primary material (slag and fines from aggregate production etc). Using waste as a carbon sink will mitigate the emissions associated with the primary product without incurring significant additional carbon emissions. The IPCC considers the costs and benefits associated with extracting silicates specifically for carbonation (Mazzotti et al., 2005). Energy requirements are between 180-2300 kWh (primarily associated with processing the raw material) and costs are between $55-430 per tonne ($t^{-1}$) of CO_2 captured using a wet carbonation reactor. However, the carbon capture potential is large (10^2 -10^4 $GtCO_2$) and is an order of magnitude larger than the anthropogenic greenhouse gas contribution to the atmosphere over the next 100 years (Lackner et al., 1995). This thesis focuses on an alternative, and complimentary, strategy to use silicates produced in waste streams where the embodied energy is shared with the primary product and the value of the material is dictated primarily by its carbon capture potential.

Delivered objective: The production of artificial silicates from a range of industrial sources has been quantified through a review of the literature and production statistics.

3.1 Geological sources of calcium-rich minerals

Although the Earth is composed of many elements, eight (Si, O, Al, Ca, Mg, K, Na and Fe) compose 98% of the continental crust (Reimens and de Caritat, 1998 -See Table 3.1). Within the context of this thesis the geochemistry of calcium and magnesium are important. During weathering of exposed silicate outcrops the elemental components of the rock are released into the environment, transported in surface water or groundwater to sedimentary basins (ocean or lake floors), and in the case of calcium and magnesium can be

precipitated as carbonate minerals calcite ($CaCO_3$) aragonite ($CaCO_3$), magnesite ($MgCO_3$), or dolomite ($CaMg(CO_3)_2$). Of course, this description is highly simplified as calcium and magnesium can form numerous intermediate products (e.g. uptake by plants and animals, sorption onto clays, and precipitation with phosphate and sulphate).

Table 3.1 – Element distribution in the continental crust based on Reimans and de Caritat (1998).

%wt	Bulk continental crust	Upper continental crust	Ultramafic rock	Ocean ridge basalt	Gabbro, basalt	Granite/ Granodiorite	Limestone	Sandstone
SiO_2	61.60	64.91	42.99	49.41	48.55	72.08	6.63	86.20
Al_2O_3	11.06	10.76	2.78	12.36	11.53	10.14	0.56	2.92
Fe_2O_3	4.02	2.87	8.74	6.60	7.99	1.86	0.46	0.93
MgO	3.65	2.24	34.48	7.63	7.63	0.83	0.66	1.16
CaO	5.39	4.12	3.50	11.75	10.35	1.26	53.16	1.82
Na_2O	2.00	2.18	0.51	1.70	1.70	2.12	0.51	1.44
K_2O	1.51	2.02	0.35	0.14	0.56	2.32	0.21	0.77
Total	89.21	89.09	93.35	89.58	88.31	90.61	62.19	95.24

Calcium and magnesium silicates are minerals which primarily contain silicon-oxygen tetrahedra coordinated with calcium/magnesium cations, although other elements may be associated including iron and aluminium (see Figure 3.1). Silicate mineral crystal structure, which influences the rate of weathering (see Chapter 6), varies depending on the silicon and aluminium to oxygen ratio in the tetrahedral matrix. Isolated tetrahedra bound together by cations (orthosilicates) have a 1:4 silicon oxygen ratio, minerals such as olivine and garnet are included in this category. However, silicate tetrahedra often share oxygen atoms as linked tetrahedra (soro/cyclosilicates 2:7, 1:3) single or double chains (inosilicates 1:3), sheets (phyllosilicates 2:5) or in a three dimensional matrix (tectosilicates 1:2). Feldspars belonging to the tectosilicates are the most abundant of silicate minerals comprising at least 50 wt% of the Earth's crust (Birkeland and Larson, 1989).

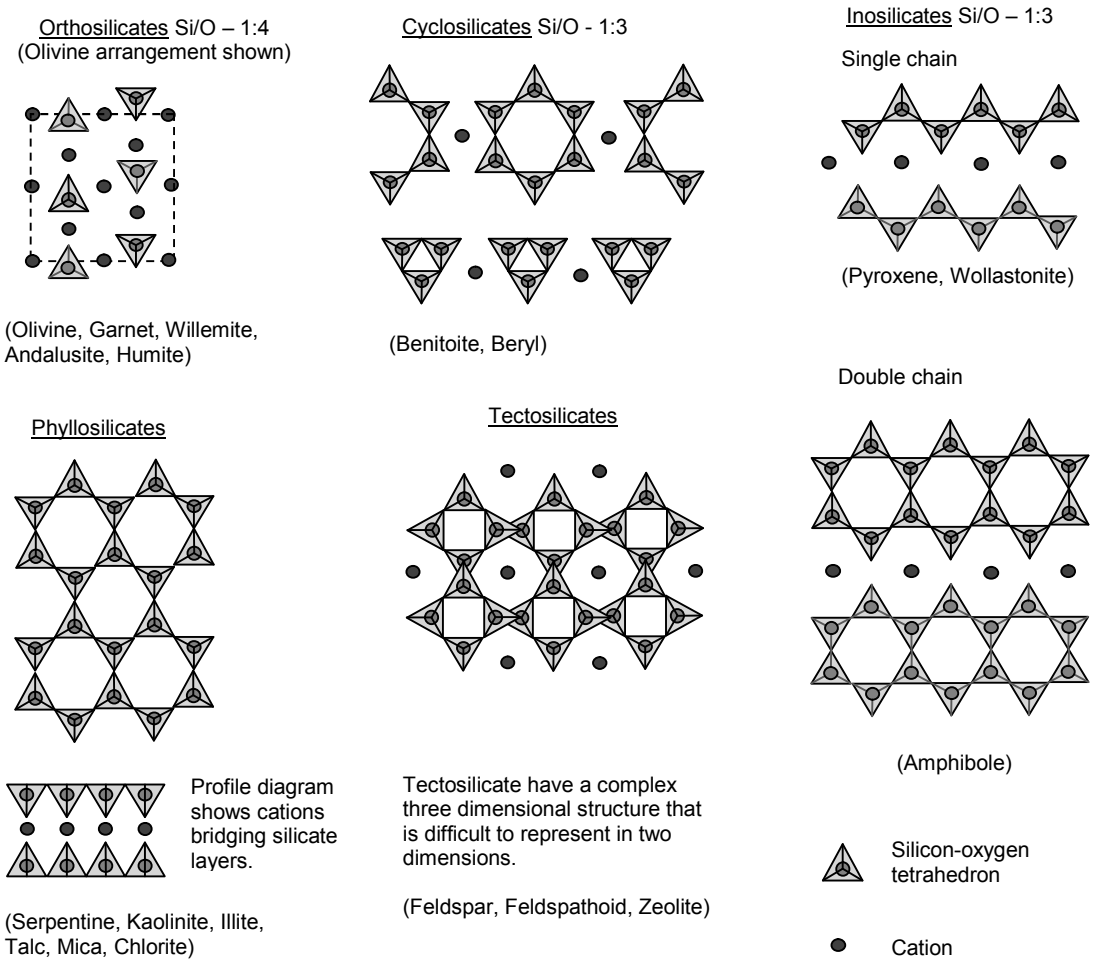

Figure 3.1 – Simplified two dimensional representations of silicate minerals. Adapted from Deer et al. (1996).

Common calcium and magnesium silicate minerals produced in human material streams vary in chemical composition, crystal structure and carbonation potential. They often occur in association with glasses and gels, and with the calcium hydroxide mineral portlandite, which also undergo carbonation. Table 3.2 gives examples of free energies (ΔGr) of carbonation reactions that produce calcite or magnesite at 25 °C, expanding on previous tabulated data (Lackner et al., 1995) to include artificial minerals. To facilitate comparison, Table 3.2 normalises the calculated values for ΔGr to the number of moles of carbonate product. It shows that it is energetically favourable for the majority of widely occurring calcium silicate minerals (and portlandite) to undergo carbonation reactions at STP.

Although the calculated free energy changes are generally favourable, the mechanisms of carbonation depend on kinetic factors, such as dissolution rate

and reactive surface area. Dissolution rate can vary by several orders of magnitude (White and Brantley, 1995). In addition, bulk materials consist of mixtures of minerals listed in Table 3.2, as well as others that may not be of interest.

Table 3.2 – Taken from Renforth et al. (2011b) - Carbonation reactions and their associated free energy changes (ΔG_r) at STP, overall and expressed normalized to the number of moles of carbonate mineral product using data from NB: reactions for jennite and tobermorite use mineral formulae corresponding to those cited in Lothenbach et al. (2008) the source of the data for ΔG_f. Formulae and values for ΔG_f for other reactants, including dissolved carbonic acid, and products, including dissolved silica, are also given. For internal consistency, all thermodynamic data except ΔG_f for jennite and tobermorite, are from Robie and Hemingway (1995)

Mineral/ material	Formula	Occurrence	ΔG_f, kJ/mol	Carbonation reaction	ΔG_r, kJ/mol	ΔG_r, kJ/mol carbonate
Portlandite	$Ca(OH)_2$	Portland cement	-898.0	$Ca(OH)_2 + H_2CO_3 = CaCO_3 + 2H_2O$	-81.50	-81.50
Larnite	Ca_2SiO_4	Cement clinker	-2191.2	$Ca_2SiO_4 + 2H_2CO_3 = 2CaCO_3 + H_4SiO_4$	-127.20	-63.60
Anorthite	$CaAl_2Si_2O_8$	Basic rocks	-4007.9	$CaAl_2Si_2O_8 + H_2CO_3 + H_2O = CaCO_3 + Al_2Si_2(OH)_4$	-57.80	-57.80
Jennite	$Ca_9Si_6O_{16}(OH)_2.6H_2O$	Hydrated cement	-2480.8	$Ca_{1.67}SiO_{1.57}(OH)_{4.2} + 1.67H_2CO_3 = 1.67CaCO_3 + H_4SiO_4 + 1.77H_2O$	-90.51	-54.20
Rankinite	$Ca_3Si_2O_7$	Cement clinker/slag	-3748.1	$Ca_3Si_2O_7 + 3H_2CO_3 + H_2O = 3CaCO_3 + 2H_4SiO_4$	-146.30	-48.77
Akermanite	$Ca_2MgSi_2O_7$	Slag	-3667.5	$Ca_2MgSi_2O_7 + 3H_2CO_3 + H_2O = 2CaCO_3 + MgCO_3 + 2H_4SiO_4$	-127.90	-42.63
Forsterite	Mg_2SiO_4	Basic rocks; slag	-2053.6	$Mg_2SiO_4 + 2H_2CO_3 = 2MgCO_3 + H_4SiO_4$	-66.80	-33.40
Wollastonite	$CaSiO_3$	Metamorphic rocks	-1549.0	$CaSiO_3 + H_2CO_3 + H_2O = CaCO_3 + H_4SiO_4$	-27.00	-27.00
Tobermorite	$Ca_5Si_6O_{16}(OH)_2.4H_2O$	Hydrated cement	-1744.4	$Ca_{0.83}SiO_{1.53}(OH)_{2.6} + 0.83H_2CO_3 = 0.83CaCO_3 + H_4SiO_4 + 0.13H_2O$	-13.66	-16.46
Diopside	$CaMgSi_2O_6$	Basic rocks	-3026.8	$CaMgSi_2O_6 + 2H_2CO_3 + 2H_2O = CaCO_3 + MgCO_3 + 2H_4SiO_4$	-26.20	-13.10
Chrysotile	$Mg_3Si_2O_5(OH)_4$	Metamorphic rocks	-4032.4	$Mg_3Si_2O_5(OH)_4 + 3H_2CO_3 = 3MgCO_3 + 2H_4SiO_4 + H_2O$	-39.20	-13.07
Tremolite	$Ca_2Mg_5Si_8O_{22}(OH)_2$	Metamorphic rocks	-11574.6	$Ca_2Mg_5Si_8O_{22}(OH)_2 + 7H_2CO_3 + 8H_2O = 2CaCO_3 + 5MgCO_3 + 8H_4SiO_4$	-33.10	-4.73
Enstatite	$MgSiO_3$	Basic rocks	-1458.3	$MgSiO_3 + H_2CO_3 + H_2O = MgCO_3 + H_4SiO_4$	0.14	0.14
Laumontite	$CaAl_2Si_4O_{12}.4H_2O$	Metamorphic rocks	-6772.0	$CaAl_2Si_4O_{12}.4H_2O + H_2CO_3 + H_2O = CaCO_3 + Al_2Si_2(OH)_4 + 2H_4SiO_4$	90.70	90.70
Water	H_2O		-237.1			
Kaolinite	$Al_2Si_2(OH)_4$		-3797.5			
Calcite	$CaCO_3$		-1128.5			
Magnesite	$MgCO_3$		-1029.5			
$(carbonate)_{aq}$	H_2CO_3		-623.2			
$(silica)_{aq}$	H_4SiO_4		-1307.8			

3.2 Silicate extraction

3.2.1 Aggregate extraction and crushing

Rocks containing silicate minerals are extracted for use in construction as building stone and aggregate. The UK extracts approximately 60 million tonnes (Mt) of igneous rock a^{-1} (70 wt% crushed and used as aggregate) which is reported to contribute £392 million to the economy and employs about 5,000 people (British Geological Survey, 2009). This is approximately 74 wt% of all hard rock production in the UK, and 28 wt% of total aggregate production (Hicks, 2008). The consumption of aggregates is typically confined to the geographic region of extraction with occasional international trade. Because of this, there is little interest in documenting the global production of the material, although limited data exist at national level. For instance, the United States produces 1.72 Gt of crushed stone a^{-1}, of which igneous rocks comprise 24 wt% (16 wt% granite, 8 wt% basic) (Willet, 2007). Bobrowsky (1998) presents various studies on aggregate production from 9 different countries, which have been collated with data from England (British Geological Survey, 2009) and the US (Wilburn and Goonan, 1998). Using cement production (USGS, 1990-2007) as a proxy, global aggregate production estimated to be around 40 Gt a^{-1} (see Table 3.3).

Table 3.3 – Aggregate and cement production statistics. Aggregate production statistics from Bobrowsky (1998), Hicks (2008), and Wilburn and Goonan (1998). Cement production statistics for the same year from the US Geological Survey Mineral Yearbook (USGS, 1990-2007).

Country	Aggregate Production (Mt a^{-1})	Cement Production (Mt a^{-1})
England	216	11.2
United States	1720	95.5
South Africa	58	7.8
Norway	50	1.7
California	121	10.1
Linear regression analysis: Aggregate production (Mt) = 18.285cement production (Mt) - 28.872 (r^2=0.996) ~ note US outlier. Average aggregate to cement ratio – 17.225.		

Aggregate raw material is extracted from surface mines by blasting a working face and crushing the resultant debris, which produces up to 20 wt% of fine material (material too small to be used as aggregate) (Lowndes and Jeffrey, 2009). Primary aggregate crushing produces between 3 wt% and 4.7 wt% of fine material depending on the method used (Guimaraes et al., 2007), which

include jaw, cone and gyratory crushing (Figure 3.2). Jaw and gyratory crushers are most frequently used for primary crushing and cone crushers are used for secondary/tertiary crushing. Lowndes and Jeffrey (2009) suggest that subsequent crushing of igneous or metamorphic materials may produce fines of up to 40 wt% of the raw material (see Table 3.4). Based on this, the production of igneous quarry fines in the UK is approximately 20 Mt a^{-1}. Globally, fines from igneous aggregate production are estimated at 3.3 Gt a^{-1} (based on the assumed total aggregate to igneous aggregate ratio of the UK and US). CO_2 emissions from crushing varies depending on which method is used, the capacity of the equipment and the particle size requirements but can be estimated between 27 – 82 gC t^{-1} of material processed (Figure 3.2).

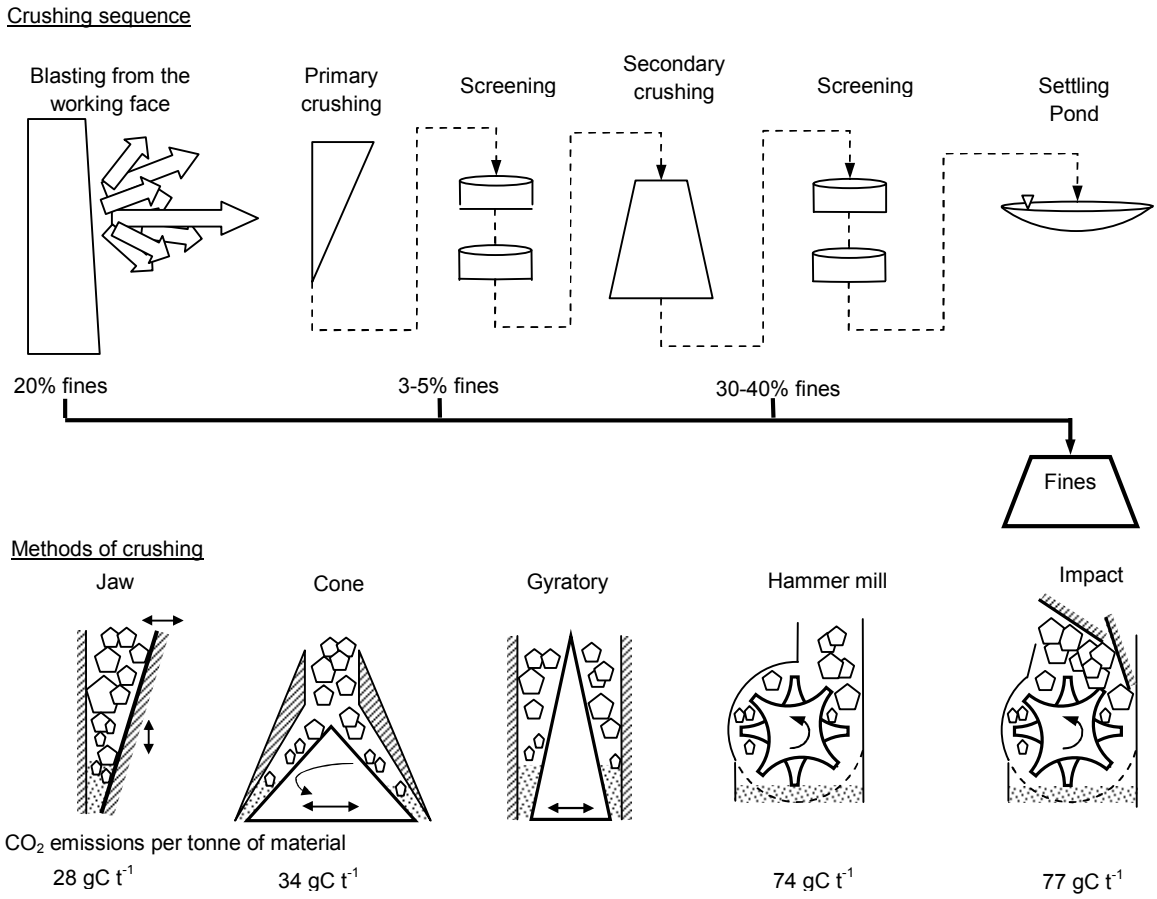

Figure 3.2 – Schematic of crushing methods adapted from Guimaraes et al. (2007).

Table 3.4 – Fine production from various crushing processes, reproduced from Lowndes and Jeffery (2009).

Production Stage	Rock Type	Fine production (and crusher type)
Primary production	Igneous & metamorphic	3-6% (jaw) to 10-15% (gyratory)
	Limestone	6-7% (jaw) to 20% (impact)
	Sandstone	1-2% (jaw) to 15-20% (gyratory)
Secondary production	Igneous & metamorphic	0-23% (cone)
	Limestone	15-25% (cone) to 30% (impact)
	Sandstone	10-15% (cone)
Tertiary crushing (and others)	Igneous & metamorphic	5-30% (cone) to 40% (impact)
	Limestone	<20% (impact) to 40% (hammer mill)
	Sandstone	~15% (cone) to 40% (impact)

The financial cost of raw material extraction in the construction industry is estimated to be approximately £8.5 t^{-1}, and the external cost (e.g. environmental impact) of producing hard rock aggregates is estimated between £0.40 and £2.62 t^{-1} (Craighill and Powell, 1999).The UK aggregates levy (£2 t^{-1}) was introduced in 2002 to account for external costs, the proceeds of which are fed into a range of benefits to the community and industry, and environmental research (Aggregates Levy Sustainability Fund). Landfill tax was introduced in the UK in 1996 to reduce the quantity of waste disposed of in landfill and is currently £2.50 t^{-1} and £48 t^{-1} for inert material (cement, untreated quarry material, ceramics, soil etc.) and standard waste respectively (Business Link, 2010). Within this framework fines production from primary aggregate manufacture is a problematic material that cannot be disposed of in landfill and often is subsequently stockpiled in quarries or used for landscaping (Woods et al., 2004).

3.2.2 Aggregate material properties

Aggregate rock is primarily used for engineering projects (road base, filler in concrete etc.). As such, interest in aggregates generally focuses on its physical properties. However, the chemistry of aggregates has received some attention due to expansion problems associated with the alkali-aggregate chemical reaction (Lea, 1970; Stanton, 1940). BS EN 12620:2002 and BS EN 1744-1:1998 stipulate the chemical analysis of aggregates that are to be used in concrete including acid soluble chloride, acid soluble sulphate, and organic

carbon, the frequency of which is presented in Table 3.5. It is typical that a detailed chemical evaluation is conducted during the initial stages of aggregate extraction. However, there is no widespread publically available reporting of aggregate chemical composition as quarrying operations progress.

Table 3.5 – Aggregate testing regime. Adapted from BS EN 12620:2002

Test	Frequency
Size grading	1 per week
Shape of coarse aggregates	1 per month
Fines content	1 per week
Fines quality	1 per week
Particle density	1 per year
Alkali-silicate reactivity	when required
Soluble chloride	1 per 2 years (more frequent when required)
Calcium carbonate content	1 per 2 years
Soluble sulphate	1 per 2 years
Organic carbon	1-2 per year

3.2.3 Mine waste

The extraction of ore from hard rock generates by products such as overburden and tailings. Tailings are the 'waste' material produced during ore refinement, the chemical composition of which is dependent on the refining process (for example: tailings from a gold mine may contain cyanates as a product of gold cyanidation) and the host geology. Tailings are hydraulically separated from the ore and stockpiled behind dams, of which there may be up to 4000 active globally (email enquiry response from Tailings.info, 2009). There is no widespread reporting of tailing quantities or mineralogy. Therefore, estimation of carbonation potential is difficult. However, with ore to tailing ratios up to 1:20 the quantity is potentially large (Deshpande and Shekdar, 2005). For example, two chrysotile mines in Northern Canada produced 50 Mt of tailings in 50 years of operation, which could be carbonated (Wilson et al., 2009). Total mine waste production between 1910-1980 in the US is reported to be approximately 40 Gt (from mining Cu, Fe, U, Mo, Zn, Au, Pb, and Ag; Dudka and Adriano, 1997). Using global production statistics for Cu, Pb, Ni, and Zn (around 40 Mt a^{-1} collectively (USGS, 2010b; USGS, 2010a)) and typical grades of ore between 0.5-25%, the global production of waste from metal mining activity is between 2-7 Gt a^{-1}. Tailings mineralogy is highly dependent upon the host geology, but in some cases may be suitable for carbon capture. It is likely that wet chemical extraction processes (if used) and subsequent storage on site has resulted in

partial carbonation of these materials. Additional work is required to assess the global carbonation potential of mine waste, the location of stockpiles and the degree to which carbonation has already occurred.

Overburden is the material removed to expose the ore, which is replaced after extraction. Potentially, this material may be carbonated prior to replacement. However, the mineralogy and chemical composition is not reported (Hartman, 1987).

3.3 Cement and construction and demolition waste

3.3.1 Cement production

Globally, approximately 2.7 Gt of cement are manufactured annually (USGS, 2004) for use as a binding material in the engineering industry. Cement is produced by heating $CaCO_3$ (quarried as limestone), silica (SiO_2) and alumina (Al_2O_3; both from clay or fly ash), to temperatures between 1300-1500°C. A range of calcium silicate minerals are produced which are colloquially known as cement clinker. The mineralogy of clinker depends on the Ca/Si ratio of the raw materials, but usually a number of di and tri-calcium silicates are formed along with free lime (CaO; Lea, 1970). The UK cement industry is dominated by four companies (Lafarge UK, Cemex UK, Castle Cement, and Tarmac Buxton Lime and Cement) which produce 12 Mt a^{-1}, employing 3,500 people between 14 production sites (The British Cement Association, 2010).

3.3.2 Life cycle analysis of cement

The production of 1 t of cement uses approximately 1.7 t of raw material and produces 150-200 kg of waste as ‘kiln dust’ (van Oss and Padovani, 2003). Worrell et al. (2001) calculate the emissions from cement manufacture to be approximately 244 kgC t^{-1} (see Figure 3.3), but can vary depending on manufacturing processes. Furthermore, this value does not account for emissions associated with mineral extraction and transport.

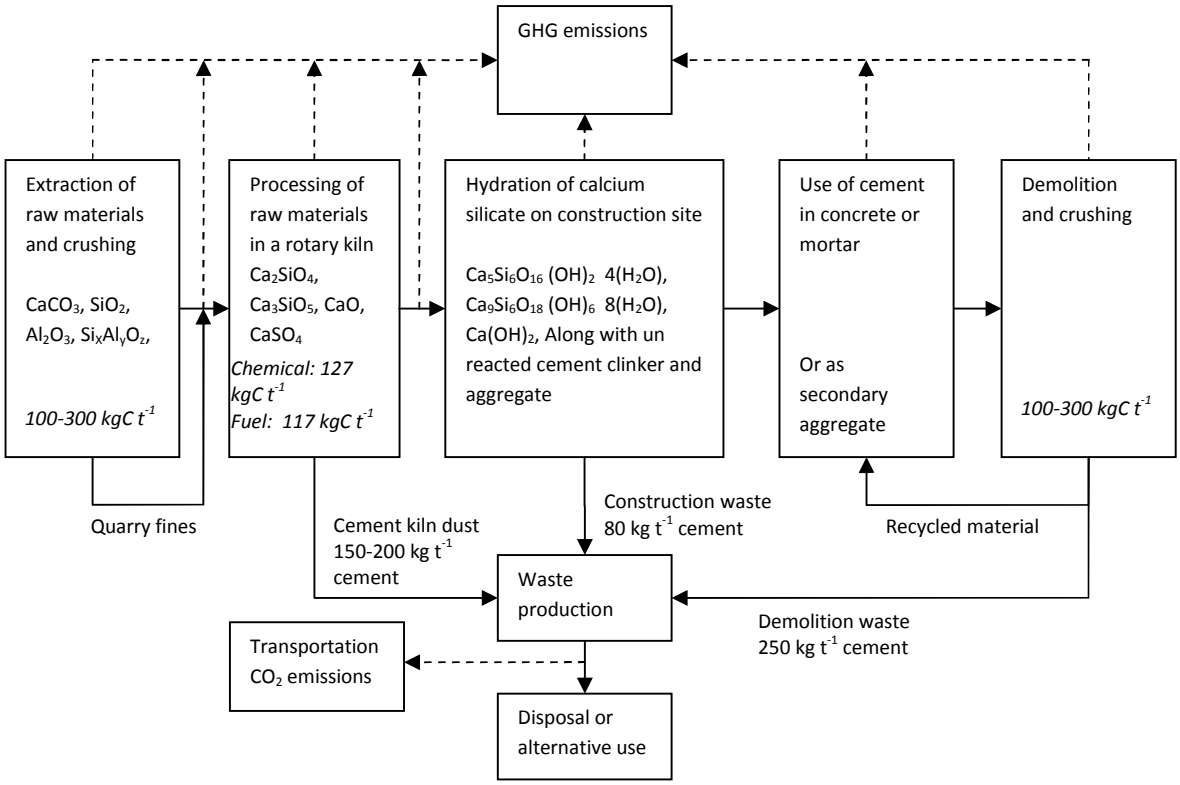

Figure 3.3 – Life cycle model of cement including mineral transformations (adapted from Worrell et al., 2001). Assumed 1:7 cement to concrete conversion.

Cement has been used for construction purposes since Roman times, when it consisted of a mixture of volcanic ash and lime. Until the start of the twentieth century, the global cement industry was dominated by the US and the UK (Lesley, 1924). Towards the middle of the twentieth century emerging economies such as Japan substantially increased their production of cement, partly because of increasing demand due to urbanisation. The most important trend recently has been the rapid growth of cement production in the so-called BRIC countries (Brazil, Russia, India and China) which account for the majority of the cement manufactured today (USGS, 2010b). Approximately 2.8 Gt of cement are produced each year and nearly 60 Gt of cement have been manufactured since the mid 1920s (Figure 3.4; BGS, 2010; BGS, 2005), contributing around 14 Gt carbon into the atmosphere (Worrell et al., 2001). Approximately 9-12 Gt of kiln dust have been produced since the 1920s, with a carbon capture potential of 1.2-1.7 GtC (based on a CaO content of 65%). Although the fate within the environment of this material is unknown, it is likely to have partially or fully carbonated.

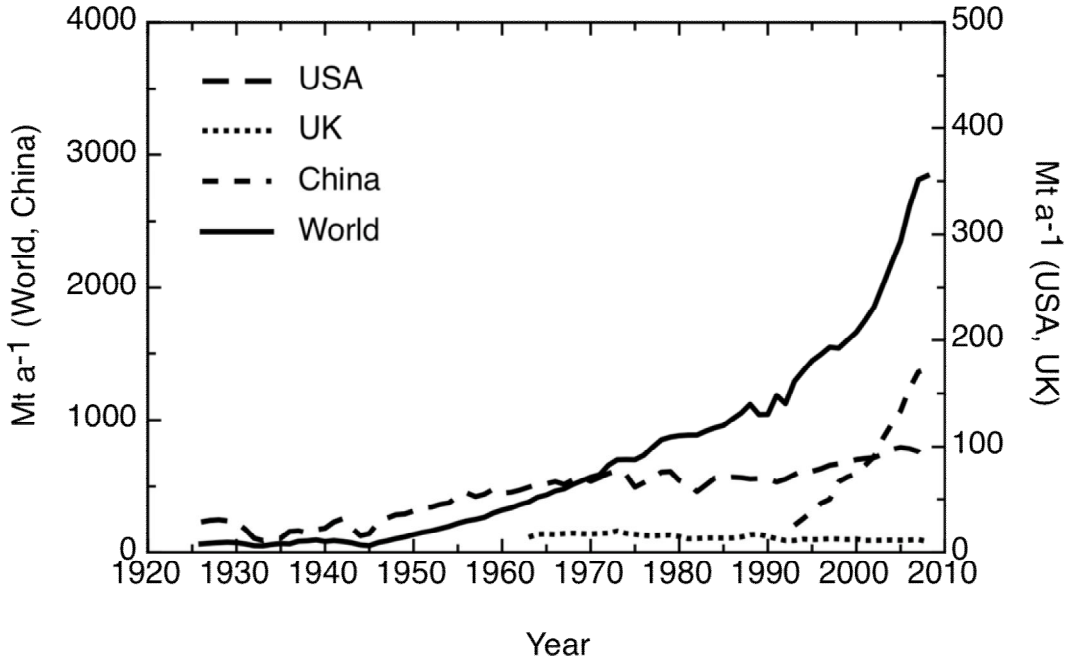

Figure 3.4 – Historic cement production since 1926 – Source: Renforth et al. (2011b).

3.3.3 Construction and demolition waste

Most of the 60 Gt of cement that was manufactured globally was used for construction. The flux of material out of this pool is a heterogeneous waste stream composed of unused/recycled material produced during the construction and demolition (C&D waste) of the built environment. A proportion of the waste is composed of calcium bearing minerals derived from hydration of cement paste. The exact quantity of C&D waste generated in the UK has not been comprehensively established, and available data are becoming increasingly dated (Lawson et al., 2001; Craighill and Powell, 1999). A recent report from the Department for Communities and Local Government (DCLG, 2007) suggests that 40-45 Mt a^{-1} of C&D waste is either spread on registered sites or disposed of in landfill; this is approximately 51 % of the total UK production of C&D waste. In this study, the total quantity of C&D waste was obtained from a survey (DCLG, 2007) of demolition crusher operators, in which the output of active crushers was calibrated against population density, assumed to be an appropriate proxy, to estimate the total recycled aggregate. C&D waste disposed of into landfill is recorded by operators using weighing stations, and was estimated nationally by extrapolation (DCLG, 2007). The accuracy of such estimates is limited, yet this study provides the baseline for current UK

government policy which calls for a 50 wt% reduction in C&D waste to landfill by 2012 (HM Government, 2008).

It is clear from the UK Government's (Department for Environment, Food and Rural Affairs -Defra -Hobbs G, 2008) attempt to disaggregate the DCLG (2007) data, that there is insufficient information to substantially quantify and characterise UK production of C&D waste. The Strategic Forum for Construction (a coalition of various construction sector stakeholders), is at the date of submission of this thesis preparing an action plan to address C&D waste accounting.

Reuse of C&D waste as a 'secondary aggregate' (Oikonomou, 2005; Khalaf and DeVenny, 2004), or as raw material for brick manufacturing (Schuur, 2000) has been suggested as a possible alternative to landfill. However, use as a structural material is limited by the possible presence of low strength or high expansion materials (bitumen, gypsum, organic matter etc.) and the possibility of aesthetic irregularities in brick manufacturing. The composition of C&D waste is dependent on the material content of the building under construction/demolition, but Lawson et al. (2001) have estimated the composition (Table 3.5). Synthesising this data with existing information on construction waste (Vetterlein, 2003; Barlow, 1996) the calcium content can be estimated. However, a similar calculation using data in Bergsdal et al. (2007) suggests that C&D waste has a CaO content closer to 20 wt% compared with 11 wt% in Table 3.6. According to Lawson et al. (2001) cement based products form the largest component of the waste stream (collectively 35.5 wt%) a magnitude approximately supported by Oikonomou (2005) and Kartam et al. (2004), but smaller than the 67 wt% suggested by Bergsdal et al. (2007), highlighting the heterogeneous nature of the material and resulting in a range of estimated CaO contents.

Table 3.6 – Composition of construction and demolition waste, figures adapted from Lawson et al. (2001).[1] Vetterlein (2003) pp210.[2] Estimation based on typical sand to cement ratio of 3:1.[3] Estimated from the stoichiometry of gypsum.[4] From Barlow, (1996) pp290. Potentially greater due to the inclusion of mortar.

Material Type	wt%	Likely material composition	CaO wt%
Construction waste			
Concrete, bricks, blocks, aggregate	7.4	Calcium silicates (hydrated and un-hydrated), Free lime CaO, $CaCO_3$ and gypsum in concrete. Calcium aluminium silicates and Fe oxides in masonry. Silica in sand and gravel.	28.6[1]
Metals	5.9	Predominantly Fe from steel and Cr from stainless steel. Cu and Zn from plumbing. Potentially trace Pb from roofing materials.	N/A
Excess mortar/concrete	2.6	Similar to concrete above	25.0[2]
Timer products	1.7	Organic carbon including lignin and cellulose	N/A
Plastics	1.9	Petroleum products	N/A
Plasterboard and plaster	0.6	Mainly gypsum	32.6[3]
Paper and cardboard	0.4	Organic carbon similar to timber products	N/A
Vegetation	0.2	Organic carbon	N/A
Soil	0.2	Silica in sand and gravel, clay, organic carbon	N/A
Demolition Waste			
Concrete	25.5	Similar to concrete above	28.6[1]
Masonry	15.3	Aluminium silicates, Fe oxides and quartz, with small quantities of free lime	2.6[4]
Paper, cardboard and plastics	12.1	Organic carbon and petroleum products	N/A
Asphalt	9.6	Petroleum products, silicates in aggregate	N/A
Wood based	2.1	Similar to timber products above	N/A
Road planings	14.0	Similar to asphalt	N/A
Total	99.5	**CaO content as a % of total material**	**10.7**

There is no widespread quantification of C&D waste which makes estimation of global production difficult to establish. The data that are available are generally for developed countries, a summary of which is presented in Table 3.7. Using population as a proxy, a crude estimate of global C&D waste production is 1.4-5.9 Gt a^{-1}. It is probable that the production of C&D waste is dependent on numerous factors including waste policy, economic prosperity, historic construction activity, availability of mineral resources and construction practice. For example, an economically developing country which boasts a strong construction sector but with little historic construction activity is likely to produce more construction waste than demolition waste, which is supported by data in Kartam et al. (2004). However, the opposite is likely to be true for a more economically developed country (Bergsdal et al., 2007; Lawson et al., 2001). A comprehensive investigation on the differences in C&D waste quantities and

characterisation has yet to be undertaken, and will be unlikely until construction practice includes the routine measurement of material flow.

Table 3.7 - Global C&D waste estimation based on a population proxy. Adapted from Kourmpanis et al. (2008), DCLG (2007), RPS-MCOS (2004) and Weil et al. (2006).

Country	C&D waste production (Mt)	Population (M)	Waste per capita (t)
France	24.0	61	0.395
UK	76.2	61	1.257
Norway	1.25	5	0.272
Ireland	6.0	4	1.463
Germany	77.3	82	0.938
Greece	2.1	11	0.196
Italy	20.0	58	0.344
Spain	13.0	40	0.322
Netherlands	11.0	16	0.671
Belgium	7.0	10	0.673
Austria	5.0	8	0.610
Portugal	3.0	11	0.283
Denmark	3.0	6	0.545
Sweden	2.0	9	0.222
Finland	1.0	5	0.192
Linear regression analysis: trend C&D production=$0.9pop^{n}+10.7$ ($r^2=0.72$), Average waste per capita is 0.559 sd = 0.341			

3.3.4 Material properties of C&D waste

The classic textbook on cement chemistry by Lea (1970) presents the typical composition of Portland cement as 64.1 % CaO, 5.5 % Al_2O_3, 3.0 % Fe_2O_3, 22.0 % SiO_2, 1.4 % MgO, 2.1 % SO_3 by weight. The Ca:Si:Al ratio can occupy anywhere in the shaded region in Figure 3.5. Calcium silicate hydrate minerals are formed during the hydration of tri/di calcium silicates (C-S-H) and are approximately 75 wt% of hydrated Portland cement (Chen et al., 2004). The most appropriate mineral comparison would be 1.4 nm tobermorite ($Ca_5Si_6O_{16}(OH)_2•4H_2O$) and jennite ($Ca_9Si_6O_{18}(OH)_6•8H_2O$), but the product is highly amorphous rendering identification using X-Ray diffraction difficult. Furthermore, other major (Fe, Mg, K, Na) and trace (Zn, Mn, Ni) elements may be incorporated into the C-S-H matrix to form a range of minerals. Lime that does not react with silica during manufacturing forms calcium hydroxide when hydrated which carbonates in the presence of atmospheric CO_2. Finally, gypsum is added to cement during manufacturing to improve workability. During hydration, some of the sulphate is incorporated into a calcium aluminium hydroxide framework as ettringite ($Ca_6Al_2(SO_4)_3(OH)_{12}•26H_2O$). Therefore, the composition of cement is a mixture of the hydration products discussed above,

and un-hydrated calcium silicates including amorphous material (Table 3.8). Combining the production statistics (by proxy) with the typical chemical compositional information, it is estimated that construction and demolition waste has a carbon capture potential of 9-37 and 24-100 MtC a^{-1} respectively.

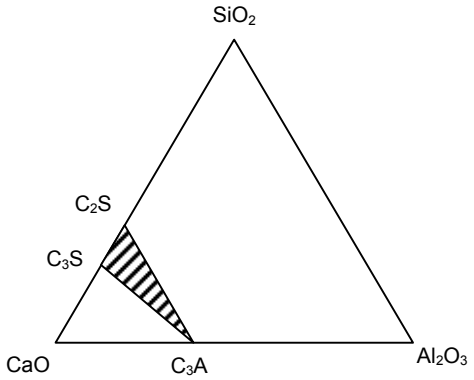

Figure 3.5 – Composition of cement clinker. Source: Manning (1995).

*Table 3.8 – Phase change during the hydration of cement. Adapted from Scivener et al. (2004) and *Lothenbach et al. (2008).*

Phase	Formula	Before hydration (%)	After hydration (%)
Alite	Ca_3SiO_5	69.9	20.4
Belite	Ca_2SiO_4	8.3	7.0
Ferrite	Fe_3O_4	6.3	4.8
Aluminate	Al_2O_4	7.5	1.9
Gypsum	$CaSO_4 \cdot 2H_2O$	2.9	-
Bassanit	$CaSO_4 \cdot 0.5H_2O$	1.5	-
Anhydrite	$CaSO_4$	0.3	-
Portlandite	$Ca(OH)_2$	0.9	15.1
Calcite	$CaCO_3$	1.1	5*
Quartz	SiO_2	0.9	-
Free lime	CaO	0.2	-
Periclase	MgO	0.4	-
Ettringite	$Ca_6Al_2(SO_4)_3(OH)_{12} \bullet 26H_2O$	-	9.1
Amorphous	-	-	34.9
Total		99.3	98.2

3.4 Iron and steel making slag

3.4.1 Slag production

3 Mt of blast furnace slag and 1 Mt of steel slag are produced annually in the UK as a by-product of the iron and steel industry (EA, 2007; Poh et al., 2006). Blast furnace slag is not classified as a waste and is often reused as secondary aggregate in concrete, as filler in road construction (Mahieux et al., 2009), or used for soil stabilisation (Poh et al., 2006). Oxides of iron, silica and alumina (from iron ore) are mixed with $CaCO_3$ and $CaMg(CO_3)_2$ (from limestone and

dolomite) as fluxing agents in a blast furnace at 1300-1600 °C to form pig iron and slag. The quantity of slag is dependent on the purity of the ore, and is usually between 250 kg t^{-1} and 1200 kg t^{-1} for purities between 20-65 % of iron (Lee, 1974). Steel is manufactured by refining pig iron or scrap steel using oxygen and $CaCO_3$/$CaMg(CO_3)_2$ as a flux in a basic oxygen furnace (Lee, 1974). The resulting slag is relatively enriched in free lime and is usually left to 'weather' prior to use. However, only 10 % of steel slag is used in the UK (Poh et al., 2006), the remainder is stockpiled or disposed in landfill.

The production of slag in the UK increased with the development of the iron and steel industry in the early nineteenth century. In the 1840s pig iron output was around 1.5 Mt a^{-1} rising to a peak of almost 18 Mt a^{-1} in the 1960s (Birch, 1967). Steel gained increasing importance in the 1860s; previously it had not been produced on a large scale. In the latter half of the century steel manufacture quickly became and remains the single largest use of UK iron (Carr and Taplin, 1962). In the latter half of the 19th century the USA became the largest producer of iron and steel (15 Mt a^{-1}) rising to around 100 Mt a^{-1} presently (Rogers, 2009). In 1992 China became the largest manufacturer of iron (and steel in 1996) producing around 970 Mt a^{-1} today (500 Mt steel and 470 Mt iron in 2008 (USGS, 2009; BGS, 1927-2008; Figure 3.6).

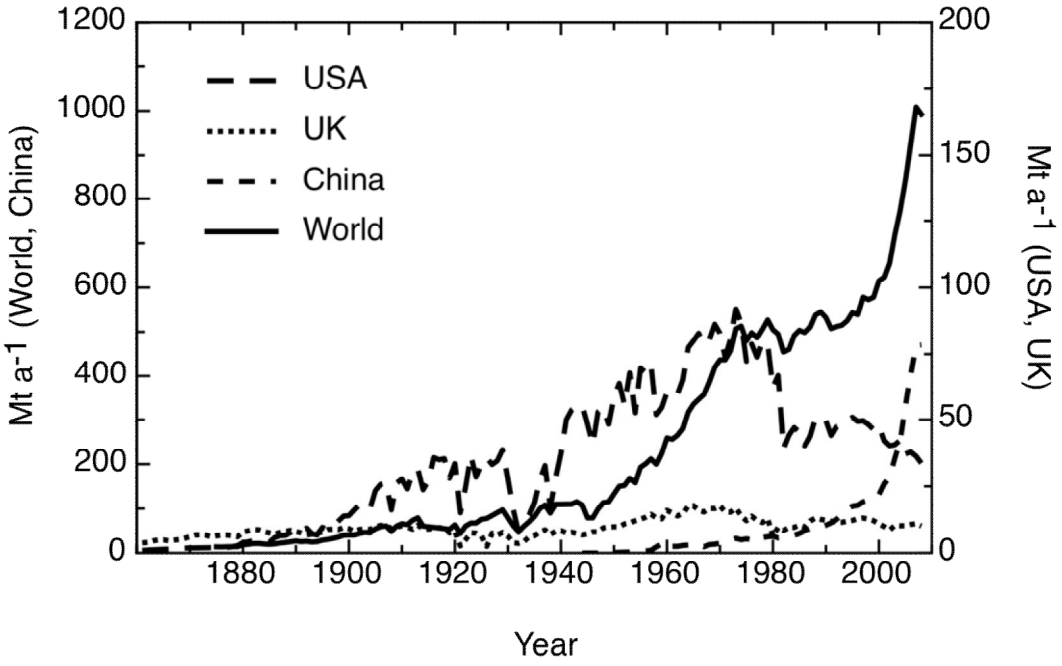

Figure 3.6 – Historic pig iron production since 1860. Source: Renforth et al. (2011b).

Stainless steel is an iron chromium alloy which is resistant to corrosion and is used for its aesthetic value in the construction industry as well as in a wide range of consumer goods. Global production is estimated to be approximately 25.9 Mt a^{-1} (ISSF, 2008) producing 6.48 Mt a^{-1} of slag assuming a similar steel to slag ratio to that produced in a basic oxygen furnace.

3.4.2 Material properties of slag

The chemical composition of iron and steel slag is variable but usually contains between 30 and 50 wt% CaO (Table 3.9). Generally, steel slag has a larger concentration of free lime than blast furnace slag and is prone to swelling during hydration. The most common minerals associated with slag are melilite ($(Ca,Na)_2(Al,Mg,Fe(II))(Si,Al)_2O_7$) and anorthite ($CaAl_2Si_2O_8$) (Lee, 1974), although rapid cooling of the molten slag, usually with water, typically forms an amorphous calcium magnesium alumina silicate glass (Fredericci et al., 2000). Ferrous slag readily weathers under ambient environmental conditions. This initially involves the dissolution of loosely bound free lime (or portlandite). Further weathering results in the breakdown of complex silicate minerals (including rankinite, larnite and akermanite – see Table 3.2) and glasses within the material (Roadcap et al., 2005). Investigation of historic slag deposits demonstrates the presence of carbonate minerals in soil (Renforth et al., 2009), both diffuse and as distinct concretions. Carbon isotope analysis has demonstrated that these carbonate minerals contain, and so sequester, C from an atmospheric source (Chapter 4). Published descriptions of the weathering of slag (Mayes et al., 2008) report high (>11) pH drainage waters containing substantial quantities of Mg, Ca, Fe, Sr and dissolved Si.

Assuming the majority of steel slag and around 20 wt% of iron slag remains stockpiled, it is estimated that 5.8-8.3 Gt of slag have been stockpiled, spread on land, or disposed of in landfill globally since the mid 19th century, with a total carbon capture potential of 0.5-1.1 GtC (based on a CaO and MgO content of 38-46% and 6-12% respectively). Furthermore, current production of slag has a maximum carbon capture potential of 44 -59 MtC a^{-1}.

Table 3.9 - Chemical composition for iron, steel and stainless steel slags (values are wt%).			
	Blast furnace slag (Proctor et al., 2000)	**Steel Slag** (Poh et al., 2006)	**Stainless steel slag** (Shen and Forssberg, 2003)
SiO_2	36.44	12.67	28.39
Al_2O_3	7.79	2.84	4.33
CaO	38.34	44.87	46.20
MgO	11.67	6.87	6.08
FeO	-	15.73	4.22 (total Fe)
Fe_2O_3	2.48	9.81	-
TiO_2	-	0.62	0.33
P_2O_5	-	1.11	-
MnO	0.71	3.81	1.69
Na_2O	-	0.11	0.06
K_2O	-	0.57	0.05
SO_3	2.57	0.00	-
Cr_2O_3	-	-	5.12
Total	100.00	99.01	96.47

3.5 Ash production

3.5.1 Fuel ash production

Various combustion products are created in coal fired power stations (fuel ash, bottom ash, boiler slag etc) as a byproduct of electricity generation; UK annual production is approximately 6 Mt (UKQAA, 2007). Other ashes potentially suitable for carbonation include biomass ash, municipal solid waste incineration ash, paper sludge incineration ash (Gunning et al., 2010), of which collectively the quantity of production is of the order of 10^2 Kt a^{-1}. However, the carbonation of ashes may form part of a waste stabilisation process undertaken to limit environmental impact. A third of the UK's electricity is produced from the annual combustion of approximately 60 Mt of coal (DECC, 2009). In the US, about half of the country's electricity is generated using coal (around 1 Gt a^{-1} (EIA, 2009)). Rapid growth in the power industry in the 1920s and 1930s came at a time when many countries, such as Japan and the USSR, were industrialising rapidly. This industrialisation required advanced electricity distribution networks, and so many countries developed their electricity generating capacity during this period. At this time coal was the only raw material from which electricity could be generated economically, and world consumption of coal rose dramatically (DECC, 2010; EIA, 2009). The second half of the twentieth century saw a rapid increase in demand for electricity in developing countries, especially India and China (EIA, 2009). Although alternative fuels such as oil

and nuclear became available, most developing countries use coal as their primary source of electricity due to its abundance and low cost. Nowadays many developed countries have invested in alternative energy sources, partly due to environmental considerations but also because of decreasing fossil fuel supplies. However many of the world's largest electricity consumers such as the US, China and India still have substantial reserves of coal, and thus the global increase in coal consumption for electricity generation shows no sign of abating. A total of approximately 6.5 Gt of coal are produced annually, and 257 Gt have been produced since 1927 (Figure 3.7; ACAA, 2008; USGS, 2008; USGS, 2006; BGS, 1927-2008).

Koukouzas et al. (2006) suggests that one tonne of lignite will produce 134 kg of fly ash, but ash content can range from 4 to 30 wt% depending on the quality of the coal (Thomas, 1992). Assuming a fuel to ash ratio of 10 % the global production of ash may be around 800 Mt (but realising the potentially large variability), which is derived from bituminous coal (73.5 wt%), lignite (16.2 wt%) and anthracite (10.3 wt%; USGS, 2004).

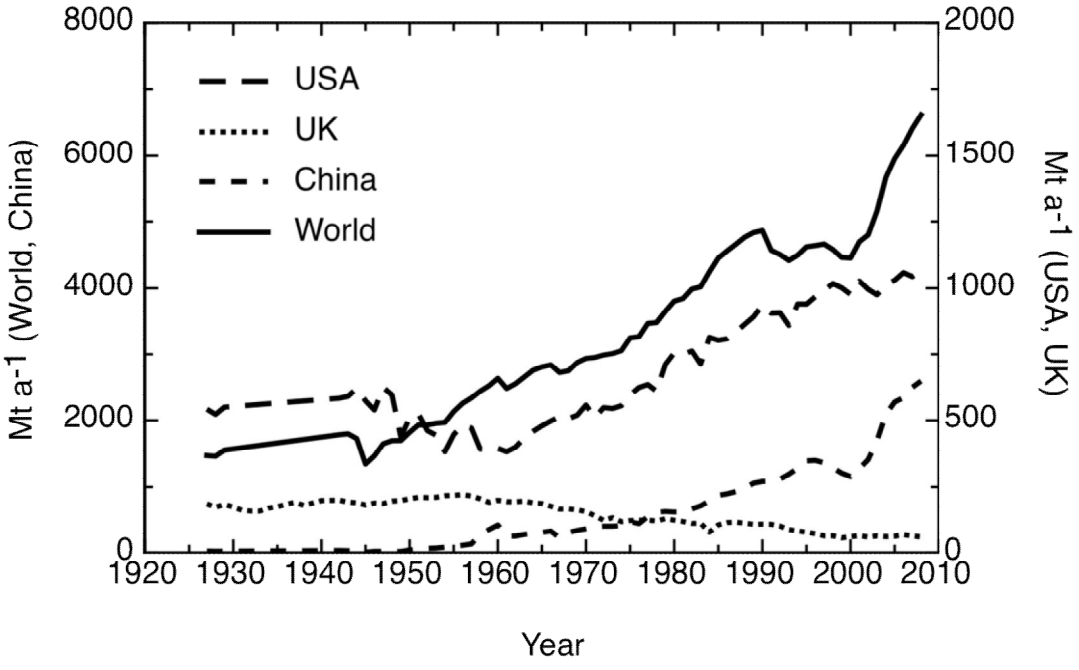

Figure 3.7 – Historic coal production since 1927. Source: Renforth et al. (2011b).

3.5.2 Material properties of fuel ash

Typically, the CaO content of fuel ash range between 1 and 10 % (UKQAA, 2004) but can be as high as 20-30 wt% in 'Type C' sub-bituminous derived ashes (Grisafe et al., 1988). Fuel ash samples from Greek lignite coal were analysed by Koukouzas et al. (2009) and shown to contain 5.7 wt% CaO, which quantitative XRD analysis suggests is largely composed of amorphous material (48.1 wt%). In an earlier paper (Koukouzas et al., 2006) the examination of Greek and Chinese derived fuel ash suggest a wide variety of calcite contents (see Table 3.10), which is apparently derived from marls or conglomerates associated with lignite deposits. However, stoichiometric evaluation against XRF derived CaO contents returns anomalous results for the fly ash samples with large concentrations of calcite (FA6,10,11). Similar analyses of anthracite and bituminous coal ash suggest CaO contents between 2.5 and 10.6 wt% (Goodarzi, 2006; Russell et al., 2002; Vassilev and Vassileva, 1997). Assuming a CaO content of 10 wt%, fuel ash has a carbon capture potential of 3-6 Mt C a^{-1}. It is estimated that between 7.6-14.6 Gt of ash have been produced since 1927.

Table 3.10 – Calcium budget analysis of quantitative XRD of ash in Koukouzas et al. (2006) – The feldspar composition was assumed as anorthite $CaAl_2Si_2O_8$ (values in wt%)

Mineral	**FA1**	**FA2**	**FA3**	**FA4**	**FA5**	**FA6**	**FA7**	**FA8**	**FA9**	**FA10**	**FA11**	**FA12**
	As reported by *Koukouzas (2006)*											
Calcite	6.2	6.6	7.9	11.7	15.6	26.5	6.1	12.5	12.5	22.3	39.7	8.7
Feldspars	8.2	11.2	9.9	5.8	6.9	5.1	5.9	8.9	8.9	9.4	2.1	10.4
Lime	3.7	3.9	3.8	4.9	4.5	6	7.5	7.2	7.2	3.1	6.9	4.4
Portlandite	1.1	1.3	1.3	2	1.2	2.2	4.4	5.8	5.8	0.8	2.1	1.5
CaO (XRF)	16.35	18.5	18.68	18.74	19.14	23.1	22.74	23.94	23.91	17.53	18.12	26.82
	Phase (from QXRD) as a % of the total CaO (from XRF)											
Calcite	21.24	19.98	23.68	34.96	45.64	64.24	15.02	29.24	29.28	71.24	122.69	18.17
Feldspars	12.04	14.53	12.72	7.43	8.65	5.30	6.23	8.92	8.93	12.87	2.78	9.31
Lime	22.63	21.08	20.34	26.15	23.51	25.97	32.98	30.08	30.11	17.68	38.08	16.41
Portlandite	5.25	5.48	5.43	8.32	4.89	7.43	15.09	18.90	18.92	3.56	9.04	4.36
Amorphous	38.85	38.93	37.83	23.14	17.30	-2.94	30.68	12.87	12.76	-5.35	-72.59	51.76

3.6 Stockpiled and other material

Material that is not recycled is disposed of using methods which have varied over time depending on material composition and legislation. Historically, the disposal of waste was less restricted, which allowed operators to dispose of material onto land or into water bodies. Evidence of these practices can be

seen adjacent to the former steelworks at Consett (County Durham UK) where 130,000 tonnes of iron and steel slag have been left since the closure of the steelworks in 1980 (Harber and Forth, 2001). Similarly, iron and steel making in Northern Illinois/Indiana (USA) since the 1830s has created 27 km^2 of new land by disposal of slag into and around Lake Michigan, where it is estimated that 52 km^2 have been covered by slag (Bayless and Schulz, 2003). The introduction of new legislation in the 1990s (e.g The Environment Act 1995 in the UK) has forced operators to dispose of materials to controlled landfills. Work by VanGulck et al. (2003) and Manning (2001) suggests that calcium carbonate is an expected precipitant of landfill leachate, which is a product of calcium from weathered minerals and carbon from putrescible material. The quantity of material stored in landfills, in controlled stockpiles or on land, and the degree to which it has carbonated is unknown but could be a substantial quantity given historic production of the material discussed in this chapter.

3.6.1 Red mud

Approximately 80 Mt of aluminium are produced each year from processing the raw material bauxite (USGS, 2010b), creating a by-product colloquially known as 'red mud'. Approximately 70 Mt a^{-1} of red mud are produced globally (Liu et al., 2007), the chemical composition of which is variable, but the CaO content may be as high as 40 wt%. Because of this, it has been suggested as a mineral carbonation material (Yadav et al., 2010).

3.7 Carbonation strategies

A variety of industrial reactor-based technologies have been proposed for the accelerated exploitation of silicate carbonation. All methods require pre-processing of the silicate material to attain small particle size, and considerable chemical and energy inputs. High temperature/pressure aqueous batch reactors such as those investigated by Huijgen and Comans (2006), are currently seen as the most attainable method, although immobility of the reactive material limits reaction rates. This is partially countered in a process patented by Geerlings (2004), in which silicate fines ($\Phi \leq 0.5$ mm) are reacted with CO_2 in a slurry bubble column. Fluidized bed reactors have also been proposed for use in forced carbonation (Zevenhoven et al., 2006), which would be more energy expensive, but offer a considerably increased rate of reaction.

Carbonates formed in soils (pedogenic) naturally occur as remobilised minerals from the bedrock and precipitate around grains or root hairs (e.g. Goudie, 1996) with zero net carbon reduction from the atmosphere. These features occur at the surface in arid environments, but are reported at depth in a range of soils as a function of rainfall (Jenny, 1941). Biological processes in soils accelerate weathering as a nutrient acquisition mechanism by decreasing pore water pH and releasing organic acids that chelate with cations in the material. Manning (2008) suggests that (providing the weathering rate was sufficiently rapid) mixing calcium/magnesium rich silicate minerals into the soil profile would precipitate carbonate minerals where the carbon is dissolved CO_2 in equilibrium with the soil pore gas, and is supplied by either organic matter degradation or diffusion from the atmosphere. This process has been documented in soils mixed with artificial silicate minerals (Renforth et al., 2009), where isotopic analysis has shown the carbon to be derived from the atmosphere.

Figure 3.8 conceptualises the range of carbonation strategies that are available. Figure 3.8 (A) represents the carbonation strategy for natural silicate outcrops or overburden from underground workings. However, this could apply to any isolated point source of silicates (e.g. blast furnace or rotary kiln). Figure 3.8 (B) represents the carbonation strategies for demolition waste in urban areas, where the waste is transported to a centralised carbonation reactor, or used in soils as part of urban redevelopment.

The potential for direct injection of CO_2 in to natural silicate formations, promoting sub-surface carbonation, has been extensively discussed as a carbon capture and storage mechanism (Kelemen and Matter, 2009; Matter and Keleman, 2009). This may be achieved by delivery of fluid or gaseous CO_2 through a borehole, or pipe network, and may be coupled with additional hydrologically mediated reactions and physical manipulation of the host rock such as pre-fracturing (see Figure 3.8 C).

Injection of CO_2 into waste silicate heaps (likes those described by Wilson et al., 2009) or landfill cells assumes many of the same principles as injection in to natural formations. This process also has the potential to exploit existing site infrastructure including boreholes, gas monitoring wells and leachate management systems. Direct injection techniques reduce the requirement for

preliminary processing and reduce mineral transportation costs, allowing *in situ* treatment at existing waste disposal sites (see Figure 3.8 C).

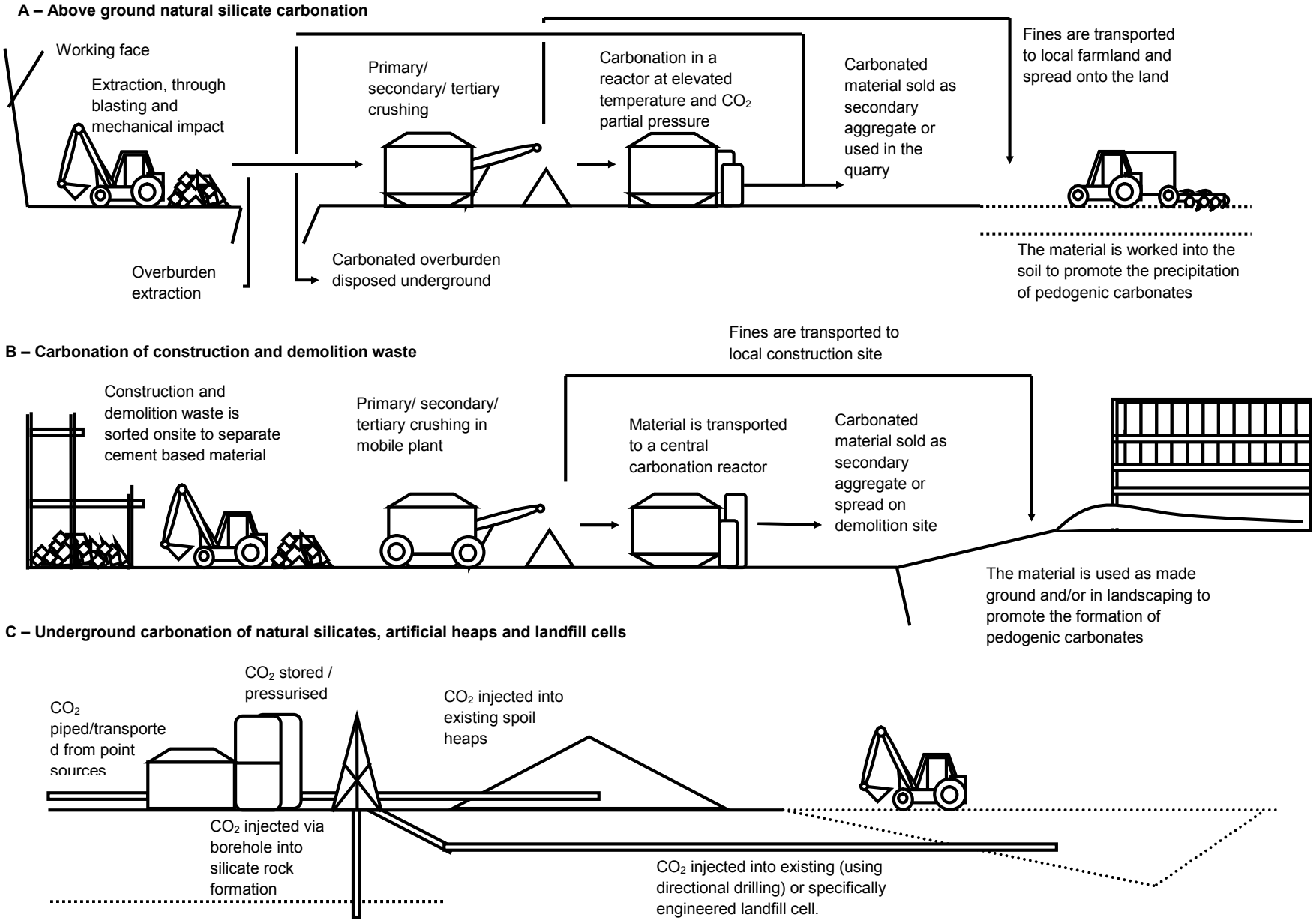

Figure 3.8 – Conceptual summary of mineral carbonation strategies.

3.8 Chapter summary

Globally, the total carbonation potential of waste silicate minerals is 190-332 Mt C a^{-1}, which does not include the carbonation of historically produced material that has been stockpiled or the production of hard rock from mineral excavation (see Table 3.11). This is comparable in potential to other carbon capture and storage technologies (Chadwick et al., 2008), and is equivalent to part of a 'stabilisation wedge' needed by 2050 to prevent atmospheric carbon exceeding 500 ppmv (Pacala and Socolow, 2004). The maximum carbon capture potential of materials historically produced that have been stockpiled is unknown, but could be of the order of 10^3 Mt C. It is likely that some of this material has carbonated in the environment, but a substantial quantity may remain unreacted in landfill cells or stockpiles.

Table 3.11 - Carbon capture potential of various waste materials [1]Based on a population proxy, [2]Lea (1970) pp16, [3]See Table 3.4, [4]Proctor et al. (2000), [5]Environment Agency (2007), [6]van Oss (2009), [7]Shen and Forssberg (2003), [8]Based on an assumed stainless steel to slag ratio similar to steel production [9]Das et al. (2007) (flue dust can be recycled through fluidised bed reactors, carbonation processes are unknown), [10]Russell et al. (2002), [11]Goodarzi, (2006).

Material	Estimated divalent content	Estimated Global Production (Mt a^{-1})	Carbon capture potential (Mt C a^{-1})	Historic production (Mt)
Quarry fines	3% CaO 3% MgO[1]	3,300	130	
Mine tailings	Unknown	2,000-6,500	Unknown	
Cement kiln dust	65[2]	420-468	59-79	9,000-12,000 (since 1926)
Construction waste	14[3]	294-1239[1]	9-37	Maximum limited by cement production around 60 Gt
Demolition waste	10[3]	1,106 – 4,661[1]	24-100	
Blast furnace slag	38% CaO 12% MgO[4]	250-300[6]	53-64	7,900-9,500 (since 1875 – 80% potentially reused)
Steel making slag	45% CaO 7% MgO	130-200[6]	23-35	4,200-6,400 (since 1875)
Stainless steel slag	46% CaO 6% MgO[7]	6.5[8]	0.6	
Blast furnace flue dust/sludge	4.9% CaO[9]	30[f,9]	0.3	
Lignite fly ash	20% CaO 1% MgO	32-61	2-3	7,600-14,600 (since 1927)
Anthracite ash	3% CaO 1% MgO[10]	20-46	0.6	
Bituminous ash	3% CaO 1% MgO[11]	146-278	1-3	
Red Mud	40% CaO 1% MgO	70	6	
Total		15,400	190-332	

The production of slag and cement in a blast furnace and rotary kiln provides a point source of CO_2 which could be captured and stored using conventional carbon capture and storage technologies. The material produced would contain a negative carbon footprint if it was subsequently carbonated (similar, in part, to ocean alkalinity modification; Kheshgi, 1995). Otherwise, the carbonation of waste silicate minerals is only partially closing the loop on the CO_2 emitted during manufacture, at best compensating for decarbonation reactions and not emissions associated with the combustion of fossil fuels. Carbonation of waste is complimentary to carbonation of silicates extracted specifically for carbon capture which has a potential to store ~GtC a^{-1}.

In Table 3.11, the maximum carbonation potential is calculated by assuming that all of the available calcium and/or magnesium in the material is converted to carbonate ($CaCO_3$, $MgCO^3$; 1 mole of cations captures 1 mole of carbon), which is unlikely in practice. Depending on the material, carbonation method and temperature, and pretreatment processes, reported carbonation efficiencies vary from 10 to 60% for untreated natural silicates to 40-90% with heating or mechanical pretreatment.22 Carbonation efficiency of artificial silicates is generally reported >70% without pretreatment. A full review of this technology is beyond the scope of this thesis.

Chapter 4

Chapter 4. Carbonate precipitation in soils

The aim of the research in this chapter is to investigate the prevalence of pedogenic (soil formed) carbonates in artificial soils as unintentionally formed analogues to an engineered soil mineral carbonation technology. Considering this thesis is the first of its kind to investigate anthropogenically mediated pedogenic carbonate formation, it is important to gather, as proof of concept, evidence of this process existing in artificial soils. Therefore, through a range of field investigations and the application of an isotope mixing line hypothesis, the quantity of atmospheric carbon captured in carbonate is presented and the rate of accumulation is interpolated over the known age of the site.

Delivered objective: A review of key literature is presented that discusses broadly pedogenic (soil formed) carbonates, focusing on soils developed on silicate parent material. To distinguish pedogenic from lithogenic carbonates stable isotopes are introduced as a tool for investigating the provenance of the carbonate components (C, O, and Ca).
Delivered objective: The prevalence of atmospheric carbon in the carbonates was quantified through the application of an isotopic mixing line hypothesis.

Delivered objective: The mixing line hypothesis was substantiated through investigations of pedogenic carbonate formation across a climate gradient.

4.1 Carbonate precipitation in natural soils

4.1.1 Field scale morphology

Pedogenic carbonates (also referred to as caliche, calcretes and rhizolith/crete/concretions) are carbonate minerals formed in the soil. They are commonly formed from remobilised carbonate bedrock where there is little net carbon sequestration (the carbon precipitated in pedogenic carbonate is ‘lost’ from bedrock during weathering).Therefore, the origin of carbonate mineral components (metal cations and carbonate anions) is important when considering the effectiveness of carbon capture.

The fieldscale morphology of calcium carbonate is widely documented in arid environments, and is reviewed in Nettleton (1991). The largest single formations of carbonate minerals are referred to as hardpans, which are unbroken strata in the soil, and can be further sub-classified according to size and shape (laminar,

massive, brecciated and nodular). However, carbonate in soil often forms isolated features in a non-carbonate host material and is only visible using microscopic analysis.

Pedogenic carbonates represent a large pool in the terrestrial carbon cycle (748 Gt; see Chapter 2). However, they are poorly documented in soils outside of arid environments. As carbonate precipitation depth is a function of rainfall (see Section 4.7.1 and Figure 4.1), and soil carbon analysis is usually confined to the top meter, 748 GtC is possibly an underestimate.

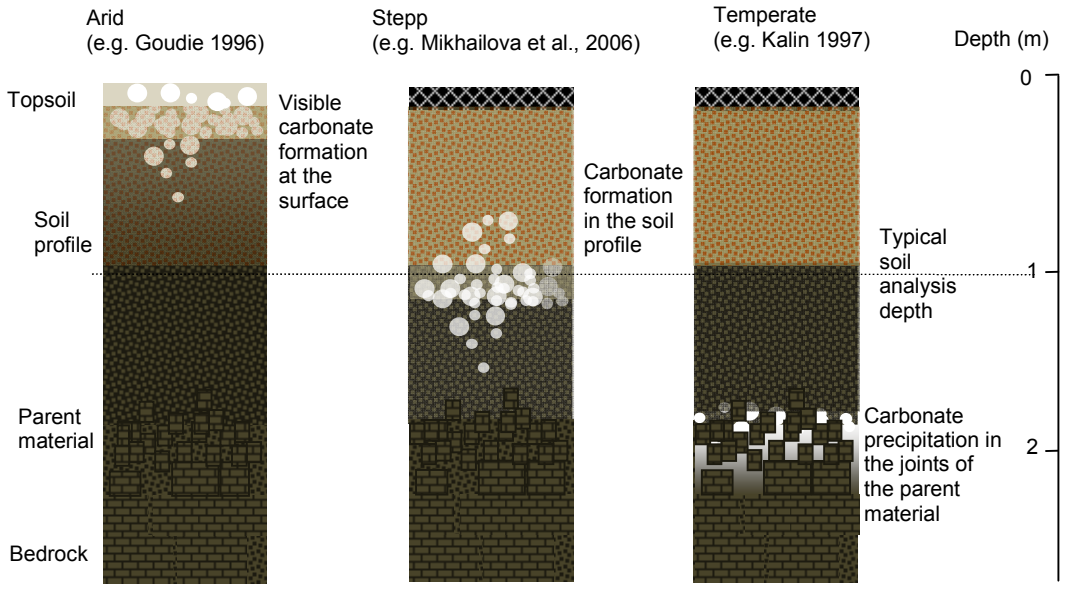

Figure 4.1 – Conceptualisation of carbonate formation depth through a typical soil profile in different climates.

4.1.2 Pedogenic carbonates formed on igneous parent material

Pedogenic carbonate formation has been globally reported on soils with igneous parent materials; the following is a brief review of these studies.

Durand et al. (2007; 2006) document the accumulation of carbonate on the Deccan Traps, an igneous province in South India. The studies investigate carbonate formation within a semi arid climate, which is located in the rain shadow of the Western Ghats mountain range. The climate of the region is said to have been stable for the majority of the past 1.8 million years. The authors discuss the presence of rhizoconcretions and calcified pseudomycelia as an indicator for biologically mediated calcite precipitation. $^{87}Sr/^{86}Sr$ analysis of the calcrete shows a similar signature to that of the local amphibolites which suggests the calcium is derived from insitu weathering.

Kalin et al. (1997) investigates the precipitation of carbonates within the joints of the Antrim Basalts, Northern Ireland. Stable isotope analysis of the carbonates reports unusually light $\delta^{13}C$ values, which the authors interpret to suggest soil CO_2 was the source of carbon in the carbonate, and radiocarbon dating places the formation of the calcite within 31 and 35 Ka before present (BP).

Anand et al. (1997) investigate the formation of calcrete on the Yilgarn Craton, a region in Western Australia dominated by granitic rock, containing hornblende and plagioclase feldspars. This study documents a correlation between the formation of carbonates and the Ca/SiO_2 content of the parent mineral (accumulation was greater on hornblende compared to granite). Dart et al. (2007) investigates the formation of carbonate across several sites in Southern & Western Australia. Investigating the $^{87}Sr/^{86}Sr$ ratios of the carbonates, the authors suggest that only 10 wt% of calcium is derived from the bedrock material and that the majority of the calcium in the carbonate is derived from marine spray and aeolean transport. However, it should be noted that most of the samples were taken within the top 30 cm of the soil profile.

Capo et al. (2000) investigated the occurrence of dolomite ($CaMg(CO_3)_2$) formed on the Kohala peninsula, Hawaii. The authors identify the $^{87}Sr/^{86}Sr$ ratio of carbonates as 0.7045-0.7048 and suggest it is indicative of chemical weathering, in which 90% of the carbonate calcium is derived from the parent material. The authors suggest that dolomite precipitates in non-saline environments, which has important ramifications for understanding the 'dolomite problem' (Arvidson and Mackenzie, 1999).

Knauth et al. (2003) documents the formation of pedogenic carbonates on volcanic lava fields in Arizona, USA. The most recent lava erupted 900 aBP which is the upper layer on a series of lava flows dating back 3 Ma. Although this study presents carbonate with light $\delta^{13}C$ value (indicating organic carbon sequestration) the authors also report unusual heavy fractionation of $\delta^{13}C$ and $\delta^{18}O$ isotopes in carbonate, as a result of rapid evaporation. Furthermore, $^{87}Sr/^{86}Sr$ suggests that approximately 55-67 % of the Ca within the carbonate is derived from insitu weathering of the parent mineral.

Ducloux et al. (1990) investigate the formation of pedogenic carbonate on the Tanecherfi Basin, a granitic region located in north eastern Morocco. The

authors suggest that the granite-calcrete relationship indicates a weathering process rather than superposition. However, chemical analysis of the bedrock indicates minerals such as othoclase feldspars, Na rich plagioclase feldspars and chlorite. Therefore, the origin of the calcium remains unclear.

These studies suggest that carbonate precipitation on igneous rocks is not uncommon in the environment, and is a product of the weathering regime that passively sequesters carbon from the atmosphere. However, carbon and oxygen stable isotope ratio analysis is required to establish the provenance of the carbonate.

4.1.3 Isotopes of carbonates in natural soils

Stable isotope analysis has been used to study carbonates since the 1950s (Craig, 1953) primarily to investigate diagenesis conditions in limestone and the influence of organic carbon during the remobilisation of calcium carbonate in soils (Hudson, 1977).

Isotopes are conventionally measured using mass and charge speciation in a mass spectrometer. The signal is compared to a standard, which in the case of carbonates is a lithogenic marine carbonate Pee Dee Belemnite (PDB), or a proxy Vienna Pee Dee Belemnite (VPDB). Thus an isotope ratio (δ) is calculated in Equation 4.1.

Equation 4.1: $$\delta\,{}^{x}M\ (‰) = \left(\frac{{}^{x}M/{}^{y}M_{Sample}}{{}^{x}M/{}^{y}M_{Standard}} - 1\right) \cdot 10^{3}$$

where x and y are isotopic masses of element M. Carbon has two stable isotope ^{12}C and ^{13}C and oxygen has three ^{16}O, ^{17}O and ^{18}O (the first and last of these are typically used for isotope ratio determination due to the abundance of ^{17}O and mass dependant fractionation difference between ^{17}O and ^{18}O).

Early work by Solomans and Mook (1976) and Cerling (1984) demonstrates the incorporation of organic carbon into pedogenic carbonates which characteristically have isotopic values between -2 ‰ and -10 ‰ and 0 ‰ and -5 ‰ for $\delta^{13}C$ and $\delta^{18}O$ respectively. Similar values have been found in more recent studies from a range of environments (Figure 4.2). Carbonate isotope values are controlled by precipitation conditions, including climate, rainfall, temperature, underlying geology and continentality (Andrews, 2006).

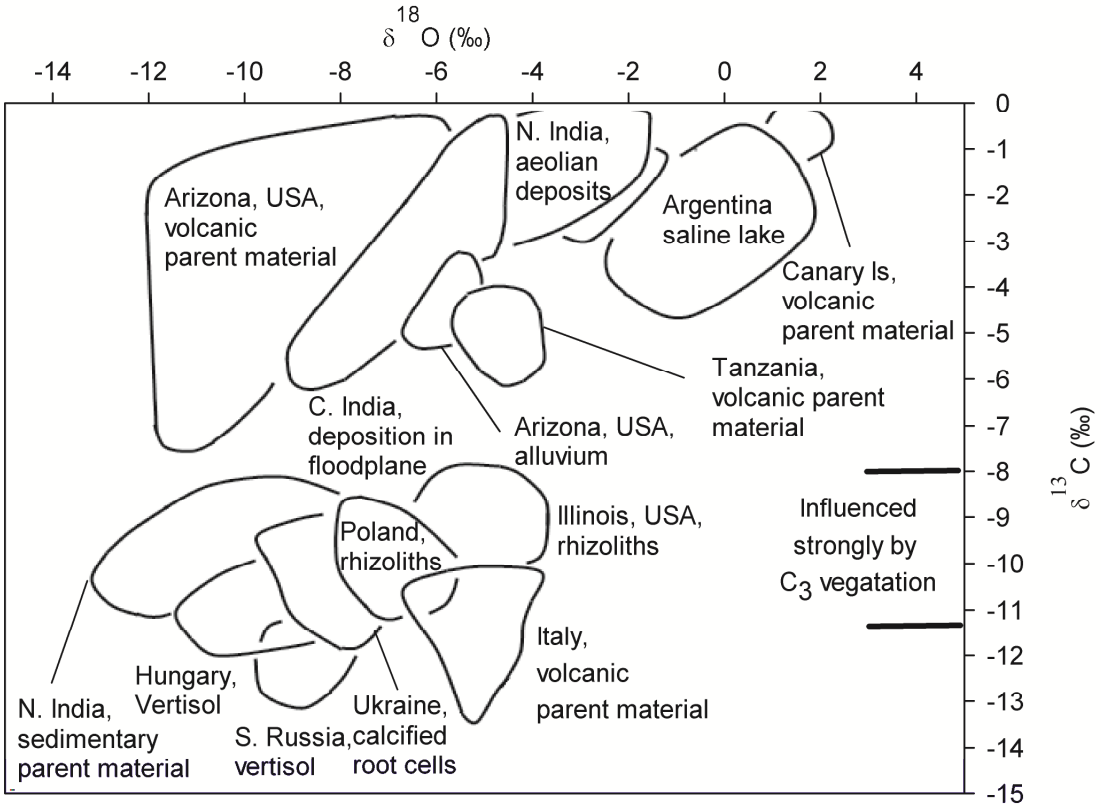

Figure 4.2 – Stable isotopes against PDB in natural pedogenic and tufaceous *carbonates. Source: Renforth et al. (2009) using existing pedogenic carbonate data (Łącka et al., 2008; Yanes et al., 2008; Sikes and Ashley, 2007; Singh et al., 2007; Wang and Greenberg, 2007; Boguckyj et al., 2006; Kovda et al., 2006; Bajnoczi et al., 2005; Zanchetta et al., 2000; Salomons and Mook, 1976).*

In Figure 4.2, the expected range of $\delta^{13}C$ values is shown for carbonates formed under the influence of C_3 vegetation (a photosynthetic carbon fixation pathway, which results in the depletion of ^{13}C compared to C_4 plants). Several studies fall within this range (Łącka et al., 2008; Singh et al., 2007; Wang and Greenberg, 2007; Boguckyj et al., 2006; Kovda et al., 2006; Bajnoczi et al., 2005; Zanchetta et al., 2000; Salomons and Mook, 1976). Organic carbon is typically reported with a $\delta^{13}C$ isotope ratio of -27 ‰ for C_3 plants, -13 ‰ for C_4 plants, and crassulacean acid metabolism falling in between (Cerling, 1984; and references therein). Zhang et al. (1995) and Turner (1982) describe the fractionation between precipitated carbonate, carbonate ions and CO_2 gas in solution, summarised by the fractionation factors (ε) in Equations 4.2-4.4

Equation 4.2: $$\varepsilon_{HCO_3-CO_2} = -(0.141 \pm 0.003)T(°C) + (10.78 \pm 0.05)‰$$

Equation 4.3: $$\varepsilon_{CO_3-CO_2} = -(0.052 \pm 0.03)T(°C) + (7.22 \pm 0.46)‰$$

Equation 4.4: $$\varepsilon_{HCO_3-Calcite} = -(1.83 \pm 0.32)‰ \ to \ (-2.26 \pm 0.31)‰$$

Therefore, C_3 and C_4 organic carbon are predicted to obtain a $\delta^{13}C$ value of approximately -10 and -3 ‰ respectively at 25 °C, when degraded to CO_2 and precipitated as carbonate, which is consistent with measured values from field investigations (Figure 4.2).

According to Andrews (2006) there is a general decrease in $\delta^{18}O$ with increasing continentality, caused by depletion of ^{18}O in meteoric water (e.g. Kendall and Coplen, 2001) and related to precipitated carbonate through Equation 4.5.

Equation 4.5: $$\delta^{18}O_{CaCO_3} = \frac{1}{3}\delta^{18}O_{H_2O} + \frac{2}{3}\delta^{18}O_{CO_2}$$

where $\delta^{18}O_{H_2O}$ (from meteoric water) ≈ -35 to -50 ‰ and $\delta^{18}O_{CO_2}$ (from the atmosphere) ≈ 8 ‰, results in a $\delta^{18}O_{CaCO_3}$ ≈ -6 to -12 ‰.

Several studies (Łącka et al., 2008; Singh et al., 2007; Wang and Greenberg, 2007; Bajnoczi et al., 2005) record the occurrence of rhizoliths, which are carbonates formed within close proximity to plant roots, the isotopic signature of which is dominated by $\delta^{13}C$ from organic carbon.

Carbon within natural pedogenic carbonates is usually a combination of that which is derived from organic carbon, and remobilisation of lithogenic carbonates. Pedogenic carbonates formed under these influences will return an isotopic signature which is between the organically-dominated region and the lithogenically-dominated region contiguous with $\delta^{13}C$ = 0 ‰, which is demonstrated in the bimodal histogram in Figure 4.3 (Hudson, 1977). However, the use of carbon and oxygen isotope ratio data to determine host geology is potentially ambiguous, demonstrated by Zanchetta et al. (2000), Sikes and Ashley (2007) and Yanes et al. (2008), who independently report differing values for carbonates formed in soils on igneous parent rocks (Figure 4.2).

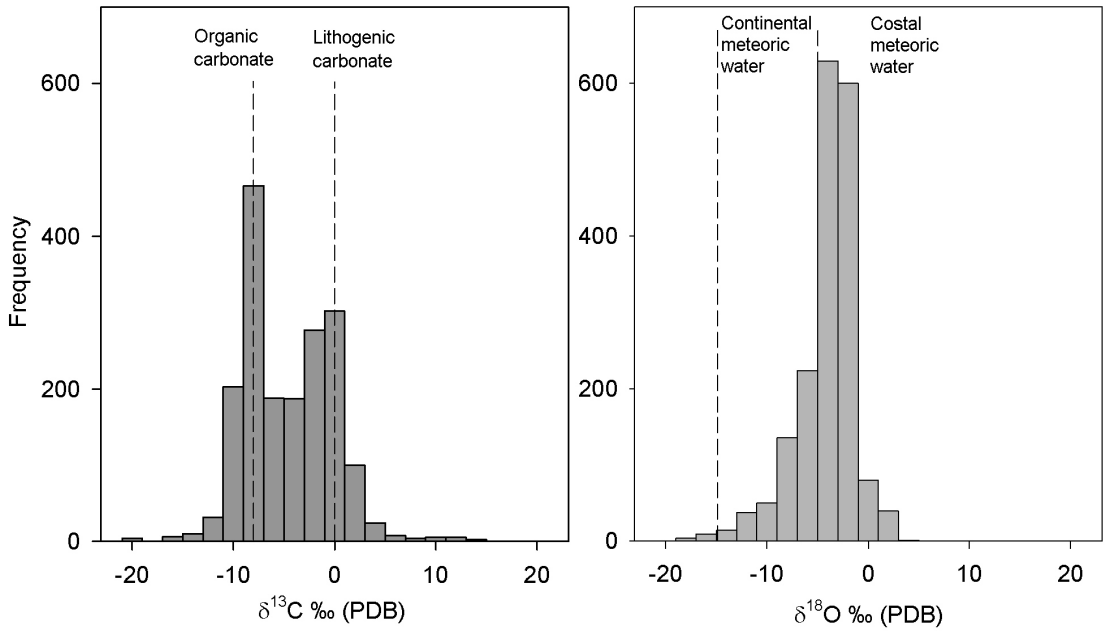

Figure 4.3 – Frequency distribution of carbonate isotope data in Figure 4.2.

4.1.4 Biological formation of calcium carbonate

Calcium carbonate is biologically produced within nature for skeletal material or to isolate parasites as seen in some *Pteriidae*. The biological mediation of calcium carbonate outside of an organism is the least understood mechanism of calcite precipitation and is suggested to be the result of a range of activities including microbial CO_2 degassing from solution or Ca released by sulphate reducing bacteria (Goudie, 1996). Ferris et al. (1994) investigate the formation of calcite on cyanobacteria. Their work suggests that bacteria both induce weathering of calcium/magnesium silicates and act as nucleation sites for carbonate growth.

Bacillus pasteurii has been shown to induce carbonate precipitation by releasing urease (DeJong et al., 2006; Bachmeier et al., 2002; Stocks-Fischer et al., 1999) which breaks down urea to produce CO_2 and ammonia (Equation 4.6), and in solution protonates to form ammonium and hydroxide (Equation 4.7). The increase of pH pushes the equilibrium in Equation 4.8 to the right and precipitates calcium carbonate on the surface of cells, which act as nucleation sites.

Equation 4.6: $$(NH_2)_2CO + H_2O \xrightarrow{urease} CO_2 + 2NH_3$$

Equation 4.7: $$NH_3 + H_2O \leftrightarrow NH_4^+ + OH^-$$

Equation 4.8: $$Cell - Ca^{2+} + CO_3^{2-} \leftrightarrow Cell - CaCO_3$$

The formation of calcium carbonate within the rhizosphere of plants has been documented in arid regions (Goudie, 1996) and is thought to be common in calcareous soils (Cailleau et al., 2004; Jaillard et al., 1991). Cailleau et al. (2004) document the accumulation of carbonate mediated by the tree *Milicia excelsa* on soils with granite parent material, and suggest the carbonate formation is a function of organic compound exudation. However, the formation mechanisms remain poorly understood.

Microscopic analysis by Verrecchia and Verrecchia (1994) highlight the importance of cells and fungal hyphae in needle fibre calcite formations. Similar, albeit larger, rhizolith structures were observed by Wang and Greenberg (2007), which are common at the surface in arid environments. The evolutionary reason for biological precipitation of carbonate is unclear (Verrecchia and Verrecchia, 1994).

The inclusion of organic-derived carbon in carbonates has been established with isotope ratio mass spectrometry, but the rate at which carbonate accumulation occurs is unknown as is the potential to accelerate carbonation. Fieldwork was undertaken in soils developed on natural silicates to investigate this further.

4.2 Investigation of the Whin Sill, Northumberland

4.2.1 Barrasford Quarry – Site description, methodology and results

Barrasford Quarry, Northumberland, UK (NY908874) is operated by Tarmac Ltd, who primarily extract dolerite from the Whin Sill to be used for construction aggregate. The Whin Sill is an igneous complex intruded between Carboniferous strata 295 MaBP, comprising numerous sills and dykes. It is estimated that 5000 km^2 of igneous intrusion underlies the region with approximate thickness of 25-30 m (Taylor et al., 1971).

In 2003 Mineral Solutions Ltd. created artificial soil plot experiments at Barrasford quarry to investigate alternative disposal routes and potential alternative fertilizers from waste quarry materials (Plate 4.1; Mineral Solutions, 2004). The plots were a mixture of Barrasford quarry dolerite or Craighouse

quarry (NT600936) basalt, with compost. The chemical composition of the dolerite and basalt are presented in Table 4.1, and the composition of the plots is presented in Table 4.2.

Table 4.1 – Chemical composition (wt%) of the Barrasford quarry dolerite (D) and Craighouse quarry basalt (B) used in artificial soil plots. Source: Mineral Solutions (2004).

	SiO_2	TiO_2	Al_2O_3	Fe_2O_3	MnO	MgO	CaO	Na_2O	K_2O	P_2O_5	SO_3	LOI	Total
D	45.53	1.85	12.79	11.39	0.15	4.54	13.24	3.10	0.91	0.40	0.43	4.90	99.24
B	44.88	3.30	13.05	14.97	0.18	7.13	7.70	3.34	1.42	1.10	0.10	2.54	99.71

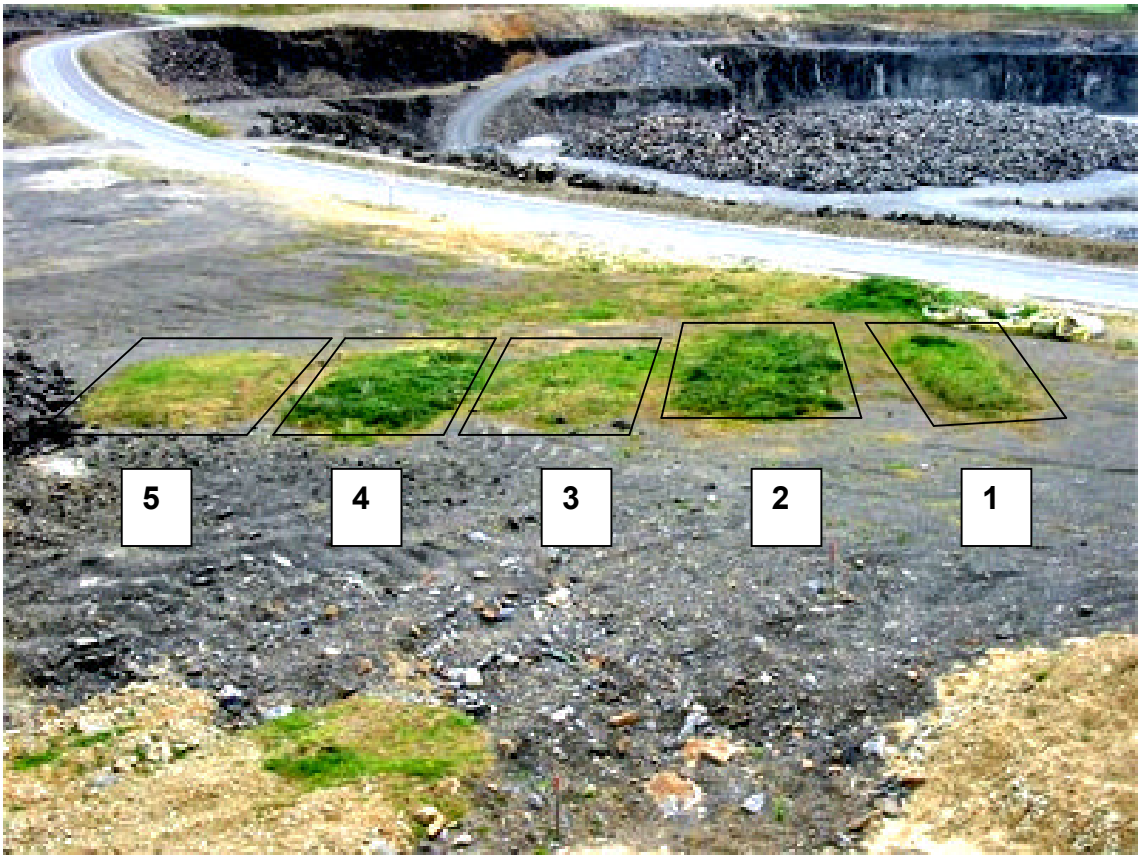

Plate 4.1 – Artificial soil plots at Barrasford Quarry (taken by David Manning October 2007).

*Table 4.2 – Chemistry of the artificial soil plots at Barrasford Quarry. Adapted from Mineral Solutions.*Material composition is a mix of dolerite (D) basalt (B) anaerobically digested compost (AD) or composted food industry waste (FI) **Estimated assuming LOI during XRF analysis of the dolerite and basalt is wholly from carbonate.*

Parameter	Plot 1	Plot 2	Plot 3	Plot 4	Plot 5
Description (see caption)*	D+AD	D+FI	B+AD	B+FI	D
Organic carbon content (wt%)	4.55	6.93	1.15	3.65	~0
Inorganic carbon content (wt%)**	0.79	0.79	0.50	0.50	1.34
CaO (wt%)	7.76	7.76	5.6	5.6	13.24

In October 2007 and 2008 soil samples were removed from the plots, air dried, sieved to passing 2 mm, and analysed for carbonate mineral accumulation (expressed here as inorganic carbon) using an Eijkelkamp calcimeter (Appendix A.1), the results of which are presented in Figure 4.4.

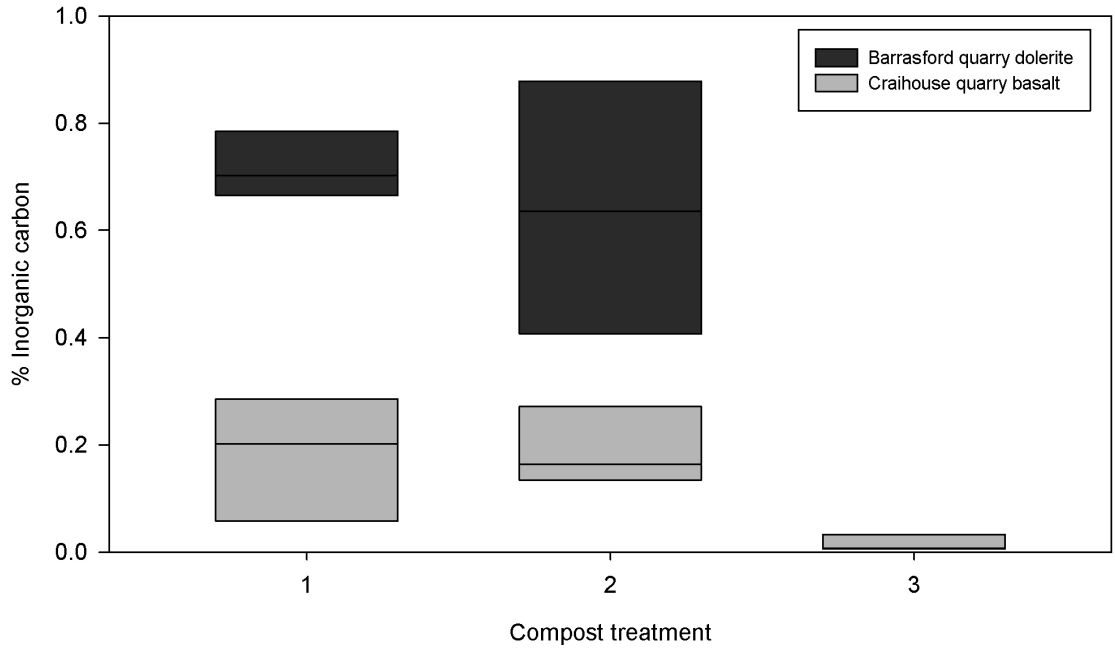

Figure 4.4 – Carbonate content of the Barrasford quarry soil plots. (1) represents the anaerobically digested compost, (2) food industry waste compost, (3) control plot with no compost. 3 samples were measured in each plot.

The compost treated plots contained significantly more ($P<0.001$) inorganic carbon (0.18 to 0.89 %) than the control (0.02 %). Stable carbon and oxygen isotope analysis conducted by Iso-Analytical Ltd. (see Appendix A.3) confirmed the inclusion of organic carbon in the carbonate matrix but suggested contamination from local lithogenic sources (Figure 4.5).

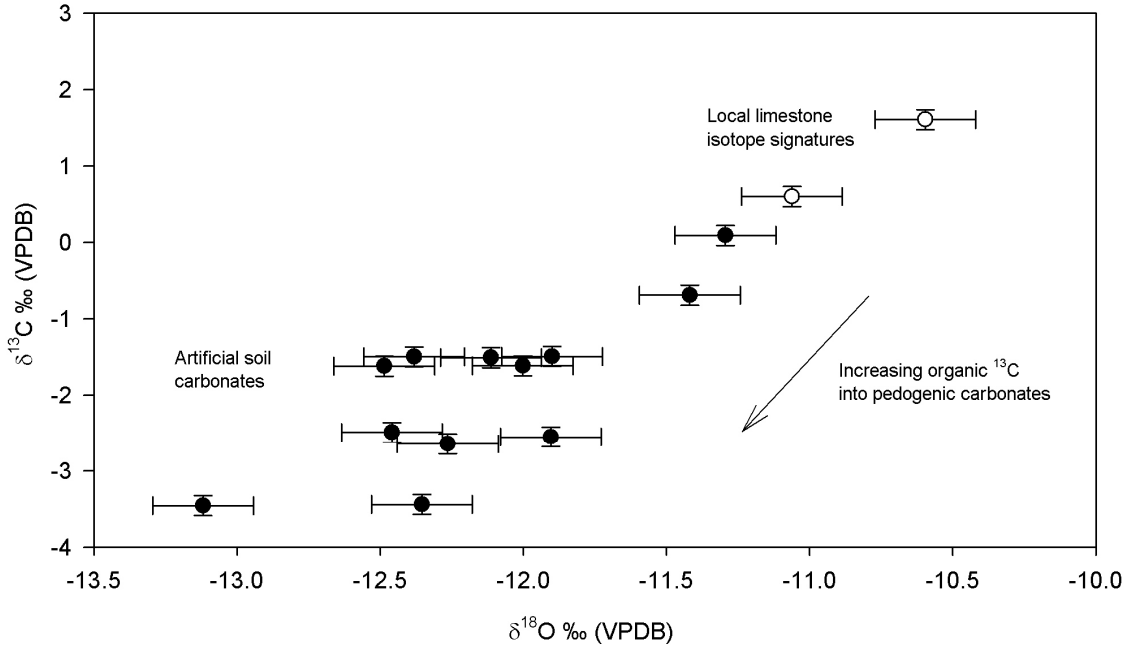

Figure 4.5 – $\delta^{13}C$ and $\delta^{18}O$ isotope ratios of pedogenic carbonates in Barrasford quarry artificial soils.

Assuming the isotope data fit on a mixing line between lithogenic ($\delta^{13}C$ = 1.1 ‰; the average of the two limestone samples) and organic (~$\delta^{13}C$ = 10 ‰; see above) end members, it is estimated between 9.1 and 41.5 % of the carbonate carbon is from organic sources. However, the isotopic fractionation during weathering of the pre-existing carbonate in the plots has not been established (e.g. Skidmore et al., 2004).

$^{87}Sr/^{86}Sr$ ratios were determined by Macaulay Scientific Consulting Ltd. Aberdeen, using thermal ionisation mass spectrometry of HF digested silicates or HCl digested carbonates. $^{87}Sr/^{86}Sr$ of the carbonates varied between 0.7090 - 0.7097, which was between the $^{87}Sr/^{86}Sr$ ratios of dolerite and local limestone samples (0.7062 and 0.7107 respectively). Assuming a mixing line between the two end members, approximately 62-78% of the carbonate calcium is derived from the dolerite.

The discrepancy between the quantity of calcium and carbon derived from lithogenic sources suggests that lithogenic carbon was re-precipitated in the soil with calcium from the weathered silicate, and the lithogenic calcium was leached out of the profile or taken up by biota (Figure 4.6).

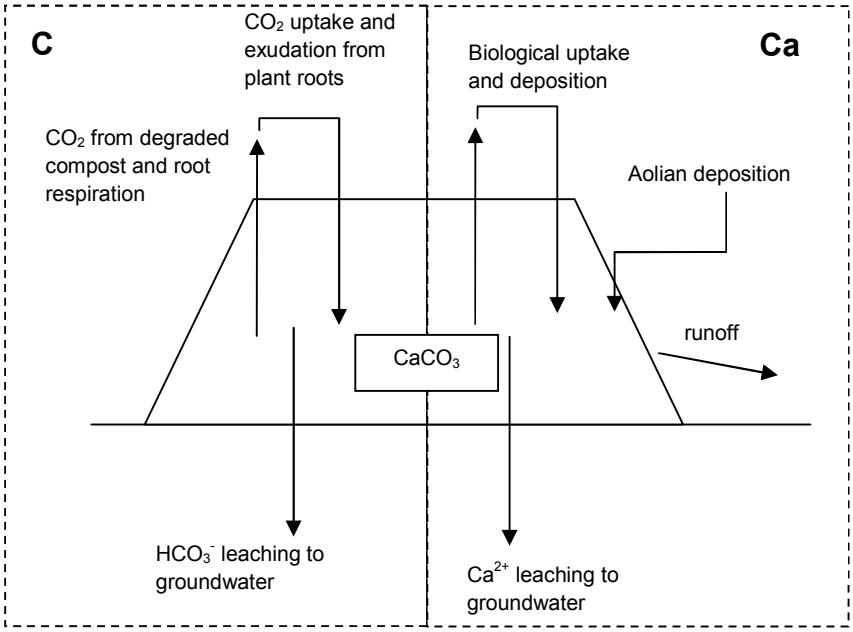

Figure 4.6 – Conceptual model of carbon and calcium dynamics in the Barrasford quarry soil plots.

4.2.2 Barrasford quarry – Discussion

The carbonate and stable isotope analyses suggest that organic carbon (most likely from the compost) has been mineralised and precipitated as calcium carbonate. Approximately 900 mgC kg^{-1}(soil) a^{-1} were removed from the atmosphere. The lack of carbonate in the control suggests that saturation has not been achieved either through lack of weathering or supply of HCO_3^- mediated by the decaying compost in the other trials, and any pre-existing carbonate minerals were weathered out of the plot. Other field investigations of soils developed on the Whin Sill (presented in full in Appendix B.1.2) did not detect the presence of mineral carbonate, which may be explained by carbonate precipitating lower in the profile between the joints in the parent material (e.g. Kalin (1997) and consistent with rainfall gradient in Jenny (1941)) or the lack of organic carbon (as a source of HCO_3^-) which is required to enhance weathering and/or saturate the soil solution with respect to calcium carbonate. The results from Barrasford quarry demonstrate that atmospheric carbon has been unintentionally sequestered as a carbonate on human relevant time scales. However, additional work is required for verification due to the presence of lithogenic carbonate.

4.3 Carbonate precipitation in artificial environments

4.3.1 Morphology of carbonate precipitation in artificial environments

Carbonate precipitation is commonly reported during the weathering of artificial silicate minerals, and may occur as hardpans similar to that detailed by Mayes et al. (2006) in the drainage regime of slag heaps, as speleothem type features on the underside of historic concrete bridges (Krishnamurthy et al., 2003; Macleod et al., 1991), or as a thin layer on the surface of concrete exposed to the atmosphere (Severinghaus et al., 1994).

4.3.2 Isotopes of carbonates in artificial environments

Isotopic analysis of carbonates formed in anthropogenic environments is used to investigate formation conditions or the provenance of the elemental components. Macleod et al. (1991), Dietzel et al. (1992), Krishnamurthy et al. (2003), and Andrews et al. (1997) have investigated the formation of carbonates in alkaline environments associated with concrete and attribute the observed negative isotopic signatures to kinetic fractionation when dissolved CO_2 reacts rapidly with hydroxide ions (from portlandite dissolution) to precipitate carbonate through Equation 4.9.

Equation 4.9: $Ca(OH)_2 + CO_{2(aq)} \leftrightarrow Ca^{2+} + 2OH^- + CO_{2(aq)} \leftrightarrow CaCO_3 + H_2O$

ΔG_r = -74.3 kJ mol^{-1}

Equation 4.10: $$CO_{2(aq)} + OH^- \overset{k}{\Leftrightarrow} HCO_3^-$$

Equation 4.11: $$r = C_0(D \cdot k \cdot [OH^-])^{0.5}$$

where k is the rate constant (cm^3 mol^{-1} s^{-1}) for hydroxylation of CO_2 (Equation 4.10; Pinsent et al., 1956). The rate of hydroxylation is governed by Equation 4.11 (Usdowski and Hoefs, 1986), D is the diffusion coefficient of CO_2 through the liquid and C_0 is the concentration CO_2 in solution. The isotope fractionation factor between CO_2 gas and precipitated $CaCO_3$ is calculated using Equation 4.12.

Equation 4.12: $$\frac{(^{13}C/^{12}C)_{CaCO_3}}{(^{13}C/^{12}C)_{CO_{2(g)}}} \cdot \frac{\alpha_b \cdot \alpha_s}{\alpha_f} = \left(\frac{^{13}D \cdot ^{13}k}{^{12}D \cdot ^{12}k}\right)$$

Equation 4.13: $\varepsilon_{i-j} = 10^3(\alpha_{i-j} - 1)$

where α_b α_s and α_f are fractionation factors for HCO_3-$CO_{2(g)}$, $CO_{2(aq)}$-$CO_{2(g)}$ and $CO_{2(g)}$-$CaCO_3$ respectively (where the fractionation factor ε between molecules i and j is related to α through Equation 4.13). Usdowski and Hoefs (1986) use α_b α_s and α_f values of 1.00874, 0.99889 and 0.98918 respectively and measured values of $\delta^{13}C_{CaCO_3}$ and $\delta^{13}C_{CO_{2(g)}}$ of -25.3 ‰ and -7 ‰ respectively to determine the fractionation factor of calcite precipitation in hydroxide solutions (Equation 4.14).

Equation 4.14: $\varepsilon_{CO_{2(g)}-CaCO_3(hydroxylation)} = -19.5\ ‰ = -0.7\ ‰(\text{diffusion}) - 18.8\ ‰\ (\text{hydroxylation})$

The log rate of hydroxylation (-4.1 moles cm^{-2} sec^{-1}) is an order of magnitude slower than diffusion of CO_2 into solution (-3.3 mol cm^{-2} sec^{-1}; Clark et al., 1992), and exerts the greatest influence on isotopic fractionation in high pH solutions (Dietzel et al., 1992; Usdowski and Hoefs, 1986), when pH>11.5 (Figure 4.7).

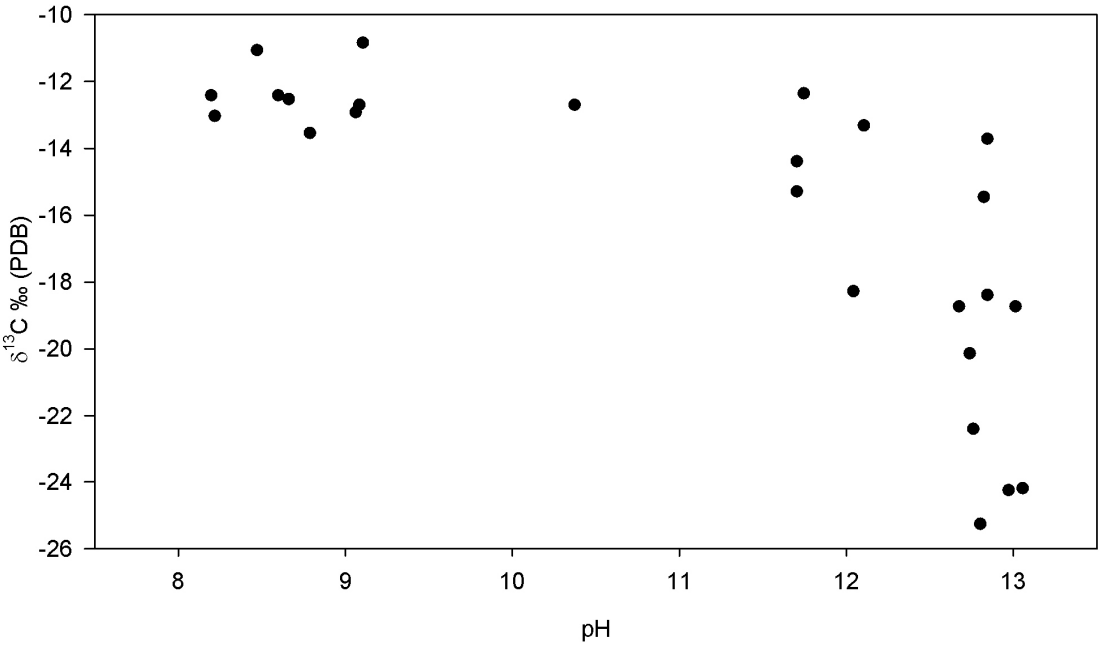

Figure 4.7 – Carbon isotope composition of carbonates as a function of pH. Source: Dietzel et al. (1992).

The carbonate mineral $\delta^{18}O$ in high pH solutions is a mixture of $\delta^{18}O$ produced from the fractionation between hydroxide and meteoric water, and atmospheric CO_2 according to (Dietzel et al., 1992; Létolle et al., 1990; Usdowski and Hoefs, 1986) Equations 4.15 and 4.16.

Equation 4.15: $$\delta^{18}O_{CaCO_3} = \frac{1}{3}\delta^{18}O_{OH^-} + \frac{2}{3}\delta^{18}O_{CO_2}$$

Equation 4.16: $$\varepsilon_{OH^- - H_2O} = -42\ ‰$$

This is generally consistent with the minimum isotope values reported in the literature (Table 4.3). Additional explanation of oxygen isotope fractionation is beyond the scope of this study.

*Table 4.3 – Measured $\delta^{18}O$ of carbonates and those predicted from $\varepsilon_{OH^-H_2O}$ *Kendall and Coplen (2001), **Tyler et al, (2007), †Sattler et al (2005) $\delta^{18}O_{CO2}$ = 9.7‰ (PDB) (Garlick, 1969).*

Study	Measured carbonate $\delta^{18}O$ (‰) PDB	Location	Meteoric water $\delta^{18}O$ (‰) PDB	Carbonate $\delta^{18}O$ (‰) PDB predicted from Equation 4.15
Andrews (1997)	-13.9 to-10.0	UK - Wales	-36	-19.5
O'Neil and Barnes (1971)	-19.9 to -4.0	California - USA	-37*	-19.8
Krishnamurphy et al (2003)	-18.0 to -15.3	Michigan, & New York, USA	-39 Michigan* -37 New York*	-20.5 to -19.8
Macleod et al (1991)	-21.8 to-14.0	UK - Scotland	-42**	-21.5
Clark et al (1992)	-16.9 to -14.0	Oman	-36†	-19.5
Fléhoc et al (2006)	-14.6 to -8.9	Paris - France	-35 to -38	-19.2 to -20.2
van Strydonck et al (1989)	-23.3 to -3.1	Brussels - Belgium	-37	-19.8
Kosednar-Legenstein et al (2008)	-25.8 to -2.6	Various - Austria	-39	-20.5

The influence of atmospheric carbon and $\varepsilon_{OH\text{-}H_2O}$ in Equations 4.15 and 4.16 reduces the effect of $\delta^{18}O$ in meteoric water, so that a natural meteoric water variation between -50 and -35 ‰ will precipitate carbonates in high pH solutions with $\delta^{18}O_{CaCO_3}$ between -24 and -19 ‰. Figure 4.9 presents isotopic data for carbonates formed in anthropogenic environments. Hydroxylation of CO_2 produces carbonate with an isotopic signature of $\delta^{18}O \approx -20$, $\delta^{13}C \approx -26.5$ ‰. It is clear from Figure 4.8 that there are a number of values more negative than hydroxylation alone suggesting additional fractionation processes.

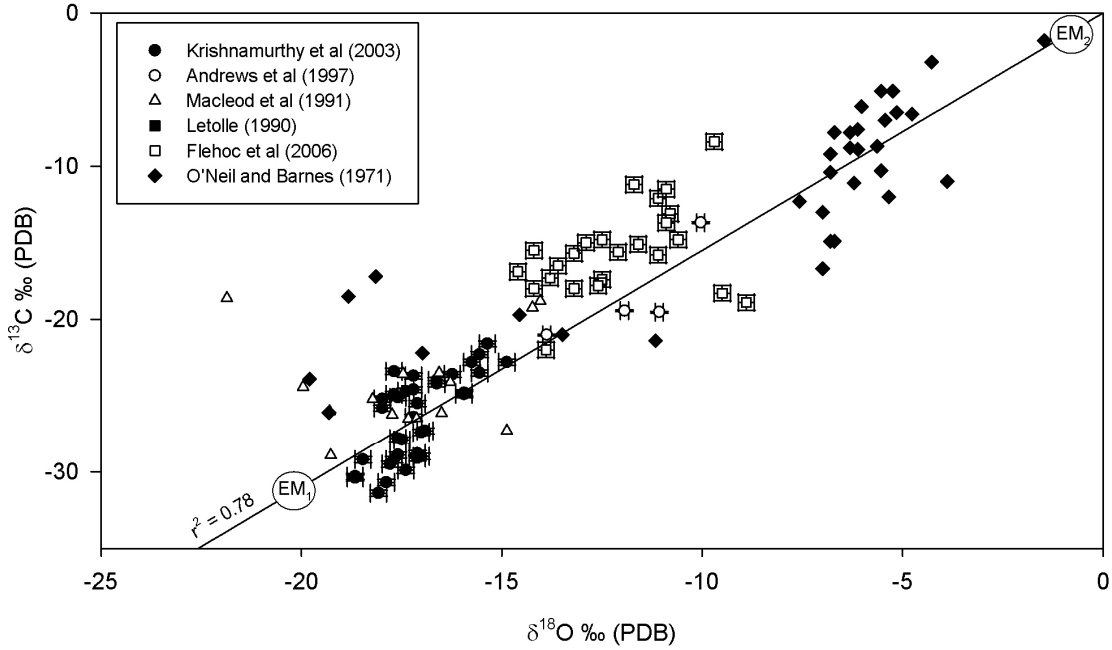

Figure 4.8 – Mixing line: Carbonate isotopic signatures in high pH environments. EM_1 and EM_2 are typical end members for high pH solutions and lithogenic carbonates respectively. Repeatability error bars are shown where given in the literature.

A recent investigation by Wilson et al. (in press) has confirmed the hypothesis by O'Neil and Barnes (1971) which suggests that there is an isotopic fractionation (α_d) governed by Graham's law (Equation 4.17) when carbonate precipitation rate exceeds the rate of diffusion of CO_2 into solution (Figure 4.9).

Equation 4.17: $$\alpha_d = \sqrt{\frac{m_2}{m_1}} = \sqrt{\frac{m^{12}CO_2}{m^{13}CO_2}} = 0.9888$$

Equation 4.18: $$\varepsilon_{CO_{2(g)}-CO_{2(aq)}} = -11.2‰$$

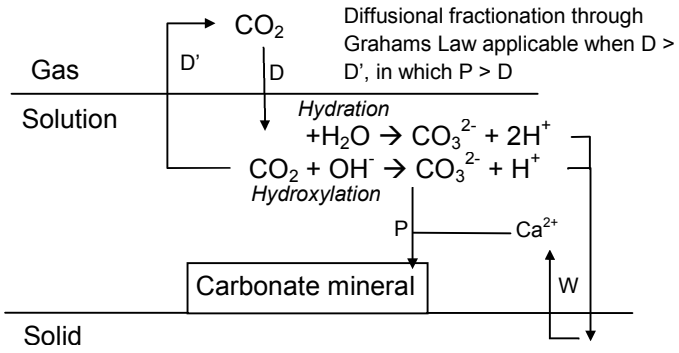

Figure 4.9 – Conceptualisation of diffusional and hydroxylation isotopic fractionation.

If $\delta^{13}C_{CO_2} \approx -8$ ‰, the total fractionation due to diffusion is $\varepsilon_{CO_{2(g)}\text{-}CaCO_3\,(diffusion)} = -21$ ‰ (taking into account an approximate $\varepsilon_{HCO_3\text{-}CaCO_3} = -2$ ‰, see Equation 4.3). The log CO_2 diffusion rate is approximately -3.3 mol cm^{-2} sec^{-1} (Clark et al., 1992; see Table 4.4), which carbonate precipitation rate can theoretically exceed when saturation is greater than 6.7. This was calculated from a mechanistic precipitation model (see Chapter 5 and Inskeep and Bloom, 1985), and assuming a 1:1 solution surface area to volume which is appropriate in the thin film model (e.g. Clark et al., 1992; Usdowski and Hoefs, 1986). Wilson et al. (in press) record a decrease in DIC which they attribute to the discrepancy between precipitation rate and dissolution rate. The precipitation rate will subsequently decrease until it is in equilibrium with CO_2 dissolution, at which point the fractionation factor (Equation 4.17) no longer applies.

Table 4.4 – Typical reaction rates for reaction steps to carbonate precipitation.

Reaction		Log turnover (mol cm^{-2} or cm^{-3} sec^{-1})	Source
Equation 4.19:	$CO_{2(g)} \rightarrow CO_{2(aq)}$	-3.3	Clark et al. (1992)
Equation 4.20:	$CO_{2(aq)} + OH^- \rightarrow HCO_3^-$	-4.1	Pinsent et al. (1956)
Equation 4.21:	$CO_{2(aq)} + H_2O \rightarrow H_2CO_3$	-2.4	Gibbons and Edsall (1963)
Equation 4.22:	$Ca^{2+} + CO_3^{2-} \rightarrow CaCO_3$	-3 for saturation of 6.8, -2 for saturation 8	see Inskeep and Bloom (1985)

It is possible that hydroxylation and diffusion fractionation occur simultaneously in solution where the resultant isotopic signature is a function of the quotient between rates (Equation 4.23), although there is no experimental work to support this.

Equation 4.23:

$$\varepsilon_{CO_{2(g)-CaCO3\,(combined)}} = \left(\varepsilon_{CO_{2(g)}-CaCO_{3\,(diffusion)}}\right) + \frac{k^H}{k^D}\left(\varepsilon_{CO_{2(g)}-CO_{2(aq)\,(diffusion)}} + \varepsilon HCO3{-}CaCO3\,(hydroxylation)\right.$$

The first bracketed term of Equation 4.23 represents diffusion fractionation and the second represents hydroxylation of the diffused CO_2. k^H and k^D are the rates of hydroxylation and diffusion respectively. This produces a carbon isotope fractionation of approximately $\varepsilon_{CO_{2(g)}\text{-}CaCO_3\,(combined)} = -34$ ‰. As hydroxylation supersedes diffusion as the primary CO_2 reaction mechanism (effectively k^H/k^D

→1) it is possible that the precipitated carbonate will be enriched in ^{12}C with a maximum fractionation factor of $\varepsilon_{CO_{2(g)}\text{-}CaCO_3\ (\text{hydroxylation following diffusion})}$ = -47 ‰. The conditions in which this fractionation applies are short lived, as dissolved CO_2 regains equilibrium with atmospheric CO_2, but may explain $\delta^{13}C$ values <-34 ‰.

A recent paper by Dietzel et al. (2009) explores the effect of precipitation rate and temperature on the fractionation of $\delta^{18}O$. Through laboratory precipitation experiments, the authors present a negative linear trend with log precipitation rate (R) for pH = 9.0 (Equation 4.24).

Equation 4.24: $$\varepsilon_{Calcite-H_2O} = -3.376 \cdot Log\ R + 33.17$$

where R is the precipitation rate in μmol m^{-2} $hour^{-1}$. A log precipitation rate of -3.3 mol cm^{-2} sec^{-1} would result in a $\varepsilon_{Calcite\text{-}H_2O}$ = -1.5 ‰. Note that the precipitation rates in the experiments of Dietzel et al. (2009) were several orders of magnitude slower at lower solution pH than discussed in this chapter. It is possible that the fractionation factor in high pH solutions is more negative than -1.5 ‰. However, such extreme fractionation is inconsistent with the majority of data from fieldwork analysis.

Summarising the mechanisms above, Table 4.5 presents possible carbonate isotope signatures.

Table 4.5 – Estimated isotopic composition of carbonates in artificial soils (against PDB).

	Mechanism	**$\delta^{13}C_{CaCO_3}$ (‰)**	**$\delta^{18}O_{CaCO_3}$ (‰)**
1	Lithogenic carbonate in soil	0	~0 to -10
2	Organic carbon degraded and precipitated as carbonate	-8 to-11	~equilibrium with meteoric water
3	Atmospheric CO_2 hydroxylated and precipitated as carbonate	-27	-20.3
4	CO_2 in soil gas diffusion fractionation due to precipitation rate	-22	~equilibrium with meteoric water
5	Mechanisms 3 and 4 operating simultaneously	-34	-
6	Mechanism 4 or 5 replaced by 3	-47	-

A confined range of values for $\delta^{18}O$ and $\delta^{13}C$ for hydroxylated/diffusional CO_2 carbonates, together with a consistent lithogenic/atmospheric carbonate end

member ($\delta^{18}O$ = 0 ‰, $\delta^{13}C$ =0 ‰; EM_2 Figure 4.9), is responsible for producing a strong linear trend (r^2 = 0.78) or 'mixing line' where the proximity to each end member reflects its contribution (e.g. Renforth et al., 2009; Kosednar-Legenstein et al., 2008; Andrews et al., 1997), which was confirmed experimentally by Létolle et al. (1990) and Pachiaudi et al. (1986). Therefore, the isotopic composition of a carbonate formed in artificial environments is summarised in Figure 4.10.

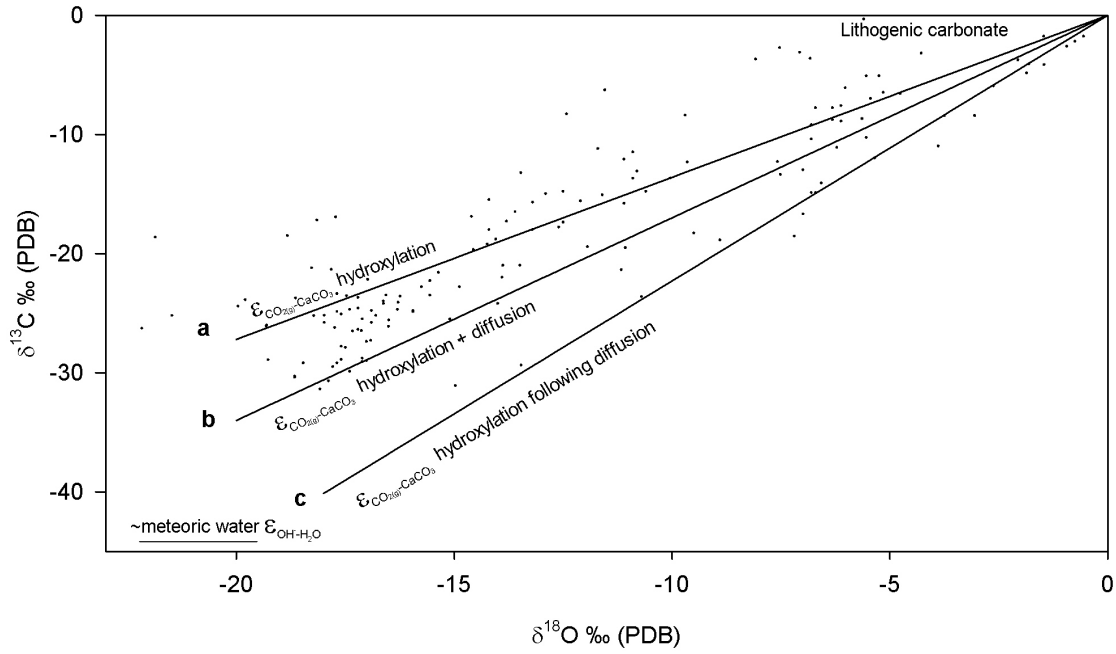

Figure 4.10 – Summary of carbonate isotope data formed in high pH solution or CO_2 limited environments. The lines represent a mixing line between (a) hydroxylation (b) hydroxylation and diffusion (c) hydroxylation following diffusion, and lithogenic carbonate end members

The Pee Dee Belemnite (PDB) standard was originally chosen because of its unusually heavy $^{13}C/^{12}C$ isotopic ratio. It is common to record variable isotopic composition in lithogenic carbonates (Hudson, 1977). Therefore, at first it may seem paradoxical that a mixing line for carbonates from a range of sites regresses linearly through the origin. However, the law of large numbers may be invoked to explain this where the average carbonate isotopic signature is close to the origin (Hudson, 1977). Additional work is required to understand the effect of variable lithogenic carbonate isotopic signatures on the mixing lines in Figure 4.10, which is beyond the scope of this thesis.

Dotsika et al. (2009), Kosednar-Legenstein et al. (2008) and van Strydonck et al. (1989) investigate the isotopic signature of carbonates formed in a mortar matrix. The results of these studies describe carbonates that are relatively enriched in ^{13}C (Figure 4.11) compared to Figure 4.10. van Strydonck et al. (1989) attribute this to a closed or partially closed system through the depth of the mortar resulting in an approximate +10 ‰ increase in $\delta^{13}C$ but with no discernable change in $\delta^{18}O$ values.

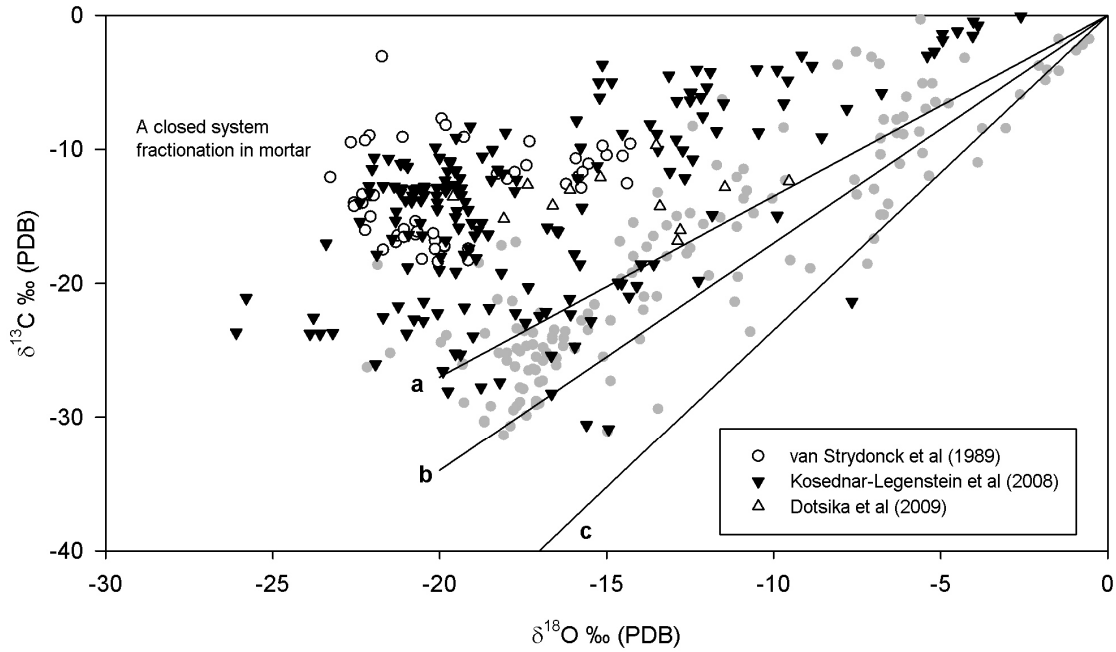

Figure 4.11 – Isotopic fractionation in closed systems as observed in mortar (Dotsika et al., 2009; Kosednar-Legenstein et al., 2008; van Strydonck et al., 1989).Lines a, b and c are the same from Figure 4.10

4.4 Investigation of the IRD site in Byker, Newcastle upon Tyne

4.4.1 IRD, Byker – Site description and methodology

An urban brownfield site was chosen in Newcastle upon Tyne approximately 2.5 km east of the city centre (GB National Grid: NZ275649 – see Figure 4.12) which was previously occupied by a concrete office complex (part of International Research and Development Ltd.) that was demolished in 1996. The site has remained unused since then, apart from storage of a soil heap excavated from an adjacent development site (approximate location shown in Figure 4.12). A contaminated land report completed by Newcastle City Council in 1998 presented soil profiles that show the presence of demolition waste throughout the site to 2–3 m in depth. Furthermore, the study found pH levels of

up to 11.8 and a sulphate content of up to 20313 mg kg^{-1} towards the north of the site indicating portlandite ($Ca(OH)_2$) and gypsum ($CaSO_4.2H_2O$) dissolution respectively. Vegetation on the site comprised of C_3 grasses (including species typical of a restoration seed mix) and C_4 ornamental garden escapes. The bedrock geology of the area is dominated by Carboniferous sandstone which is superficially overlain by glacial till. The site has been heavily modified by industrial activity and substantial thickness (>3 m) of made ground is present.

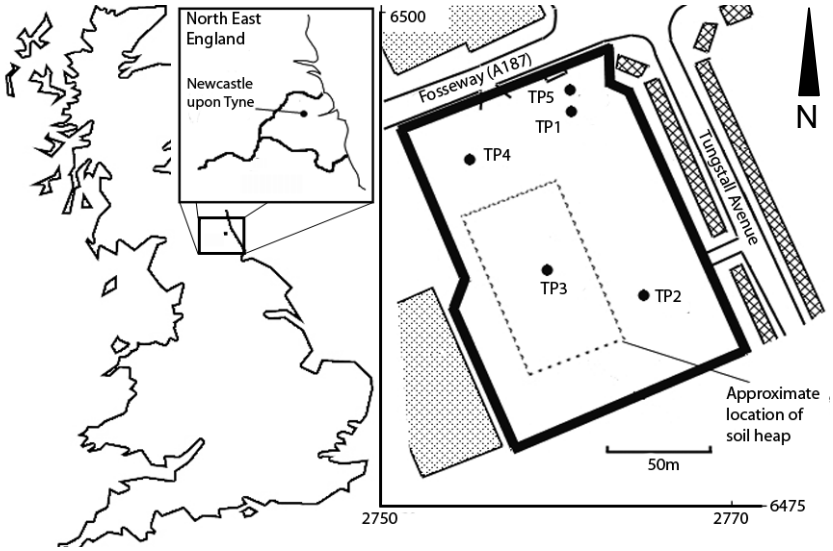

Figure 4.12 – Plan and location of the IRD brownfield field site, Byker, Newcastle upon Tyne. Source: Renforth et al. (2009).

Ian Farmer Associates (www.ianfarmerassociates.co.uk) were contracted in March 2008 to excavate five trial pits to 3.5 m. Samples were collected through the soil profile at both sites, air-dried and sieved to <2 mm. Calcium carbonate content was determined using an Eijkelkamp calcimeter (Appendix A.1), the residue was collected, washed, filtered and oven dried at 80 °C and used for the determination of organic C isotope ratios. Soil pH was analysed according to ISO 10390 1994, using a Jenway 3020 pH meter. Isotope ratio mass spectrometry (IRMS) was conducted using a Europa Scientific 20-20 IRMS (Iso-Analytical, Cheshire UK) for $^{13}C/^{12}C$ and $^{18}O/^{16}O$ for $CaCO_3$ and $^{13}C/^{12}C$ for organic C collected from the calcimeter residues (see Appendix B.1.3). Mineralogical analysis was determined using X-ray powder diffraction (XRD; Appendix A.4).

4.4.2 IRD, Byker – Results

In some trial pits, visible precipitates of $CaCO_3$ occurred as coatings and concretions on demolition rubble (Figure 4.2). Acid digestion determined inorganic carbon quantities within the soil to be between 0.26 and 2.38 ± 0.07 wt% ($\bar{x}$ = 1.14 % s = 0.62). Trial pits TP1, TP4 and TP5 showed negative correlation of inorganic carbon concentration with depth (r^2 = 0.78, 0.99 and 0.50, respectively, after removal of outliers from the basal clay in TP1, for which a carbonate content of 4.3 % was measured compared with values between 11 % and 20 % returned for other samples from the same trial pit, and sand in TP5, which had a similar lower value than the other samples from the same pit). There was no variation in carbonate content with depth in TP2 and TP3 (Figure 4.13).

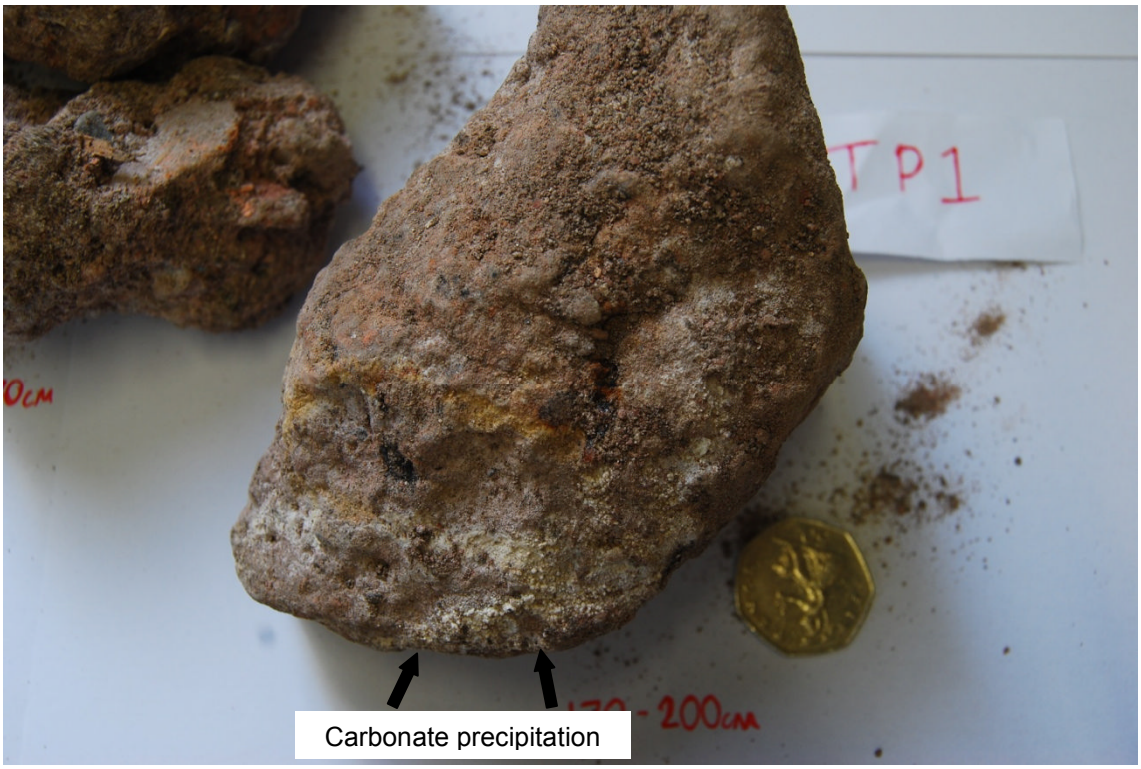

Plate 4.2 – Visible carbonate precipitation on demolition rubble.

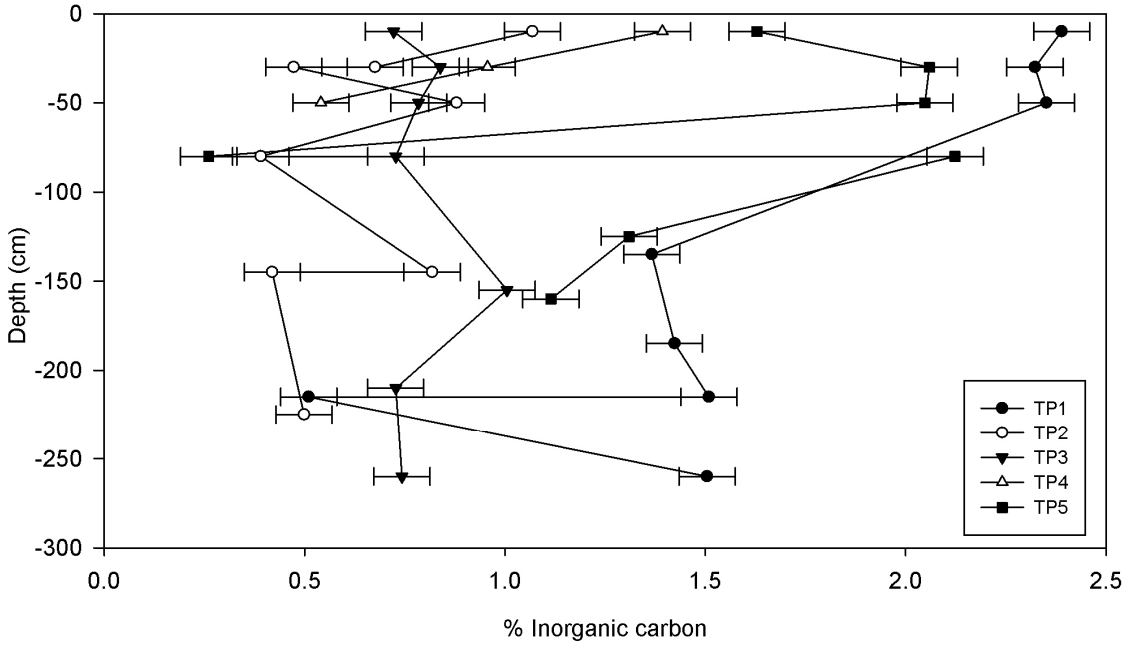

Figure 4.13 – Carbonate concentration with depth in the 5 trial pits at the IRD site, Byker (error bars represent repeatability).

Carbon and oxygen isotope analysis of the carbonates gave $\delta^{13}C$ values between -6.3 ‰ and -27.5 ‰ and $\delta^{18}O$ between -3.9 ‰ and -20.9 ‰ (Figure 4.14). The most negative carbon isotope values (between -13.3 ‰ and -27.5 ‰) were detected in precipitates on demolition rubble. There is a positive correlation between inorganic O and C isotope values (r^2 = 0.66 or 0.86 after the removal of outliers). Analysis of the organic C isotope ratios gave values between -19.0 ‰ and -24.0 ‰ $\delta^{13}C$ (all but one value lies within 1 standard deviation of the mean of -22.9 ‰). Comparison of pH values recorded in this study with those presented in the contaminated land report suggest a decline in soil pH over time (from 12 to 7 at the present day). However, a comparison is speculative due to variation in sampling locations.

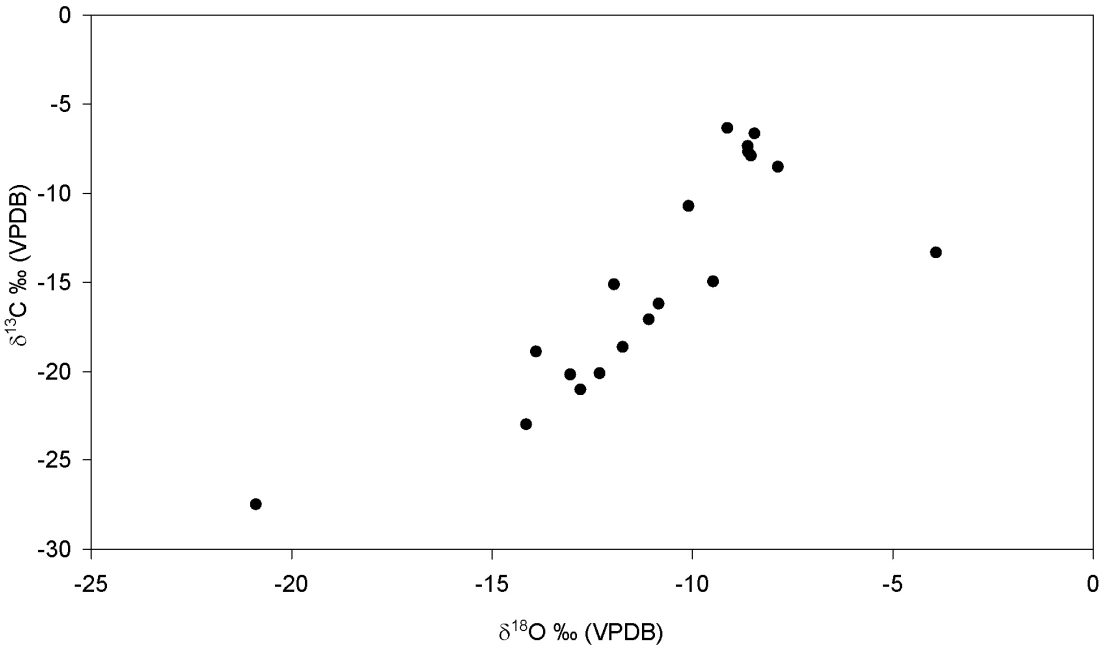

Figure 4.14 – Carbon and oxygen isotope ratios in carbonates from the IRD site (see Renforth et al., 2009) Note repeatability error bars are within the size of the point.

XRD analysis detected the presence of quartz (SiO_4), calcite ($CaCO_3$), dolomite ($CaMg(CO_3)_2$), illite ($(K,H_3O)(Al,Mg,Fe)_2(Si,Al)_4O_{10}[(OH)_2,(H_2O)]$) and kaolinite ($Al_2Si_2O_5(OH)_4$). The clay mineral peaks were more pronounced in TP3 and TP4, whereas calcite and dolomite peaks were more pronounced in TP1 and TP2 (Figure 4.15).

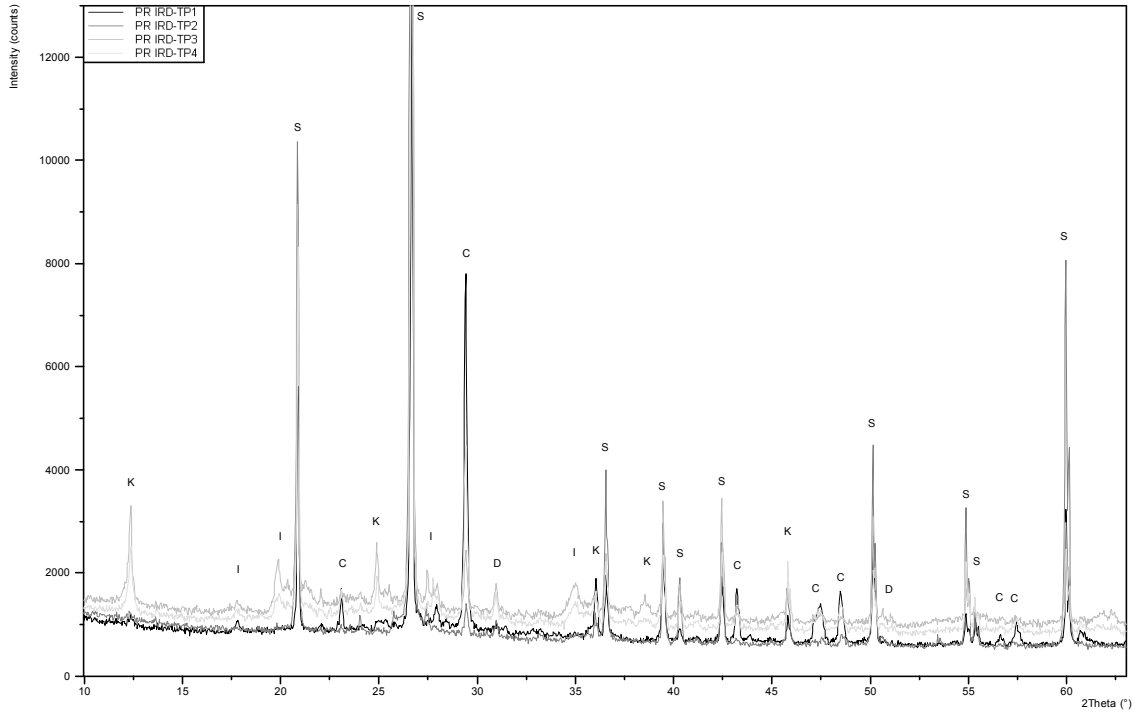

Figure 4.15 – XRD diffractogram of soils at the IRD Site in Byker. C – Calcite ($CaCO_3$), S – Quartz (SiO_4), D – Dolomite ($CaMg(CO_3)_2$), I – Illite ($\sim(K,H_3O)(Al,Mg,Fe)_2(Si,Al)_4O_{10}[(OH)_2,(H_2O)]$), K – Kaolinite ($Al_2Si_2O_5(OH)_4$).

4.5 Investigation of Consett Steelworks, County Durham

4.5.1 Consett Steelworks – Site description and methodology

A second site was selected adjacent to a former steel works in Consett (GB National Grid: NZ094492), County Durham, England which was closed in the 1980s creating 290 ha of derelict land. In a review of the contamination problems typically associated with iron and steel making, Harber and Forth (2001) describe remodelling of the ground profile at the Consett site with the emplacement of 'clean slag'. At the site, slags of different types have accumulated as steel making processes evolved since the early 1800s. The basic slag used for the cover is a lime-rich Ca silicate glass, containing Ca silicate minerals (such as merwinite, melilite and larnite; Fredericci et al., 2000), Ca oxide as Ca ferrite and portlandite as well as Fe oxides (Harber and Forth, 2001). The final stage in restoration involved emplacement of top soil, from which the samples were taken. Subsequent analysis of the area (Mayes et al., 2006) has discovered pH values of 12.5 within leachate draining the site which

was attributed to the weathering of portlandite and Ca silicate minerals. The waters were supersaturated with respect to calcite and showed a relationship between precipitation and biological activity, coupled with attenuation of pH through a pond and calcareous wetland which has developed on a watercourse draining the former steel works area. A calcareous hardpan has formed at the surface adjacent to the pond and covers an area of approximately 400 m^2. The bedrock geology of the area is dominated by the Carboniferous mudstones of the Lower Coal Measures, but the landscape has been considerably altered by industrial activity.

At the former steelworks at Consett in June 2008, soil samples were collected with a hand auger to depths up to 20 cm prior to contact with large fragments of slag. Furthermore, sediment was collected from the bottom of the high pH pond (locations are shown in Figure 4.16). Carbonate and isotope values were determined as described in Section 4.4.1 (see Appendix A.3 and B.1.4).

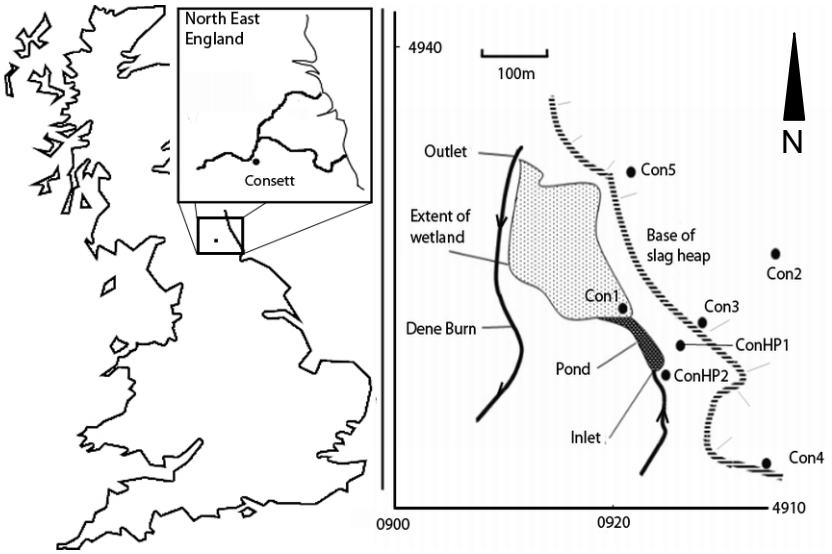

Figure 4.16 – Plan and location of the Hownsgill valley, former steelworks, Consett. Source: Renforth et al. (2009). The solid black line represents the route of the watercourse (Dene Burn) and the dashed line represents the foot of a slag mound. Points are the sampling locations

4.5.2 Consett Steelworks – Results

Calcium carbonate occurred in both the soil (pedogenic carbonate) and within the drainage system of the site (tufaceous carbonate). Quantities of inorganic carbon ranged between 0 % and 11.21 % ($\bar{x}$ =3.55 % s = 4.23) over both

systems. The largest concentration of inorganic carbon was recorded in the sediment of the pond (>10 % or >90 %as $CaCO_3$) and the hardpan (3.84–10.40 %). The concentration of pedogenic carbonate was extremely variable (between 0 % and 4.59 %C, $\bar{x}$ = 0.84 % s = 1.68) and there appears to be no relationship between concentration and depth. Carbonate isotope ratios were between -17.6 ‰ and -22 7 ‰ for $\delta^{13}C$ and -11.3 ‰ and -16.1 ‰ for $\delta^{18}O$ (Figure 4.17).

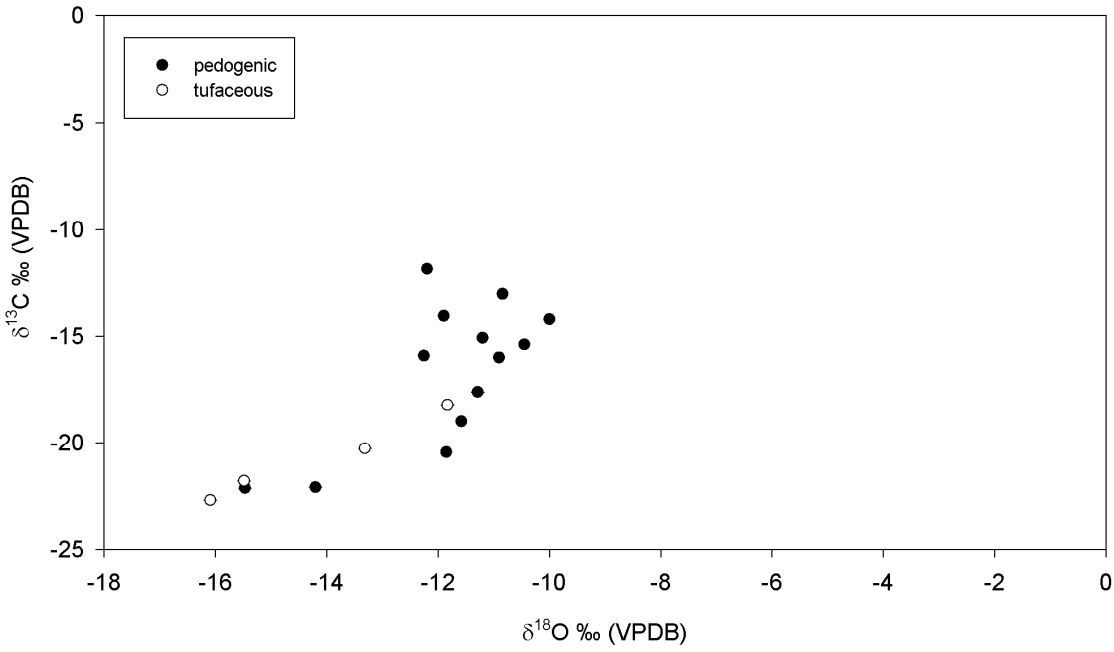

Figure 4.17 – Carbon and oxygen isotope ratios in carbonates from the former steelworks site, Consett (see Renforth et al., 2009). Note, repeatability error bars are within the data points.

4.6 Investigation of Science Central, Newcastle upon Tyne

4.6.1 Science Central – Site description and methodology

Science Central is a 10 ha development in the centre of Newcastle upon Tyne (see Figure 4.18; NZ240564). The site was formerly occupied by Scottish and Newcastle Breweries, until it was bought by a partnership between Newcastle University, Newcastle City Council and One North East in 2008. The structures on the site were demolished, the debris of which was distributed forming a layer of ‘made ground’. Profile data from intrusive investigation reports compiled by Northwest Holst Soil Engineering were collated, modelled in GIS software (ESRI© ArcScene™ and ArcMap™ 9.3), and used to determine the thickness of

made ground (Figure 4.18), which varies between 6 m towards the south east and <0.5 m in the north west quarter of the site.

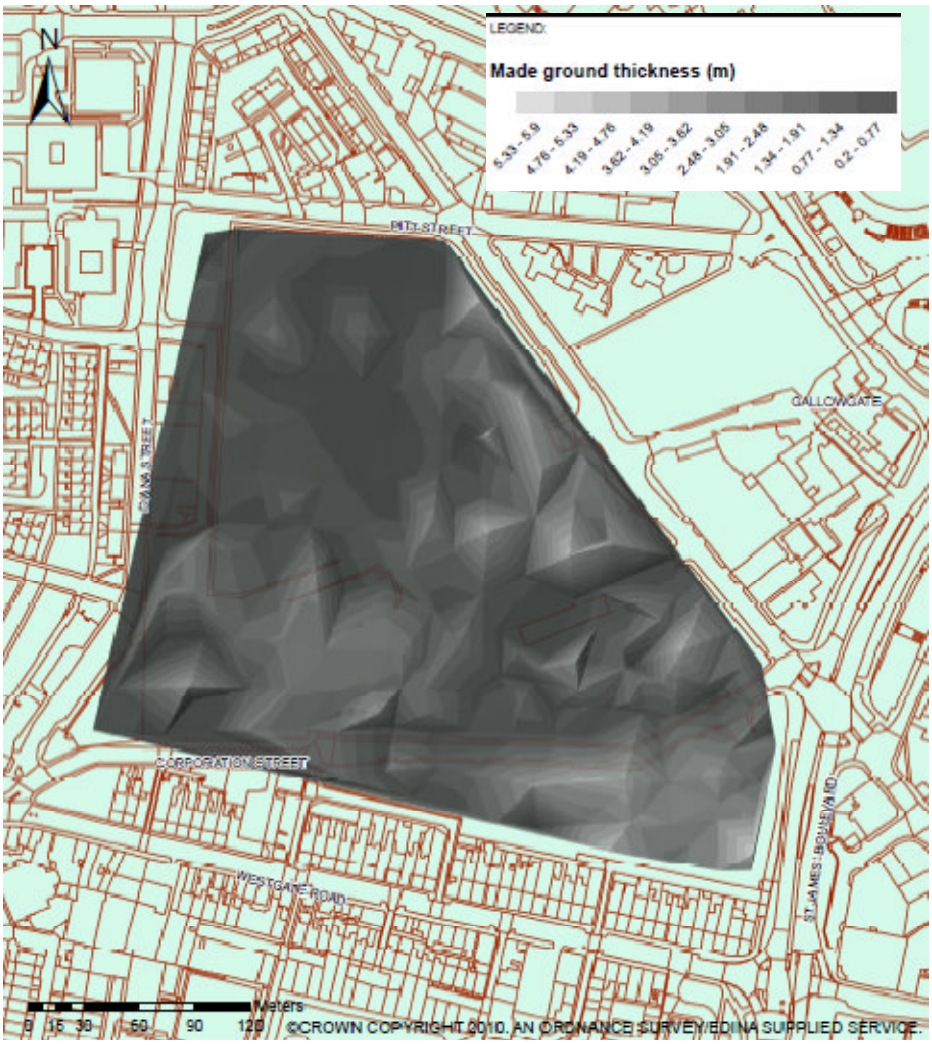

Figure 4.18 – Made ground thickness at Science Central. Data was collated from intrusive ground surveys and processed in ArcMap and ArcScene software.

Assuming a density of made ground of ~1800 kg m^{-3} (confirmed in the site investigation reports), it is estimated that 1 Mt of material overlay the site. pH (5.9-12.5) and surface elevation (53 – 78 mAOD) also vary spatially (Figure 4.19).

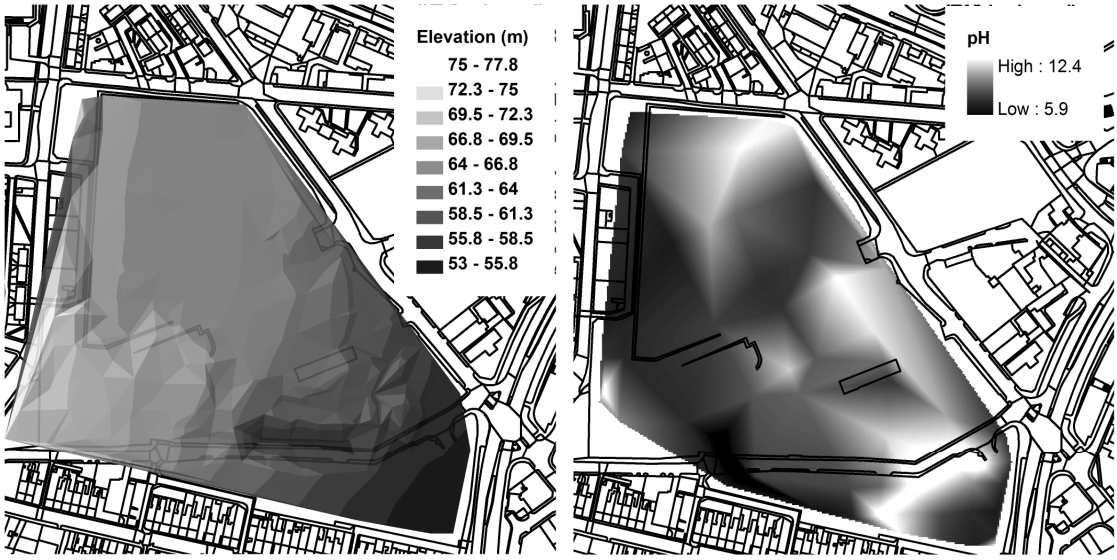

Figure 4.19 – Surface elevation and made ground pH at Science Central. Data was collated from intrusive ground surveys and processed in ArcMap and ArcScene software.

In September 2010 (in collaboration with Carla-Leanne Washbourne -PhD student, the School of Civil Engineering and Geosciences, Newcastle University), the surface material at Science Central was sampled in a 20 m x 20 m grid (Figure 4.20) using hand tools, and sieved on site to passing 2 mm. 137 samples were oven dried at 80 °C. Inorganic carbon content and carbon and oxygen stable isotope were determined as outlined in Section 4.4.1. The samples were powdered using a Siebtechnik Tema mill and analysed for organic carbon using a Leco CS244 Carbon/Sulphur Analyser (Appendix A.5). A subset of 38 samples was analysed using XRF by Leicester University (Appendix A.6).

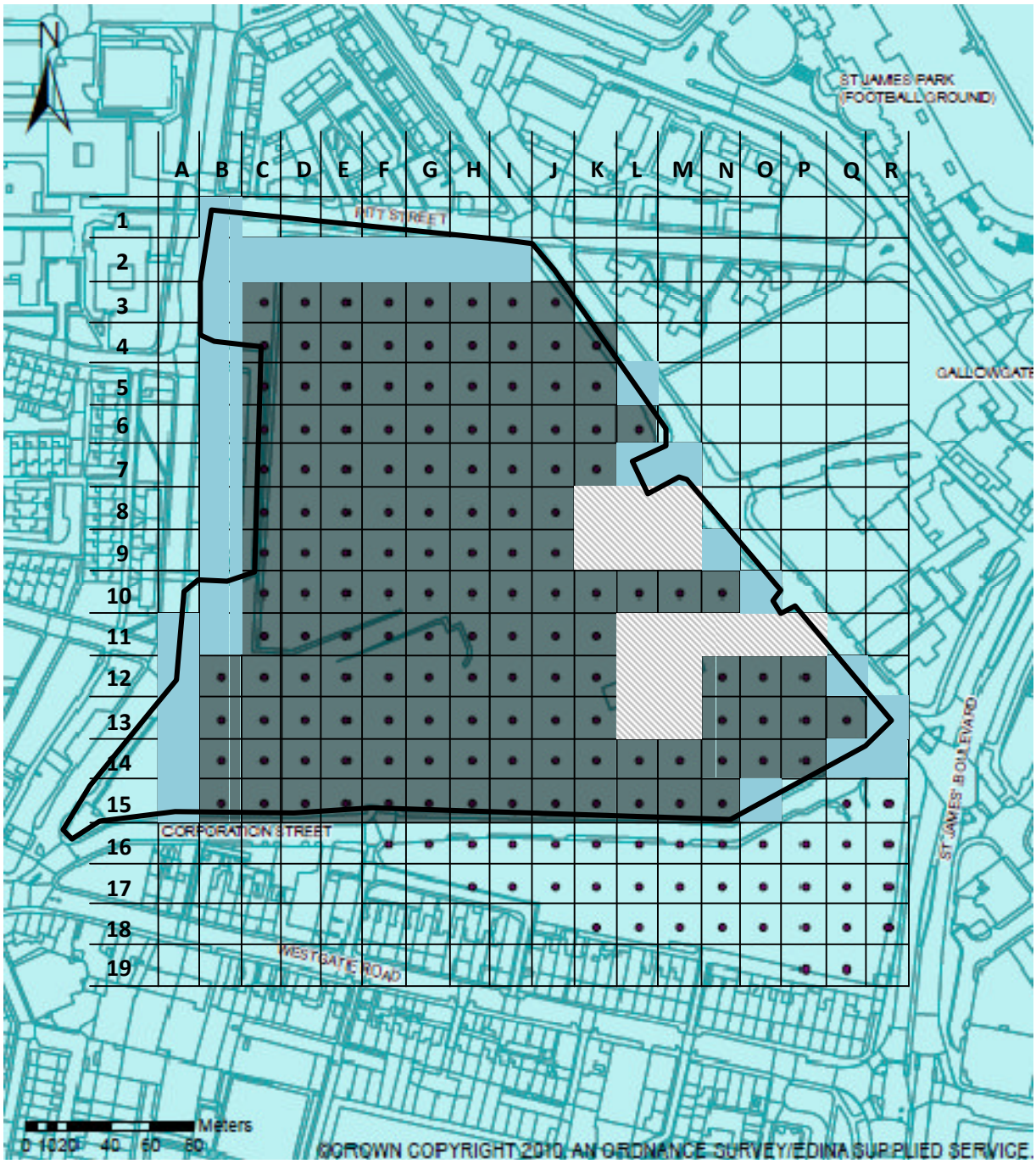

Figure 4.20 – Science Central survey locations denoted by the dark grey shading.

4.6.2 Science Central – Results

Inorganic carbon concentrations ranged from 1.40 to 3.85 ± 0.07 wt% ($\bar{x}$ = 2.58 wt% s = 0.48) with a small discrepancy between the east and west sides of the site (Figure 4.23). Organic carbon concentrations were between 0.27 and 5.67 ±.0.52 wt% ($\bar{x}$ = 1.80 % s = 0.63). Isotopic composition varied between -3.13 ‰ and -13.55 ‰, and -8.10 ‰ and -12.13 ‰ for $\delta^{13}C$ and $\delta^{18}O$ respectively, (Figure 4.21).

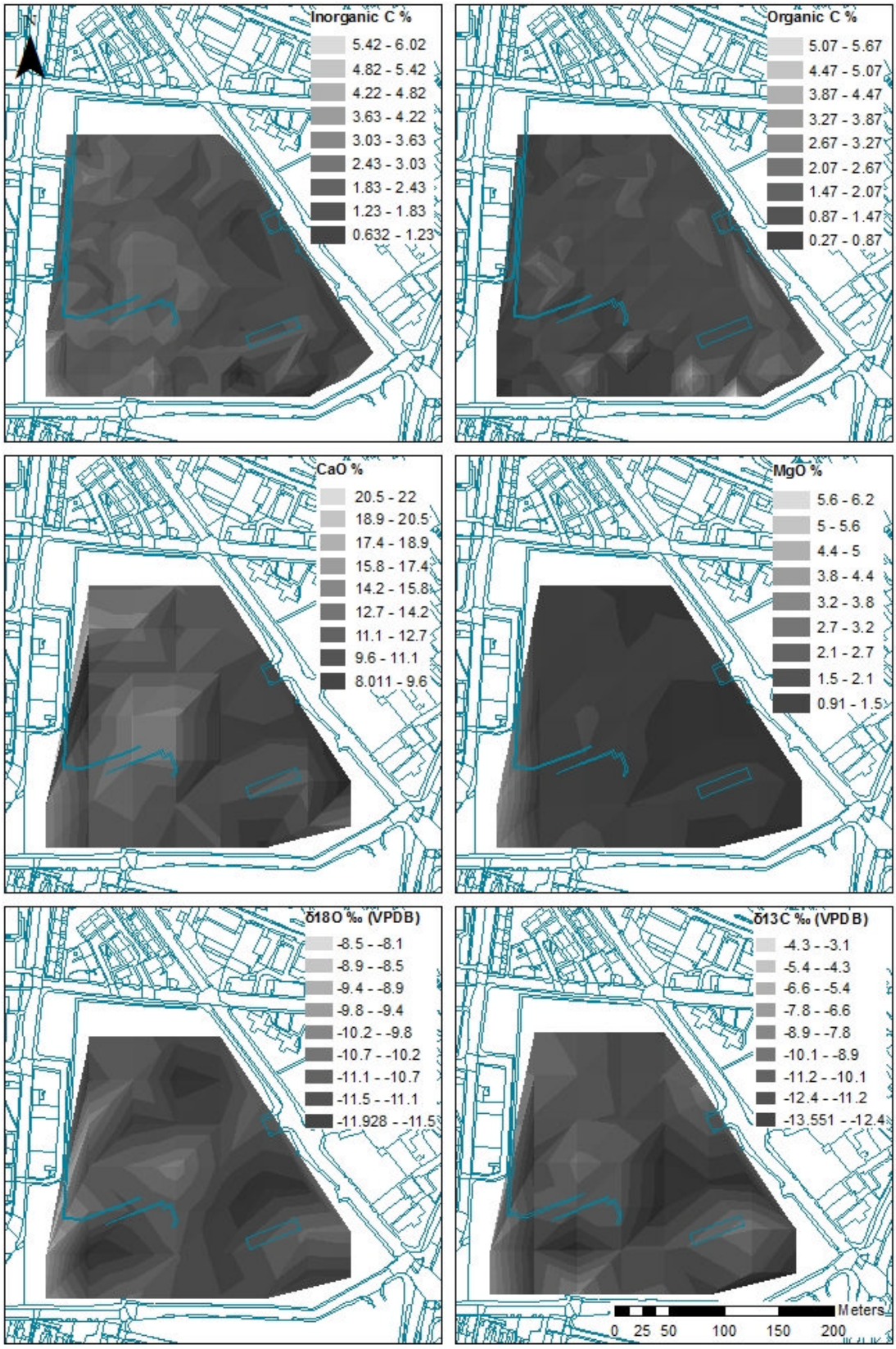

Figure 4.21 – Organic carbon, inorganic carbon, calcium, magnesium, and carbon and oxygen stable isotopic ratios of carbonate at Science Central. Data collated from XRF analysis and processed in ArcMap and ArcScene software.

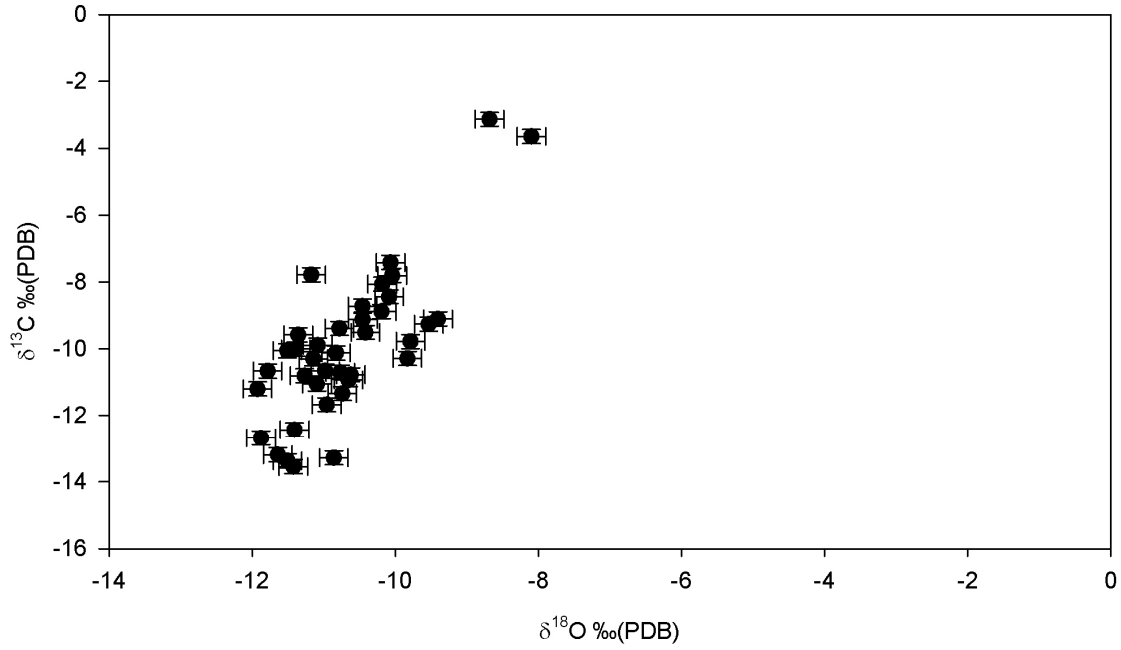

Figure 4.22 – Carbon and oxygen isotope signatures in soil carbonates at Science Central. Error bar represent repeatability.

SiO_2, CaO and MgO concentration were between 38.9 wt% to 65.1 wt%, 8.0 wt% to 22.0 wt% and 0.9 wt% to 6.2 wt% respectively. A full table of results is presented in Appendix B.1.4. There was strong negative correlation between CaO and SiO_2 content (r^2 = 0.85; Figure 4.23) suggesting the presence of calcium carbonate minerals in the sample, which is confirmed by the similarly strong relationship between calcium content and inorganic carbon (r^2 = 0.78; Figure 4.24). The intercept with the % inorganic carbon = 0 axis suggests ~3 %CaO is not contained in the carbonate phase. The CaO intercept with the %SiO_2 = 0 axis suggests that the carbonate phase is not purely calcite and may include ~35 % dolomite. However, the relationship between MgO, SiO_2 and inorganic carbon is not as well defined and there was greater variation in CaO concentration on site than MgO (Figure 4.21).

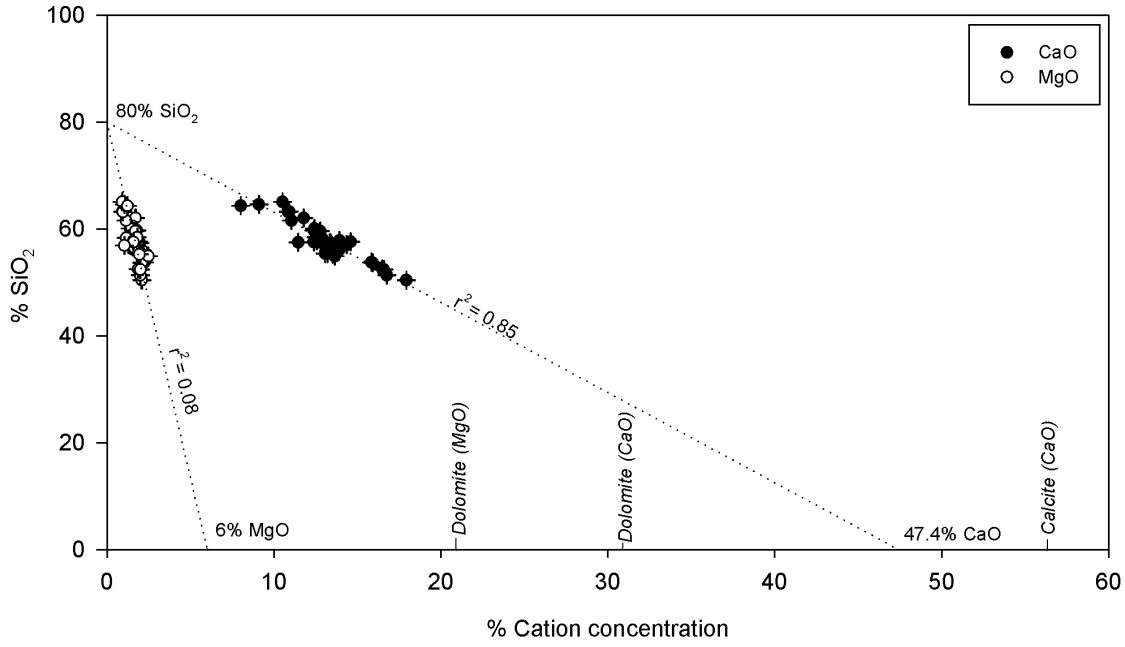

Figure 4.23 – MgO and CaO against SiO_2 concentration, Science Central (repeatability error is within the size of the data points).

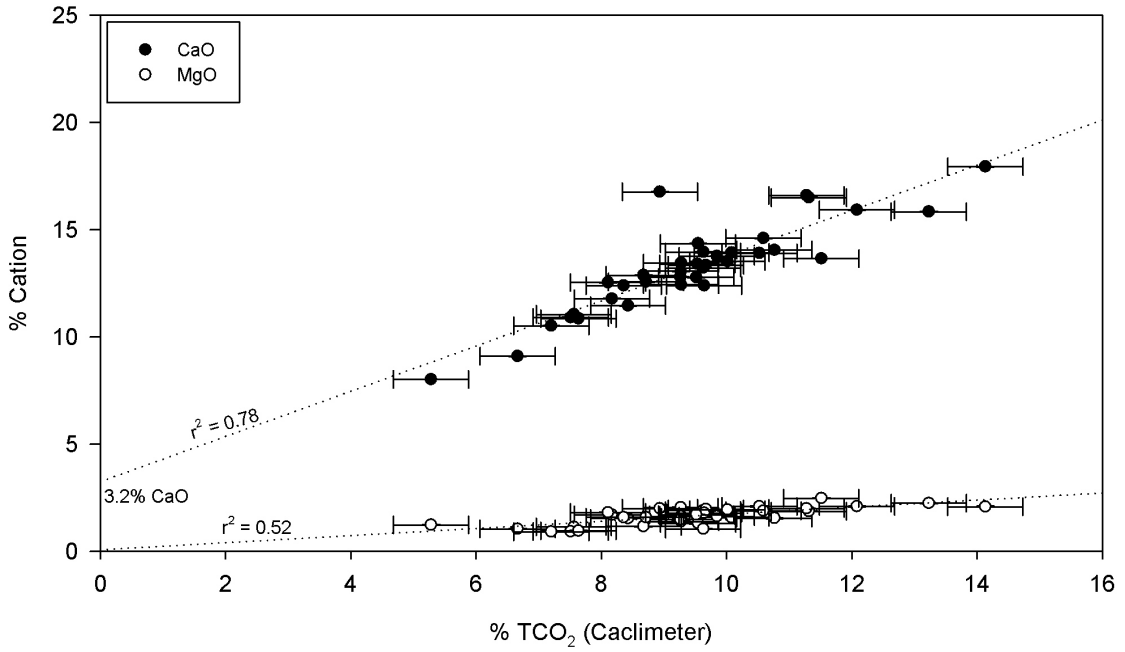

Figure 4.24 – MgO and CaO against mineral carbonate concentration (as $\%CO_2$), Science Central. Error bars represent repeatability.

Comparing the loss on ignition undertaken during XRF analysis with the separate and combined organic and inorganic carbon (expressed as CO_2) data shows a strong correlation and a 1:1 gradient (*m*) with the combined CO_2 (Figure 4.25).

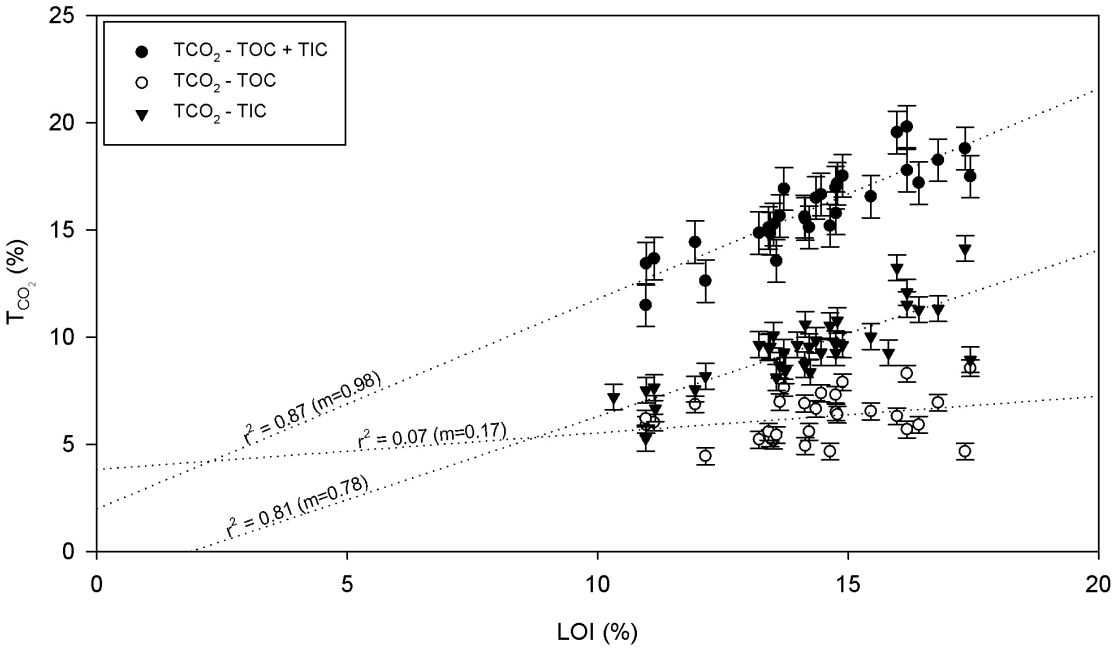

Figure 4.25 – Comparison of loss on ignition with total inorganic carbon (TIC) values obtained from acid digestion and organic carbon (TOC) determined using a Leco CS244 Carbon/Sulphur Analyser (expressed here as T_{CO_2}). Error bars represent repeatability.

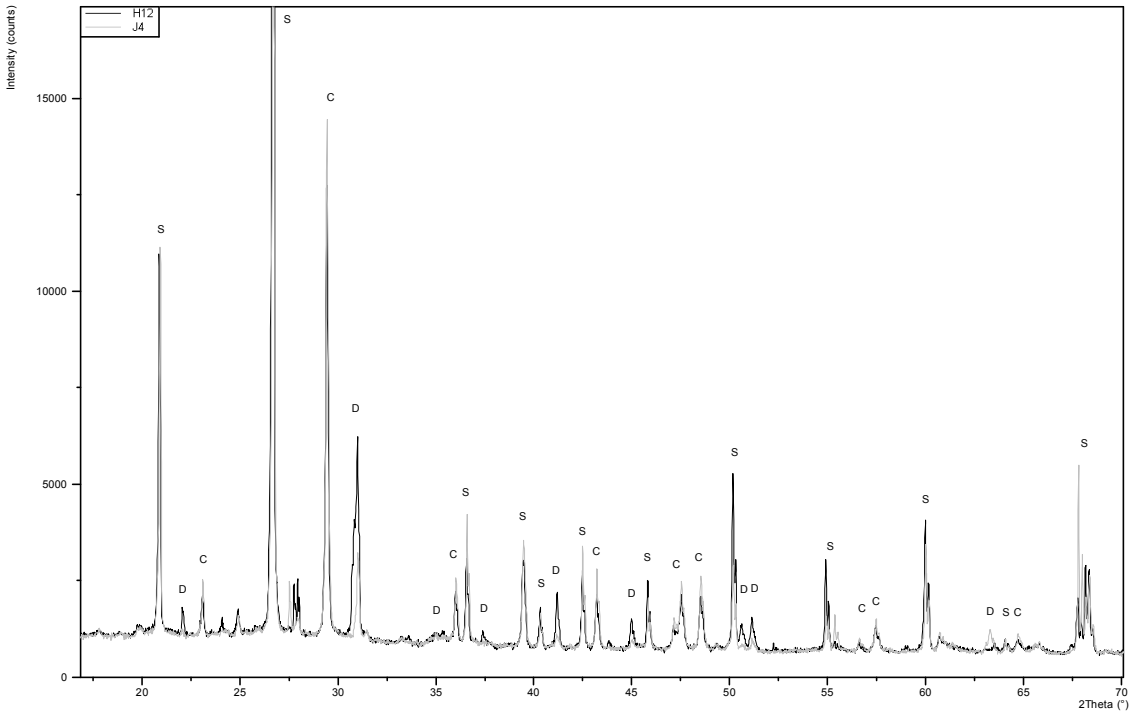

Figure 4.26 – XRD diffractogram of two samples from Science Central. C – Calcite ($CaCO_3$), S – Quartz (SiO_4), D – Dolomite ($CaMg(CO_3)_2$).

Interpretation of spectra patterns from XRD analysis suggest the soils at Science Central are largely composed of silica, calcite and dolomite (Figure 4.26). Relative intensity analysis of the dolomite and calcite peaks (e.g. Chung, 1974) suggests that between 55 and 74 % of carbonate is contained within the calcite and 26 to 45 % of the carbonate is within dolomite.

4.7 Site investigation interpretation

4.7.1 Soil inorganic carbon content

Inorganic carbon ranged from 0.26 to 2.38 %, 0 to 11.21 %, and 1.4 to 3.85 ± 0.07 % in the soils at IRD, Consett and Science Central respectively. The average inorganic carbon concentration between the three sites was 1.86 % with a standard deviation of 2.61 %, reflecting the heterogeneity of the soil. This equates to approximately 20-30 kgC m^{-2} (for dry densities between 1 – 1.5 t m^{-3}, and assuming 1 m soil depth), which exceeds typical organic carbon concentration in urban soils (Table 4.6) and is consistent with other reported inorganic carbon concentrations (Lorenz et al., 2006).

Table 4.6 – Organic carbon content of urban soils. Source: Renforth et al. (2011)

Location	Vegetation cover	Mean soil organic carbon (kg m^{-2})	*N*	Soil depth (cm)	Source
Baltimore, USA	Grassland	9.9	2	100	Pouyat et al. (2006)
Tokyo, Japan	Grassland	8.2	17	30	Takahashi et al. (2008)
Moscow, USA	Grassland	3.6	3	30	Smetak et al (2007)
UK	Grassland	7.1	5	15	Rawlins et al. (2008)
Baltimore, USA	Grassland	12.2	18	100	Pouyat et al. (2006)
Chicago, USA	Grassland	16.3	24	60	Jo and McPherson (1995)
Moscow, USA	Grassland	2.1	6	30	Smetak et al. (2007)
Fort Collins, USA	Grassland	6.9	3	30	Kaye et al (2005)
UK	Grassland	9.7	25	15	Rawlins et al. (2008)
Phoenix, USA	Xeric	1.8	22	30	Kaye et al. (2008)
Phoenix, USA	Mesic	1.0	23	30	Kaye et al. (2008)
Baltimore, USA		6.0	61	15	Pouyat et al. (2002)
Baltimore, USA		12.0	5	100	Pouyat et al. (2009)
Baltimore, USA		9.5	1	69	Groffman et al. (2006)
Tokyo, Japan		12.0	13	30	Takahashi et al. (2008)
Baltimore, USA		5.1	37	15	Pouyat et al. (2002)
New York, USA		6.1	N/A	10	Pouyat et al. (2002)

Rate of accumulation is calculated between two time points (the first of which, t=0, it is assumed that inorganic C concentration is 0). The log accumulation rate is on the order of -12 molC cm^{-3}(soil) sec^{-1} (Table 4.7).

Table 4.7 – Estimated rate of carbon accumulation in artificial soils from fieldwork.

Site	Age of site (a)	Inorganic carbon concentration (%)	Rate of accumulation	
			Log molC cm^{-3} (soil) sec^{-1}	KgC m^{-3} a^{-1}
IRD site	11	1.14	-12.79	2.07
Consett Steelworks	27	3.55	-12.68	2.63
Science central	2	2.58	-11.69	25.80

4.7.2 Carbonate isotope signatures

Carbonate isotope ratios were between -3.1 ‰ and -27.5 ‰ for $\delta^{13}C$ and -3.9 ‰ and -20.9 ‰ for $\delta^{18}O$ (Figure 4.27) The IRD site and Consett Steelworks had the lightest isotope signatures largely consistent with hydroxylation and diffusional fractionation, whereas the carbonates at Science Central were consistent with hydroxylation alone.

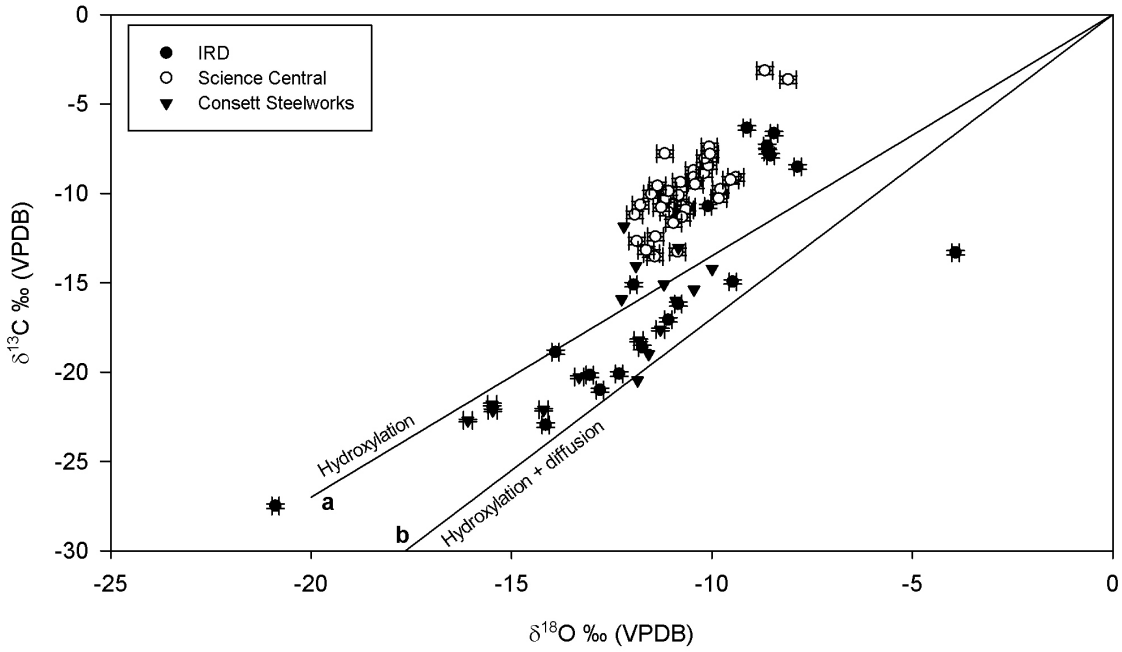

Figure 4.27 – Combined $\delta^{13}C$ and $\delta^{18}O$ *isotope data for the IRD site, Science Central and Consett Steelworks. Lines a and b represent mixing lines as presented in Figure 4.11. Error bar represent repeatability.*

Assuming that atmospheric CO_2 is the only source of carbon in hydroxylation and diffusion isotopic fractionation, the proximity of the carbonate to these end members can be used to determine the quantity of sequestered atmospheric CO_2. Table 4.8 suggests that between all of the sites approximately 47.7 to 55.2 % of the carbonate carbon is derived from the atmosphere. Sample proximity to three possible $\delta^{13}C$ end members makes interpretation complex. For instance, the hydroxylation end member ($\delta^{13}C$ = -20 ‰) may be appropriate for the carbonates at Science Central, but returns impossibly high values for the IRD site and Consett Steelworks. The average of carbon end members is presented in Table 4.7 which has a linear relationship (r^2 = 0.67, with the removal of two outliers at the IRD site) with estimates from $\delta^{18}O$= -20 ‰ (Figure 4.28).

Table 4.8 – Proportion of field site pedogenic carbonate carbon derived from the atmosphere (after the removal of outliers).

Site	**% of carbon from the atmosphere for specific end members in**							
	$\delta^{18}O$ = -20		$\delta^{13}C$ = -27		$\delta^{13}C$ = -34		$\delta^{13}C$ (average)	
Absolute values	min	max	min	max	min	max	min	max
IRD site	19.6	70.7	23.5	85.1	18.7	67.5	21.1	76.3
Consett Steelworks	50.0	80.5	43.9	84.1	34.8	66.8	39.4	75.4
Science Central	40.5	59.6	11.6	50.2	9.2	39.9	10.4	45.0
Average values	$\bar{x}$	s	$\bar{x}$	s	$\bar{x}$	s	$\bar{x}$	s
IRD site	51.8	12.5	52.2	20.3	41.5	16.1	46.8	18.2
Consett Steelworks	62.0	9.0	65.4	12.6	51.9	10.0	58.6	11.3
Science central	53.4	4.2	36.9	8.2	29.3	6.4	33.1	7.3
Total	**55.0**	**9.1**					**42.4**	**15.9**

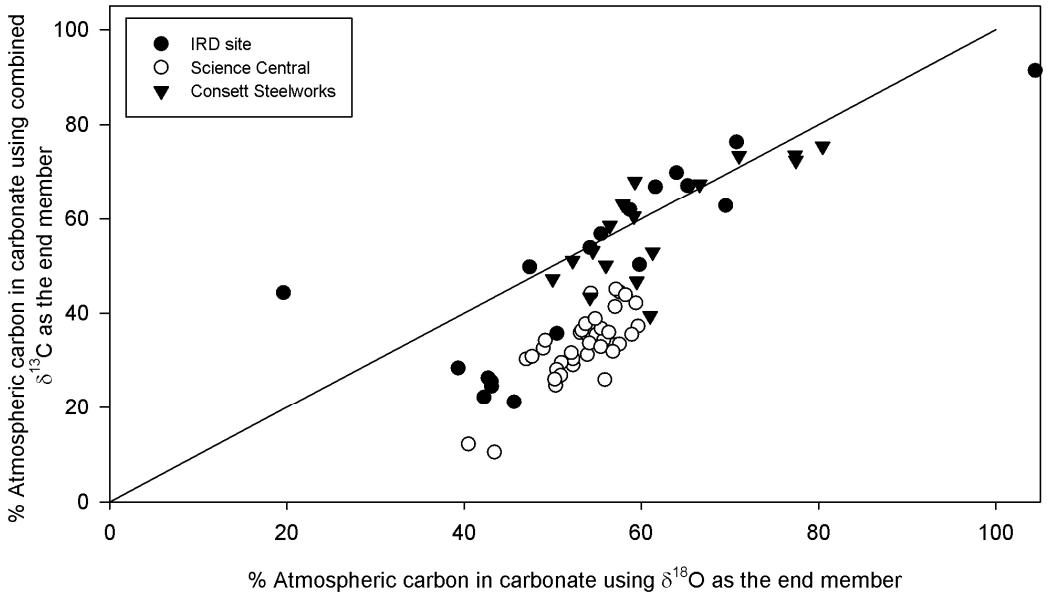

Figure 4.28 – % of atmospheric carbon in soil carbonates. Line represents 1:1 gradient.

4.7.3 Carbon capture potential at Science Central

The XRF, inorganic carbon and isotope data for Science Central can be used to determine the extent of carbonation and the additional carbonation potential for the material. The total inorganic carbon (C_t) is assumed to be contained within calcite (C_c) and dolomite (C_d; Equation 4.25).

Equation 4.25: $$C_t = C_d + C_c$$

If the MgO content is wholly comprised in the dolomite phase, the relative proportions of calcite and dolomite can be estimated (Equation 4.26), the values of which are approximately supported by the relative peak intensities in XRD analysis and the x = 0 intercept in Figure 4.26).

Equation 4.26: $$C_d = \frac{\%MgO \cdot 2M_c}{M_{MgO}}$$

where M_c and M_{MgO} is the molecular mass of carbon and MgO respectively. The total calcium contained in a carbonate phase can be estimated through Equation 4.27.

Equation 4.27: $$\%CaO_{carbonate} = \frac{M_{CaO}}{M_c}\left(\frac{C_d}{2} + C_c\right)$$

where M_{CaO} is the molecular mass of CaO. Subtracting $\%CaO_{carbonate}$ from the total calcium returns an estimate of the calcium available for additional carbonation. From this it is estimated that between 2.1 and 8.2 %CaO ($\bar{x}$ = 3.5 % s = 1.1 %) is available for carbonation and is distributed across the site according to Figure 4.29. The corresponds approximately to a carbon capture potential of 7500 tC for the 1 Mt of material overlaying the site. It is interesting to note the area of the site with the largest carbonation potential is from a recently disturbed stockpile suggesting carbon content variations through the material. However, additional work is required to investigate the soil profile to its full depth.

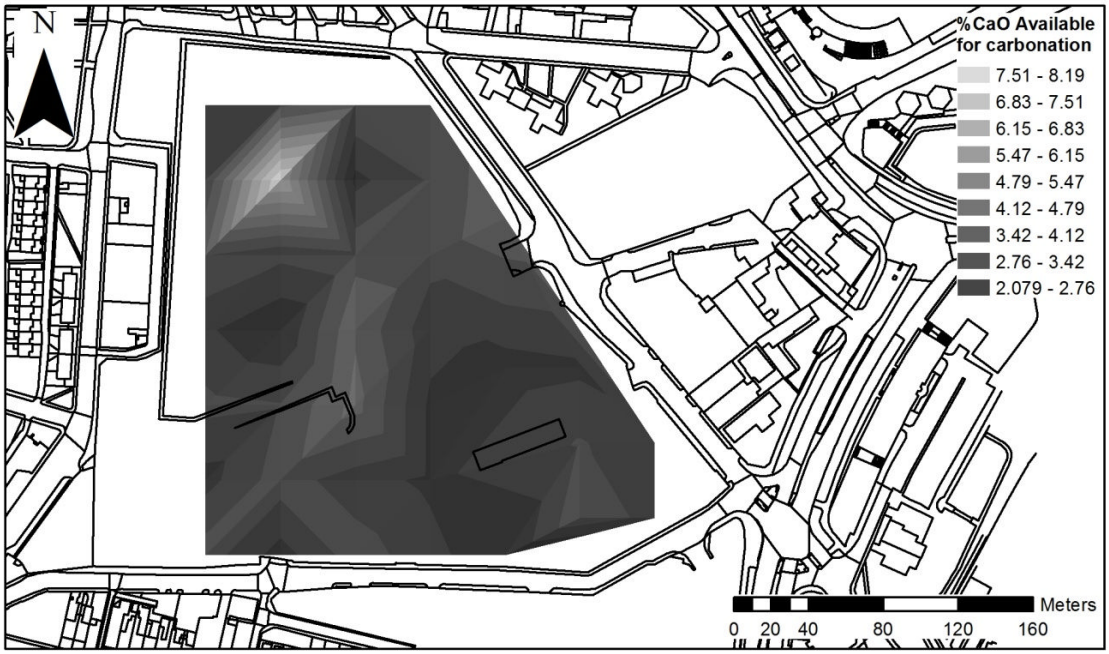

Figure 4.29 – Potentially available CaO% at Science Central for carbonation.

4.8 Precipitation of carbonate across a climate gradient

4.8.1 Carbonate precipitation as a function of rainfall

The formation of carbonates has traditionally been associated with soil formation on calcareous parent material in semi arid/ arid climates where precipitation is less than the potential evapotranspiration (Goudie, 1996; James, 1972). Contemporary studies have demonstrated that pedogenic carbonate precipitation is not limited to semi arid climates.

The classic work by Jenny (1941) documents a linear relationship between mean annual precipitation (MAP) and carbonate accumulation depth. Similarly, Stevenson et al. (2005) noted a correlation between carbonate accumulation depth and MAP in loess soils in Washington State, USA. Further to this, they demonstrated a strong correlation between MAP and carbonate isotope values which suggests that carbonates may be used as a long term indicator of plant productivity, providing the carbonate carbon is derived solely from organic carbon.

The importance of rainfall on isotopic signatures in natural pedogenic carbonates warrants a similar investigation on artificial pedogenic carbonates. Furthermore, as discussed in Section 4.3.2, the isotopic fractionation of carbon and oxygen is potentially a function of temperature (Dietzel et al., 2009; Pinsent

et al., 1956). Therefore, it is important to determine whether the mixing lines used as the basis for interpreting fieldwork data are a function of temperature rather than mixing between isotopically distinct carbonate minerals. To this end, artificial soil carbonates were sampled across a climate gradient in California, USA.

4.8.2 California – Site description and methodology

Seven sites in California, USA, were identified to investigate the precipitation of carbonate in artificial soils across a climate gradient, including four associated with the University of California (UC) system (Davis, Merced, Santa Barbara and Santa Cruz) and three waste transfer and storage stations (Compton, Sacramento and San Leandro; Figure 4.30). The climate in California is well documented by the Western Regional Climate Centre (http://www.wrcc.dri.edu), in which the northern half of the state receives typically ~8-13 mm month^{-1} more rainfall and the annual average temperature is 2-3°C cooler compared to the south (see Table 4.9 for site descriptions).

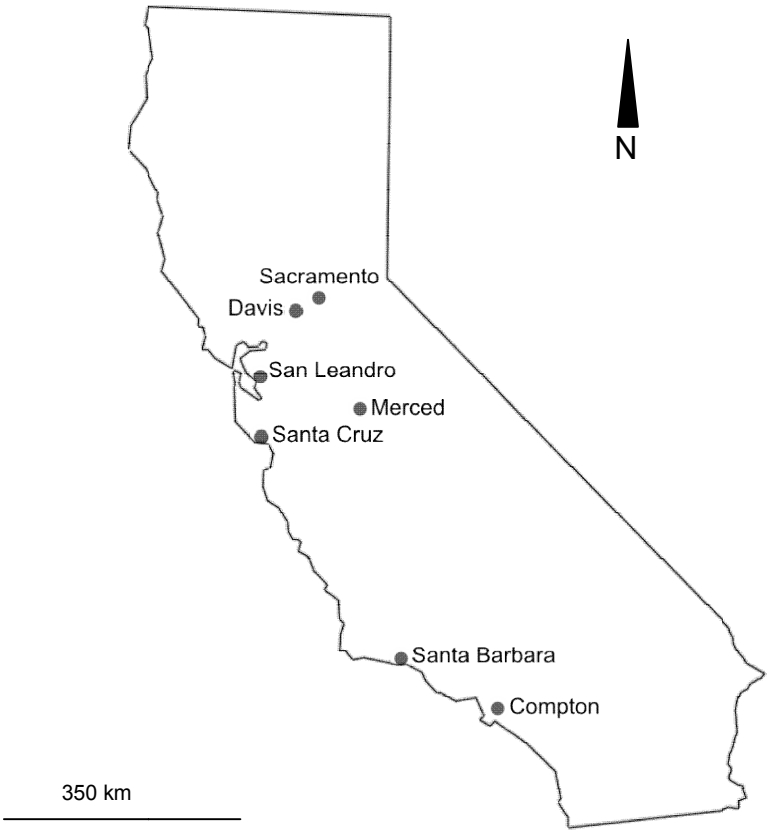

Figure 4.30 – Distribution of sampling locations in California, USA.

Over a three week period in October 2009 soil at these sites was collected, oven dried at 85 °C, sieved to passing 2 mm and shipped back to the UK for analysis. Laboratory work in California was undertaken in collaboration with Dr Jason DeJong (University of California at Davis). Carbonate contents were determined using HCl acid digestion in an Eijkelkamp calcimeter (Appendix A.1). Carbon and oxygen stable isotope analysis was undertaken in collaboration with Professor Tony Fallick (Scottish Universities Environmental Research Centre, East Kilbride) using a Prism III mass spectrometer (Appendix A.3).

*Table 4.9 – Field site description and locations in California. Climate data from http://www.wrcc.dri.edu- accessed 6th December 2010,*taken the average between Vacaville and Sacramento **Watsonville data used.*

Site	Coordinates	Av a temp (°C)	Av rainfall (mm a^{-1})	Description
UC Davis (UCD)	38°32'10.37"N 121°45'50.98"W	16.3*	504*	Under the direction of grounds staff, samples were taken from adjacent to a new structure where construction material was stockpiled. Substantial landscaping was observed.
UC Merced (UCM)	37°21'54.62"N 120°25'34.79"W	16.4	268	University campus constructed in 2005. Samples were removed from soil where construction rubble was stockpiled.
UC Santa Cruz (UCSC)	36°59'58.15"N 122° 3'27.67"W	13.7**	486**	Soil samples were taken from adjacent to recent construction activity.
UC Santa Barbara (UCSB)	34°25'3.62"N 119°51'9.70"W	14.8	439	Samples removed from soil where construction materials are occasionally stored.
North Area Recovery Station – Sacramento (SAC)	38°38'56.87"N 121°23'26.30"W	16.1	428	Site is a waste transfer station serving the northern districts of Sacramento. Samples were taken of soils adjacent to stockpiled construction and demolition waste.
Davis Street Station for Material Recycling & Transfer - San Leandro (SLA)	37°42'39.69"N 122°11'34.80"W	14.5	523	The site is a municipal solid waste transfer station serving 2 million homes in the Bay area. The site produces 1000 t $month^{-1}$ of MRF (a mix of organic material and construction waste). Samples taken from soils disturbed with MRF and construction waste.

*Table 4.9 – Field site description and locations in California. Climate data from http://www.wrcc.dri.edu- accessed 6th December 2010,*taken the average between Vacaville and Sacramento **Watsonville data used.*				
Site	**Coordinates**	**Av a temp (°C)**	**Av rainfall (mm a^{-1})**	**Description**
Atkinson Brick Company – Compton (CMP)	33°54'24.31"N 118°15'25.44"W	18.6	373	Site has been operational since 1939 as a clay mine and brick works. This site function was short lived becoming a landfill for construction waste in the early 1940s. The site is continuously sprayed with water to control dust.

4.8.3 California – Results and discussion

Inorganic carbon contents of the soil ranged between 0.01 to 1.45 ±0.07 % ($\bar{x}$ = 0.36 % s = 0.34 %; Figure 4.31). The soils at the field site in Compton had significantly more carbon than the other locations (P<0.001), but all sites contained less carbon than the average content of soils sampled in the UK.

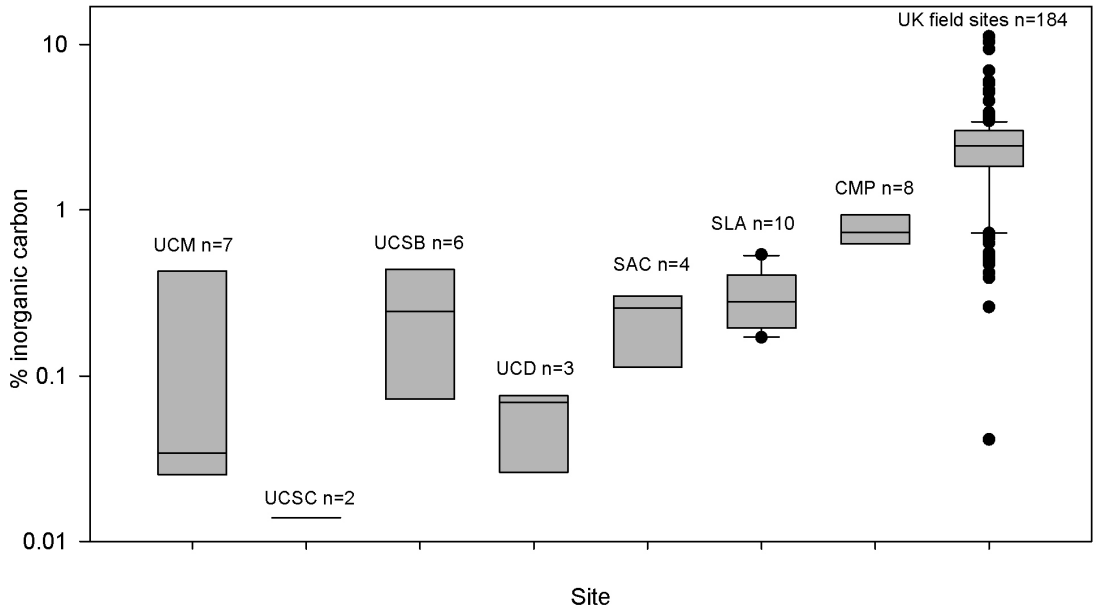

Figure 4.31 – Carbonate content (expressed as inorganic carbon) of soils at field sites in California and compared to UK fieldwork results (n represents the number of samples).

Isotopic composition varied between -7.95 ‰ and -21.57 ‰, and -6.77 ‰ and -29.85 ‰ for $\delta^{13}C$ and $\delta^{18}O$ respectively (Figure 4.32). The results are generally

consistent with the isotopic mixing lines discussed in Section 4.3.2, with two outliers with $\delta^{18}O$ <-25 ‰. There appears to be minimal variation in $\delta^{13}C$ and $\delta^{18}O$ values with temperature and precipitation (Figure 4.33), although the quantity of additional water added to the soil by human activity is unknown.

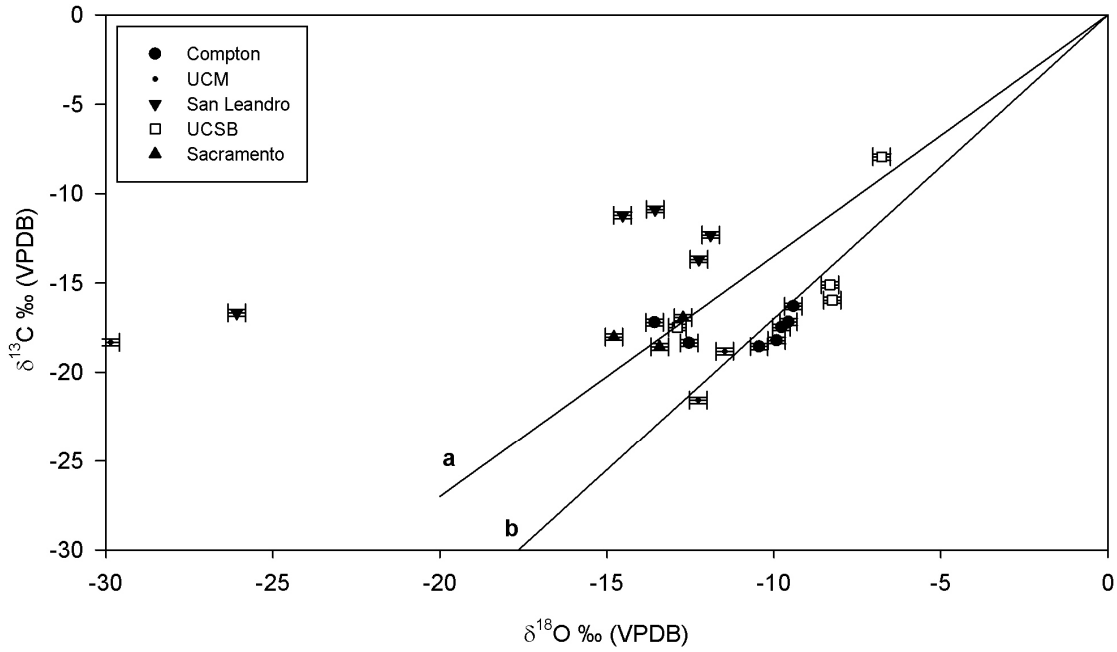

Figure 4.32 – Carbon and oxygen stable isotope analysis of artificial pedogenic carbonates, California. Mixing lines a and b are shown as presented in Figure 4.11.

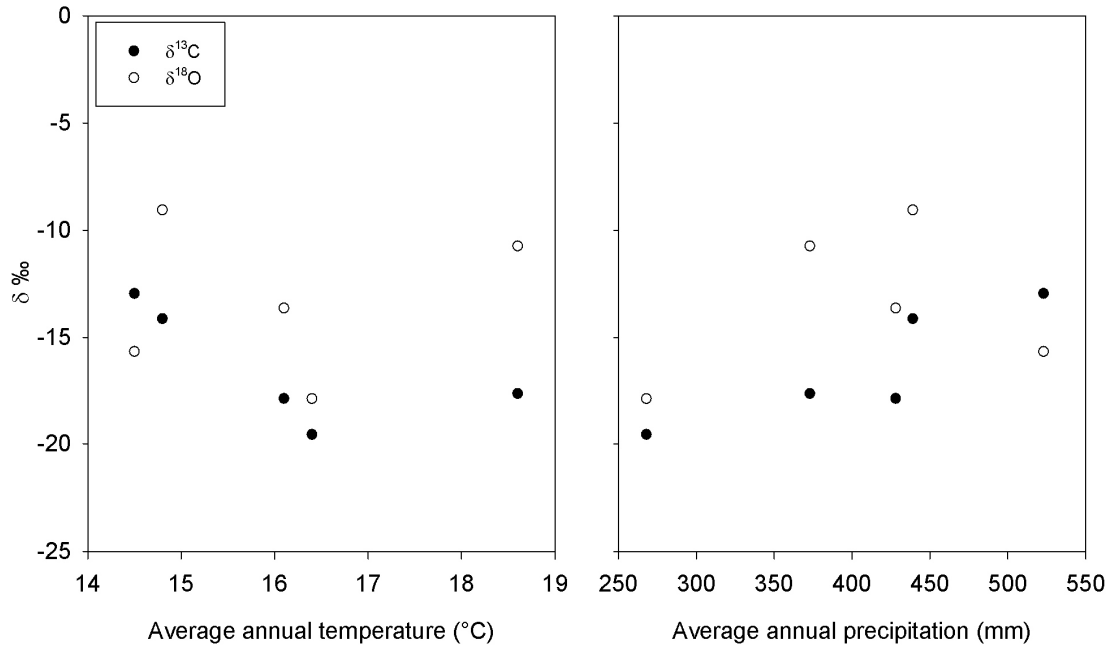

Figure 4.33 – Isotope change with temperature and precipitation.

The isotopic signatures of carbonates formed in soils modified with artificial silicates across California do not show a relationship with climate, suggesting

that temperature and precipitation are not the primary controlling mechanisms in isotope fractionation. This supports the mixing line hypothesis (e.g. Renforth et al., 2009; Andrews et al., 1997) used to establish the quantity of carbon sequestered from the atmosphere compared with the interpretation by Dietzel et al. (2009) which suggests isotopic fractionation due to temperature and precipitation rate variations.

4.9 Conclusions

A review of published literature has shown that carbonate precipitation on silicate rocks is not uncommon in the environment. Stable isotope ratios of naturally occurring pedogenic carbonates demonstrate organic carbon sequestration, with $\delta^{13}C$ between -8 and -10 ‰.

A field investigation of soils developed on natural silicates (Barrasford quarry) have demonstrated that organic carbon was mineralised and sequestered into inorganic carbonate with an upper rate of approximately 900 mgC kg^{-1}(soil) a^{-1}, which is two orders of magnitude quicker than organic carbon accumulation on restored agricultural land (<5 mgC kg^{-1} a^{-1}; Lal, 2003). Carbon concentrations in the soils were up to 8.9 gC kg^{-1}, up to 40% of which was sequestered from the atmosphere.

Carbonate formation is also common on artificial silicate minerals (in cement, slag etc), but the isotopic interpretation is more complex due to fractionation from hydroxylation and diffusion. However, this Chapter develops an existing mixing line hypothesis to interpret carbonate formation in soils perturbed with artificial silicates.

Interpretation of pedogenic carbonate isotopes in soils mixed with artificial silicates suggests that the rate of accumulation is greater than natural soils. If diffusion of CO_2 into solution is rate limiting, then the log precipitation rate is greater than -3.3 mol m^{-3} sec^{-1}, which equates to a carbon accumulation rate of 38 gC kg^{-1} a^{-1} (assuming a surface area of soil 500 m^2 g^{-1}). Field measurements report concentrations of up to 20 gC kg^{-1} (10-15 kgC m^{-2} for 1 meter deep soils which is equivalent or greater than organic carbon concentrations in natural soils) sequestered from the atmosphere on soils in 2-10 a. However, the

conditions in which diffusional fractionation occurs are possibly short lived and the majority of carbonate is produced from hydroxylation.

The soils investigated here unintentionally removed carbon from the atmosphere as a product of the weathering regime. Fieldscale trials are required to investigate the accumulation of carbon in soils designed for carbon capture.

Chapter 5

Chapter 5. Silicate mineral weathering

The ‘unintentional’ accumulation of inorganic carbon has been investigated in the previous chapter for artificial soils. Mineral weathering/carbonation is a well defined process that occurs on geological time scales (as discussed in Chapter 2). Therefore, it is important to understand the processes that may limit the rate in soils (on a human time scale), particularly the supply of divalent metal cations to the carbonate reaction. The aim of the research presented in this chapter is to investigate the weathering of artificial silicates in soils to asses the rate of calcium supply to the carbonate reaction. Although investigations have described the fate of artificial silicates in the environment, there are no data which express weathering as a function of surface area. In this chapter, concrete and cement are weathered in batch trials, using similar methods to those applied to natural silicates. The weathering rate is estimated as a function of geometric and BET determined surface area. Finally, the hydration and calcium-silicon properties of the gels are investigated.

Delivered objective: Key literature was reviewed that broadly describes the field of mineral weathering, and specifically investigates the chemistry of artificial silicates in the environment.

Delivered objective: A series of weathering experiments has been undertaken to quantify the rate of artificial silicate weathering expressed as a function of surface area. Experiments have been conducted using organic acids as a proxy for natural plant root exudates (Chapter 6).

5.1 Mechanisms of mineral weathering

There are four regularly quoted mechanisms of silicate mineral dissolution (see White and Brantley, 1995 for a thorough discussion), which include protonation of the bridging oxygen between the Si and Al tetrahedra, protonation/ deprotonation of dangling surface oxygen atoms, hydrogen exchange with surface cations and complexing of anionic ligands with cations at the surface (particularly those that are multi-valent, primarily Al^{3+} and Ca^{2+}). The first three are thought to be the primary dissolution mechanisms, the rate of which can be expressed as:

Equation 5.1: $$\mathbf{rate} = \mathbf{k_a N_s}\left[\frac{\mathbf{k_H}\,[\mathbf{H^+}]}{\mathbf{1+k_H[H^+]+k_X[X^+]}}\right]^{\mathbf{0.5}}$$

Where K_a is the rate constant, K_H and K_X are equilibrium constants for absorption species, $[H^+]$ and $[X^+]$ are hydrogen and end member cation activities at the mineral surface and N_s is the surface concentration of exchange sites. This equation highlights the importance of pH on dissolution rate which has been empirically confirmed and is represented in Figure 5.1. It can be seen that dissolution rate is greatest at low or high pH.

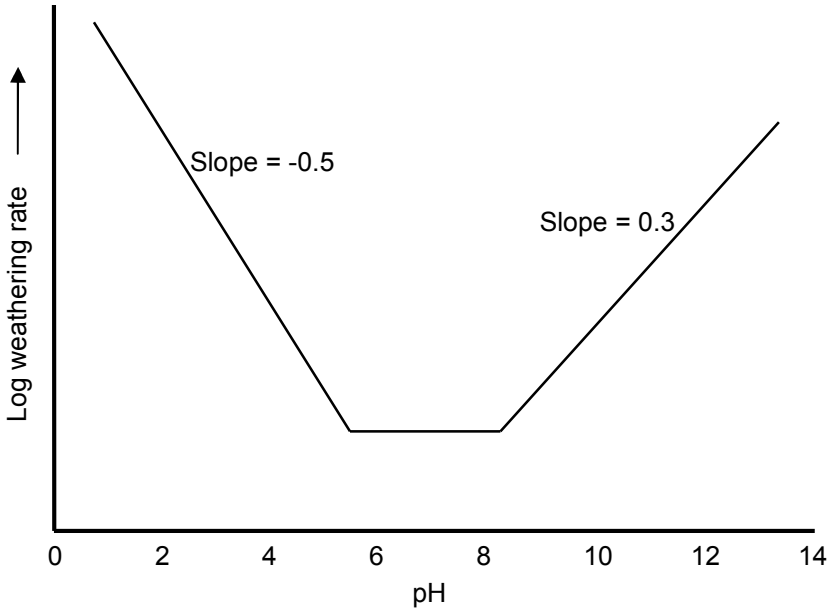

Figure 5.1 – Weathering rate relationship with pH, measured from cation concentrations, Source: Blum and Stillings (1995).

Furthermore, Equation 5.2 demonstrates the importance of the ionic character of the solution on dissolution kinetics, where dissolution is the greatest when the solution is furthest from equilibrium. The rate constant, K_a, is dependent on temperature as described by the Arrhenius equation:

Equation 5.2: $$\mathbf{k_a} = \mathbf{A e}^{\frac{-\mathbf{E_{app}}}{\mathbf{RT}}}$$

Where A is the pre exponential terms, E_{app} is the apparent activation energy, R is the gas constant and T is temperature. The activation energy is the combination of the transport in solution (~21 kJ mol^{-1}) and bond breaking in the crystal (160-400 kJ mol^{-1}).

Complexing of organic acids and inorganic anions with surface cations is thought to increase the rate of dissolution, however, separating the effects of

protonation with those of complexing is difficult, which a limited number of studies have investigated independently (e.g. Berg and Banwart, 2000; Manning et al., 1991).

5.2 Silicate weathering in laboratory studies

In the 1980s, there was a concerted effort to quantify silicate dissolution. The primary laboratory methodologies deployed are usually a variation of batch or flow-through weathering.

Batch weathering describes the process whereby material is placed into a closed container with a fixed volume of solution. The container is agitated over a pre-defined period during which aliquots are removed for analysis. The change in solution concentration of silicon or a metal cation is used to calculate the rate of dissolution as a function of surface area. This is the simplest technique of mineral dissolution experiment and has been used to estimate rate constants for a range of silicate minerals (Velbel and Losiak, 2008; Neaman et al., 2006; White and Brantley, 1995; van Grinsven and van Riemsdijk, 1992). During the dissolution of a silicate it is possible that secondary minerals (kaolinite, calcite etc.) will precipitate on the exposed surface. The precipitation of secondary minerals inhibits further dissolution by reducing ‘active’ surface area and solute concentration. These are the primary limitations when using batch weathering experiments and result in substantially lower rate constants than those determined using flow through weathering apparatus. To mitigate these effects, researchers have periodically replaced the solution.

Amrhein and Suarez (1992) review various experimental factors affecting anorthite dissolution including wetting and drying cycles, drying temperature, variation in agitation methods, particle size and ionic strength. Their conclusions demonstrate the complexity of weathering rate determination, notably a lack of homogeneity in reaction sites across the surface, non uniform weathering profiles through the grain, and the effect of varying agitation on the weathering rate. Weathering profile variation was confirmed by Nesbitt and Skinner (2001) and their finding represented in Figure 5.2, which shows the ‘weathering front’ progressing through the mineral over the course of the experiment.

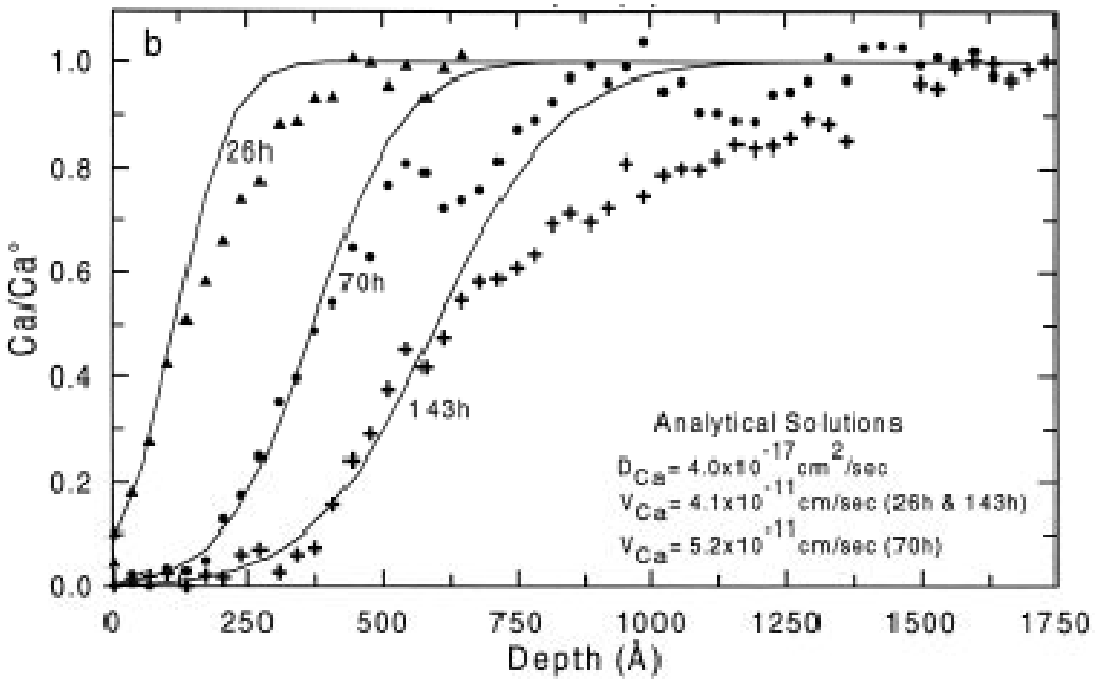

Figure 5.2 – Calcium weathering (ratio of calcium to initial calcium) through the cross section of a grain after 25, 70 and 143 hours of weathering using an ion beam coupled with X-ray photo electron spectroscopy. 1 Angstrom = 10^{-10} m. Source : Nesbitt and Skinner (2001).

In flow-through weathering experiments the solution is continually replaced in well mixed vessels. The concentration of the solute in the effluent is used to calculate the weathering rate over the period of the experiment. Unlike batch weathering trials, a flow- through reactor can be used to minimise the effects of equilibrium and secondary precipitates.

Weathering rates are expressed as a function of surface area, which is determined using a range of methods.

- Geometric surface area (S) is calculated by assuming spherical particles with known diameters and densities (abbreviated in Equation 5.3; Hodson et al., 1998) Chapter 7, Equation 7.7
- Gas absorption of nitrogen on particle surfaces has been used extensively to quantify surface area. The Brunauer-Emmett-Teller (BET) method (Brunauer et al., 1938) is the most commonly used, in which nitrogen gas forms a monolayer at ~77 K. While BET is appropriate for most solids, limitations exist when the material is excessively porous

(Sing, 2001). For BET analysis in this chapter, a Micromeretics Gemini Surface Area Analyser was used at the University of Reading operating at pressures between 0.05 and 0.3 atm.

The limitations of weathering experiments (including the precipitation of secondary phases, variations in ionic character of the solution, experimental procedure, and inaccuracies in surface area calculations) result in large (2-3 orders of magnitude) variations in potential rates (e.g. Table 5.1). A weathering rate determined in the laboratory should be verified by field investigations.

Table 5.1 – Feldspar dissolution rates under varying experimental conditions. Source: Blum and Stillings (1995).

Phase	Solution – acid	Temp (°C)	pH	Epp (kJ mol^{-1})	Log Rate (mol fsp cm^{-2} sec^{-1})
Albite	Acetic (0-70 mM)	100-150	3.4-6	32.2 to117.0	-10.28 to- 14.84
	Oxalic (0-10.0 mM)	25-100	2.9-6.5		-12.90 to-15.57
	Malonic (0-0.1 mM)	70	3.9-10.0		-14.50 to-15.3
Oligoclase	Acetic (0.2 mM)	100	3.4	46.1 to 80.3	-14.66
	Oxalic (0-2.0 mM)	25	2.9-9.0		-14.65 to-16.42
	Citric (5.5 mM)	20	5.1		-16.78
	Mor extract (45.0 g l^{-1})	20	5.1		-16.26
Andesine	Acetic (0-1.0 mM)	25	3.9-9.3		-13.77 to-14.76
	Pyruvic (0-0.1 mM)	25	5.8-6		-14.45 to-14.76
	Oxalic (0-8.0 mM)	25	3.0-9.3		-13.61 to-15.69
	α-ketoglutaric (0-1.0 mM)	25	3.1-9.3		-13.18 to-14.7
Labradorite	Acetic (1.0 mM)	21-60	3.9-4.0	48.1 to 66.4	-14.92 to-15.91
Bytownite	Acetic (0-1.0 mM)	25	3.9-4.9		-12.85 to-14.2
	Propionic (0-1.0 mM)	25	3.9-4.9		-12.64 to-14.2
	Oxalic (0-2.0 mM)	25	3.0-7.8		-12.34 to-15.15
	Succinic (0-1.0 mM)	25	3.6-4.5		-12.25 to-13.35
	α-ketoglutaric (0-1.0 mM)	25	3.8-4.0		-12.10 to-12.89
	Citric (0-10.0 mM)	25	2.7-5.9		-11.89 to-14.12
Anorthite	Acetic (0.2.0 mM)	100	3.4	18.4 to107.0	-14.39
	Oxalic (0-2.5 mM)	25	5.3-6.6		-14.62 to-16
K-feldspar	Acetic (0.1-0.2 mM)	100	3.4-6.0	35.0 to 78.3	-14.37 to-15.59
	Oxalic (0-20.0 mM)	25-70	1.0-9.0		-13.75 to-16.03
	Malonic (0-0.1 mM)	70	3.9-10.0		-14.40 to-15.5
	Citric (0-5.5 mM)	20-25	5.1-5.7		-14.80 to-16.52
	Mor extract (0-45 g l^{-1})	20	5.1		-16.52 to-16.64

The effect of inorganic solutes has been shown to alter the dissolution rate depending on the pH of the solution (Stillings and Brantley, 1995; Schweda, 1990). In high pH solutions, dissolution has been shown to increase with the concentration of cations. Blum and Stillings (1995) suggest that weathering at high pH is controlled by the detachment of Si and the absorption of cations onto deprotonated surface sites. Inorganic ligands (f^-, Cl^- HCO_3^- etc.) promote the dissolution of silicates as a function of their ability to alter the charge

characteristics of the mineral surface, where large heavily charged M-ligands promote larger rates of dissolution (Casey and Ludwig, 1995).

5.3 Silicate weathering at a field scale

5.3.1 Weathering of natural silicates

There is considerable uncertainty when up-scaling the dissolution rates determined from laboratory experiments to field scale. Various factors influence the rate of weathering including soil temperature, soil thickness, the composition of the parent material, vegetation type and density, and precipitation frequency and intensity (see Dessert et al., 2003; Oliva et al., 2003; White, 1995).

Using chemical flux data (Dessert et al., 2003; Oliva et al., 2003; Moulton et al., 2000; see Appendix C1) the logarithmic mineral weathering rate for silicates at field scale can be estimated to be between -12 and -17 mol m^{-2} sec^{-1} (assuming a surface area between 0.1-10 m^2 g^{-1}, a soil depth between 1-3 m, and a density between 1.8-2.5 t m^{-3}). It can be seen that the weathering rates are broadly several orders of magnitude slower than those determined in the laboratory (Table 5.1). The explanation given by White (1995) attributes this discrepancy to a range of factors including soil age, saturation, hydrological heterogeneity and climate. All of them can act to reduce the weathering rate at field scale.

5.3.2 Biological enhancement of weathering

Recent research attempts to quantify the role of plants, microflora and microorganisms in mineral weathering for a range of environments, typically in order to understand the supply of rate limiting trace nutrients to ecosystems (van Breemen et al., 2000; Rogers et al., 1998; Jackson and Voigt, 1971).

van Hees et al. (2002), Moulton et al. (2000), and Cochran and Berner (1996) investigate the role of plants, particularly organic root exudates, on the dissolution of feldspars. All three studies demonstrate increased weathering induced by organic compounds.

Using weathering fluxes on vegetated and un-vegetated areas of Iceland, Moulton et al. (2000) were able to show the effect of plants on the weathering rate of plagioclase (x2 increase) and pyroxene (x4 increase). van Hees et al.

(2002) demonstrated similar increases in bed reactors for microcline and labradorite at pH 5. Cochran and Berner (1996) investigated the weathering of young basalts by vascular plants and lichen on Hawaii, USA. They suggest that vascular plant roots play a more important role in basalt weathering than microflora. Balogh-Brunstad et al. (2008) determined the log rate of weathering of biotite and anorthite to be approximately -6.5 mol (∑cations) m^{-2} sec^{-1} in experiments cultured with a range of microorganisms compared to -7.6 mol (∑cations) m^{-2} sec^{-1} in the abiotic control.

Using carbon isotopic signatures in drainage waters, Das et al. (2005) were able to separate silicate and carbonate weathering on the Deccan Traps in India, They compared the $\delta^{13}C$ isotope ratio against the Si/HCO_3^- content of water courses and discovered a strong negative correlation ($r^2 = 0.80$). Values with low Si/HCO and heavy $\delta^{13}C$ values are said to be influenced by carbonate geology, whereas, a water course with a light $\delta^{13}C$ value and a high Si/HCO_3^- is said to be influenced by silicate geology, suggesting elevated weathering due to biotic processes.

5.3.3 Field scale weathering of artificial silicates

The environmental impact of artificial silicates produced in human material streams is poorly understood. This section expands on the summary presented in Chapter 3 Section 7 to describe the weathering processes of these materials.

It is estimated that 60 Gt of cement have been produced since 1926 (see Chapter 3), most of which was initially used in the construction industry (although 9-12 Gt of cement dust were immediately disposed of or stockpiled). The fate of this material in the environment is not completely understood, but can be estimated through an analysis of historic waste management practices and observational evidence. For example, carbonate precipitation is typically reported on the outer surface of concrete structures (Krishnamurthy et al., 2003) suggesting weathering and precipitation in close proximity. In the Biosphere 2 experiment, carbonation of the concrete surfaces in the enclosure removed CO_2 more efficiently than photosynthesis was able to convert it to oxygen resulting in the failure of the study (Severinghaus et al., 1994). Similarly, concrete used in contact with shallow groundwater, where the dominant anion is HCO_3^-

(Chebotarev, 1955) often shows signs of carbonation (Plate 5.1 and Dietzel et al., 1992).

Plate 5.1 – Arlanda airport underground train station, Stockholm, Sweden (taken by the Author February 2010). Note, the concrete tunnel lining shows evidence of carbonation.

Demolition of a structure produces a solid waste that is often categorised with construction waste as 'C&D waste'. The disposal of solid waste into the environment was uncontrolled until the introduction of legislation in the 1960s and 1970s (see Pichtel, 2005). It is possible that this material has substantially weathered and carbonated, although no evidence is available to support this. The introduction of the Environment Act 1995 in the UK stipulated that solid waste be disposed of into controlled landfill. Landfill cells have a heterogeneous composition and it is difficult to separate the weathering regime of C&D waste in landfill leachate. That withstanding, Bennett et al. (2000) and Manning (2001) have independently demonstrated that carbonate minerals are a typical precipitate in landfill leachate. This is confirmed in laboratory simulations (Townsend et al., 1999), and highlights the importance of organic compounds to accelerate the weathering of cement and supply carbonate through

mineralisation. This is confirmed by Bertron et al. (2005), who used organic acid composition of silage effluent to simulated the degradation of concrete retaining structures. It is unknown to what extent cement products in landfill have already carbonated, but it is possible that the material has not fully weathered/carbonated. Presently, the introduction of landfill tax (£48 t^{-1} for active wastes, rising £8 t^{-1} a^{-1}, and £2.50 t^{-1} for inert wastes) and the aggregates levy (£2 t^{-1}) has promoted the reuse of C&D waste as secondary aggregate. The most recent (but outdated) figures for C&D waste suggest that half is disposed of in landfill (DCLG, 2007).

The dissolution rate of concrete was investigated by Galle et al. (2004), who showed the degradation rate is proportional to exposed surface area. Interpreting the authors' data the logarithmic weathering rate was found to be between -4.5 and -3.9 molCa m^{-2} sec^{-1}. They found that pH was rapidly buffered at 9.5 throughout the experiment, which was conducted on concrete cylinders (40 mm in diameter and 80 mm in height).

The fate of cement products used underground has been extensively studied as part of the Nirex Safety Assessment Research Programme investigating underground storage of radioactive wastes (e.g. Hodgkinson and Hughes, 1999; Rochelle et al., 1998). Laboratory experiments, investigations of naturally occurring cement minerals, geochemical modelling and studies on historical mortar have shown that cement gels are potentially stable for 10^3-10^6 years in groundwater and surface systems. The weathering products are dependent on host geology, and carbonate precipitation/ dissolution is controlled by the supply of dissolved inorganic carbon.

Since 1875 12-16 Gt of slag have been created as a by-product of the iron and steel industry (see Chapter 3). Similar to cement waste, a proportion of this material has been disposed of, uncontrolled, into the environment. The evidence of this is present adjacent to former iron and steel works where large stockpiles of slag have been incorporated into the landscape (Bayless and Schulz, 2003; Harber and Forth, 2001). Subsequent analysis of this environment has demonstrated carbonate formation in the drainage regime and soil (Renforth et al., 2009; Mayes et al., 2006). Analysis also shows continued weathering (and carbonate precipitation) 30 years after the material was

deposited, which demonstrates that this material may be exploited for additional carbonation.

7-15 Gt of ash have been produced since 1927 as a by product of coal combustion. The fate of this material in the environment is unknown but it is often stockpiled adjacent to the point of production (see Chapter 3). Analysis of metal concentration in an ash stockpile shows the presence of potentially toxic metals and elevated pHs (Lee and Spears, 1997). Modelling this data using Solmineq (Kharaka et al., 1988) demonstrates that carbonate minerals are likely to precipitate (Figure 5.3).

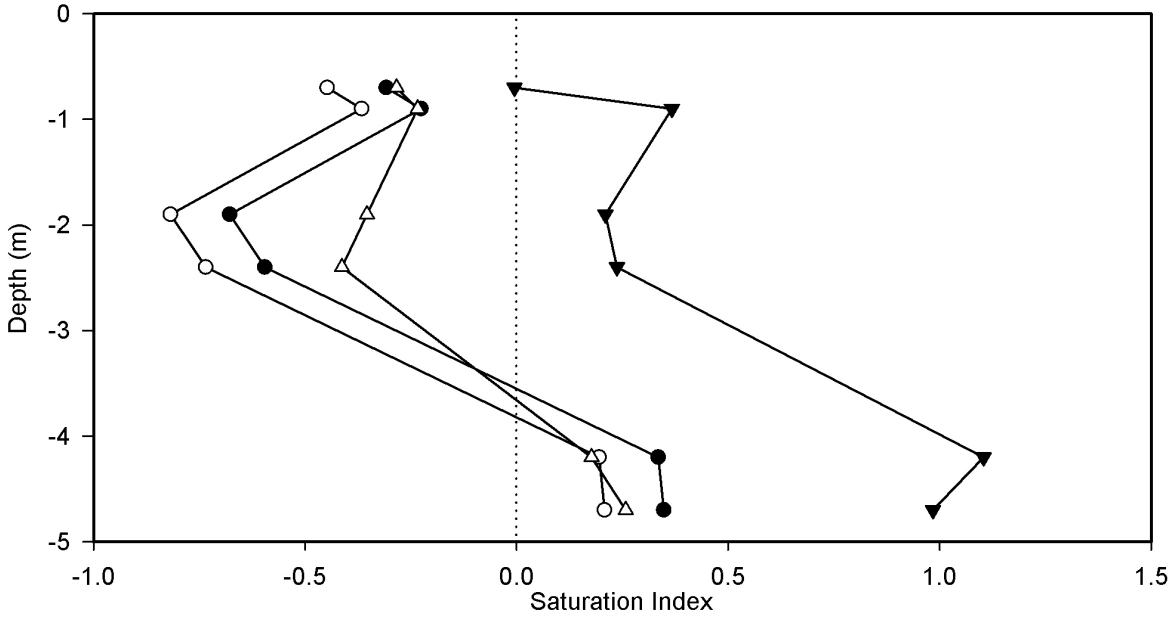

Figure 5.3 – Saturation index predicted using Solmineq from data presented in Lee and Spears (1997). ○ –Aragonite, ● – Calcite, Δ – Cerrussite, ▼ – Dolomite.

The investigations described above demonstrate both the longevity and lability of silicate glasses/gels in the environment, which carbonate readily when exposed to dissolved CO_2.

5.4 Calcium silicate minerals, gels and glasses

5.4.1 Silicate glasses and gels

Artificial silicate rich material produced from high temperature processes are usually associated with (or wholly consisting of) amorphous gels or glasses. Glasses and gels are composed of poorly crystalline amorphous material and

are typically described using the crystalline mineral counterpart, for instance calcium silicate hydrate (C-S-H) gels found in cement are often regarded as ‘tobermorite-like’ or ‘jennite-like’(Chen et al., 2004). Common artificial calcium silicate minerals are presented in Table 3.2 (Chapter 3).

A study comparing the weathering rate of an albite glass to its crystalline counterpart has demonstrated enhanced cation leaching from the surface layer by 2-3 orders of magnitude greater in the glass (Hamilton et al., 2000).

While silicate glasses and gels are the largest component of some human material streams, they are often associated with other minerals. Free lime (CaO) and portlandite ($Ca(OH)_2$) are typical constituents of cements, slags and fly ashes, and readily carbonate in the presence of dissolved CO_2. $Ca(OH)_2$ dissolves in water with a solubility constant of approximately 5.19 (Duchesne and Reardon, 1995) and buffers the pH to >11. Reardon and Fagan (2000) suggest that portlandite placed in subsurface environments will convert to calcite acting as a sink for gaseous CO_2. Gypsum ($CaSO_4.2H_2O$) is added to cement clinker during production which reacts with $Ca(OH)_2$ and alumina during hydration to form ettringite ($Ca_6Al_2(SO_4)_3(OH)_{12}.26H_2O$). Ettringite is stable at pH>10.7, below which it dissolves to from gypsum and aluminium hydroxides (Myneni et al., 1998).

Cement is a complex mixture of unhydrated cement clinker, poorly crystalline C-S-H gels, portlandite, gypsum and ettringite. Furthermore, iron, aluminium and magnesium may be incorporated into the silicate framework. For simplicity, solubility characteristics have been determined for pure C-S-H gels (Chen et al., 2004; Rothstein et al., 2002; Jennings, 1986). Solubility is considered a function of the Ca/Si ratio in the solid, which is related to mean chain length in a silicate (Figure 5.4). A comprehensive study of the solubility of a range of cement minerals is presented in Matschei et al. (2007). The calcium contents in Figure 5.5 are those from pore fluids in equilibrium with cement minerals, and do not relate to the rate of weathering.

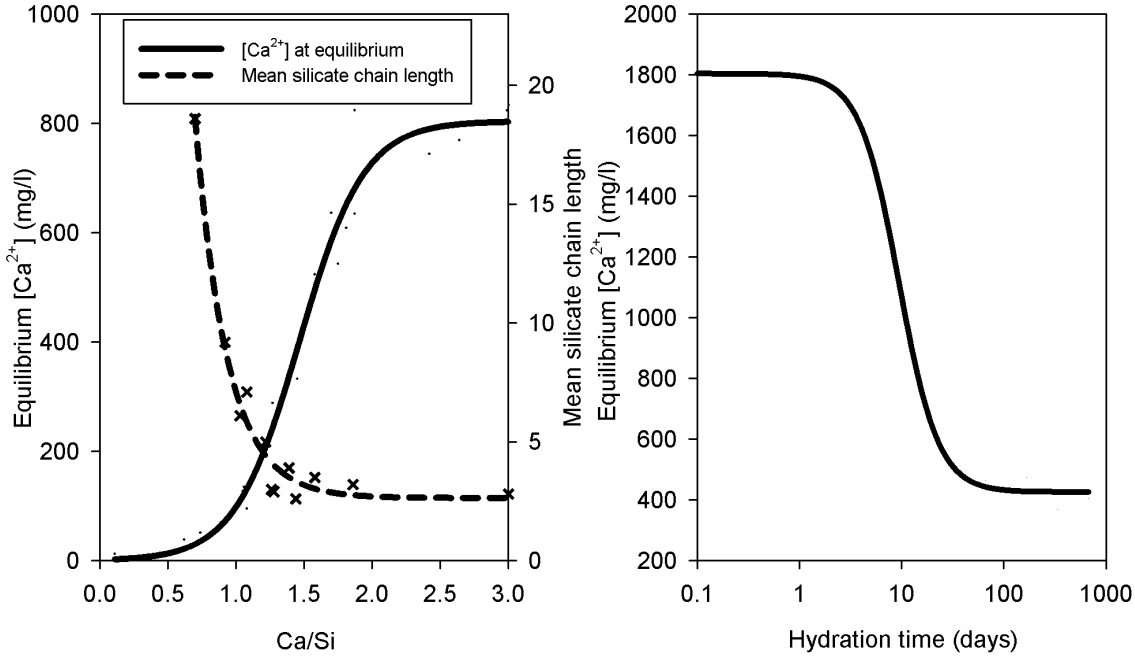

Figure 5.4 – Solubility of C-S-H as a function of Ca/Si ratio in the solid and hydration time, Source: adapted from Chen et al (2004) Rothstien et al. (2002).

5.4.2 Identification using X-ray diffraction (XRD) and thermogravimetric (TGA) analysis

X-ray diffraction (XRD), a standard mineral identification technique, is inappropriate when routinely analysing amorphous material (as the glasses and gels appear as a poorly defined 'hump' on the diffractogram). XRD has been successfully employed to investigate the structure of hydrothermally formed crystalline phases in cements (Shaw et al., 2000a) which are chemically related to the C-H-S gels but are stable at different temperatures (Figure 5.5).

Small/wide angle X-rays scattering coupled with thermogravimetric/differential scanning calorimetry has been used to characterise the breakdown of hydrated minerals under varying thermal conditions (Shaw et al., 2000b). The results demonstrate dehydroxylation and water loss from the hydrated minerals (Table 5.2) and subsequent re-crystallisation into low temperature wollastonite at approximately 750-800°C.

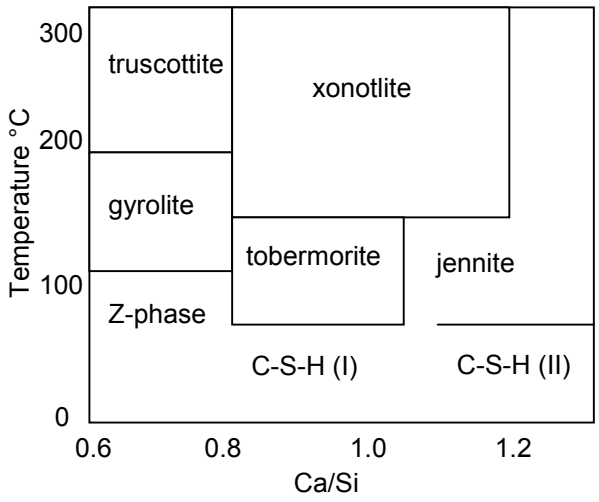

Figure 5.5 – Stability diagram for calcium silicates under hydrothermal conditions. Source: Shaw et al. (2000a).

Table 5.2 – Thermogravimetric analysis of calcium silicate hydrate minerals. Source: Shaw et al. (2000b).

Mineral	CaO%	Ca/Si	H_2O%	Dehydroxylation temperature (°C)
Xonotilite	46.9	1.0	2.5	750-800
Tobermorite	35.2	0.8	12.2	20-320
Hillebrandite	58.7	2.0	9.5	450-650

5.5 Knowledge gaps and experimental methodology

While studies have investigated the impact of artificial silicate weathering on the environment and the solubility characteristics of individual cement minerals, there are no data that express weathering rates as a function of surface area. Weathering rates expressed in this way are used to up-scale to the catchment size, and are important when considering the potential of soils to capture carbon. To this end, the experiments described in this chapter used methodologies developed to investigate weathering of natural silicates for the determination of cement weathering rate. Ordinary Portland Cement (OPC; Lafarge – see Appendix B.2.1 for chemical composition) has been used because of its ubiquity and relatively safety when handling, but is used in the discussion to broadly describe the weathering rate of amorphous artificial calcium silicates. Silica fume (Tarmac – see Appendix B.2.1 for chemical composition) was used to control the calcium-silicon ratio. The approach taken is similar to that presented by environmental engineers investigating the potential of wastes to contaminate

the environment (e.g. Dijkstra et al., 2006). Dijkstra et al., (2006) investigates the leaching behaviour of municipal solid waste bottom ash. Using partially characterised material these authors provide data that connects theoretical individual phase dynamics (presented in earlier papers) with real environmental conditions. The investigations presented herein provide estimates of weathering characteristics of hydrated cements without full characterisation of individual phases in the material. To simulate the enhanced weathering conditions in soils, a citric acid - sodium citrate buffer was used (organic acids are discussed in greater depth in Chapter 6).

5.6 Methodology

5.6.1 Batch weathering of concrete (Experiment 5A)

Concrete manufactured at Newcastle University was crushed to passing 3 mm. The composition of the concrete was approximately 1 part by volume of OPC, 2 parts by volume silica sand (63 μm < Φ < 150 μm) and 3 parts per volume coarse (~5 mm) aggregate (partially weathered dolerite supplied by Tarmac Ltd. from Barrasford Quarry, Northumberland). 10 g of the material were measured into 250 ml centrifuge bottles and mixed with 100 ml of solution (deionised water or 10 mmol l^{-1} sodium citrate buffered to an initial pH 5). Solution aliquots were taken at 1, 3, 5, 10, 20, 40, 60, 80 and 100 day time intervals after solid solution separation using a Sorvall RCSB PLUS centrifuge at 9000 rpm for 15 minutes. All of the solution was removed and replaced after each sampling interval to minimise equilibrium effects. The aliquots were filtered and analysed for calcium using AAS (Appendix A.10).

5.6.2 Batch weathering of calcium silicate hydrate to analyse changes in solution chemistry (Experiment 5B)

Cement is composed of various calcium rich minerals namely portlandite formed from hydrated free lime ($Ca(OH)_2$), calcium silicate hydrate gels and minerals ($Ca_xSi_yOH_z$), un-reacted calcium silicates (e.g. belite - Ca_2SiO_4), gypsum ($CaSO_4.2H_2O$) and ettringite ($Ca_6Al_2(SO_4)_3(OH)_{12}.26H_2O$) and calcite ($CaCO_3$). Hydrated cement contains approximately 15 wt% portlandite (Scrivener et al., 2004), which is an important constituent when considering the carbon capture potential of cement based materials. However, it is important to

distinguish between this and the weathering rate of calcium silicate gels, which form the largest constituent of hydrated cements.

To this end, cement clinker was hydrated in controlled conditions to limit the formation of free lime/portlandite and subsequent carbonation of these materials. Deionised water was boiled for 30 minutes to remove dissolved CO_2 and allowed to cool in a depressurised desiccator (approximately 0.7-0.8 atm). 36.9-57.5 g of OPC cement clinker were mixed with 42.5-63.1 g of oven dried powdered silica fume and hydrated using 20 ml of CO_2 stripped deionised water (Table 5.3).

Table 5.3 – Hydrated cement properties for batch weathering experiments.

Material	Mass of cement (g)	Mass of silica fume (g)	Ca/Si Ratio (confirmed using XRF)	Carbonate content after hydration wt %	Hydration % (LOI% – carbonate % expressed as CO_2)	BET surface area (m^2 g^{-1})
1	36.9	63.1	0.54	2.31	7.23	29.10
2	44.8	55.2	0.66	2.66	7.33	20.39
3	57.5	42.5	1.03	2.88	8.18	14.76

The resulting mixtures were cured at ambient laboratory temperatures (~20°C) over 14 days, crushed using a Siebtechnik Tema mill, rehydrated with an additional 10 ml of CO_2 stripped deionised water, and left for 10 days in the depressurised desiccator. The cured material was hand crushed using a pestle and mortar, oven dried to constant weight and sieved between 150 μm < Φ < 212 μm. The absence of free lime (<0.1% CaO) was determined using the method described in Appendix A.7. XRF and loss on ignition analysis interpreted using the lever rule (e.g. Manning 1995) indicate that the material is likely to have some (<7-30 %) un-hydrated cement clinker (Figure 5.6), the presence of which was confirmed using XRD analysis. However, all samples contained similar quantities of hydrated cement. A normally distributed surface area for the grain size was calculated geometrically as 0.03 m^2 g^{-1}. However, BET analysis suggests a surface area three orders of magnitude greater at 29.10, 20.39 and 14.76 m^2 g^{-1} for Ca/Si ratios of 0.54, 0.66 and 1.03 respectively, which suggests the presence of an internal surface area or smaller particles attached to the surface of the larger particles (confirmed later using SEM).

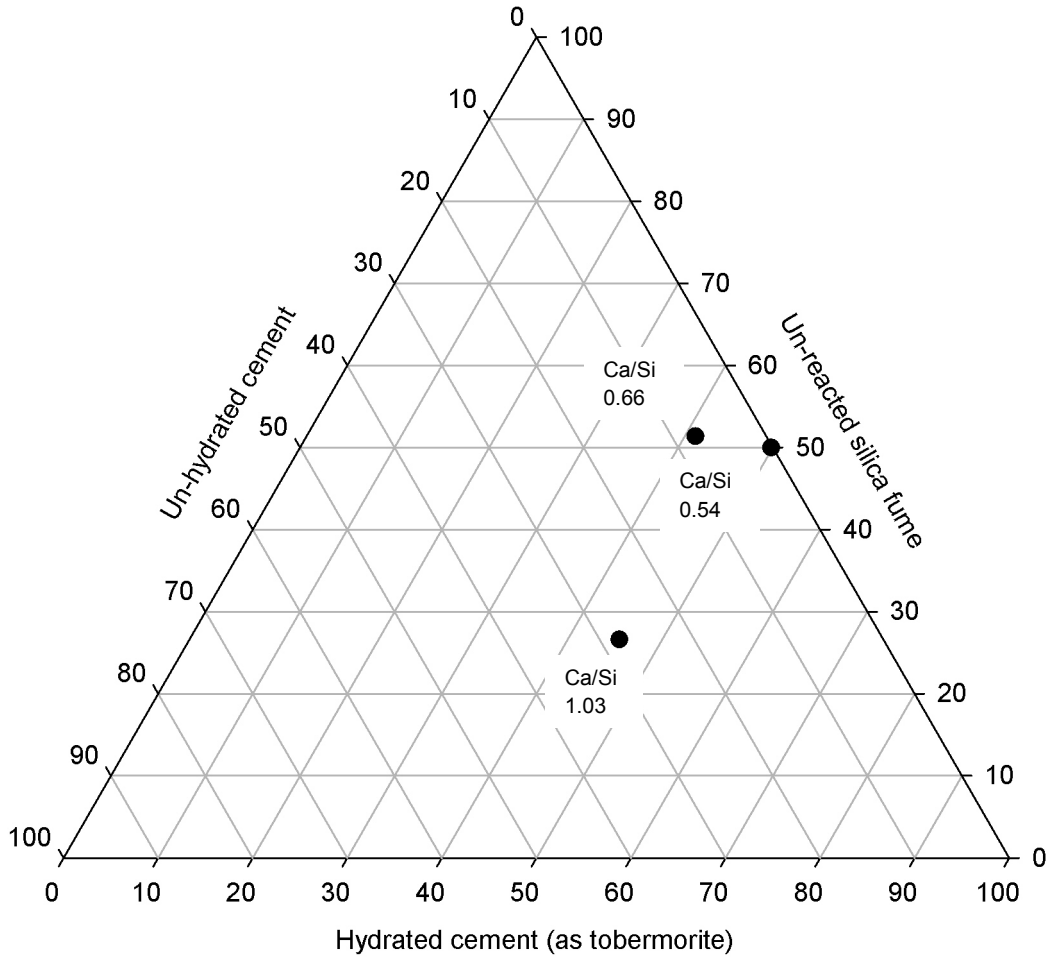

Figure 5.6 – Interpretation of XRF data, <7 – 30 % of the material remains as un-reacted cement clinker.

0.2 g of each hydrated cement sample were measured into 250 ml centrifuge bottles and immersed in 150 ml of 10 mmol l^{-1} sodium citrate solution buffered to pH 5. The mixture was shaken and aliquots were taken after 1, 2, 3, 4 and 5 hours, wholly replacing the solution at each interval, and analysed for calcium using AAS. This is a development on the method used in the previous batch weathering experiments in order to reduce the experimental running time, while simultaneously increasing the temporal resolution by increasing the surface area to solution ratio. Furthermore, the method described here reduces the dilution factor for AAS and subsequently the magnitude of the repeatability error, which is especially important when considering cumulative effects. The experiment was repeated using deionised water instead of the sodium citrate buffer solution.

5.6.3 Batch weathering of calcium silicate hydrate to determine solid material transformations (Experiment 5C)

A further experiment was undertaken to determine the change in solid material composition as a result of weathering.10 g of each material was immersed in 150 ml of sodium citrate buffer solution for 1 week. The solution was centrifuged, filtered, acidified, diluted and analysed for calcium concentration using AAS. The material was oven dried over night and analysed for calcium carbonate as detailed in Appendix A.1. Images were taken using an Environmental Scanning Electron Microscope (Appendix A.8) to compare the raw and weathered material. The mineralogy of the samples was investigated using XRD (Appendix A.4).

5.6.4 The effect of Ca/Si ratio on hydration (Experiment 5D)

Prior to batch weathering of controlled calcium silicate hydrate gels, an investigation was undertaken to determine the effect of silica fume on the hydration of cement paste. OPC and silica fume were mixed in varying quantities to create desired Ca/Si ratios (Table 5.4). The material was hydrated with CO_2 stripped deionised water and cured over 20 days in a depressurised dessicator. The solid material was powdered using a Siebtechnik tema mill. Using thermo-gravimetric analysis (Appendix A.9) the mass change was measured during heating up to 900 °C.

5.7 Results and Discussion

5.7.1 Batch weathering of concrete (Experiment 5A) - Results

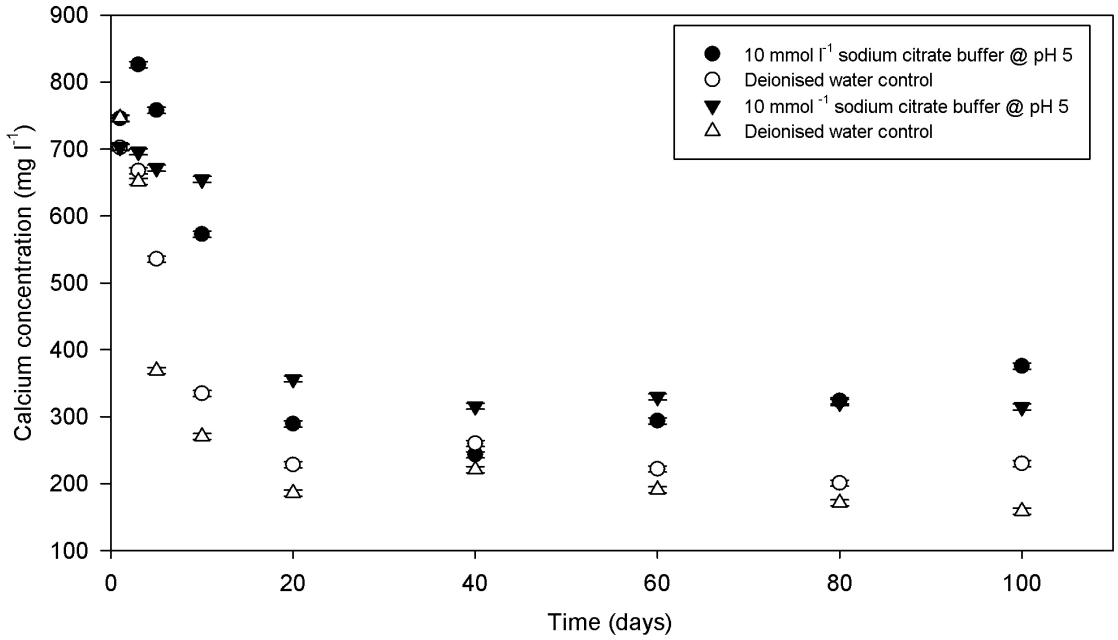

Figure 5.7 – Calcium content of the solution during the weathering of concrete. Error bars represent repeatability.

The calcium content decreased rapidly between 0 and 10 days (Figure 5.7) for all treatments, the largest decrease being that with sodium citrate (826 to 314.5 ± 4.5 mg l^{-1}) compared (P=0.03) with deionised water (746.5 to 158.8 ± 4.5 mg l^{-1}). The pH was measured before and after replacing the solution (Figure 5.8). Although a sodium citrate buffer was used, it can be seen that the pH fluctuated between 11.3 and 12.3, and a rapid decrease of pH (to between 11.9 and 9.4) was noted after the refreshing of the buffer solution.

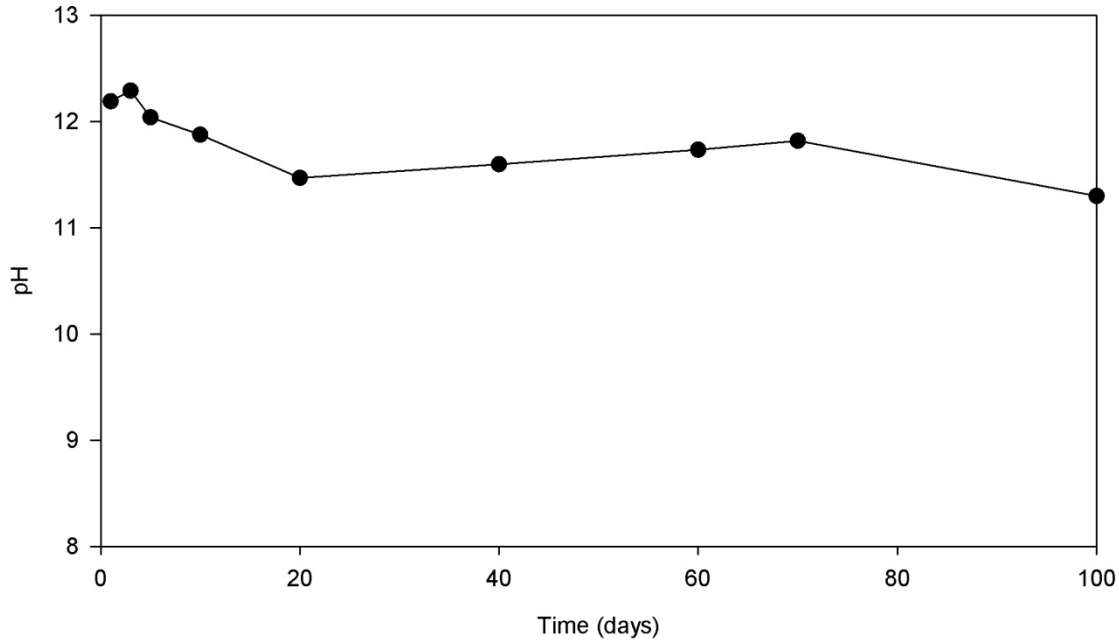

Figure 5.8 - Solution pH, aggregated and averaged for both solid and solution composition experiments. Repeatability error is within the size of the data point.

To analyse the change in solid composition, the trial was repeated for 40 days using the same sodium citrate solution and sacrificial treatments (where the solid was removed at the appropriate time interval). The solids were oven dried and analysed for carbonate content using an Eijkelkamp calcimeter (Appendix A.1). Figure 5.9 presents the change in carbonate content of the solid. The carbonate content increased to 5.2 ± 0.6 wt% in 10 days. This fits to the sigmoidal relationship (Equation 5.4 r^2 = 0.99).

Equation 5.4 $$y = 0.3 + 4.8\ (1 - e^{-2.2x})^{1.5\times10^5}$$

Differentiating and solving for x = 8 provides an estimate of the maximum rate of growth = 0.713 wt% day^{-1} or 8.5 mgC day^{-1} for a 10g sample.

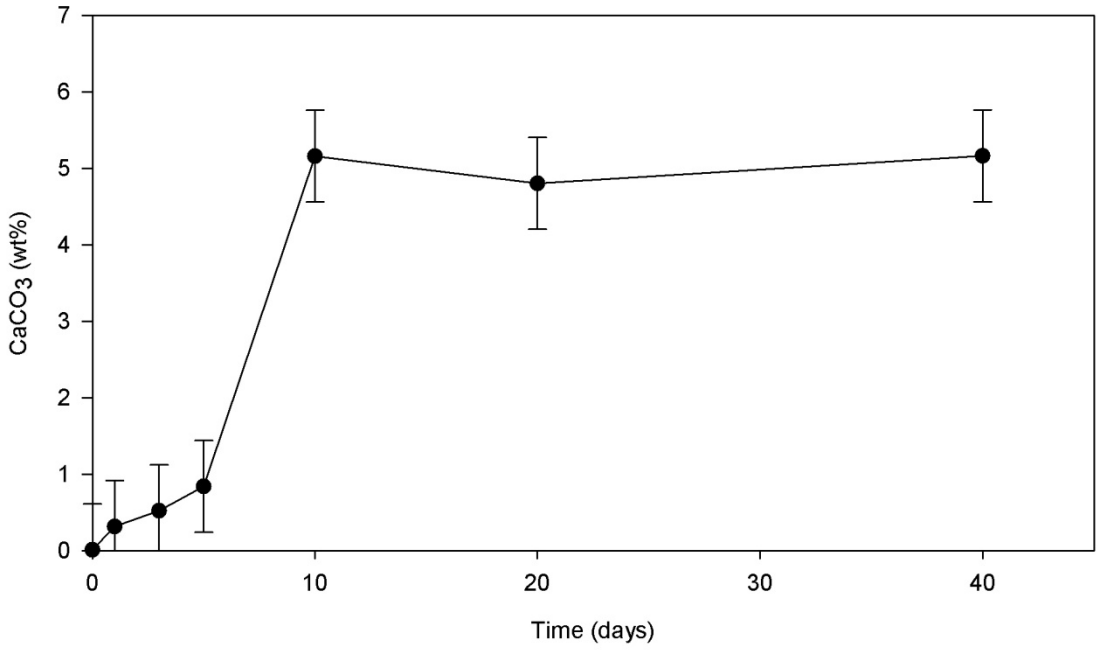

Figure 5.9 - Carbonate content of solid during weathering of concrete in Na-buffer solution. Error bars represent repeatability.

Repeating the experiment for 30 days, the matrix was tested for sensitivity against particle size and initial solution pH. Concrete samples were sieved so that the diameter of particle was between 63 μm < Φ < 212 μm and 300 μm < Φ < 600 μm. 10 g of solid were immersed in 150 ml of 10 mmol l^{-1} sodium citrate solution buffered to pH 3, 5 and 6. Aliquots were taken at 1, 3, 7, 15 and 30 day intervals, completely replacing the solution at each interval. Silica sand was used as a control solid.

Similar to the previous batch weathering experiment, the cumulative calcium content decreased between 966 and 136 ± 43.8 to 87.6 mg l^{-1} over 30 days of weathering (Figure 5.10), and pH fluctuated between 11.8 and 12.5 (with no discernable difference between the various concrete treatments, but the pH 3 and 5 solutions were significantly different (P=0.02) and the silica sand control pH was successfully buffered at 3 and 5 but failed at 6; Figure 5.11). Concrete weathered in pH 3 sodium citrate returned the largest (statistically significant when compared to the pH 5) cumulative calcium content.

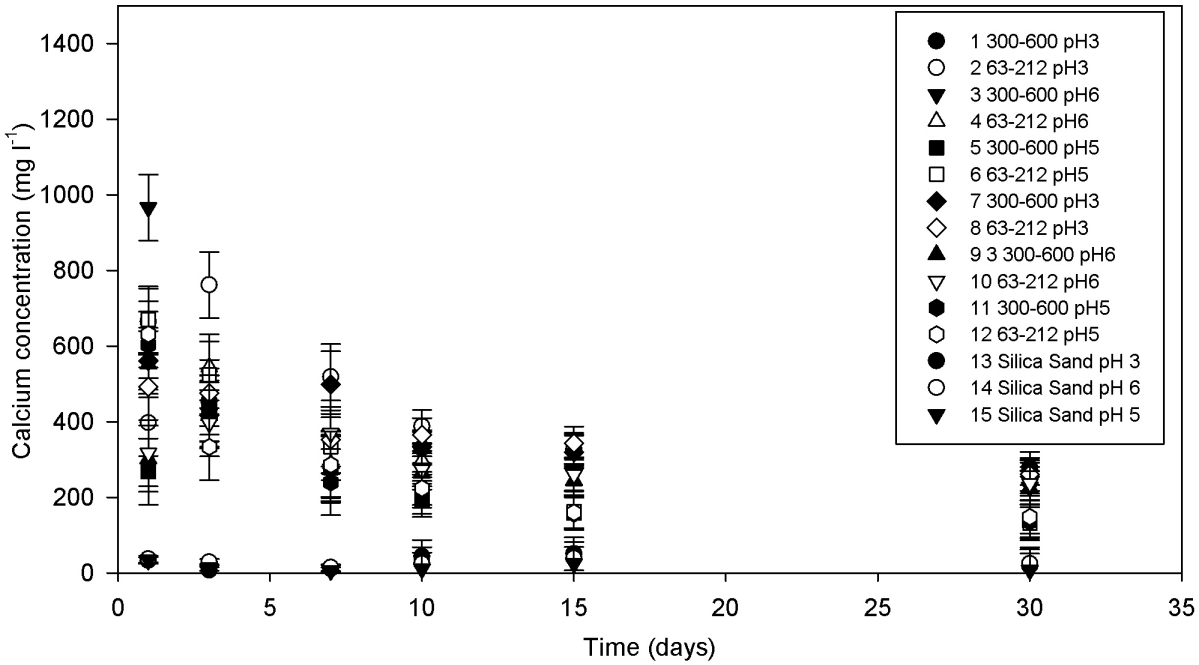

Figure 5.10 – Calcium concentration in solution during repeated batch weathering of concrete varying particle size and pH. Error bars represent repeatability.

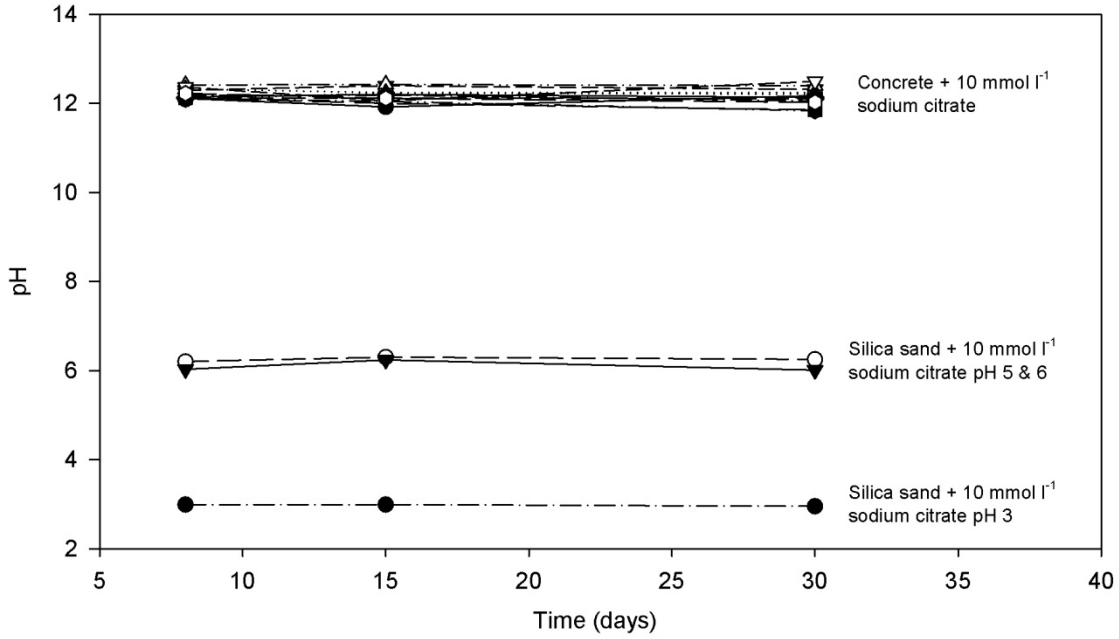

Figure 5.11 – pH of concrete weathering experiment. Repeatability error is within the size of the data point.

5.7.2 Batch weathering of concrete (Experiment 5A) - Discussion

Concrete weathering tests show calcium readily leaches from the material. The geometric surface area of grain sizes normally distributed between 63 μm < Φ <

212 μm and 300 μm < Φ < 600 μm range from 0.003-0.018 m^2 g^{-1} respectively (using Equation 7.7 Chapter 7). Therefore, the log weathering rate can be expressed as between -3.85 to -2.90 molCa m^{-2} sec^{-1} for respective particle size distributions. These values are several orders of magnitude larger than those recorded for natural silicate weathering, but are similar to that measured by Gaulle et al. (2004).

The chemical composition of the concrete as a composite material was not confirmed, but can be estimated using the chemical composition of OPC, dolerite (Randall, 1989) and densities for OPC, silica sand and crushed dolerite. Using the calcium content of the material (~16 wt%CaO), it is estimated that between 10.8 wt% and 20.3 wt% of the calcium was leached in 30 days (Figure 5.12; Appendix C.3 for calculations).

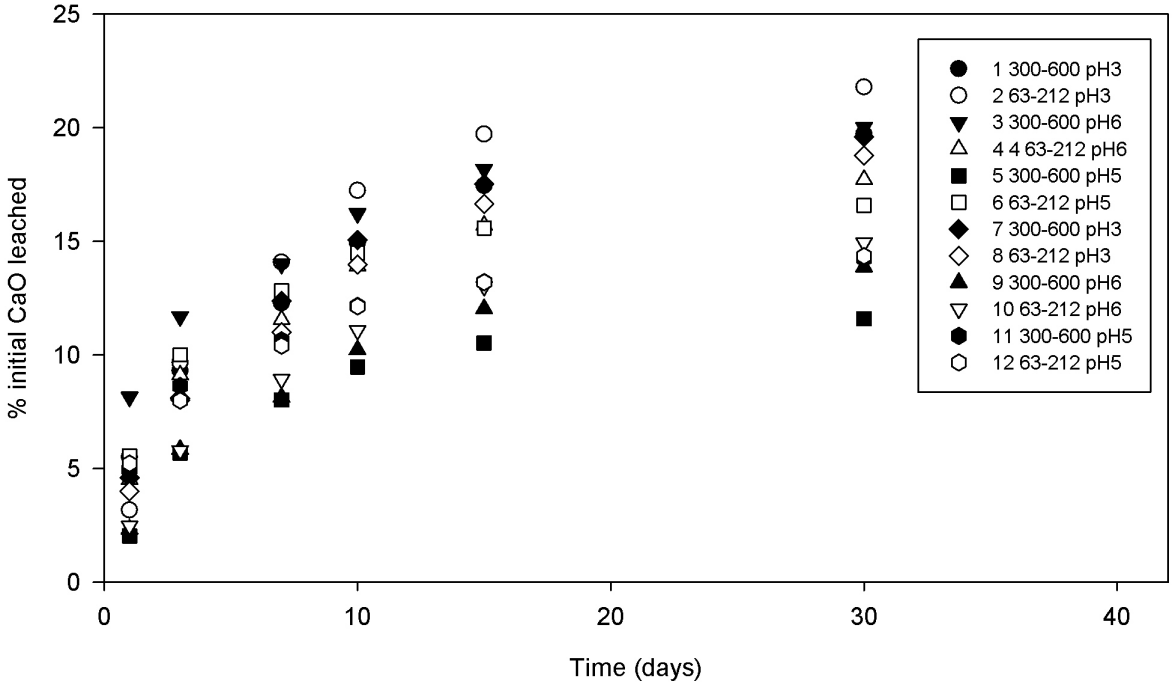

Figure 5.12 – Weathering expressed as a % of the total calcium content of the material.

5.7.3 Batch weathering of calcium silicate hydrate to analyse changes in solution chemistry (Experiment 5B) – Results

The calcium content in the solution decreased with each successive sampling to 129.6 to 3.2 ±1.7 mg l^{-1} over the 5 hour experiment (Figure 5.13; a significant difference ($P<0.001$) over the control deionised water which decreased between 17.8 and 6.4 ± 1.7 mg l^{-1}). The solid with the Ca/Si ratio = 1.03 leached

significantly more calcium into solution (P=0.006), with no discernable difference between the other two Ca/Si ratios. pH was successfully buffered between 5.01 and 5.60 over the 5 hours (the control was not buffered and fluctuated between 9.7 and 10.5 (Figure 5.14).

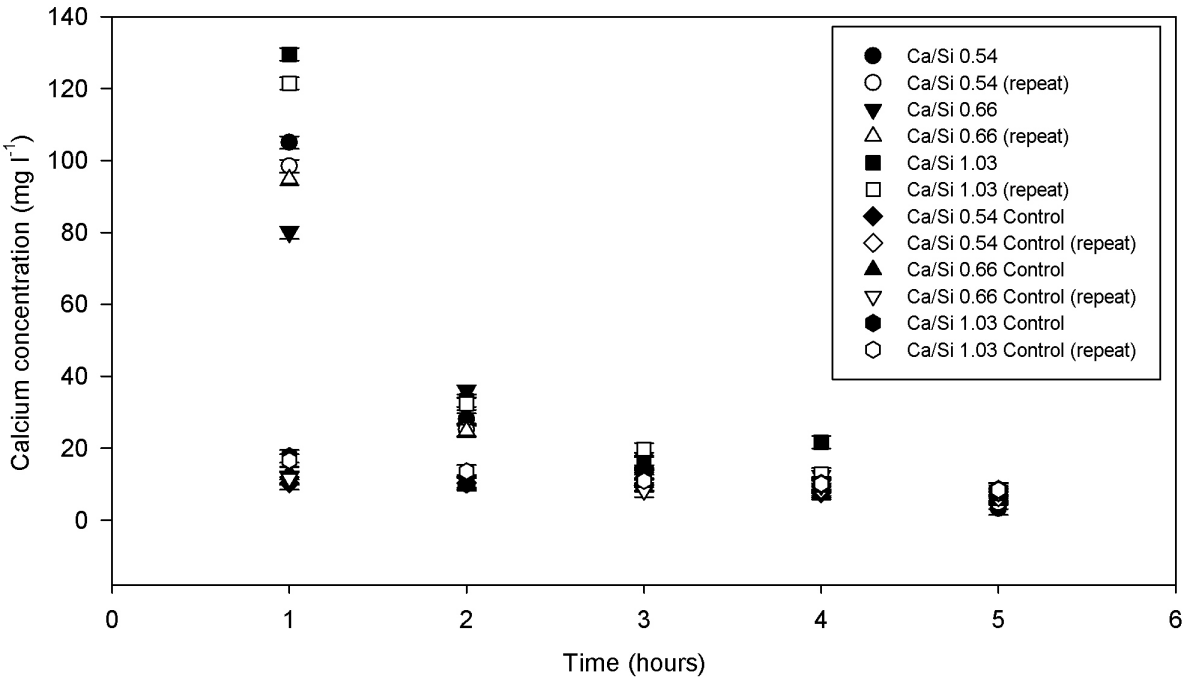

Figure 5.13 – Calcium concentration in solution during C-S-H weathering in Na-citrate solutions and deionised water control. Repeatability error bars are within the size of the data point.

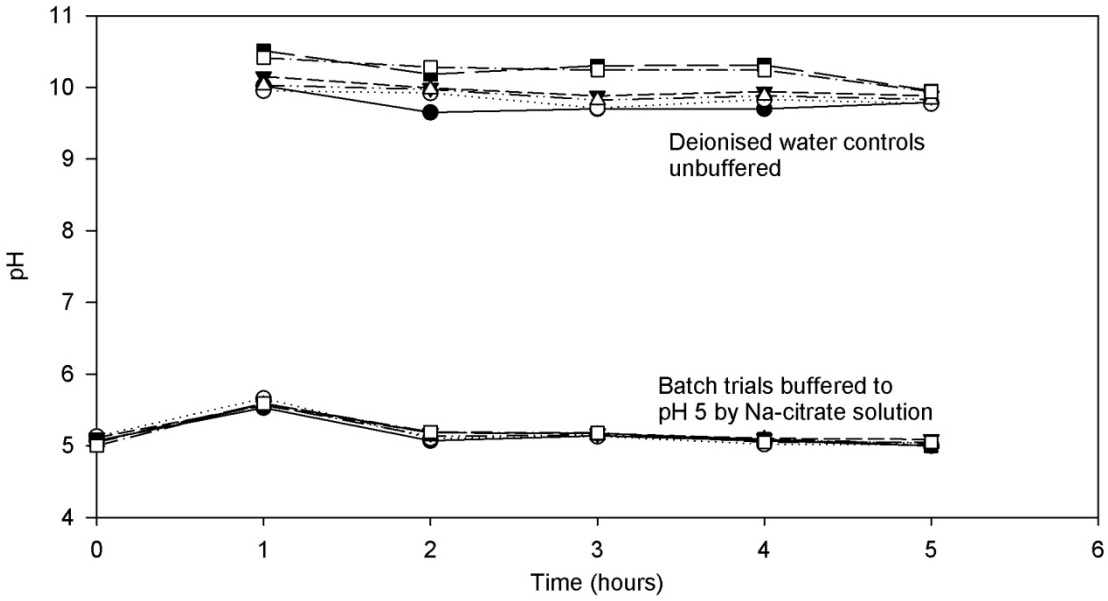

Figure 5.14 – pH of batch weathering experiment of C-H-S. Repeatability error is within the size of the data point.

In order to determine the dynamics of weathering in the first hour a batch experiment was run in which 0.2 g of the same material were immersed in 20 ml of 10 mmol l^{-1} sodium citrate buffered to pH 5 in a 30 ml centrifuge tube. The smaller tubes were used in this instance to reduce the required centrifuge time to 2 minutes, at 12,000 rmp. The tubes were placed on a reciprocating shaker and aliquots were taken after 8, 16, 24 and 33 minutes, wholly replacing the solution after each interval. The samples were filtered, diluted, acidified and analysed using AAS. The cumulative calcium concentrations are presented in Figure 5.15.

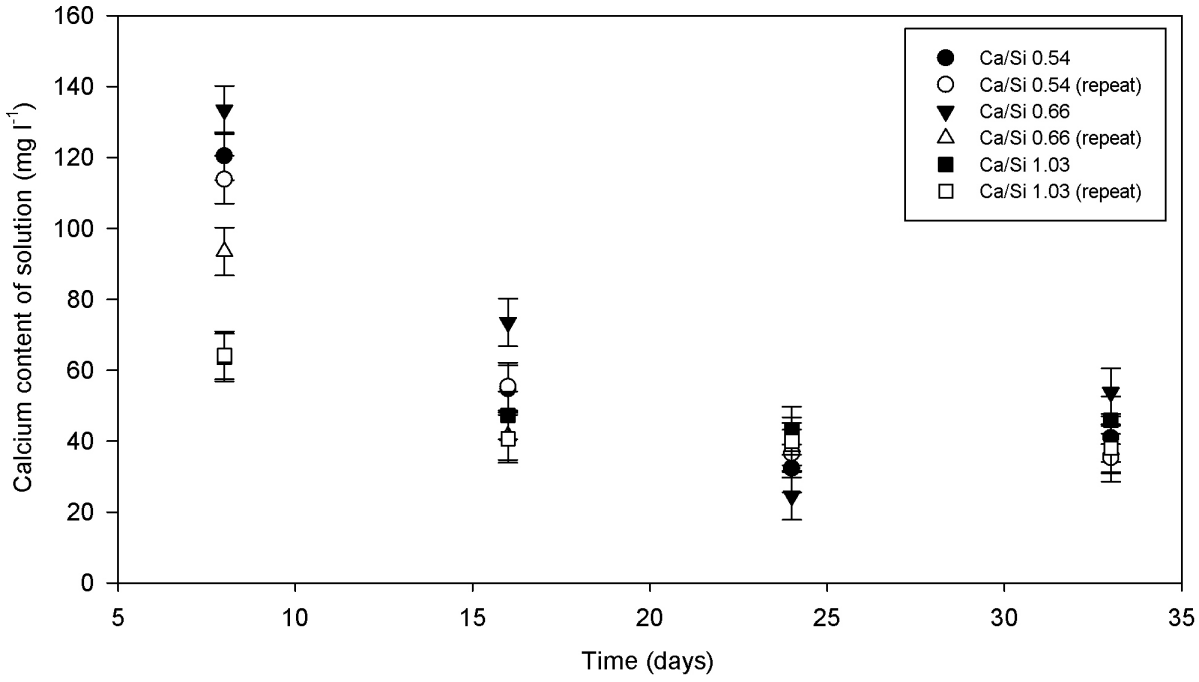

Figure 5.15 – Calcium content of 33 minute batch weathering experiment. Error bars represent repeatability.

The smaller tube weathering experiments show similar calcium concentrations to that of the previous weathering experiment, with concentrations ranging up to 133.4 ± 6.7 mg l^{-1} in 8 minutes of running (with no statistically significant variation between solids ~P = 0.27). pH was buffered between 5.2 and 5.7 over the experiment.

5.7.4 Batch weathering of calcium silicate hydrate to determine solid material transformations (Experiment 5C) - Results

SEM images taken of the grains before and after the weathering experiment show a range of particle sizes present in the material, which appear (at 80x

magnification; Plate 5.2) to have changed little over the course of the experiment. Plate 5.2A and 5.2B both show small particles attached to the surface of the grain (annotated as ‘a’) Images taken at higher magnification (1000-2000x; Plate 5.3) show a change in the surface texture over the course of the experiment. Growth of fibrous crystals (annotated as ‘b’; possibly crystallised calcium silicate hydrate minerals) formed on the surface of the weathered material.

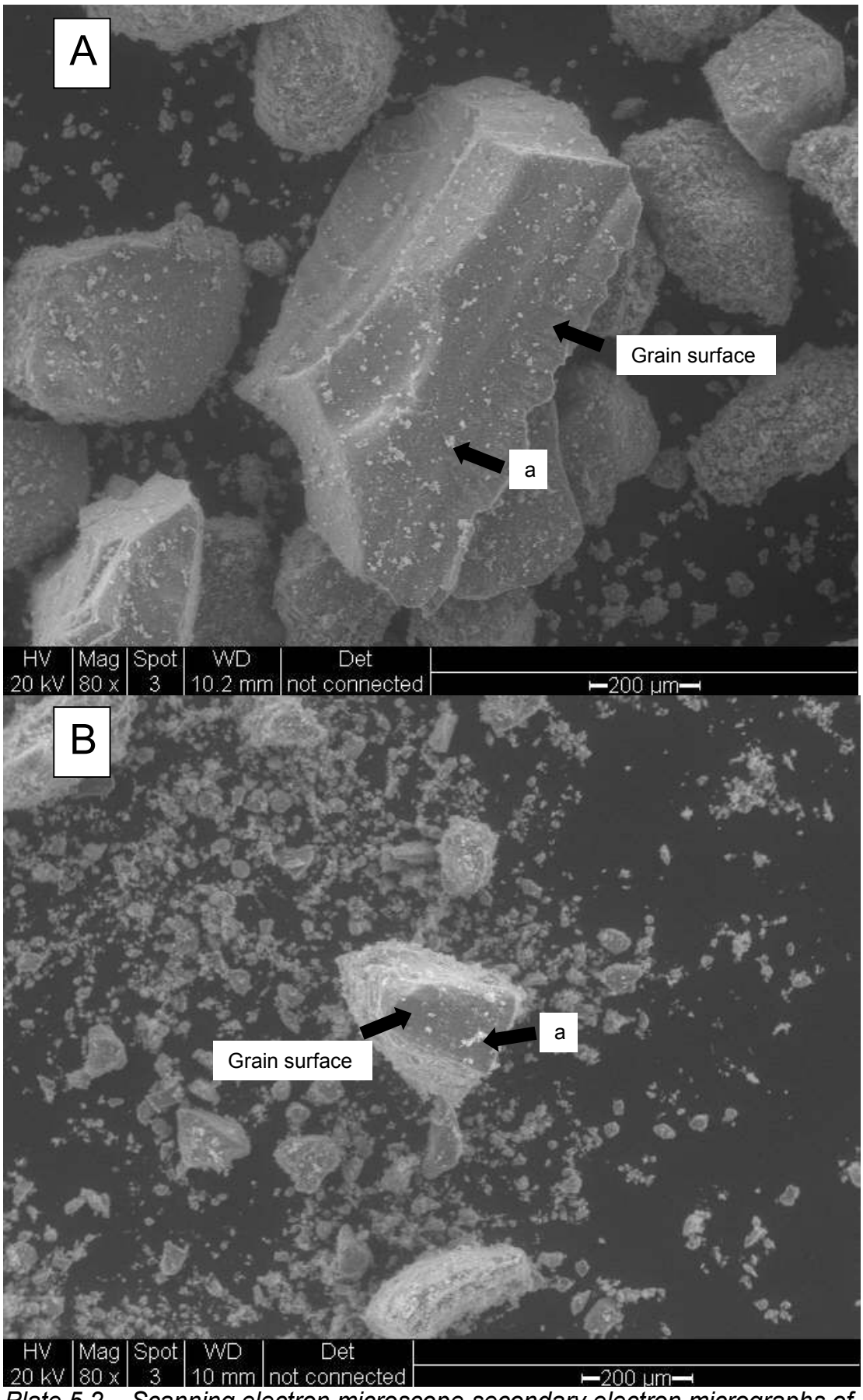

Plate 5.2 – Scanning electron microscope secondary electron micrographs of un-weathered (A) and weathered (B) cement minerals at 80x magnification and 20 kV. Explanation of the annotation given in the text above.

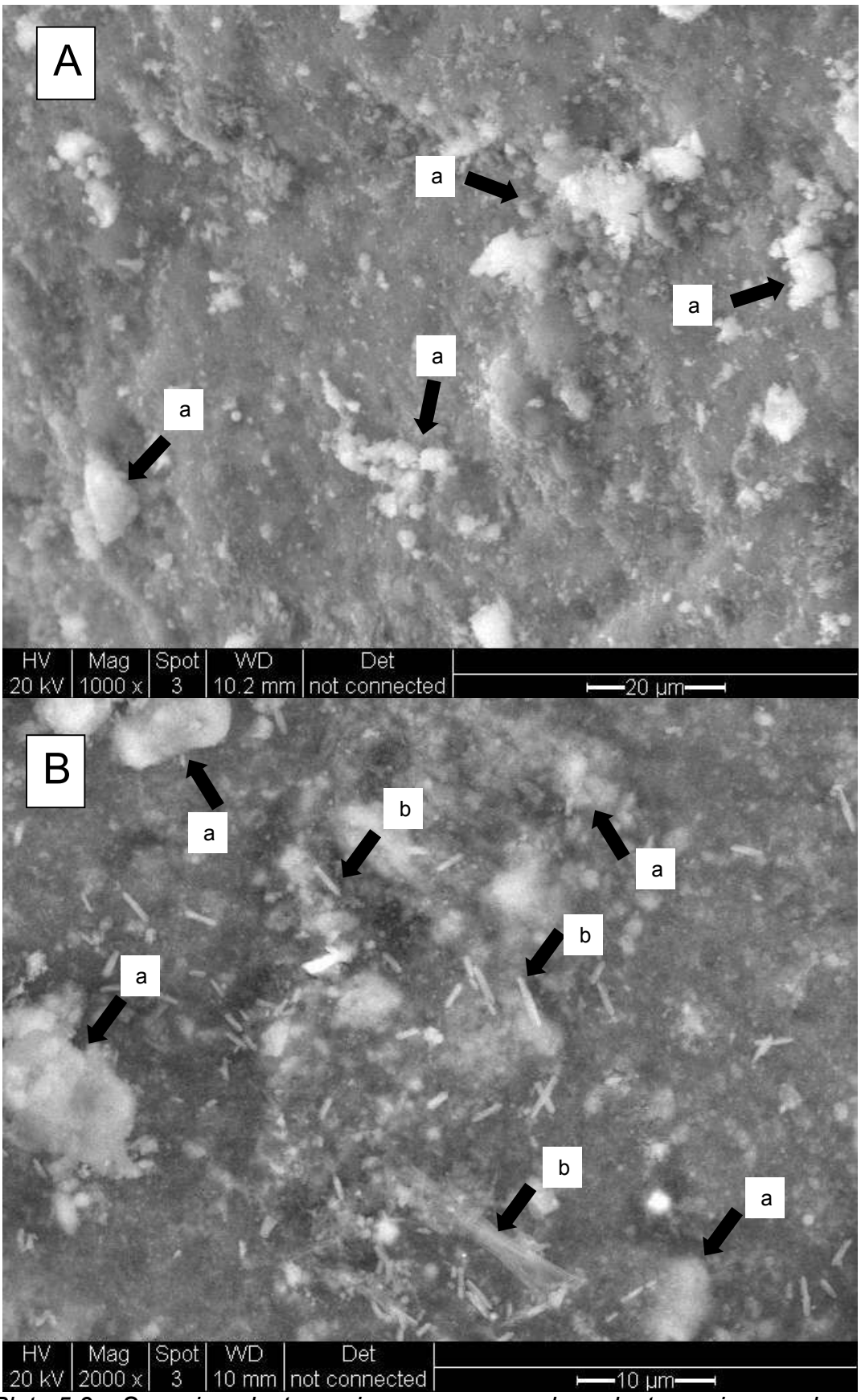

Plate 5.3 – Scanning electron microscope secondary electron micrographs of un-weathered (A) and weathered (B) cement mineral surfaces at 1000x (A) and 2000x (B) magnification, and 20 kV. Explanation of the annotation given in the text above.

Using X-ray spectroscopy (coupled with SEM), the elemental composition of the surface particles (labelled a in Plates 5.2 and 5.3) was semi-quantitatively determined (Figure 5.16).

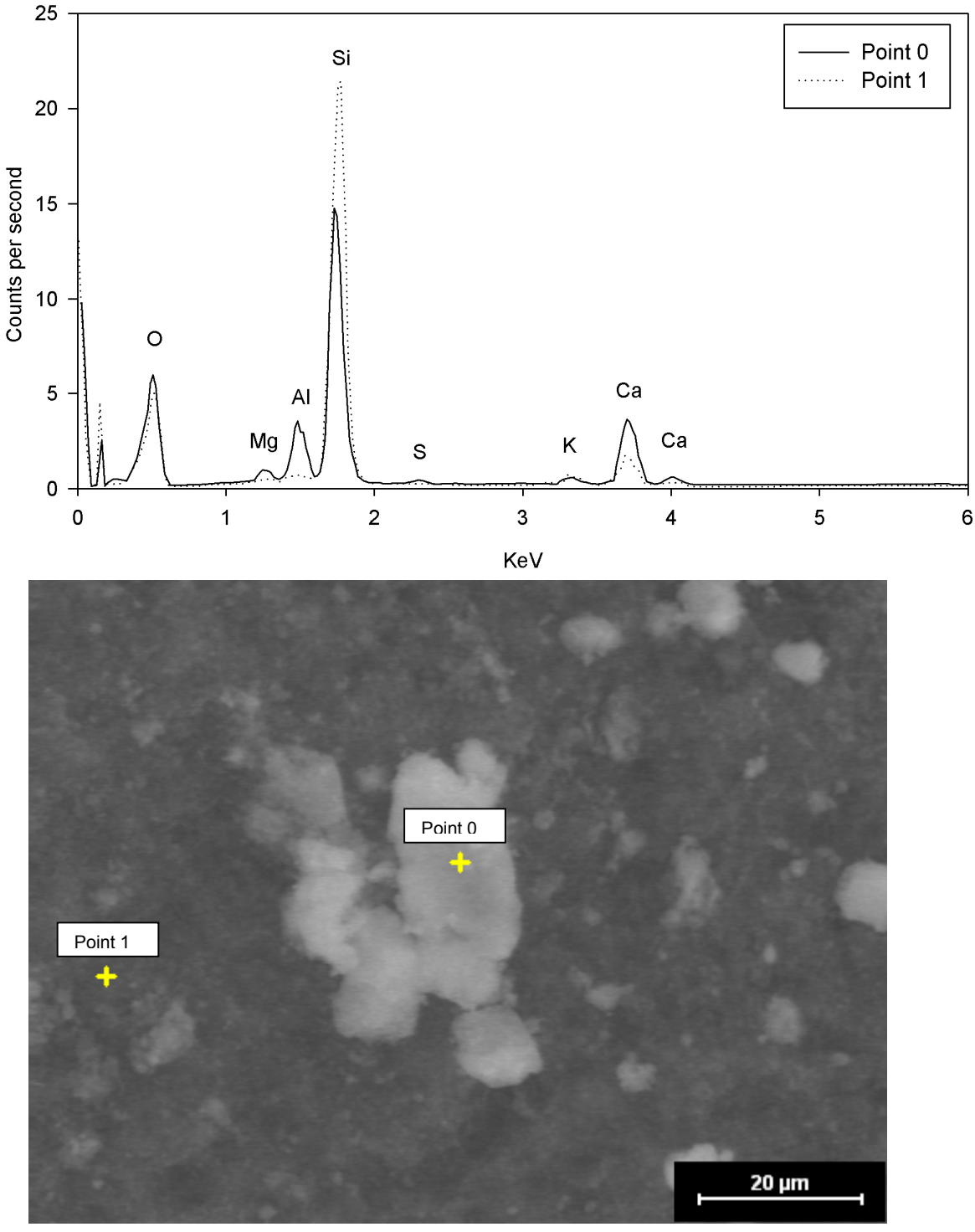

Figure 5.16 – Characteristic X-ray spectra of surface anomaly compared with the background material.

For this example, the characteristic X-ray spectra suggest that the particles have larger concentrations of Ca, Mg and Al compared to the background matrix.

X-ray diffraction (XRD; Appendix A.4) was used to investigate the changes in mineralogy during weathering. Cement is composed of numerous, poorly crystalline, minerals, the phases of which can be distorted by the interference of other cations in the silicate framework. This complicates the interpretation of XRD diffractograms. However, analysis of the clinker (Figure 5.17 A) confirms the presence of cement minerals larnite/belite (Ca_2SiO_4), brownmillerite ($Ca_2(Al,Fe)_2O_5$) and calcite probably formed from free lime carbonation with ambient CO_2 during manufacturing. Analysis of the cement hydration products (Figure 5.17 B) shows the reduction in peak intensities of un-hydrated cement minerals and the growth of an amorphous 'hump' between 14-28 2θ, suggesting that the hydration products are primarily amorphous gels, which is confirmed by the lack of crystalline calcium silicate hydrate minerals in spectrum B.

XRD analysis of the weathered minerals shows systematic variations in mineralogical composition (Figure 5.18) particularly the increased intensity and the appearance of additional calcite peaks, the reduction in larnite peak intensity and the increased intensity of the amorphous hump. Furthermore, weathering appears to have had little effect on the brownmillerite peak, suggesting a range of recalcitrance in the mineral phases.

The growth of carbonate in the samples was confirmed through acid digestion using an Eijkelkamp calcimeter. Calcium carbonate concentration in the un-weathered material was 2.31, 2.66 and 2.88 ± 0.6 % for Ca/Si 0.54, 0.66 and 1.03 respectively. The weathered material had a mean carbonate concentration 4.21 % (s = 1.1). AAS confirmed that the calcium content of the solution was 204.7 – 326.2 ± 5.2 mg l^{-1}, which is likely to be in equilibrium with the calcium silicate phases in the material.

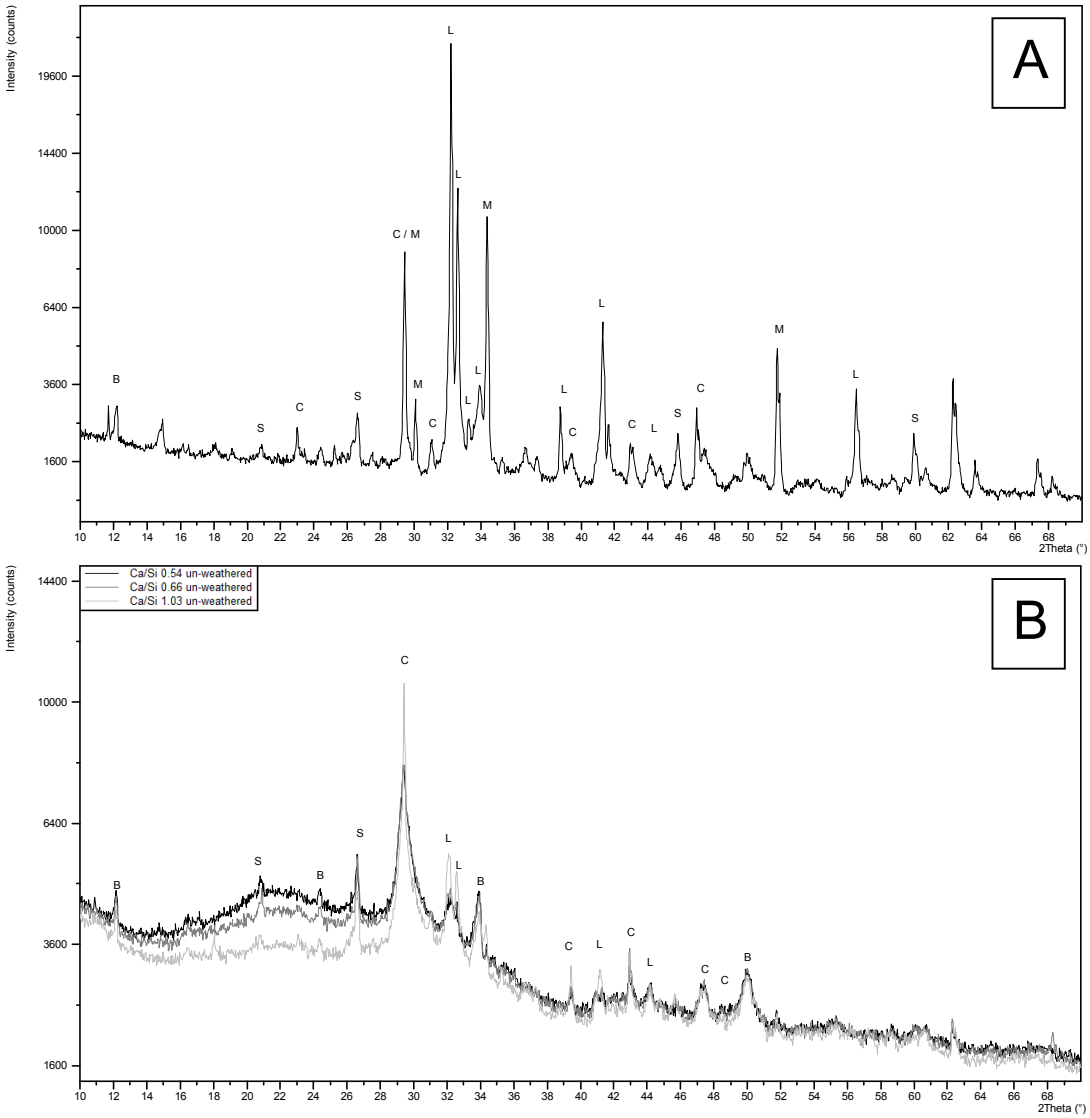

Figure 5.17 – X-ray diffractogram of cement clinker (A) and the un-weathered hydrated cement paste (B). B – brownmillerite ($Ca_2(Al,Fe)_2O_5$) C – calcite ($CaCO_3$) L – larnite/belite (Ca_2SiO_4) M – calcium, magnesium, aluminium silicate S- quartz (SiO_4).

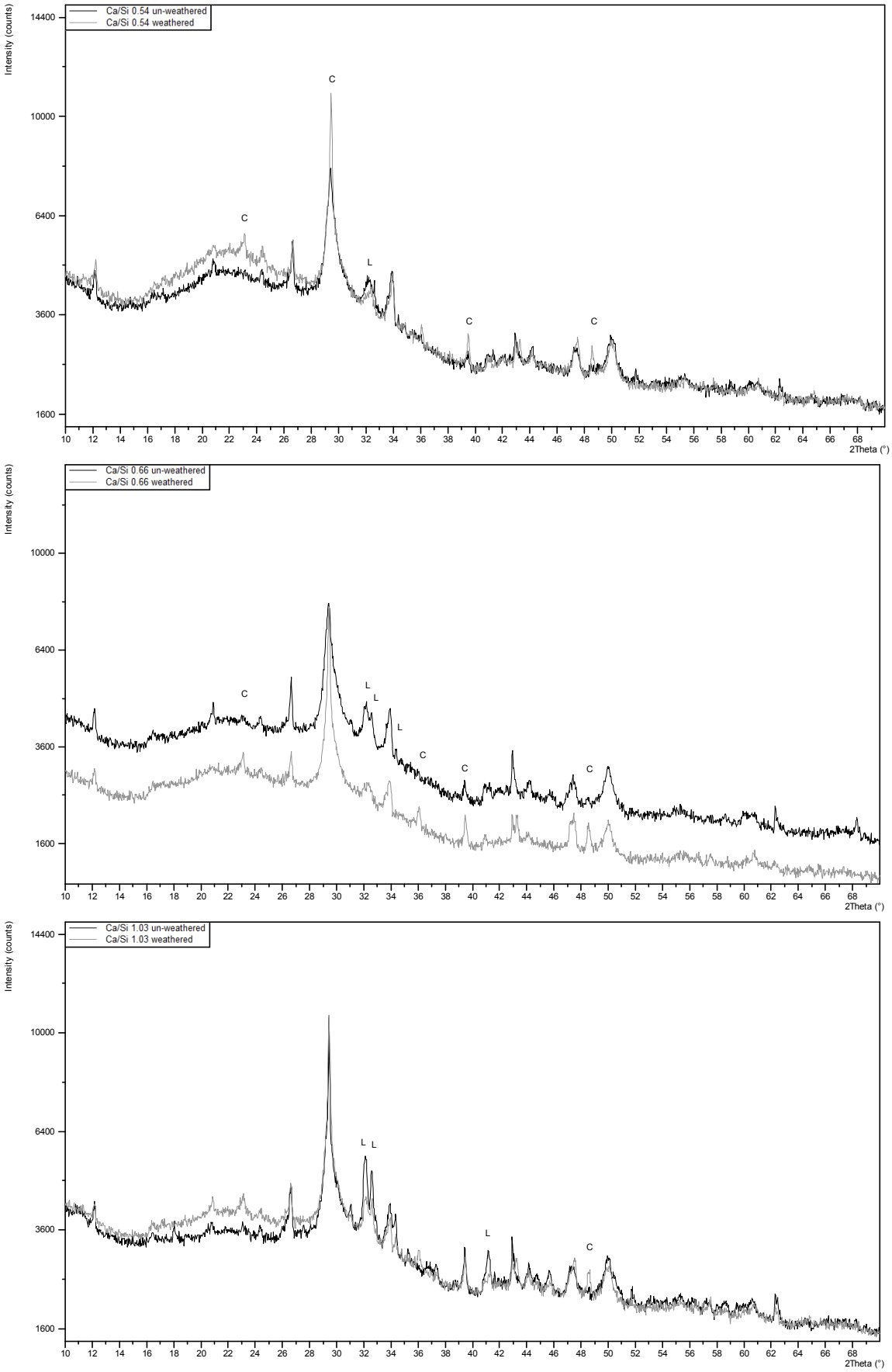

Figure 5.18 – Comparison of diffractograms from weathered and un-weathered materials. L –Larnite (Ca_2SiO_4) C- calcite ($CaCO_3$).

5.7.5 Calcium silicate hydrate weathering (Experiment 5B and 5C) – Discussion

Using the same interpretation as that in Section 6.5.2, and a BET determined surface area between 14.76-29.19 m^2 g^{-1}, the log rate of weathering (from the data in Section 5.7.3) is calculated between -8.26 to -6.86 molCa cm^{-2} sec^{-1}.This is equivalent to that calculated in Experiment 5A. Expressing the weathered calcium as a percentage of the initial total calcium in the material it can be estimated that between 62.7 and 75.5 wt% is leached out within 5 hours of the trial, compared to the deionised water control which leached 19.1 and 22.9 wt% (Figure 5.19).

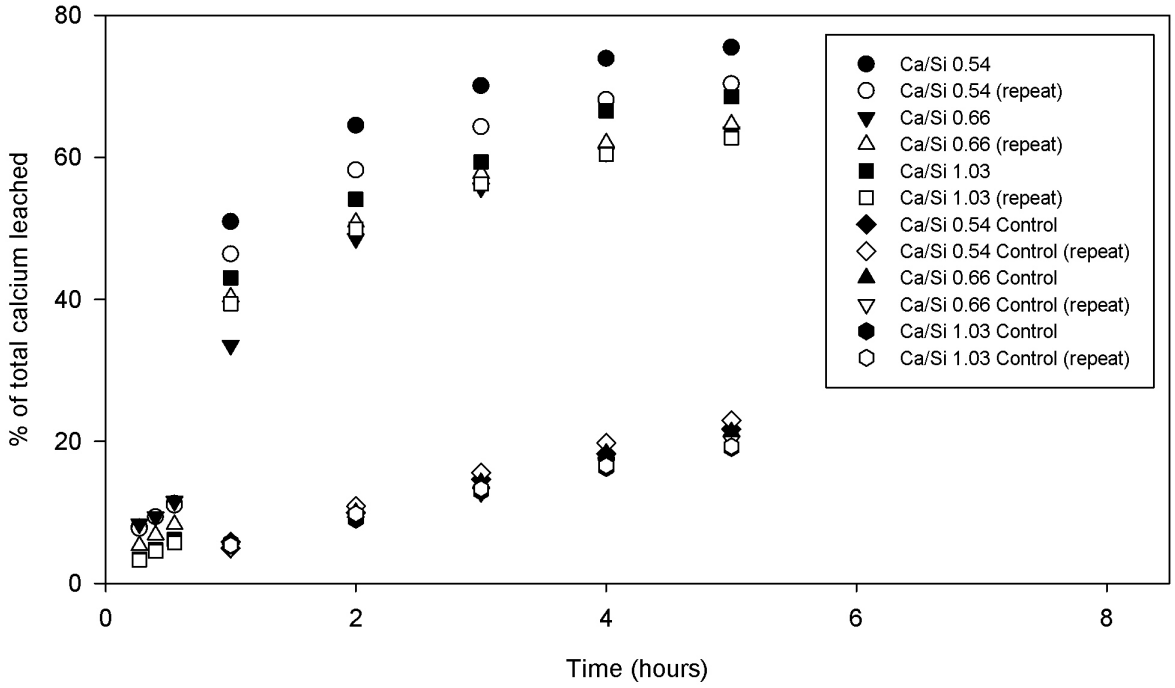

Figure 5.19 – Calcium weathered as wt% of the total calcium in the initial material.

The rate of calcium weathering is several orders of magnitude greater than those reported for natural silicates in the laboratory. However, the similarity between the 1-week, 5-hour and 30-minute experiments suggests that the C-S-H gel may have been in partial or full equilibrium with the solution, and the weathering rate is greater than that reported here. This suggests that C-S-H gels are highly soluble and rapidly equilibrate with solutions, which agrees with the solubility data presented in Chen et al. (2004). There is a discrepancy between the rates of weathering in the 30 minute experiment compared to the 5 hour experiment when normalised against solution/material ratio, which

highlights the variability in determining weathering rates from laboratory experiments. Interpretation of the maximum weathering rate potential is:

- The upper limit of calcium weathering (62.7% and 75.5%) is controlled by the mineralogy of the cement. The calcium weathered in this experiment originated in a soluble phase and the remaining calcium is fixed in less soluble minerals representing 25-35% of the initial CaO content. This is supported by SEM images which possibly show the presence of crystalline calcium silicate hydrate minerals on the surface of the weathered material.
- The upper limit is a function of the depth of a weathered surface layer, in which the underlying calcium rich core is protected from weathering by a silica rich outer layer. The depth of the surface layer can be estimated to between 11-17 μm depending on grain size (see Appendix C.4 for calculations) which is 2 orders of magnitude greater than that reported by Nesbitt and Skinner (2001).
- Secondary minerals have precipitated on the outer surface of the cement grains and reduced the active surface area available for weathering (supported by XRD analysis and carbonate concentrations).Furthermore, precipitation of calcite would subsequently remove solute from solution. A 2 % increase in calcite concentration equates to 10-15 % of the calcium content of the initial material.

Both experiments have shown that cement based minerals readily weather when crushed and exposed to continually replaced solutions. The presence of an organic acid enhances the weathering rate by a factor of 3-4, although this could be attributed to a buffered pH in the sodium citrate trial, compared to that in the control.

5.7.6 The effect of silica fume on cement hydration (Experiment 5D) – Results and discussion

Generally the samples lost between 2.77 and 5.60 wt% of their mass up to 600 °C. Within this, there was a discrete mass loss between 200 and 300 °C in all samples, most likely representing the dehydroxylation or water loss from a semi crystalline hydrated mineral (although this was not detected in the XRD diffractogram, see below). Mass loss between 650-750 °C represents the

volatilisation of CO_2 in carbonate minerals (0.64-0.81 wt% as CO_2) probably formed by unintentional dissolution of CO_2 during cement curing or ambient CO_2 carbonation with clinker during manufacturing (Figure 5.20).

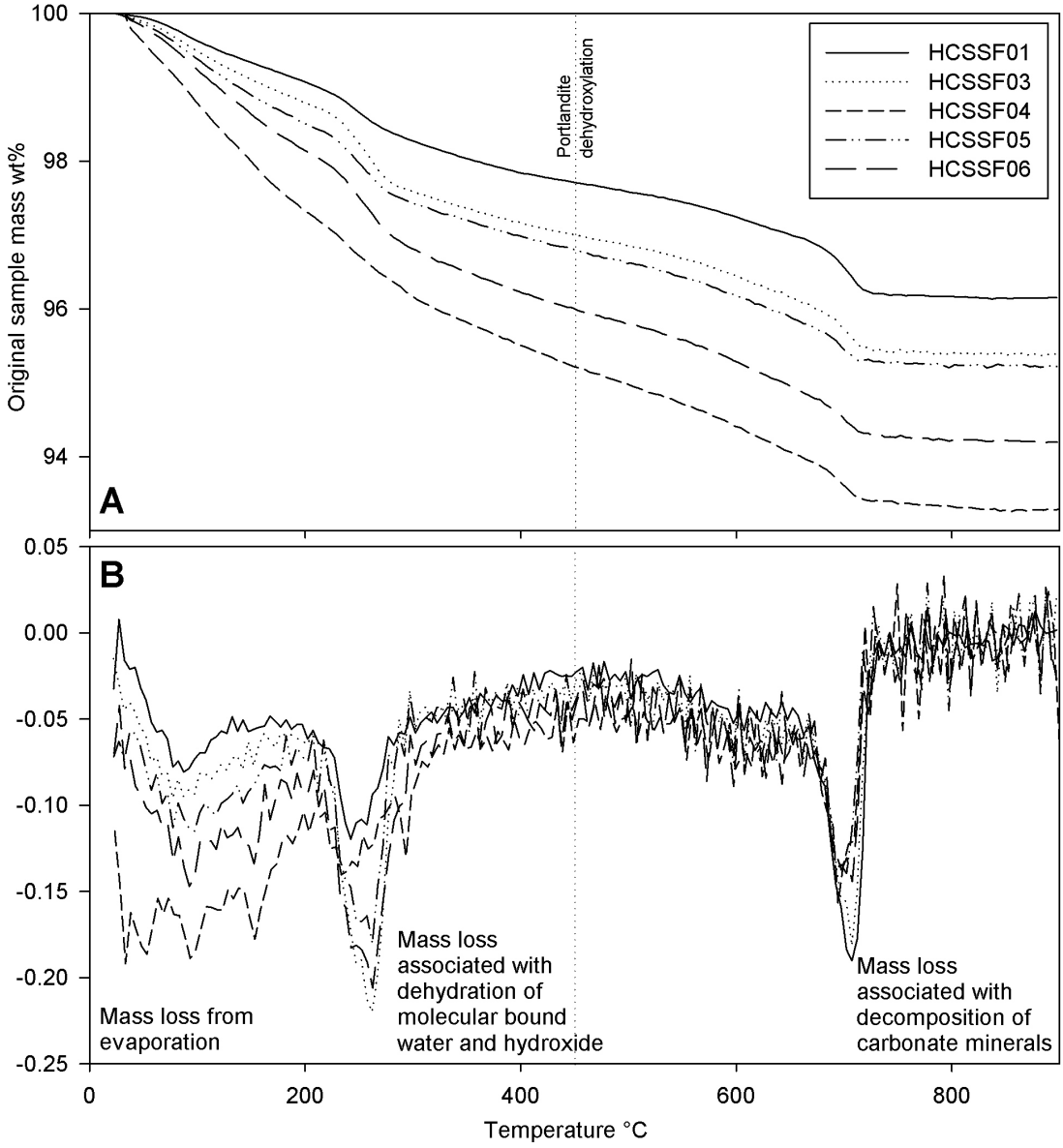

Figure 5.20 – (A) Mass loss of hydrated cements during thermal analysis (B) differentiation of the mass loss lines in (A).

Table 5.4 – The effect of the calcium/silicon ratio on cement hydration.

Sample	Ca/Si	Mass loss 200-300°C (%)	Mass loss 0-600°C (%)	Mass loss 650-750°C (%)
HCSSF 1	3.03	0.79	2.77	0.81
HCSSF 3	1.26	1.20	3.56	0.75
HCSSF 4	0.98	1.16	5.60	0.69
HCSSF 5	0.80	1.07	3.83	0.64
HCSSF 6	0.67	1.32	4.71	0.71

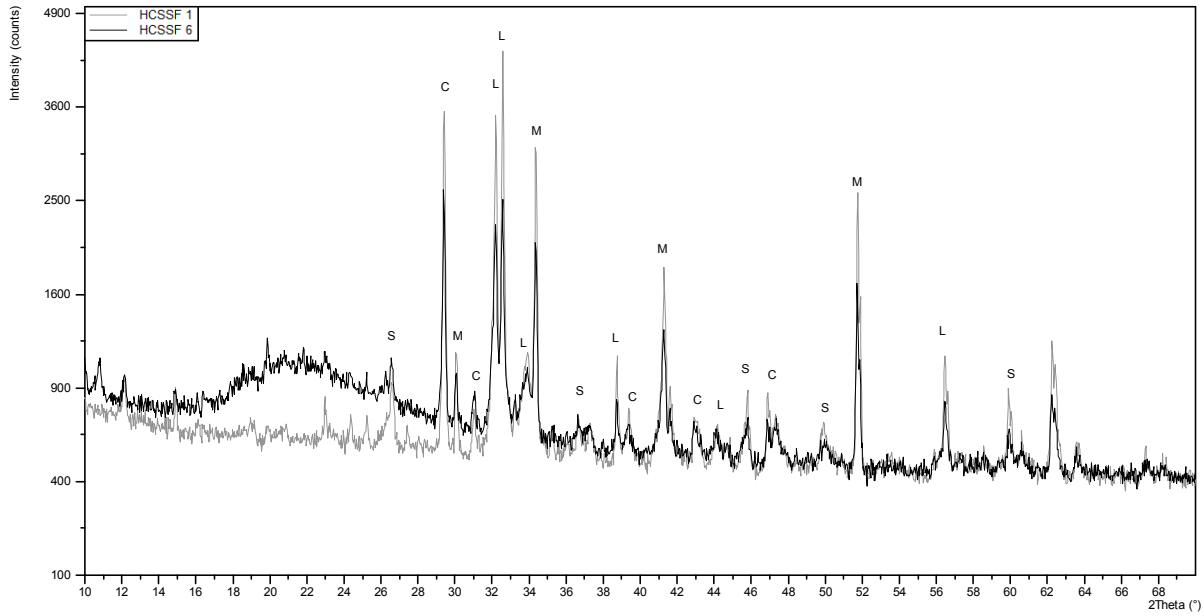

Figure 5.21 – XRD diffractogram of hydrated cement. C – calcite ($CaCO_3$), L – larnite/belite (Ca_2SiO_4), M – calcium, magnesium, aluminium silicate, S- quartz (SiO_4).

The XRD diffractogram of the hydrated cement minerals are similar to that in Experiment 5C where the minerals calcite, quartz, larnite and a calcium magnesium aluminium silicate were identified. However, Figure 6.21 identifies the variation in amorphous material as a function of Ca/Si ratio. HCSSF 6 (Ca/Si = 0.67) has the larger amorphous hump compared with HCSSF 1 (Ca/Si = 3.03).

5.8 Discussion and conclusions

All experiments demonstrate that calcium readily weathers from cement. Applying a similar technique to that used in natural silicate weathering experiments, it is possible to define cement weathering as a function of surface area (Table 5.5). The log weathering rates presented here are several orders of magnitude greater than natural silicate weathering, and some are similar to that presented in Galle et al. (2004), who investigated concrete dissolution. If the geometric surface area (~0.03 m^2 g^{-1}) is used instead of those determined using BET, the weathering rate is two orders of magnitude greater. This highlights the importance of surface area in weathering calculations and the potential variability in laboratory results, which are compounded when up-scaling.

*Table 5.5 – Weathering rates calculated from Na-citrate buffered batch weathering experiments. *Denotes geometric surface area calculations, the other surface areas were determined using BET.*

Experiment	Ca/Si	pH	Particle Size (μm)	Surface area ($m^2 g^{-1}$)	Log weathering rate (molCa $cm^{-2} sec^{-1}$)	%CaO Leached h^{-1}
concrete, 60 mg ml^{-1}	0.77	3	300-600	0.05-0.10*	-8.43 to -8.13	0.03
concrete, 60 mg ml^{-1}	0.77	3	63-212	0.14-0.47*	-9.09 to - 8.57	0.03
concrete, 60 mg ml^{-1}	0.77	6	300-600	0.05-0.10*	-8.49 to - 8.19	0.02
concrete, 60 mg ml^{-1}	0.77	6	63-212	0.14-0.47*	-9.18 to -10.66	0.02
concrete, 60 mg ml^{-1}	0.77	7	300-600	0.05-0.10*	-8.60 to -8.30	0.02
concrete, 60 mg ml^{-1}	0.77	7	63-212	0.14-0.47*	-9.20 to -8.68	0.02
cement paste, 1.3 mg ml^{-1}	0.54	5	150-212	29.1	-8.23	15.09
cement paste, 1.3 mg ml^{-1}	0.54	5	150-212	29.1	-8.26	14.07
cement paste, 1.3 mg ml^{-1}	0.66	5	150-212	20.4	-8.09	12.71
cement paste, 1.3 mg ml^{-1}	0.66	5	150-212	20.4	-8.09	12.94
cement paste, 1.3 mg ml^{-1}	1.03	5	150-212	14.8	-7.81	13.70
cement paste, 1.3 mg ml^{-1}	1.03	5	150-212	14.8	-7.85	12.54
cement paste, 10 mg ml^{-1}	0.54	5	150-212	29.1	-7.07	13.26
cement paste, 10 mg ml^{-1}	0.54	5	150-212	29.1	-7.10	12.97
cement paste, 10 mg ml^{-1}	0.66	5	150-212	20.4	-6.86	13.66
cement paste, 10 mg ml^{-1}	0.66	5	150-212	20.4	-6.99	9.81
cement paste, 10 mg ml^{-1}	1.03	5	150-212	14.8	-6.87	7.32
cement paste, 10 mg ml^{-1}	1.03	5	150-212	14.8	-6.92	6.74

The non-cumulative calcium concentration in solution during the experiments ranged from 80-966 mg l^{-1}. The upper values approximately equate to the solubility data presented in Chen et al. (2004), suggesting that the solution reaches equilibrium with calcium silicate hydrate minerals within minutes. Modelling the calcium solubility data in Chen et al. (2004) with dissolved carbon dioxide at atmospheric pressure, it can be seen that calcite is predicted to precipitate (Figure 5.22).

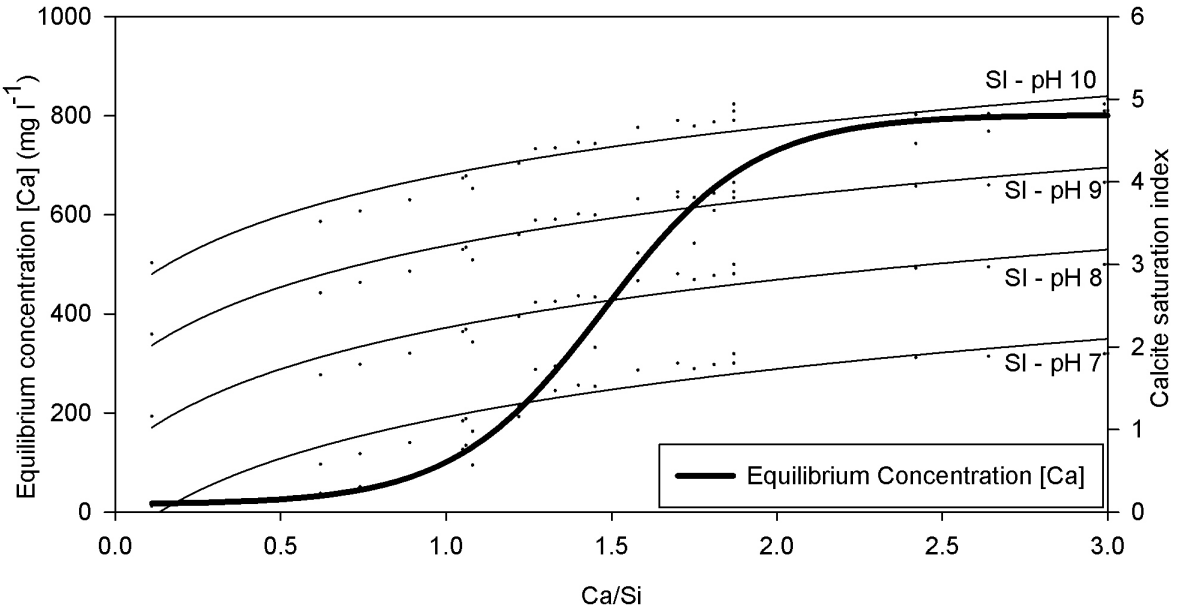

Figure 5.22 – Calcite solubility calculated using data in Chen et al. (2004) and estimates of dissolved carbon dioxide.

Between 10 – 75 % of the initial calcium was removed from the material during the experiments. This upper limit is possibly a function of the following mechanisms:

- A weathered layer was created that is protecting an un-weathered core.
- A less soluble calcium phase exists in the material, suggested by the presence of brownmillerite in XRD diffractograms and SEM-characteristic X-ray analysis.
- Secondary minerals have precipitated on the surface reducing the area exposed to the solution, consistent with carbonate concentrations determined through acid digestion and additional calcite peaks in XRD diffractograms.

The solubility and weathering potential of a calcium silicate material is governed by the calcium silicon ratio. Increased solubility is attributed to alterations in the silicate gel framework by calcium inclusion, which also affects the degree to which the material hydrates. The work in this chapter is the first step in creating a characterisation methodology that can be applied to waste silicate materials to determine the likely carbon capture potential and the rate at which it will carbonate.

Chapter 6

Chapter 6. Biological activity in high pH environments

The importance of organic acids in weathering reactions has been discussed in the previous chapter to elucidate on the rate of cation efflux from the silicate mineral lattice. The rate of carbon supply to the carbonate reaction in soil is a function of a number of mechanisms including gas diffusion of CO_2 through soil and into solution, the efflux of CO_2 from plant roots and the mineralisation of organic carbon. While these processes are well defined for natural soils, they are less well understood for alkaline environments. In this chapter the contribution of plant derived organic acids to the dissolved carbon dioxide pool is investigated using a number of controlled microcosm experiments with particular focus on high pH environments. This is part of a field of study concerned with the impact of silicates on the environment. Therefore, qualitative evidence was collated to discuss the environmental impact of artificial silicates in soils.

Delivered objective: A review of key literature was conducted to describe carbon dynamics in soils, with particular focus on organic acids. This is contextualised in a discussion of biological activity in extreme environments.

Delivered objective: A series of microcosm experiments has been undertaken to quantify the rate of citrate mineralisation in high pH solutions.

Delivered objective: Qualitative evidence was collated from field investigations in Chapter 4 and a growth trial conducted to assess the potential impact of artificial silicates on the environment.

6.1 Biological growth in extreme environments

6.1.1 Biodiversity in extreme conditions

Life, from microorganisms to plants and animals, has been shown to survive in an extraordinary range of environments (Rothschild and Mancinelli, 2001). However, insights into simple ecosystems in extreme environments (Wall and Virginia, 1999) suggest that they are vulnerable to disturbance. This is important when considering the environmental perturbation of using silicate minerals in soils to enhance carbonation. Soils developed on silicate (including artificial) minerals may not be the most extreme environment, nonetheless they present

immediate challenges to resident ecosystems, particularly plant growth on soils with elevated pH.

6.1.2 Biological response to elevated pH

There are few studies that investigate biological activity in ultra-alkaline environments, where most studies are confined to carbonate buffered alkaline soils (e.g. Strom et al., 2005; Strom et al., 2001). Mayes et al. (2009; 2006) investigated wetland formation on high pH drainage waters originating from artificial silicates. The study highlighted a wide range of plant species that grow in these environments. Indeed, some organisms, collectively known as alkaliphilic, have developed mechanisms for surviving in high pH environments (Krulwich, 1995). These organisms are documented in investigations of alkaline groundwater on the Colombia Plateau, USA and Cabeço de Vide in Portugal, Maqarin, Jordan (pH 8.5-12), in which large and diverse microbial communities survive in these environments (Pedersen et al., 2004; Tiago et al., 2004; Stevens et al., 1993).

The biological deterioration of concrete, in which pore waters are often buffered pH >11, has been extensively studied, particularly in sewers. Sulphur oxidising bacteria utilise the hydrogen sulphide produced in the waste to create sulphuric acid (Nogami et al., 1997; Islander et al., 1991). This occurs at up to pH 10, but is optimal at around pH 7 (Islander et al., 1991). The degradation of concrete by *Fusarium*, a common fungus found in soils and concrete structures, is associated with the exudation and chelating of organic anions with metal cations in the concrete (Gu et al., 1998).The excretion of organic compounds on nutrient poor environments is documented as a mechanism for nutrient acquisition that is available to some plants (Dakora and Phillips, 2002). These studies suggest that pioneering communities of plants and microbes exude organic and inorganic compounds as a survival mechanism in extreme pH environments.

6.2 Organic molecules in soils

6.2.1 Input of carbon into the soil

The importance of soil in the carbon cycle is discussed in Chapter 2. This section expands the explanation of carbon input into the soil. The review papers

by Kuzyakov (2006) and Kuzyakov and Domanski (2000) distinguish three primary methods of carbon input into soils namely, degradation of below ground soil organic matter, above and below ground degradation of plant residues, and organic substance release from living organisms. Table 6.1 presents the partitioning of carbon in plants, which demonstrates that a large quantity of carbon fixed during photosynthesis is passed-through or degraded-in the soil as organic compounds (71% in wheat and 63% in pasture) when assuming that the below and above ground biomass decompose to CO_2 in the soil. In practice, above ground biomass is removed by livestock or sold commercially. Nevertheless, the majority of plant carbon is cycled through the soils and the degradation pathway of this remains poorly understood.

*Table 6.1 – Carbon partitioning in plants and soils, units are wt% of total carbon assimilated during photosynthesis.*organic compounds that are degraded through the soil profile. Source: Kuzyakov (2006).*

	Fate	**Wheat**	**Pasture**
Carbon in plant shoot*	Forms a layer of debris on the soil surface (litter). Organic contents degrade at the surface or lower in the soil profile to CO_2 which diffuses to the atmosphere.	50.0	30.0
Shoot respiration	Direct flux of CO_2 back into the atmosphere	25.0	30.0
Carbon in root cells*	Degrades in soil through a range of organic molecules to CO_2 which returns to the atmosphere.	13.0	20.0
Soil+ Microorganisms(SOM)*		3.0	5.0
Root respiration	Flux of CO_2 into soil gas which diffuses to the atmosphere	4.3	7.2
Rhizomicrobial respiration*	Degradation of organic carbon exuded from plant roots into the atmosphere	4.7	7.8
Total		100.0	100.0

Rhizodeposition is a term used to collectively describe the mechanisms by which plants release organic compounds into soils (Nguyen, 2003). This refers to the secretion of organic compounds, and the ‘sloughing off’ of root cells as part of the functional metabolism of plants. These processes are highly species dependant (Nguyen, 2003) but have been compartmentalised to model the total turnover of carbon in soils (see Chapter 2; Jenkinson et al., 1990), where the more rapid processes are collectively described with cell respiration.

Concentration of exuded compounds from maize roots have reported concentrations of 86 mmol l^{-1} for sugars, 9.5 mmol l^{-1} for amino acids, and 10-20 mmol l^{-1} for organic acids (Nguyen, 2003) that turnover rapidly. The complex relationship between soluble, insoluble, labile and recalcitrant compounds, some of which are degraded (possibly through a range of intermediate organic compounds) into CO_2, renders measurement and analysis challenging. For instance, Brookes et al. (2008) suggest that low molecular weight organic compounds may be used as 'trigger molecules' to catalyse the mineralisation of larger compounds. Below is a short explanation of organic carbon compounds in soils, which is partially expanded from Chapter 2, Section 2.1.3.

6.2.2 Stable soil organic matter

Soil organic matter (SOM) is a heterogeneous mixture of numerous compounds, which are (partially/fully) degraded from plant and microorganism biomass (Schnitzer and Khan, 1978). The largest component of this is comprised of humic substances, which are partially degraded/polymerised organic compounds. Despite this varied chemical composition, cellulose, hemicellulose and lignin constitute a large proportion of SOM mass. Lignin is a structural component of plant cells responsible for rigidity (Crawford and Crawford, 1976) and is relatively recalcitrant to microbial decomposition under normal soil conditions. Cellulose and hemicelluloses are important parts of plant cell walls and decompose more readily in soils. Both lignin and cellulose decompose as a function of soil moisture content and temperature (Donnelly et al., 1990), degrading into smaller, more soluble compounds (Guggenberger et al., 1994).

6.2.3 Low molecular weight organic compounds

It is possible that intermediate low molecular weight compounds are produced during the mineralisation of larger organic molecules (described above). However, these pathways remain poorly understood in soils (Jones et al., 2003). Low molecular weight organic compounds (measured concentration are typically on the order of 10 mmol l^{-1}), which including sugars, amino acids and organic acids are secreted by plants but are difficult to measure in-situ due to their lability. Hill et al. (2008) have demonstrated the turnover of sugars in soils to occur within minutes ($t_{1/2}$ generally within 10 minutes) with natural background concentrations of 50 µmol l^{-1}. Approximately 2-5 wt% of the organic

carbon in soil is composed of amino acids (Senwo and Tabatabai, 1998) with solution concentrations of 8 μmol l^{-1} (Fischer et al., 2007). Organic acids turn over in days and comprise the largest component of low molecular weight compounds in solution.

6.3 Low molecular weight organic acids in soils

A review of organic acid dynamics in soils can be found in Jones et al. (2003), Ryan et al. (2001) and Jones (1998), this is summarised in Figure 6.1 and is discussed in more detail below. Organic acids are investigated closely in this section because of their ability to enhance the weathering rate of silicate minerals (Chapter 5). They may also be used as a proxy to discuss generally the degradation of low molecular mass organic compounds in soils.

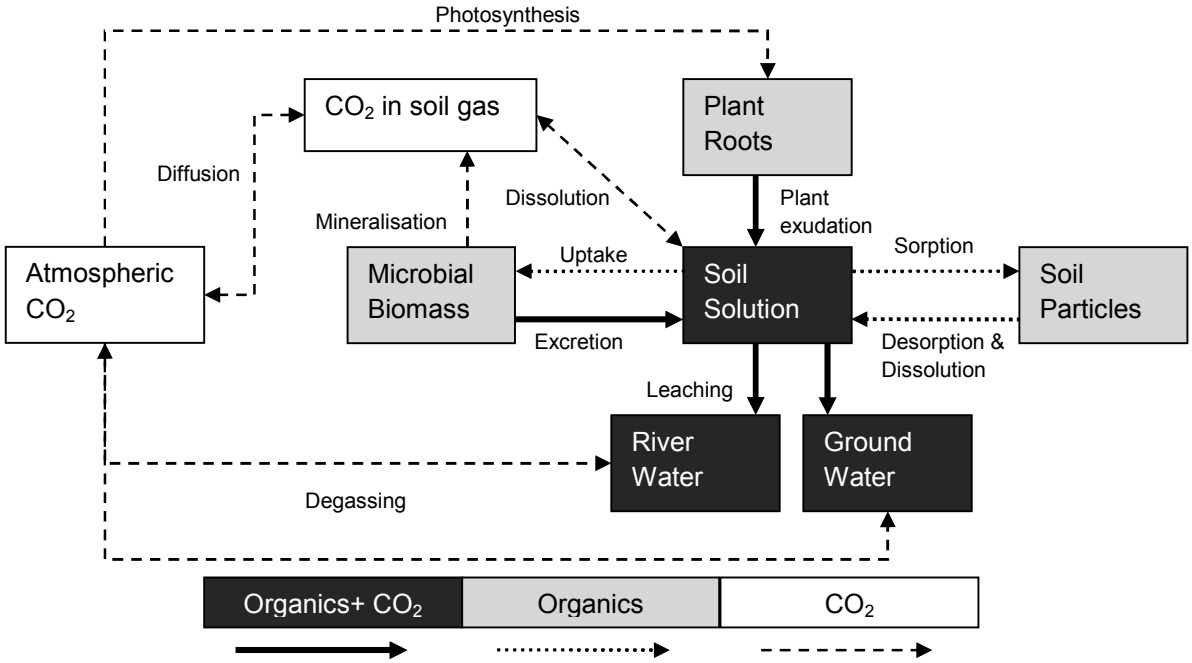

Figure 6.1 – Conceptualisation of organic acid and CO_2 dynamics in soil. Adapted from Jones et al. (2003).

6.3.1 Organic carbon degradation pathways

The tri-carboxylic acid (or 'Krebs') cycle denotes a well known organic acid degradation pathway, in which citrate is transformed by enzymatic activity to oxaloacetate through various organic intermediaries producing CO_2 and NADH (a coenzyme essential for biological redox reactions; Figure 6.2).

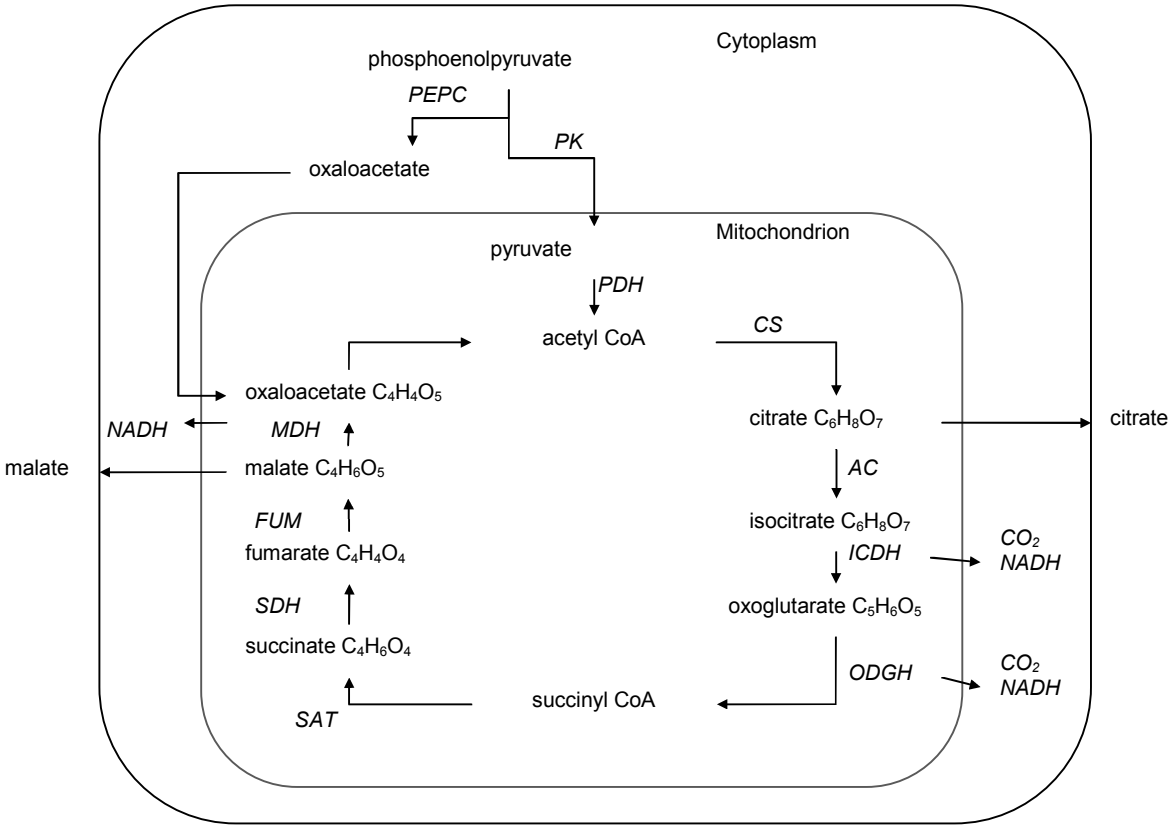

Figure 6.2 – Krebs cycle. Enzymes: PEPC: pyruvate dehydrogenase, CS: citrate synthase, AC: aconitase, ICDH: isocitrate dehydrogenase, OGDH: 2-oxoglutarate dehydrogenase, SAR: succinate thiokinase, SDH: succinate dehydrogenase, FUM: fumurase, MDH: malate dehydrogenase. Source: Adapted from Ryan et al. (2001).

In soils, the degradation of organic carbon is not necessarily confined to the tricarboxylic acid cycle, and may be degraded through other pathways, confirmed by the presence of a range of organic acids in soil solutions (Bylund et al., 2007). Pyruvate is an important intermediate organic compound, which is used by numerous enzymes, and is formed from glycolysis (Figure 6.3).

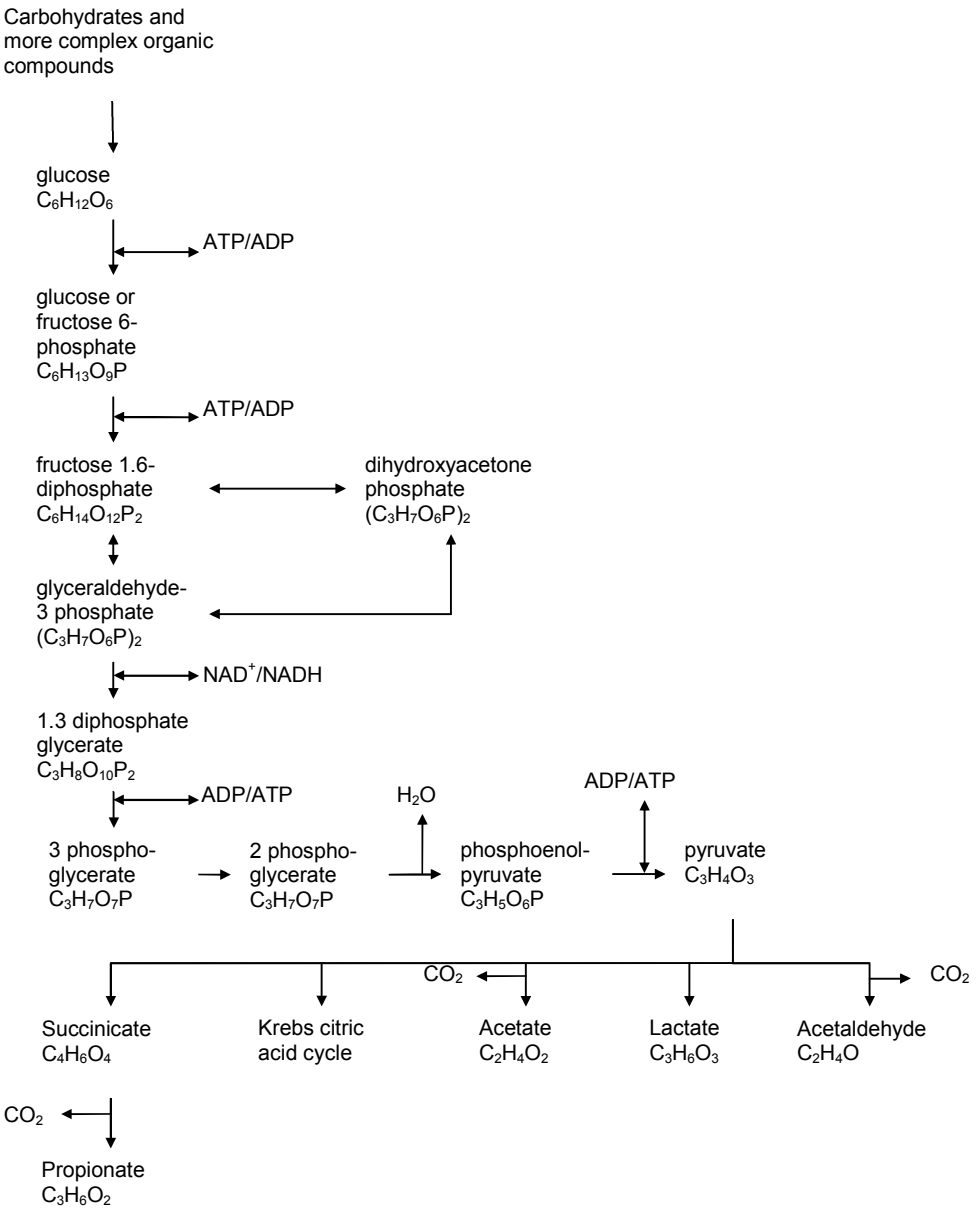

Figure 6.3 – Transformation of glucose to pyruvate and some products of pyruvate transformation. Source: Gray (2004).

6.3.2 Exudation by plants and turnover rates in soils

Concentration of organic acids in the root structure and exudation thereof is controlled by three variables; root area, charge differences (ionic charge inside and outside of the root and membrane potential) and temperature.

There is a substantial body of research investigating organic acid exudation from plant roots which is brought together by Jones (1998), Ryan et al. (2001), Jones et al. (2003) and Nguyen (2003). Collectively, these papers

comprehensively cover the science of rhizodeposition by collating over 600 publications on the subject. They cover similar points regarding organic carbon within soils with variations of emphasis on different components of the organic carbon pool. Table 6.2 presents maximum recorded organic acid concentrations in soil solutions and their associated environmental stimuli.

Table 6.2 – Maximum organic acid concentrations detected in soil solutions. Source: Jones (1998) and Ryan et al. (2001).

Organic acid	**Maximum detected concentration (mmol l^{-1})**	**Comments**	**Reported stimuli**
Acetate	3.2	*Elytrigia* residues	
Formate	2.3	*Elytrigia* residues	
Citrate	4.7	Exuded from *Lupinus albus*	$+Al^{3+}$, -P, -Fe, +Cu
Malate	1.4	Exuded from *Trifolium*	$+Al^{3+}$, +Er, -P
Oxalate	0.6	Decomposing wood	$+Al^{3+}$

Although the topic of each paper varies slightly, the concluding statements are remarkably similar and can be summarised as:

- The exudation rate of low molecular weight organic acids is dependent on a multitude of environmental stimuli including; soil nutrient deficiency, metal toxicity, soil pH, atmospheric CO_2 concentration and anoxic soil conditions. The relative importance of each stimulus varies with plant species.

- Further work is required to determine the flux between the roots and soil, the molecular transformation of organic C and the flux between organic C and the atmosphere. Current methods used to measure rates and quantities of organic carbon mineralisation are either destructive (placing the soil into a centrifuge and decanting the organic acid) or manipulate the environment (hydroponics) to an extent that the results may not be representative of a plant system within nature. There is no passive system for organic carbon measurement within soils.

- The role of microflora in the rhizosphere is not fully understood

- There is a lack of research investigating the fate/impact of organic acids within/on the environment.

6.3.3 Organic acids from laboratory to field scale

Laboratory dissolution of soil minerals has suggested that organic acids are essential to soil formation, particularly podsolisation (leaching of metals to lower in the soil profile to create an acidic A horizon; van Hees et al., 2002). Field scale analysis of organic acid dynamics has suggested that dissolved organic carbon is an important factor in weathering and ion transport (particularly calcium; Vestin et al., 2008). However, parent material plays only a minor influence on organic carbon exudation, highlighting the potential for other plant growth parameters to become rate limiting (Nambu et al., 2008).

6.4 Knowledge gaps and experimental methodology

From the previous chapter and the research described above, it is apparent that low molecular weight organic compounds are important in the weathering of soil minerals as a nutrient acquisition mechanism. They are also essential in mitigating the effects of harmful environments on ecosystems and represent a substantial component of the carbon cycle which is rapidly cycled by soil microorganisms. However, the dynamics of these compounds in soil are poorly understood, and the available research is concerned primarily with natural soils. Therefore, there is a need to explore the turnover of organic carbon in high pH environments and the potential microbial degradation pathway, for soils perturbed with artificial silicate minerals. More generally, the response of ecosystems to high pH environments is important when considering the large scale implementation of a soil carbon capture technology. To this end, the following sections present results from numerous microcosm trials that investigate the breakdown of citrate (for continuity with previous weathering trials) in high pH solutions. Finally, growth trials and field observations are used to explain the potential environmental impact of artificial silicate on the environment.

6.5 Methodology

6.5.1 Microcosm experiments investigating citrate degradation – Experiments A, B and C

An organic acid microcosm experiment method used by Strom et al. (2001), in which the degradation of organic carbon is measured on carbonate rich soils, was adapted for this study. Material was collected from the soil directly adjacent to an ultra alkaline drainage pond (pH>11) in the Hownsgill Valley slag heaps (British national grid reference NZ094492; described in Mayes et al. (2006), Renforth et al. (2009), and Chapter 4– Plate 6.1). Field moist soil was passed through a 2 mm sieve and refrigerated at 5 °C. 10 g of moist soil was measured into 250 ml centrifuge bottle and immersed in either 3 mmol l^{-1} sodium citrate (~240 mgC l^{-1}) buffered to pH 5 or deionised water (see Table 6.3). A proportion of the soil was sterilised using mercuric chloride (Trevors, 1996).Trials 1-3 and 7-9 were buffered to pH>11.5 using approximately 100 mg of calcium hydroxide. Sub samples of the material were oven dried, powdered and analysed for carbonate (Appendix A.1) and total organic carbon (Appendix A.5). The un-treated soil contained 72.3 wt% $CaCO_3$, and 5.0 wt% organic carbon.

Plate 6.1 – Highly alkaline drainage pond at Consett steelworks described in Mayes et al. (2006) and Renforth et al. (2009). (Taken by author June 2008).

Table 6.3 – Microcosm matrix for experiments A&B.				
Material	**162 mol l^{-1} sodium citrate + calcium hydroxide buffered to pH 11.5**	**162 mol l^{-1} sodium citrate buffered to pH 5**	**Dionised water + calcium hydroxide buffered to pH 11.5**	**Dionised water, unbuffered**
Field moist soil	1)	4)	7)	10)
Field moist soil + mercuric chloride	2)	5)	8)	11)
No material (control)	3)	6)	9)	12)

The tubes were placed on a reciprocating shaker at 150 rpm. At 24, 48 and 168 hour time intervals the tubes were removed from the shaker and the pH of the solutions were analysed (Appendix A.2). The tubes were placed in a Sorvall RCSB PLUS centrifuge and settled at 9000 rpm for 15 minutes. Approximately 7 ml aliquots were removed and filtered using l ml luer loc syringes and 0.2 µm cellulose nitrate syringe filters, and refrigerated prior to analysis. The aliquots were analysed for total organic and inorganic carbon using a Shimadzu-TOC-5050A Total Carbon Analyser (Appendix A.11). The experiment was repeated and the results of both trials are presented in Figures 6.5, 6.6 and 6.7, referred herein as 'A&B'. Organic carbon degradation was recorded in one of the experiments which was repeated and extended to 336 hours (Experiment C)

6.5.2 Microcosm experiments investigating citrate degradation – Experiment D

Repeating the methodology in A and B but substituting sodium acetate in the place of sodium citrate, the effect of organic acid composition was investigated (Experiment D).

6.5.3 Microcosm experiments investigating citrate degradation – Experiment E

To understand the importance of nutrient supply on degradation rate, the methodology in A and B was repeated but the initial citrate solution was controlled to include the concentrations of major and trace elements outlined in Table 7.4, denoted as Experiment E.

*Table 6.4 – Composition of starting solution in Experiment 'E' *not including the addition of calcium hydroxide.*	
Element	**mg l^{-1}**
N	224.00
K	235.00
Ca	160.00*
P	62.00
S	32.00
Mg	24.00
Cl	1.77
B	0.27
Mn	0.11
Zn	0.13
Cu	0.03
Mo	0.05
Fe	1.12

6.5.4 Plant growth on soils amended with concrete

A trial was designed to provide qualitative evidence of plant growth on soil mixed with concrete waste. Cuttings of *Salix nigra* (black williow) were supplied by JPR Environmental (http://www.jprwillow.co.uk). A *Salix sp*. was selected because of its known brownfield remediation potential (Strycharz and Newman, 2009), and experience from unsuccessful pilot experiments using *Lupinus Albus* and *Brassica sp*. The cuttings were placed in green waste compost (degraded from vegetation collected at Moorbank botanical gardens, Newcastle University) and allowed to re-shoot in a cold temperature greenhouse (10-15°C) for 30 days. Concrete (made for weathering trials see Chapter 6 Section 6.5.1) was mixed with compost (supplied from Newcastle City Council – Newburn green waste facility) and silica sand, where the ratio of concrete to sand to compost was 1:2:7 by volume. Four healthy willow cuttings were divided between two identical lysimeters (height 1.5 m diameter 0.3 m), one was filled with the concrete/sand/compost mixture, and the other was filled with sand to compost of 3:7 by volume. As a semi quantitative indicator of plant health, relative chlorophyll content was measured using Opti-Sciences CCM-200 chlorophyll content meter over an 11 month period.

6.6 Results and discussion

6.6.1 Microcosm experiments investigating citrate degradation – Experiments A and B

Reduction of dissolved organic carbon (82.8-119.7 mg l^{-1}) was recorded in solutions containing field moist soil treated with a sodium citrate buffer (Experiment 4A and B Figure 6.4). This corresponded to an increase in dissolved inorganic carbon (74.2-81.3 mg l^{-1}; Figure 6.5). Generally, dissolved organic carbon increased in the other trials (<30 mg l^{-1}).

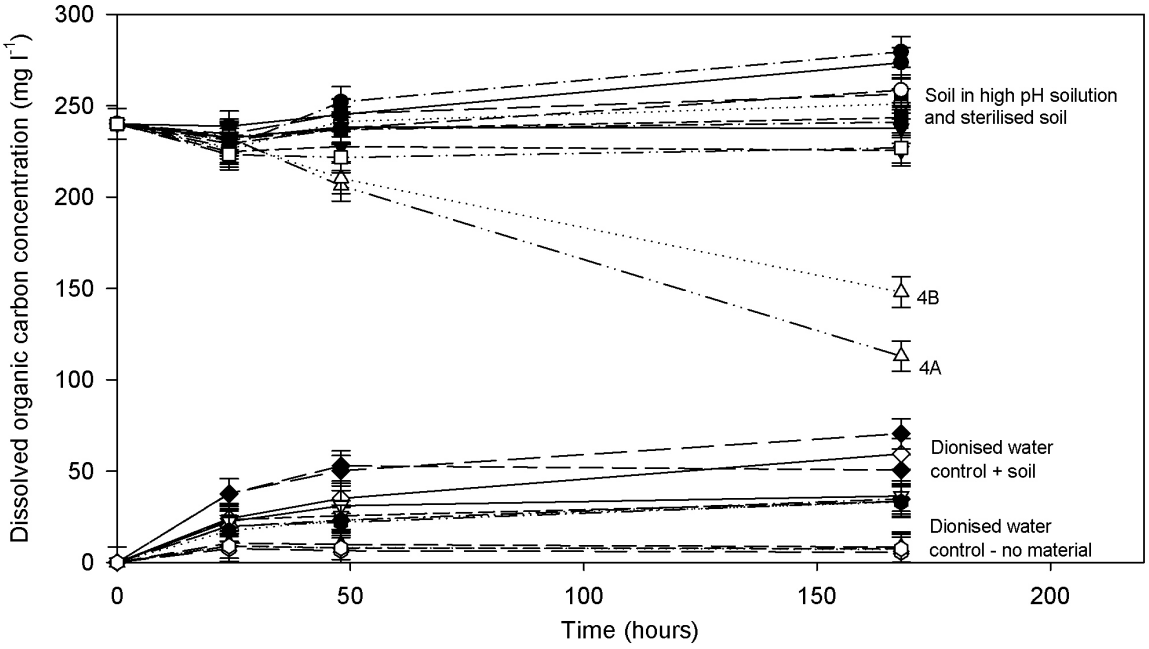

Figure 6.4 – Dissolved organic carbon content during A&B microcosm trials, error bars represent repeatability.

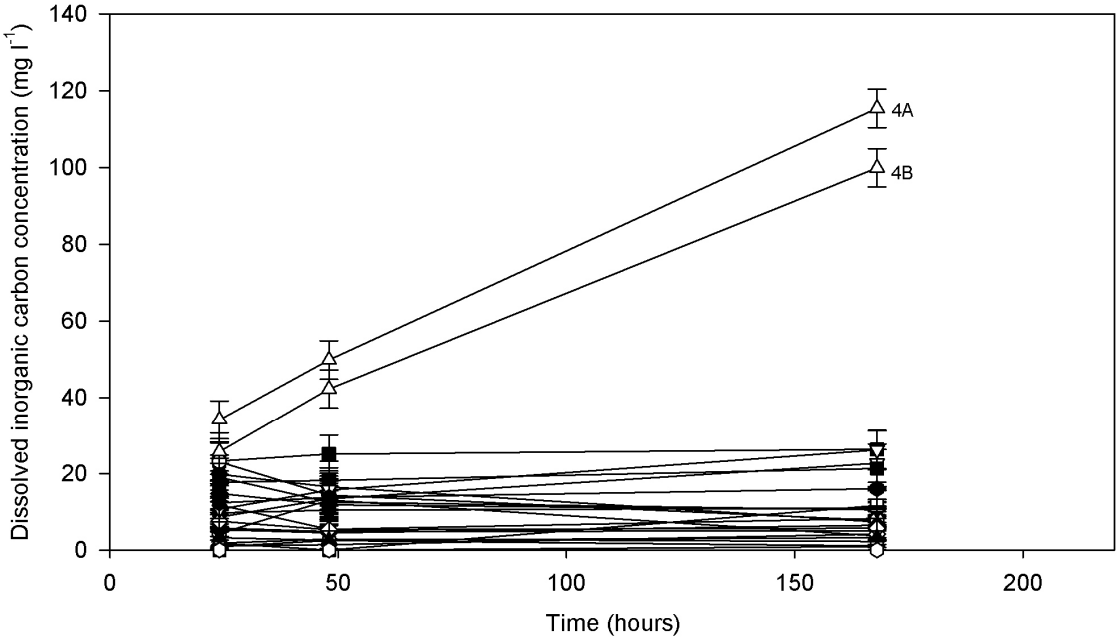

Figure 6.5 – Dissolved organic carbon concentration during A&B microcosm experiment, error bars represent repeatability.

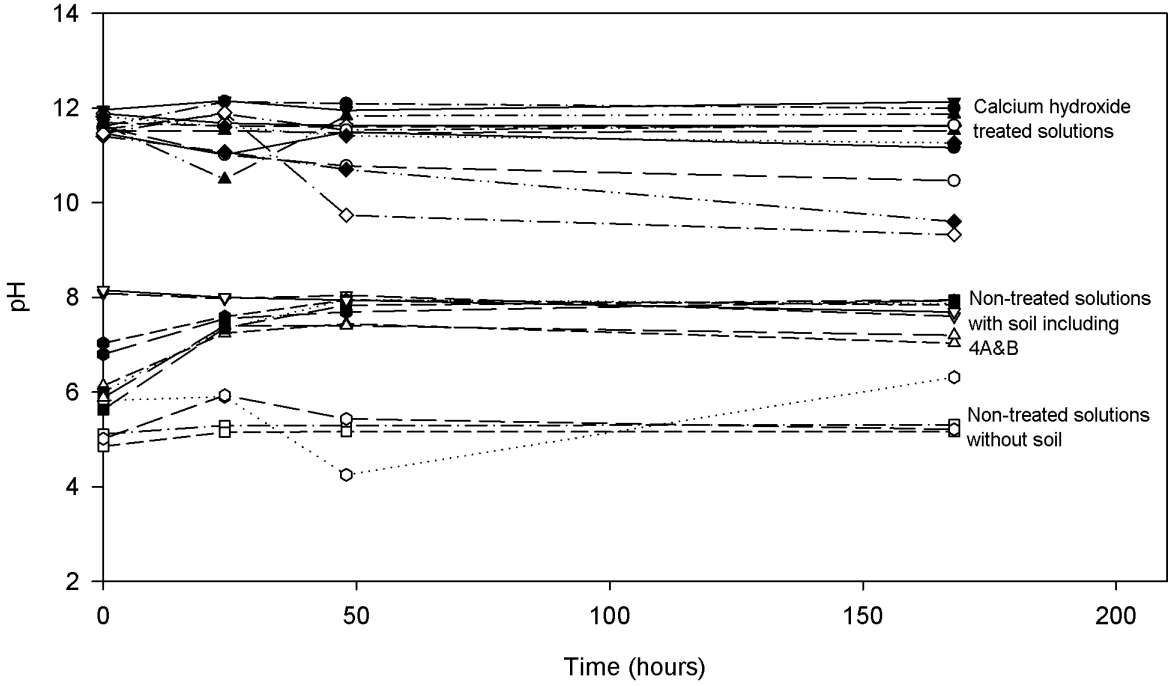

Figure 6.6– pH of solutions during the A&B microcosm trial. Repeatability error is within the size of the data point.

The solutions treated with calcium hydroxide were buffered to pH > 10, with only two trials drifting below to pH > 9.5. Untreated solutions were buffered to pH 7-8 in the presence of soil and 5-6.5 in those without soil (Figure 6.6).

6.6.2 Microcosm experiments investigating citrate degradation – Experiment C

To confirm the rate of degradation, trial 4 was repeated over a two week period taking samples at 24, 96, 168, 240 and 336 hour intervals, described herein as 'C'. The organic carbon content of the solution decreased from 153.4 mg l^{-1} after 24 hours to 47.6 mg l^{-1} after 168 hours (Figure 6.7). This corresponded to an increase in inorganic carbon content (34.5 – 103.5 mg l^{-1}). The linear change in concentration between 24 and 168 is consistent with zero order kinetics.

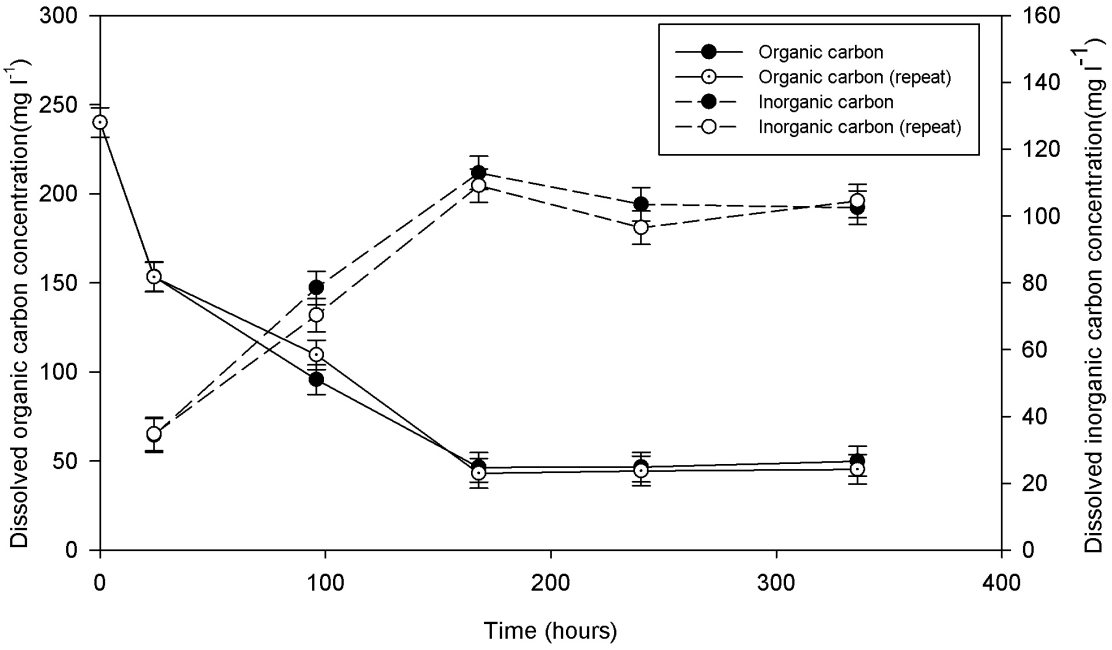

Figure 6.7 – Organic carbon content in a sodium citrate matrix during microcosm C, error bars represent Repeatability.

6.6.3 Microcosm experiments investigating citrate degradation – Experiment D

Normalising the dissolved carbon degradation against initial organic carbon content to facilitate comparison with sodium citrate from the previous trials, it can be seen that between 10-50 wt% of the dissolved organic carbon was degraded during the 168 hour experiment (Figure 6.8) at a comparable rate to the previous experiments. Organic carbon degradation was measured in the solutions treated with calcium hydroxide, corresponding to a decrease in pH (Figure 6.9) over the experiment.

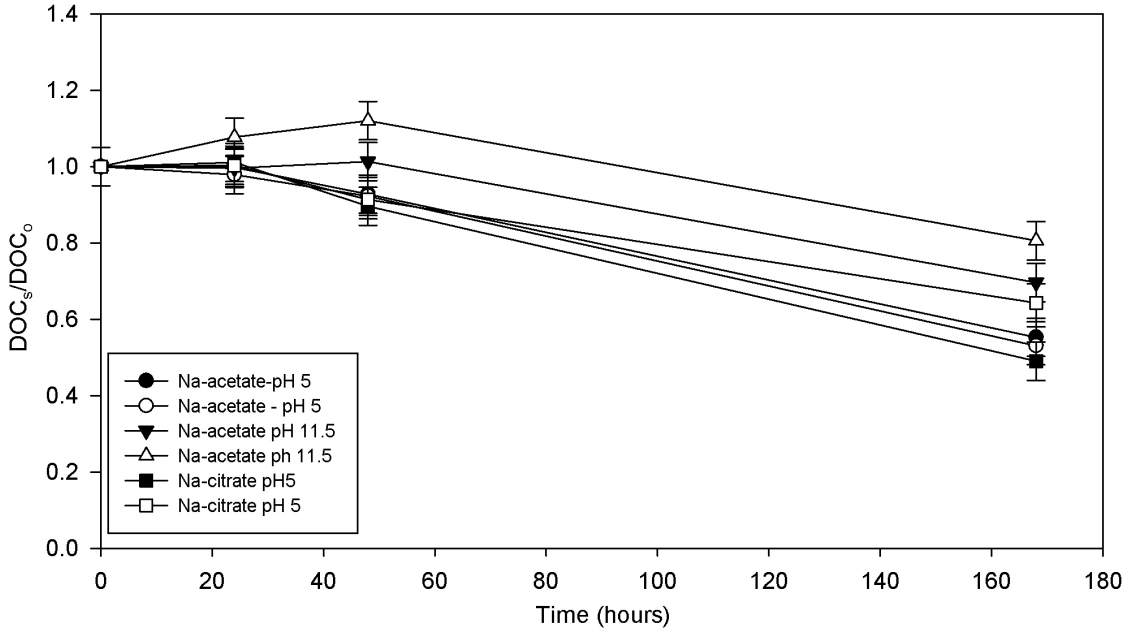

Figure 6.8 – Dissolved organic carbon content of the solution (DOC_s) normalised against initial carbon content (DOC_o) for microcosms A, B and D. error bars represent repeatability.

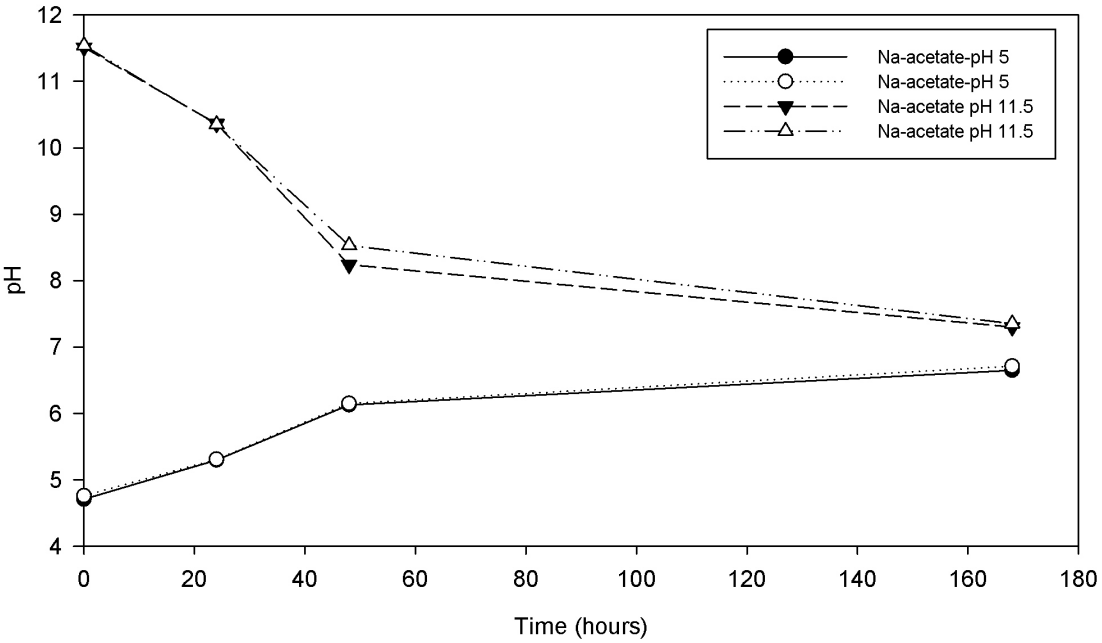

Figure 6.9 – pH of sodium acetate degradation experiment. Repeatability error is within the size of the data point.

The residue from each trial was oven dried, powdered and analysed for carbonate and organic carbon content. There was no substantial systematic variation in carbonate and organic carbon content (see Appendix B.3) over the

range of treatments. This, together with the non-fluctuating inorganic carbon content of the high pH and sterilised soils (Figure 6.5) suggests the existing carbonate content of the soil is relatively stable. Sequestration of the degraded organic carbon (~1 $mgCO_2\ g^{-1}$ soil) is undetectable using the methods described above. However, deviations in carbon and oxygen stable isotopes would be detectable in the samples if the organic carbon was degraded and precipitated as a carbonate mineral. The methodology used in A and B above was repeated using a control material collected from a garden topsoil (British National Grid reference NZ292764). The results show no variation on that found using soil from the ultra alkaline drainage pond in the Hownsgill Valley, and are presented in full in Appendix B.3.

6.6.4 Microcosm experiments investigating citrate degradation – Experiment E

Increasing the concentration of available nutrients in the solution appeared to have limited effect on the microcosms with initial pH 5 (reduction of 58.1 mg l^{-1} between 24 and 168 hours), but stimulated the degradation and reduction of pH in the microcosms with initial pH 11.5 (reduction of 45.2 mg l^{-1}; Figure 6.10). The solutions treated with calcium hydroxide were buffered originally to pH 11.5, but decreased over the course of the experiment to pH 7.3. Similar to previous experiments, the solutions buffered to an initial pH 5 rose to pH 6.8 (Figure 6.11)

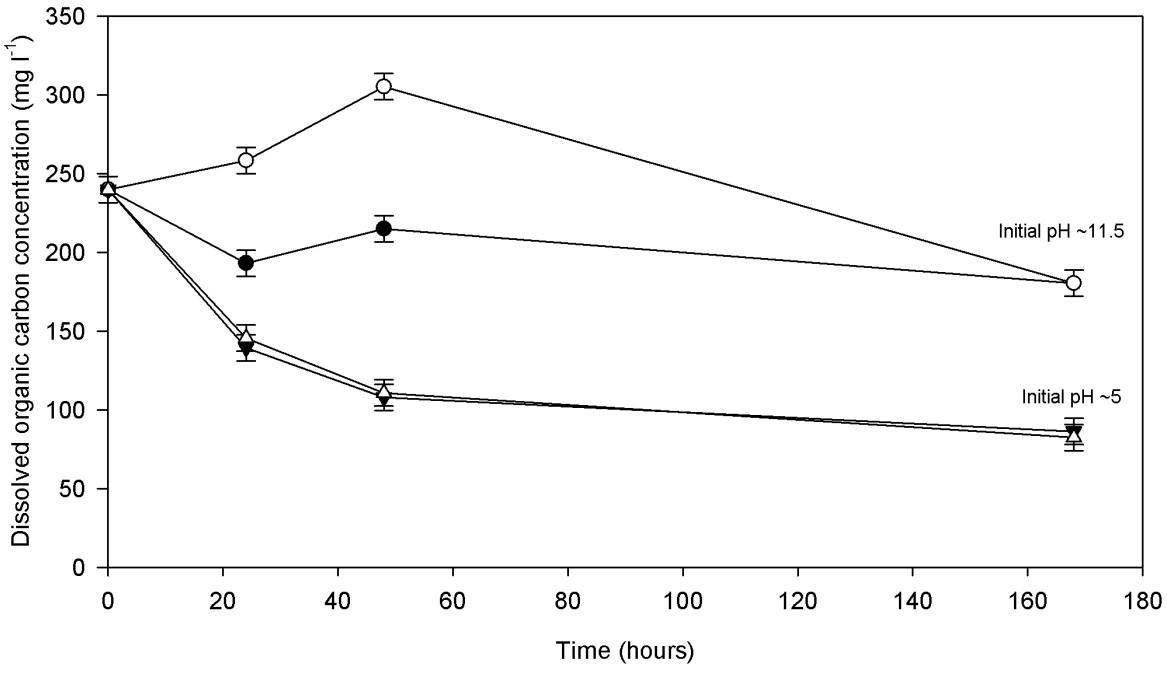

Figure 6.10 – Dissolved organic carbon content of solutions in Experiment E error bars represent repeatability.

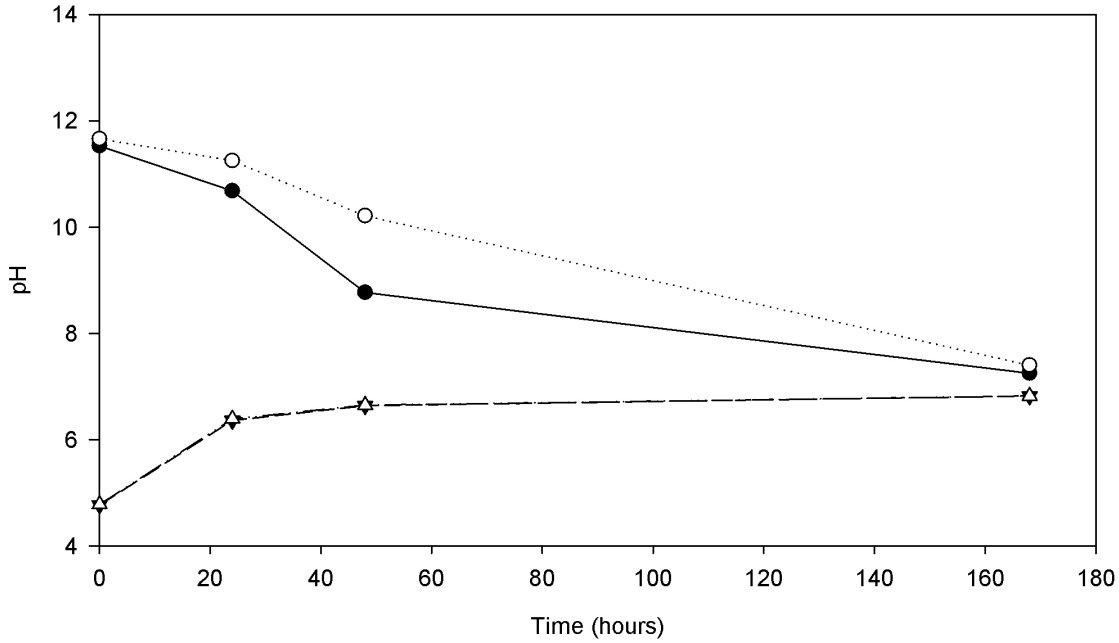

Figure 6.11 – pH change in Experiment E. Repeatability error is within the size of the data point.

6.6.5 Microcosm experiments investigating sodium citrate degradation - Discussion

The studies presented above demonstrate that microorganisms are inhibited by exposure to high pH solutions. The stability of citrate in high pH solutions was confirmed using liquid chromatography coupled with mass spectrometry at Mid Sweden University, the methods and results of which are presented separately and in full in Appendix D. In solutions where the pH is between 7 and 8, the log degradation rate was 3.9×10^{-4} mmol g^{-1}(field moist soil) sec^{-1} (1414.5 mmol Kg^{-1} $hour^{-1}$), which is the same order of magnitude to that recorded by Strom et al. (2001) on natural soils when results are normalised against initial organic acid content. No change in rate was experienced after the addition of nutrients (Figure 6.10). Therefore, it is possible that the supply of other reactants were rate limiting resulting in the zero-order kinetics in Figure 6.7. It is interesting to note that the degradation of acetate was not inhibited by solution pH, suggesting varying sensitivity of enzymes to extreme conditions. The initial solution concentration was maximised (3 mmol l^{-1} in this trial compared to µmol l^{-1} concentrations used by Strom et al., 2001) so that any degradation would be noticeable against organic carbon leaching from the soil and to obtain solution concentrations within the detection range of the Shimadzu-TOC-5050A Total

Carbon Analyser. ^{14}C radiolabelling can be used to investigate the degradation rate of organic compounds in solutions at realistic concentrations against leaching of carbon from the soil material in accordance with existing organic acid degradation methodologies (Hill et al., 2008; Strom et al., 2001 etc.).

6.6.6 Plant growth in concrete – Results and discussion

It can be seen that the chlorophyll content was variable in each lysimeter (Figure 6.12). A 2 sample t test performed on the results at each time interval shows that the treatments were not statistically different during the first four months of growth. However, the second season of growth in the control lysimeter had statistically significant more chlorophyll than the willow grown in concrete treated lysimeter (Figure 6.13). The results here suggest that growth is inhibited on short-medium time scales, and several growing seasons may be required before the environmental impact is mitigated.

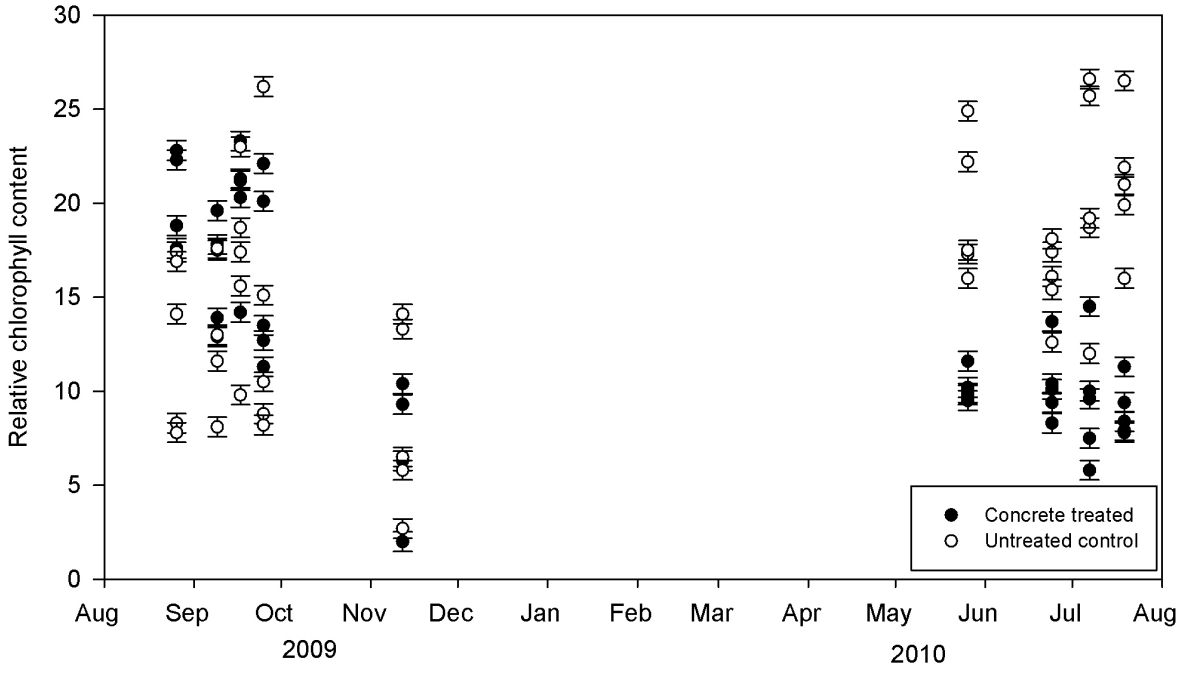

Figure 6.12 – Relative chlorophyll content of Black Willow growth trial.

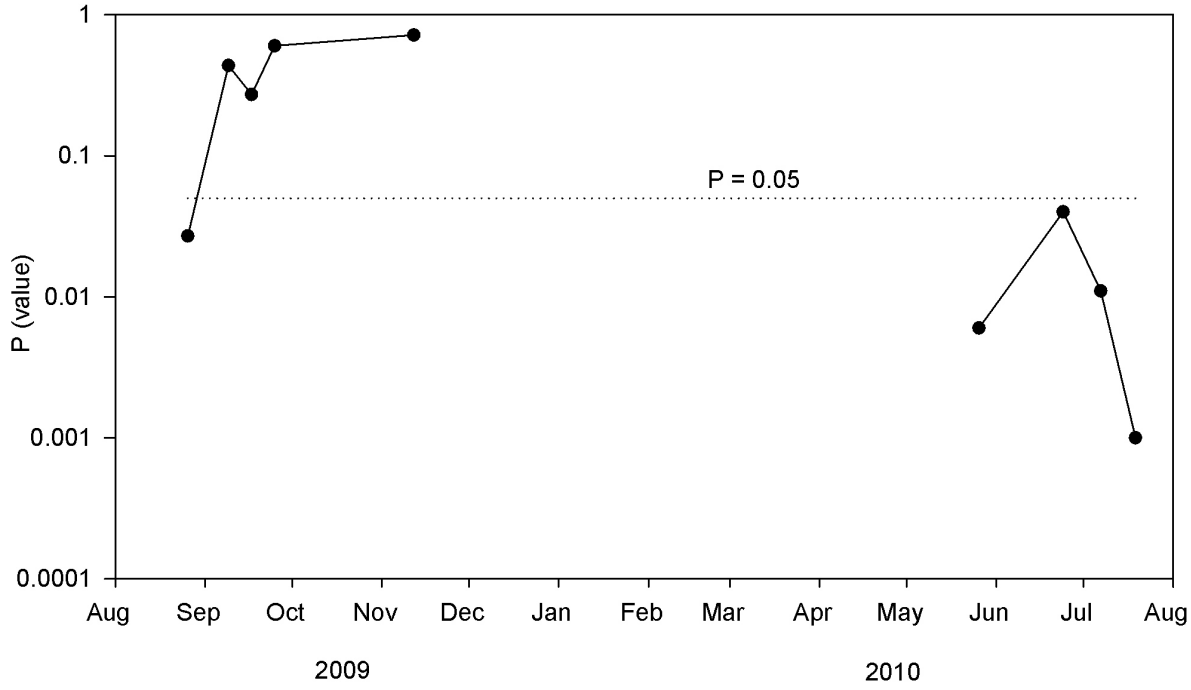

Figure 6.13 – 2 sample t test analysis of differences between treatments at discrete time intervals.

6.6.7 Plant growth in extreme environments –Discussion

Investigating the dynamics of organic carbon in the laboratory is useful for simulating small components of the environment. However, a larger investigation is required to understand the impact of artificial silicates on ecosystems. Such an investigation is outside the scope of this project. However, a short discussion is presented here which aims to inform further research. Chapter 4 details extensive field investigations in which artificial silicates have been incorporated into the soil. The carbon capture and the environmental impact of this material is an unintended consequence of waste disposal strategies. Field observations are summarised here to describe site progression with time and the potential strategies that may be employed to mitigate environmental impact.

Plant community development on artificial soils is analogous to primary succession on natural soils, in which biomass quantity and species diversity increase with time (Aplet et al., 1998). However, primary plant succession and soil development at natural sites can take 10^2-10^3 years, whereas soil and plant development at artificial sites may take decades. This is possibly an artefact of increased weathering rates reported in Chapter 5. Examples of early site

development are presented in Plates 6.2 and 6.3. The surface soil layer at waste transfer stations, like that found in Compton California (Figure 6.15), is continually disturbed by site activity. Therefore, plant development on the site is maintained at an early stage. The area at Science Central, Newcastle, UK, was cleared of buildings in 2008 and covered with a layer of demolition rubble. Both sites host pioneering plant communities, commonly shrubs of the genera *Buddleja* (Tallent-Halsell and Watt, 2009) and annual weedy species such as *Senecio and Taraxacum etc*.

The IRD site in Byker, Newcastle upon Tyne and the Hownsgill Valley slag heaps, Consett, County Durham (see Chapter 4 for description – Plates 6.4 and 6.5 respectively), were disturbed in 1996 and 1980 respectively. The sites have recovered to host a diverse mixture of plants (Table 6.5), even under the continued stress of ultra alkaline drainage waters in the Hownsgill Valley. These sites have recovered naturally over decades, but it may be possible to accelerate the recovery through engineering activity.

Table 6.5 – Plant species at the IRD site and Hownsgill Valley slag heaps.

Site	**Description**
IRD Site, Newcastle, UK. Identified with aid from staff in the School of Biology, Newcastle University (see acknowledgements).	Trees and Shrubs: *Buddleia G*, *Alnus sp.*, *Salix sp.*, *Rubus sp., Rosa sp.*, *Epilobium sp*, *Alnus sp.*, *Betula sp.* Grasses: *Agropyrum repens, syn. Elymus repens*, *Tussilago farfara*, *Rumex obtusifolius*, *Poa trivialis*, *Anthriscus sylvestris, Trifolium pratense & repens*, *Vicia cracca*, *Ranunculus sp., Holcus lanatus*, *Festuca vivipara*, *Alopecurus pratensis*, *Galium sp*. *Achillea millefolium, Tanacetum vulgare, Matricaria discoidea*
Hownsgill Valley slag deposits, Consett Co Durham (and similar environments; Mayes 2009)	Wetland plants: *Typha latifolia, Phragmites australis, Iris pseudacorus, Sparganium erectum, Carex flacca & nigra, Juncus effusus, Equisetum fluviatile &. palustre, Schoenoplectus tabernaemontani*

The black willow growth trial conducted at Moorbank botanical gardens demonstrated that the addition of compost could mitigate some of the impact of the elevated pH. Similarly, the addition of nutrients into the soil could catalyse biological activity to mediate pH, similar to that presented in Figure 6.11.

Plate 6.2 – Plant growth on demolition rubble at Compton waste transfer station, California USA 33° 54' 27"N, 118° 15' 21"W (taken by author October 2009)

Plate 6.3 – Plant communities at Science Central, Newcastle upon Tyne – British National Grid Reference NZ241164 (taken by Carla-Leanne Washbourne, September 2010).

Plate 6.4 – (A) Profile of soil development on demolition rubble (taken by author March 2008), (B) Plant growth and diversity on the IRD site, GB National Grid Reference NZ275649 (see Chapter 4, taken by author August 2010).

Plate 6.5 – Plant growth adjacent to a hyper alkaline drainage pond at Howsgill Valley slag heaps, Consett, County Durham, GB National Grid Reference NZ094492 (taken by author June 2008).

6.7 Discussion and conclusions

Using microcosm experiments, the results of this chapter have shown that high pH solutions can inhibit the degradation of some organic acids, suggesting the effects of high pH environments are microbial or enzyme species dependent. Acetate was shown to degrade in solutions whereas citrate did not, and promote a decrease in solution pH. In low pH solutions, organic carbon degradation was similar to that recorded by others. The supply of nutrients to the microcosms was shown to catalyse biological activity, reduce pH and degrade dissolved carbon. Aconitase, the enzyme responsible for the breakdown of citrate, is sensitive to deficiencies in transition metals (Fortnagel and Freese, 1968) which are less soluble in high pH solutions (Tack et al., 1996). The soil used in the microcosm experiments originated from a high pH environment (Plates 6.1 and 6.5), in which the resident organisms have adapted to the extreme conditions. The inhibition of citrate degradation is paradoxical in this respect. Therefore, an explanation of the biological adaptation to the environment at Consett may be summarised as:

- The exuded organic carbon at Consett is limited to smaller molecular weight organic compounds that are more available to microbial degradation. This reduces the pH allowing microbial breakdown of the larger organic molecules.
- The formation of carbonate in the soil buffers pore solution pH providing a less extreme microenvironment for biological activity. This may be an important survival mechanism for plants that have evolved to exude more carbon (organic or inorganic) on high pH soils and promote the precipitation of carbonate minerals.
- Mayes et al. (2008; 2006) recorded variable concentrations of metals in the drainage waters of the slag. The metals, that are usually considered a pollutant, may act to stimulate biological activity at the site, which explains the decrease in concentration along the watercourse.

Growth trials using Black Willow cuttings have demonstrated inhibited growth on soils modified with crushed concrete. It is possible that the environmental stress induced by the concrete will diminish as the material weathers, and similar

growth will be recorded after several seasons. This is rapid in the context of natural site development where sites are biologically productive after decades.

The use of artificial silicates in soils presents a number of challenges to the environment which should be understood before wide scale implementation. This chapter is a preliminary investigation in this field, which should be developed to include the following:

- Expand the microcosm experiments conducted in this chapter for a range of organic acid buffer solutions (malate, oxalate, lactate, succinate etc.) where the organic carbon has been radiolabelled to facilitate detection of reactants and products at soil pore waters concentrations.
- Use chromatography/mass spectrometry analysis to determine the degradation pathway of organics in high pH solutions, expanding on the LC-MS/MS work presented in Appendix D.
- Long term field scale growth trials are required for a range of plant species to understand the weathering dynamics of the material, organic and inorganic carbon accumulation in the soil and the biological response. This can be used to optimise the soil carbon capture technology.
- The previous task would be aided by a detailed investigation of plant primary succession on demolition sites. This can be achieved by using a detailed (flora and fauna species, soil and solution chemistry etc.) chronosequence of sites as a proxy for redevelopment (expanding on the discussion above).

Chapter 7

Chapter 7. Modelling mineral carbonation in soils, economics of silicate transportation and implications for engineers

The aim of the research presented in this chapter was to investigate the application of soil mineral carbonation and how that may be optimised through engineering activity. The models presented herein have been constructed to simulate key (previously un-explored) components of the application of soil mineral carbonation.

Delivered objective: A numerical model was constructed that simulates soil weathering/carbonation as a function of geotechnical (bulk density, particle size distribution, surface area, soil moisture content) and geochemical parameters (cation content of the solid). Carbonate precipitation is influenced by a number of controllable and uncontrollable variables (e.g. 'active' surface area on mineral weathering (and carbonation) is discussed in Chapter 5, and the association between pedogenic carbonate formation and rainfall is discussed in Chapter 4). Therefore, a numerical model was constructed which simulates carbonate precipitation in soils as a function of geotechnical parameters and identifies the rate- and efficiency-limiting variables in soil mineral carbonation.

Delivered objective: A numerical model was constructed that simulates the feasibility of transporting silicate minerals as a function of carbon price. The cost of soil mineral carbonation includes that from extraction/processing (Discussed in Chapter 3), transport to the appropriate site and the cost of application (spreading on agricultural land or incorporation into engineered soils). The costs associated with the latter are well understood from the agricultural practice of liming or the development of made ground. The economics associated with the transport of silicates for mineral carbonation are poorly understood, which justifies the modelling exercise undertaken here.

7.1 Introduction

The importance of soils in the global carbon cycle has prompted the development of numerous models to describe carbon dynamics (e.g. Sohi et al., 2001; Jenkinson et al., 1990). These models generally focus on organic carbon; whereas less work is available on pedogenic carbonates (see Chapter 4). Similarly, models have been created that investigate weathering of minerals

during soil formation (Sverdrup and Warfvinge, 1988) or mineral carbonation on geological time scales (Berner, 1994). Finally, soils are extensively modelled to predict geotechnical properties as part of engineering developments (e.g. DeJong et al., 2006). These disciplines are brought together in this chapter to describe mineral carbonation in engineered soils.

The most significant 'new' cost associated with soil mineral carbonation is the transportation of silicate material from the production site to the application site. To this end, a model is presented in Section 7.4, which was developed from first principals, to simulate the interaction between the value of carbon, cost of material and transportation distance.

7.2 Linking silicate weathering to carbonate precipitation in soils

7.2.1 Scope of model

A model was constructed to simulate carbonate precipitation as a function of silicate weathering in soils. The primary purpose of this is to understand the influence of soil physical properties on carbonate precipitation to aid in the design of application sites. To this end, various assumptions and simplifications have been made:

- The weathering of silicates and solution chemistry is confined to Ca^{2+}, Na^{+} and K^{+}. In reality, Al and Si would also be weathered from the material. However, their solubility is low and secondary phases (gibbsite, kaolinite etc.) would probably precipitate. Therefore, their omission from solution chemistry is reasonable for this model.
- For simplicity, pH, weathering rates and temperature remain constant.
- A generic calcium silicate is the only weathered solid phase and calcite is the only precipitate.
- The soil freely drains and any solution retention is a function of permeability. The retained solution forms a homogeneous unconnected fluid on the mineral surface (consistent with thin film models), evaporation loss was ignored. The only loss of solute is from one dimensional advection where the flow remains constant.
- Biological uptake and absorption of solute into solids was ignored.

- HCO_3^- and CO_3^{2-} are the only anions in solution, where their combined concentration is initially in equilibrium with atmospheric CO_2 at standard temperature and pressure. The concentrations are modified to maintain charge neutrality during the simulation.

The following section describes components of the model, most of which have been standardised to a given unit of volume.

7.2.2 Bulk density, porosity and void ratio

Various geotechnical parameters were employed in this model, which are defined in Table 5.1.

Table 7.1 – Formulae of basic geotechnical properties. Source: Craig (1992).

Parameter	**Formula**
Porosity (n) is the ratio of void volume to total volume	Equation 7.1: $n = \frac{V_v}{V}$
Void ratio (e)	Equation 7.2: $e = \frac{n}{1-n}$
Bulk density (ρ) is the total mass to the total volume	Equation 7.3: $\rho = \frac{M}{V}$
Specific gravity of the soil (G_s) is the density of the soil particles (ρ_s) to the density of water (ρ_w)	Equation 7.4: $G_s = \frac{\rho_s}{\rho_w}$
Saturation ratio (Sr) is the volume of water to the volume of voids	Equation 7.5: $Sr = \frac{V_w}{V_v} = \frac{wG_s}{e}$
Dry density (ρ_d) is the mass of the solid to the total volume	Equation 7.6: $\rho_d = \frac{M_s}{V}$

7.2.3 Particle size distribution, permeability and surface area

Particle size distribution of a material is measured against retention on a series of sieves with decreasing aperture, the size of which usually varies between 10 mm and 63 μm. The quantity of particles smaller than 63 μm is determined through differential settling in solution (see Schiebe et al., 1983). The general size distribution of particles were specified according to ‘gravel’, ‘sand’, ‘silt’ and ‘clay’ and averaged into a series of discreet intervals (Figure 7.1) and the surface area S_m was geometrically determined according to the relationship:

Equation 7.7: $$S = \left[S_i \left(\frac{M_i}{\rho_s \cdot V_i}\right)\right]_i + \left[S_{i+1} \left(\frac{M_{i+1}}{\rho_s \cdot V_{i+1}}\right)\right]_{i+1} \ldots \left[S_j \left(\frac{M_j}{\rho_s \cdot V_j}\right)\right]_j$$

Where ρ_s is the density of solid particles with M, V, and S volume, mass and particle surface area respectively normally distributed between i and j particle diameters. While this is the crudest method of surface area determination, it is comparable to more complex methods for solid grains with minimal internal surface area when accounting for size distribution (Hodson et al., 1998).

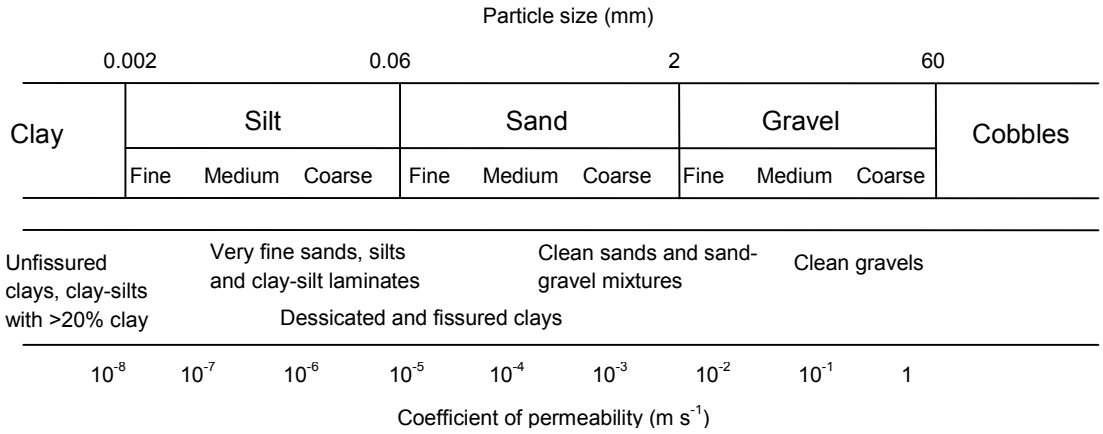

Figure 7.1 – Particle size classification and coefficient of permeability. Adapted from Craig (1992).

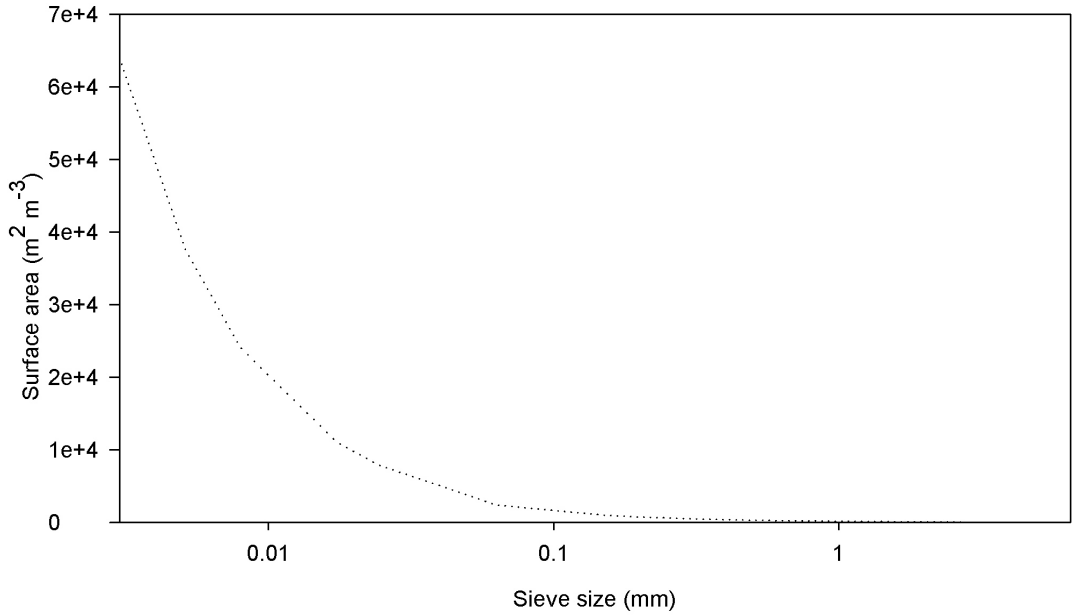

Figure 7.2 – Example of surface area of size fractions for a soil of a sand to silt ratio of 1.

Permeability is a function of particle size (Chakraborty et al., 2006) and can be determined for a size distribution through the Equation 7.8:

Equation 7.8: $$K_s = \frac{cn}{\pi}\sum_{c=1}^{y} \emptyset_i^{(x-2)} w_i [0.667 e^{P_i(1-\alpha)}]^{\frac{(x-2)}{2}}$$

where K_s is the coefficient of permeability (m s^{-1}), c and x are empirically derived parameters that describe the shape and tortuosity of the pores, P_i is the number of particles in the size distribution, w_i is the particle mass and S_i is a scaling parameter (Arya et al., 1999) in the i^{th} size fraction. S_i is related to the number of particles in the size distribution through Equation 7.9.

Equation 7.9: $$S_i = \log P_i$$

Log K values between -8.0 and -6.8 are calculated for a range of sand/silt ratios (Figure 7.3), which corresponds approximately to the fine silt region in Figure 7.1 (for log c and x values of -3.3 and 3.4 respectively, which were determined for sandy clay loam and can vary depending on soil texture; Chakraborty et al., 2006).

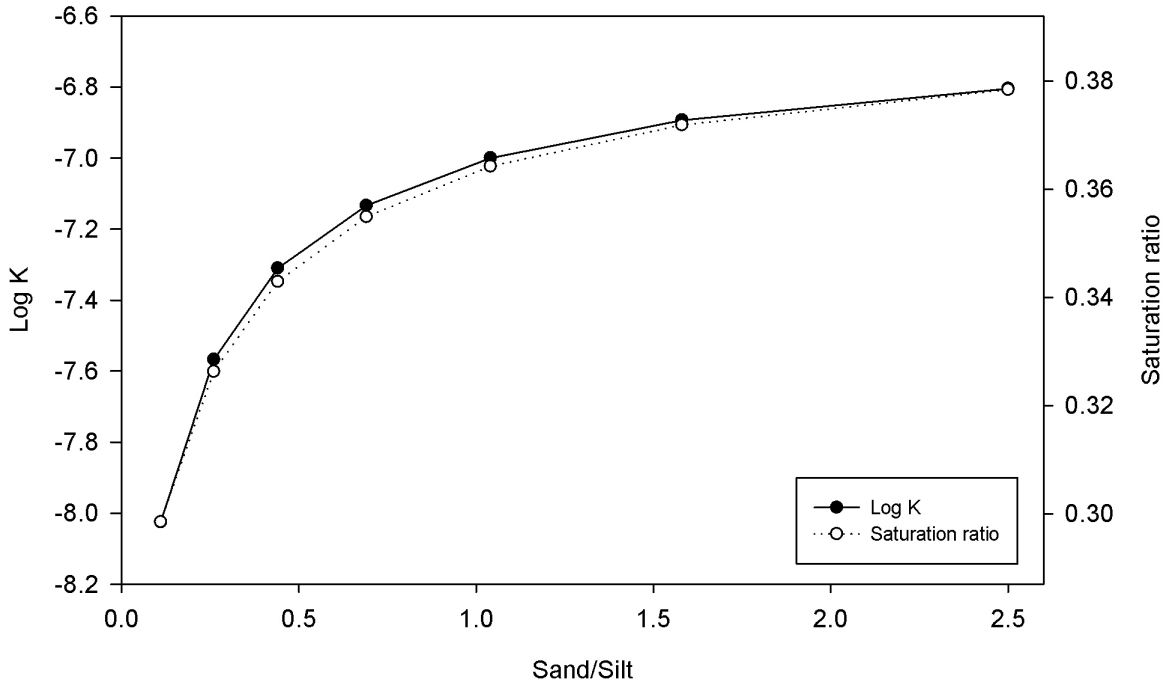

Figure 7.3 – Coefficient of permeability and saturation ratio for a range of sand to silt ratios.

Finally, the degree of saturation is related to the coefficient of permeability through Equation 7.10 (modelled and empirically determined for a clay loam; Fredlund et al., 1994), and varies with sand/silt ratio (Figure 7.3).

Equation 7.10: $$K_s = 10.1 \cdot 10^{-3} Sr^{11.335}$$

7.2.4 Carbon dioxide in solution

Carbon dioxide dissolves as a function of the partial pressure of CO_2 in the gas phase (Henry's law), and by convention is represented completely as carbonic acid (Equation 7.11), which de-protonates as a function of pH (Equations 7.12 and 7.13). For simplicity, the quantity of carbonic acid or carbonate is assumed to be zero at high and low pH respectively.

Equation 7.11: $$CO_{2\,(aq)} + H_2O \leftrightarrow H_2CO_3$$

Equation 7.12 and 7.13: $$K_1 = \frac{[HCO_3^-][H^+]}{[H_2CO_3]} \qquad K_2 = \frac{[CO_3^{2-}][H^+]}{[HCO_3]}$$

where the reaction constants K_1 and K_2 vary with temperature (Figure 7.4)

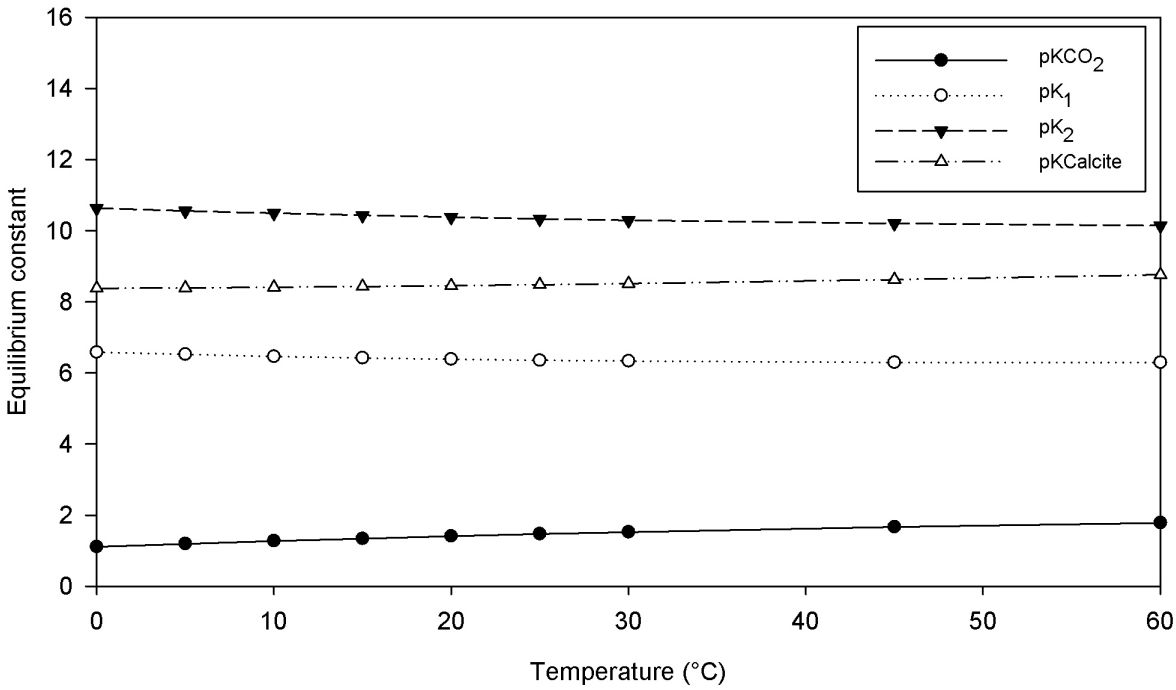

Figure 7.4 – Variation of equilibrium constants with temperature. Source: Drever (1997).

7.2.5 Carbonate precipitation

The degree to which carbonate precipitates in solution is represented through Equation 7.14.

Equation 7.14: $$\Omega = log_{10} \frac{\alpha Ca^{2+} \cdot \alpha CO_3^{2-}}{K_{calcite}}$$

where a saturation index (Ω) = 0 describes a solution in equilibrium with calcite, and positive and negative variations describe supersaturated or under-saturated solutions. $K_{calcite}$ is the solubility constant, which varies with temperature (see Figure 7.4). The activity of calcium and carbonate is a function of the ionic strength of the solutions through the Debye-Huckel equations (Equations 7.15 - 7.18; Appelo and Postma, 2005).

Equation 7.15: $$I = \frac{1}{2} \sum M_i^z z_i^2$$

Equation 7.16: $$\alpha M_i^z = y_i \cdot [M_i^z]$$

Equation 7.17: $$logy_i = \frac{-Az_i^2\sqrt{I}}{1+Ba_0\sqrt{I}} \qquad I < 0.1$$

Equation 7.18: $$logy_i = \frac{-Az_i^2\sqrt{I}}{1+Ba\sqrt{I}} + bI \qquad 0.1 < I < 0.5$$

where y_i is the activity coefficient of the i^{th} ion with z charge, and A, B, a_0, a, and b are empirically derived ion specific coefficients (Table 5.2).

Table 7.2 – Coefficients of activity for Ca^{2+} ad CO_3^{2-}. (Appelo and Postma, 2005; Drever, 1997; and references therein).

Coefficient	**Ca^{2+}**	**CO_3^{2-}**
A at 25°C	0.5085	
B at 25°C	0.3281 x 10^8	
a_0	6x10^{-10}	4.5x10^{-10}
a	5x10^{-10}	5.4x10^{-10}
b	0.165	0

Carbonate precipitation kinetics have been substantially researched, a review of which can be found in Morse et al. (2007), Inskeep and Bloom (1985) and Dreybolt (1981). Generally, precipitation rates are a function of the activity of calcium and carbonate relative to their equilibrium concentration. The further a solution is from equilibrium the more rapid the precipitation rate. Precipitation is divided into discrete steps; the transport of the ions to the mineral surface from the bulk solution through a boundary layer, absorption of the solutes to the

surface, a concentration gradient to the reaction site and finally the reaction (Morse et al., 2007). The rate equations may therefore include terms to account for interferences from the reaction steps. However, for simplicity, the mechanistic model of Nancollas and Reddy (1971), which has been verified extensively through seeded precipitation experiments, was used in this model (Equation 7.19)

Equation 7.19: $$R_p = Ks([Ca^{2+}][CO_3^{2-}] - K_{calcite})$$

where K is the empirically derived rate constant, which can vary considerably depending on the precipitation model and experimental conditions but is reported by Inskeep and Bloom (1985) as 119 dm^6 mol^{-1} m^{-2} sec^{-1} at 25°C (for atm<0.01), which is approximately supported by Compton and Daly (1987). s is the surface area of the crystal taken in this model to be 0.2 m^2 m^{-3} (Inskeep and Bloom, 1985). Parentheses around the ions represent activities.

7.2.6 Solution composition

The concentration of solute $[M^+]$ is a function of mass input from weathering (discussed in detail in Chapter 6), advection loss and precipitation loss. The solution is modelled as a homogeneous unconnected layer on the surface of the soil particles and losses due to diffusion have been ignored. The concentration of solute at time t therefore is represented through Equation 7.20,

Equation 7.20: $$[M_i^+]_t = \frac{R_w \cdot t \cdot p_m \cdot S_m}{V_s} - \frac{Q \cdot [M_i^+]_{t-j}}{n} - R_p \cdot t$$

Where $R_w \bullet p_m$ is the rate of weathering as a proportion of the solute in the material. S_m is the surface area of the solid phase and V_s is the volume of solution. Q is the flow of solution through the material with porosity n, and $[M^+]_{t-j}$ is the concentration of solute at t-*j* time increment. Electrical neutrality is maintained through Equation 7.21.

Equation 7.21: $$\sum([M_i^+] \cdot z_i) + [H^+] - [OH^-] - [HCO_3^-] - 2[CO_3^{2-}] = 0$$

7.3 Soil carbonate precipitation modelling results

7.3.1 Model results

Using the values presented in Table 5.3, the above model was simulated for 250 days.

Table 7.3 – Typical initial parameters for geochemical modelling.

Parameter	Value
CaO (%wt)	8
Na_2O (%wt)	1
K_2O (%wt)	2
Gravel (%wt)	1
Sand (%wt)	49
Silt (%wt)	49
Clay (%wt)	1
Density of soil particles ρs(kg m^{-3})	1800
Volume of solids (Vs) (m^3 m^{-3})	0.4
Flow Q (mm m^{-2} $month^{-1}$)	80
pH	11
Log weathering rate (mol m^{-2} sec)	-10
incremental time increase (days)	1

Calcium concentration in solution was buffered to 15.6 mg l^{-1} by advection loss and precipitation, whereas sodium, potassium, carbonate and bicarbonate increased (Figure 7.5). The efflux of cations into solution represented a small (~0.2 %CaO) loss of concentration in the solid phase (Figure 7.5).

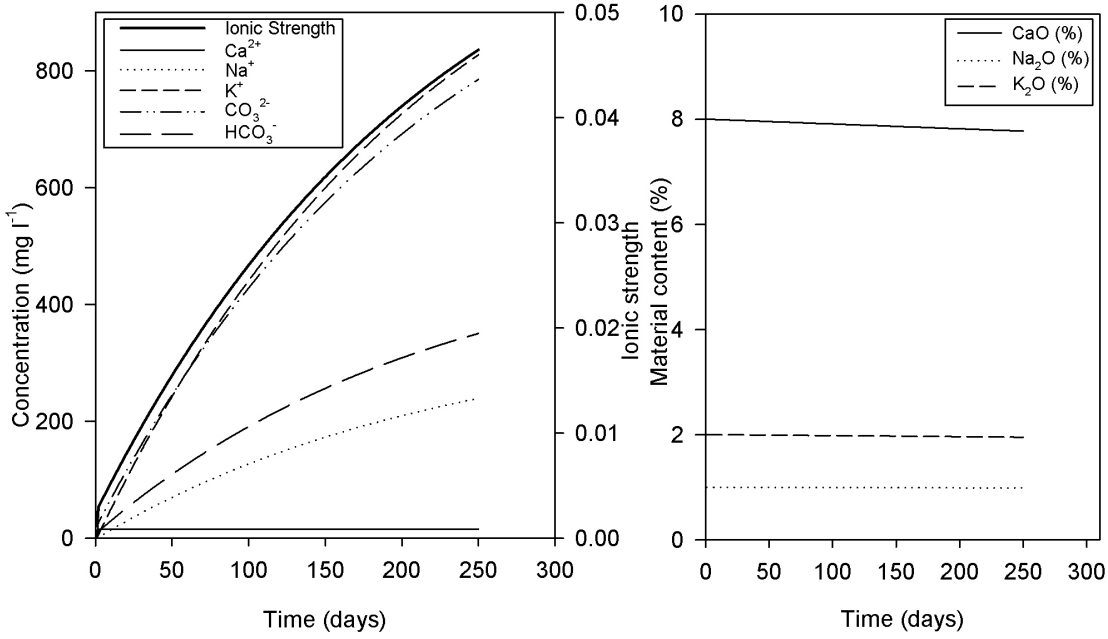

Figure 7.5 – Composition of solution (left) and solids (right) during the simulation.

The carbonate ion concentration increased with cation concentration to maintain charge balance (Figure 7.5; assuming a constant pH). Using the solution chemistry described in Figure 7.5, the saturation index of calcite can be calculated (Figure 7.6), which promotes a log precipitation rate of -6.5 to -4.4x10^{-5} mol dm^{-3} sec^{-1}; similar to that reported in Compton and Daly (1987) and Inskeep and Bloom (1985).

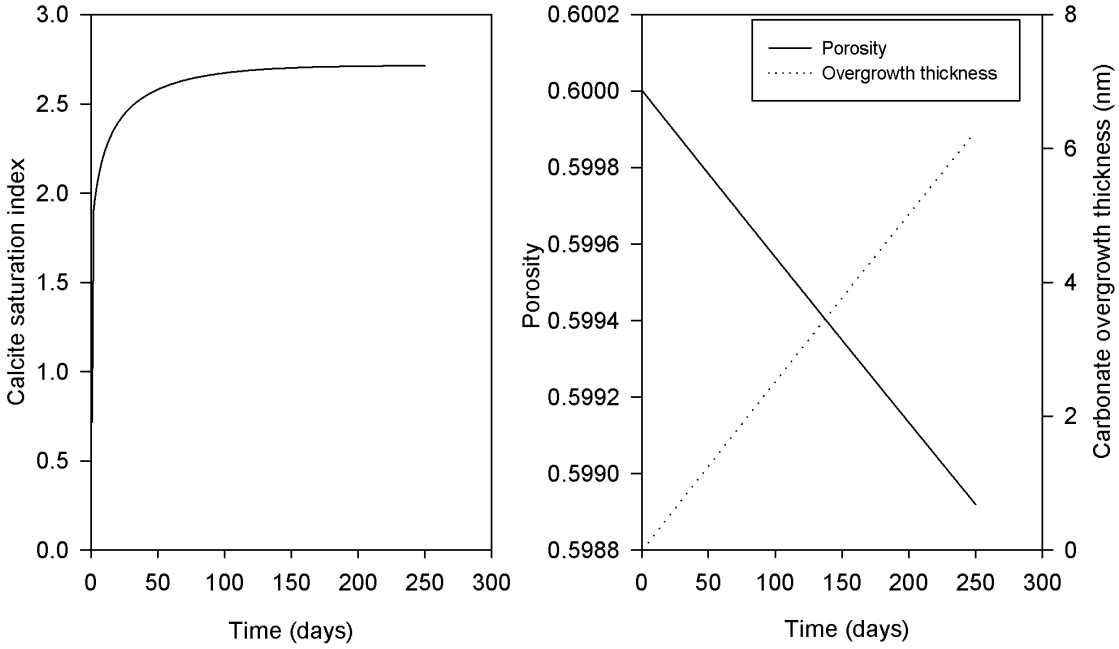

Figure 7.6 – Calcite saturation index (left), and porosity and overgrowth thickness (right) during the simulation.

The growth of a nm thick carbonate layer on the surface of the particles has a small impact on the porosity (Figure 5.6), however the log K permeability constant varied little from -6.9 m s^{-1}. In reality, the relationship between carbonate precipitation and the physical properties of soil (porosity, permeability, bulk density etc) is more complex than modelled here (see DeJong et al., 2006; Ferris et al., 1994).

The model calculates a carbonation rate of 18.72 mgC kg^{-1} (soil) day^{-1}, which is in the same order of magnitude as those calculated from studies of field sites (Chapter 4), and a carbonation efficiency (the ratio of calcium precipitated to that removed from the material) of 21.6 %.

7.3.2 Sensitivity analysis

The parameters presented in Table 5.3 were simulated for a range of realistic values to determine model sensitivity. The results of this exercise are presented in Figure 7.7 A and B. Changes in density of solids (ρ_s) and flow had little effect on the carbonation rate and efficiency. Varying the sand/silt ratio had little influence on the carbonation efficiency, but a larger silt component increased the rate of carbonation possibly as a function of surface area. A similar explanation could be attributed to increases in carbonation rate with volume of solids. The efficiency of carbonation is reduced with increases in V_s as a result of enhanced advection loss from reductions in porosity and a more rapid flow velocity (Equation 7.21).

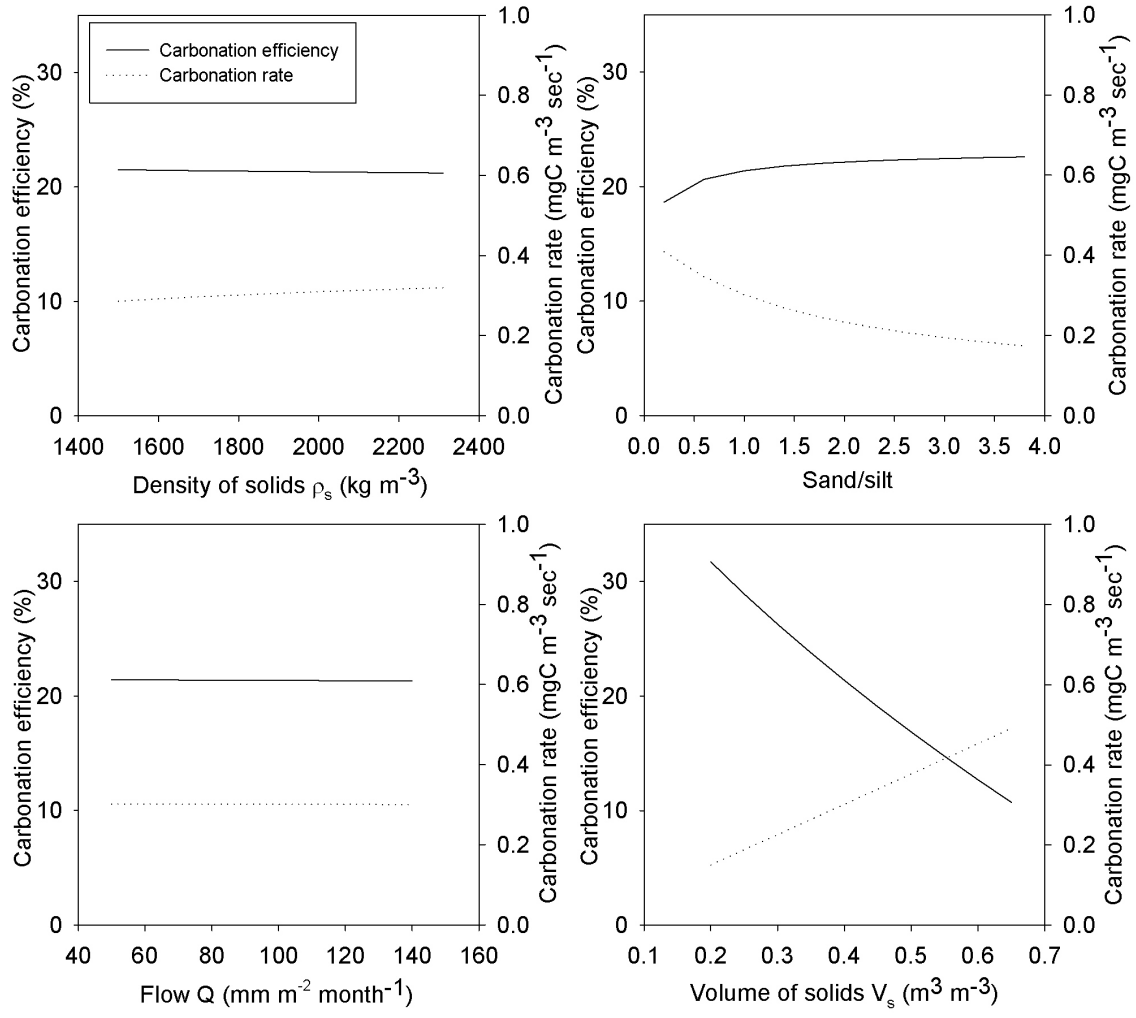

Figure 7.7 A – Sensitivity of carbonation efficiency and rate against realistic changes in input parameters.

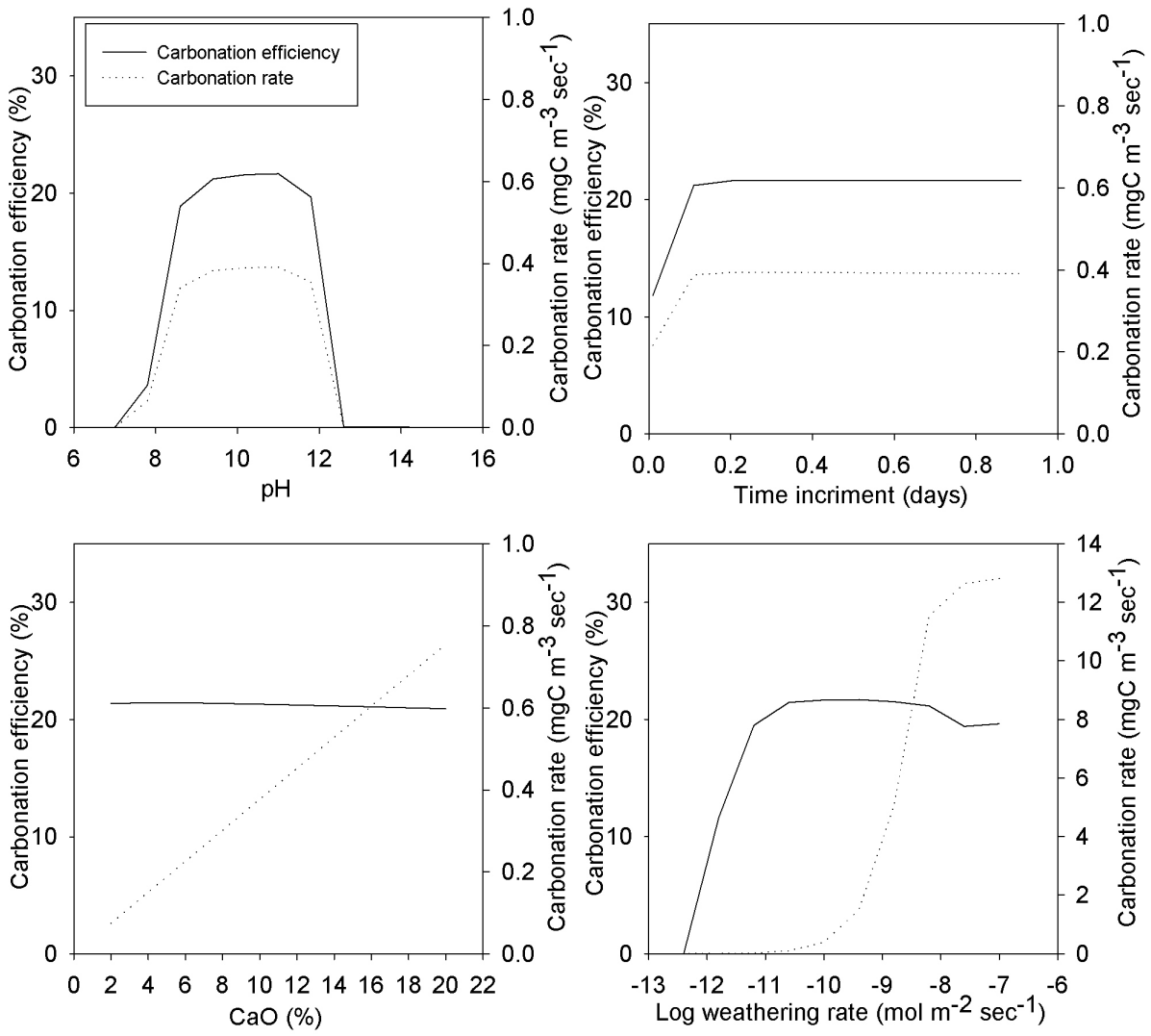

Figure 7.7 B – Sensitivity of carbonation efficiency and rate against realistic changes in input parameters.

Analysis of the model over a pH range of 7.5 – 13 shows a consistent carbonation efficiency and rate between pH values of 8.6 and 11.8, with substantial decreases either side (Figure 7.7 B). This is an artefact of the protonation of carbonate at low pH and hydroxide ion dominance in charge balancing (Equation 7.21) at high pH (Figure 7.8), which reduces calcite saturation. Changes in CaO content of the solid had little effect on carbonation efficiency, but increased carbonation rate. The largest variation in carbonation rate was recorded with changes in weathering rate, which is a function of increased cation flux into solution and calcite saturation. The ionic strength of the pore waters increases exponentially above a log weathering rate of -8 mol m^{-2} sec^{-1}(Figure 7.9) making the model results unreliable.

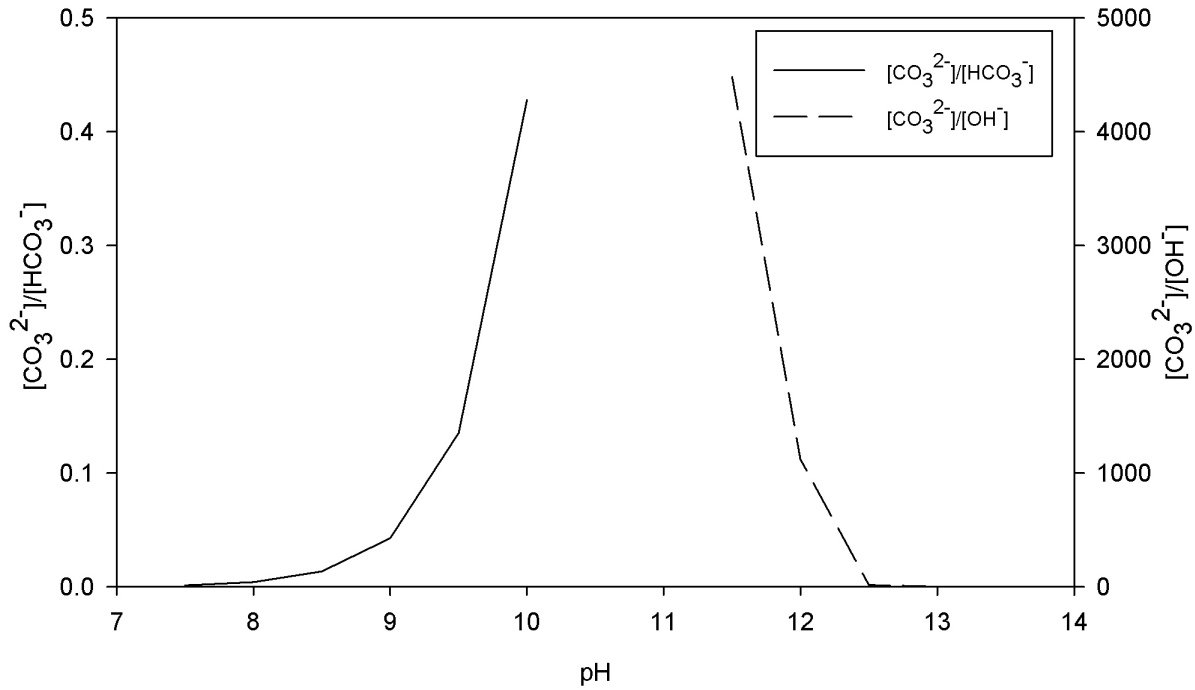

Figure 7.8 – Carbonate ion concentration ratios between pH 7 and 14.

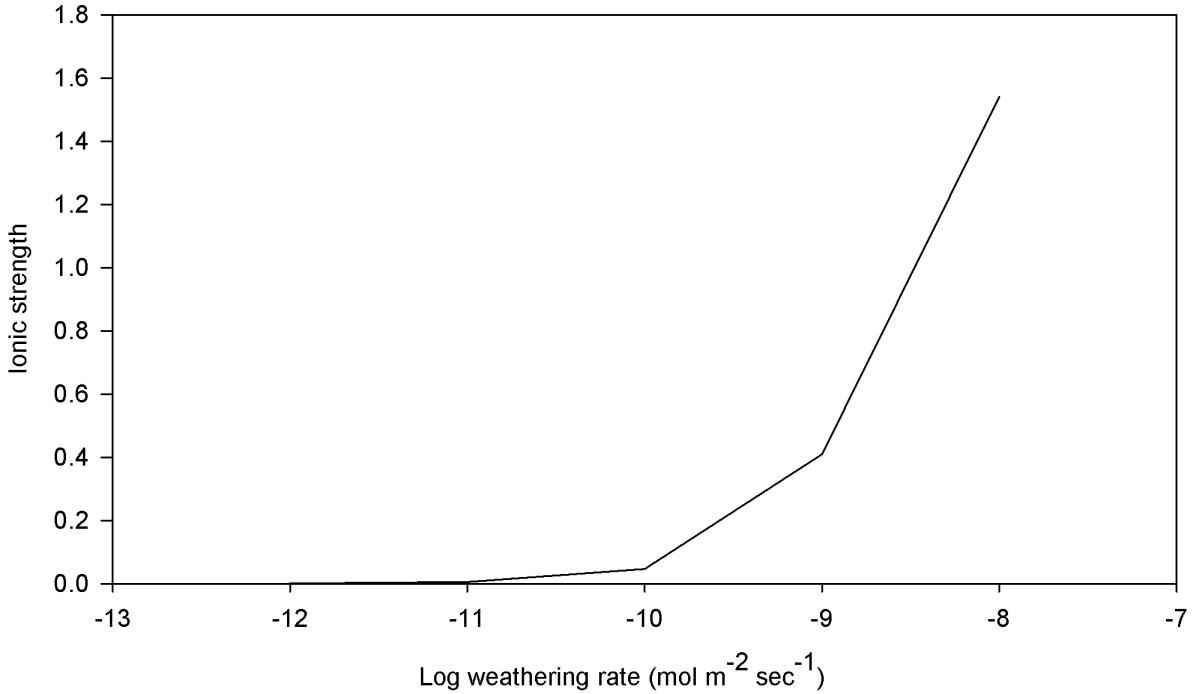

Figure 7.9 – Ionic strength in comparison to range of weathering rates.

7.4 The economics of mineral carbonation in soils

In a strict economic sense, the feasibility of carbonating silicate materials in soil or high temperature/pressure reactors is a trade off between the costs

associated with transporting the material from the source to the carbonation site, the cost during carbonation, and the value of the carbon sequestered.

The value of carbon is determined through the potential impact on the environment and society. Its true cost is subject to large uncertainties. A substantial report commissioned by DEFRA (Downing et al., 2005) values carbon at £35 t^{-1} but recognises the uncertainties in calculation with cited figures ranging between £0-1000 t^{-1} often with standard deviations greater than the mean. Carbon is undervalued on emissions trading markets (e.g. http://ec.europa.eu/clima/policies/ets/index_en.htm) at < £20 t^{-1}. Therefore, there is limited economic incentive for investing in carbon sequestration technologies. However, the required value of carbon for economic feasibility of soil carbon capture can be estimated. In the following calculation it is assumed that the cost of application is minimal in comparison to the transportation costs.

Equation 7.22 presents a relationship between various transportation factors and the maximum transportable distance as a function of the value of carbon.

Equation 7.22: $$D = \frac{10^3\ MPG}{2.08 \cdot A}\left(\frac{C_{mol} \cdot P \cdot M_{ox} \cdot E_c \cdot}{M_{mol}} - \frac{T_{cost}}{C_{value}}\right)$$

where D is maximum transport distance (km), P is the payload of the vehicle (t), M_{ox} and M_{mol} are the wt% and molecular mass (g mol^{-1}) of metal oxide (Ca, Mg) in the material respectively, E_c is the efficiency of carbonation, T_{cost} is the total transport costs (£) and C_{value} is the value of carbon (£ t^{-1}). A is a coefficient to account for congestion and other inefficiencies during transport and C_{mol} is the molecular mass of carbon (g mol^{-1}). Total transportation cost is itself a function of distance represented by Equation 7.23.

Equation 7.23: $$T_{cost} = D\left(\frac{F_£}{0.354 \cdot MPG} + \frac{W_£}{V} + S_£\right) + P \cdot M_£$$

where $F_£$, $W_£$, $S_£$ and $M_£$ are the cost of fuel (£ $Litre^{-1}$), Labour (£ h^{-1}), standard vehicle charge (£ km^{-1}) and material (£ t^{-1}) respectively. V is the average velocity of the vehicle (km h^{-1}). MPG is the fuel consumption of the vehicle which is related to payload through Equation 7.24, although this relationship varies slightly with engine power (Coyle, 2007).

Equation 7.24: $$MPG = -0.140 \cdot P + 10.8$$

Solving Equations 7.22 to 7.24 using typical boundary conditions for the variables (Table 7.4) it can be demonstrated that the value of the material is the dominating variable (£-42 < $M_{£}$ < £3) where D = -12.7 $M_{£}$ + 20.4. Alternatively, Equations 7.22 and 7.24 can be solved to return a value of carbon per unit of distance. There is a positive linear trend between material cost and carbon value where C_{value} = 31.1 $M_{£}$ + 2.4 (see Figure 7.10). The required value for carbon exponentially increases for decreasing concentrations of divalent cations. It substantially increases in this case when CaO <10 %.

Table 7.4 – Typical range of variables in transport modelling equations.

Variable	**Typical value**	**Maximum**	**Minimum**
$F_{£}$ (Fuel Cost)	1 £ l^{-1}	0.5 £ l^{-1}	1.25 £ l^{-1}
$W_{£}$ (Labour cost)	9 £ h^{-1}	13 £ h^{-1}	6 £ h^{-1}
$S_{£}$ (Standard vehicle charge)	1.1 £ km^{-1}	2 £ km^{-1}	0.5 £ km^{-1}
P (Payload)	20 t	40 t	10 t
M_{ox} (Calcium content of material)	20%	50%	2%
E_{ff} (Efficiency of carbonation)	75%	Assumed constant	
V (Average velocity)	50 km h^{-1}		
A (Congestion and transport inefficiencies)	1.4		
M_{mol} (Molecular weight of divalent cation)	56 (g mol^{-1})	Assumed as calcium for simplicity	

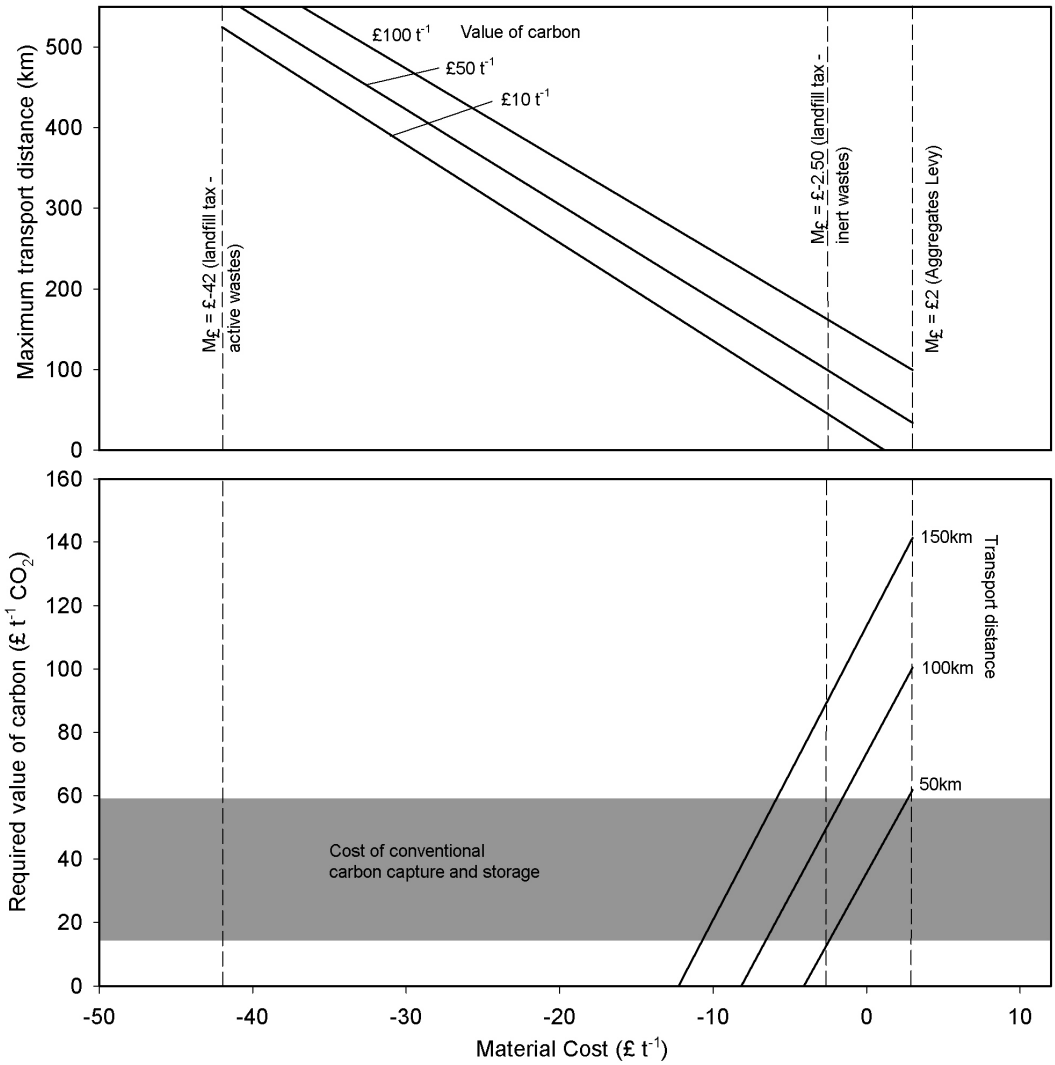

Figure 7.10 – Material cost against transport distance and value of carbon.

7.5 Discussion and conclusions

7.5.1 Important geotechnical parameters in soil mineral carbonation

The soil mineral carbonation model, that was developed for this thesis and is included on an attached CD-rom, describes carbonation as a function of soil properties. Using 'typical' parameters, the model returns carbonation efficiency and rate equivalent to those found in field investigations (Chapter 4). Interrogating the model over a range of input parameters highlights the model sensitivity to change, and the importance of each parameter on carbonation. Increasing the volume of solids and the calcium content of the soil promoted a more rapid carbonation rate; however, the former also decreased carbonation efficiency. The supply of material is probably the primary limiting factor in site design (see Chapter 3). Therefore, to maximise carbonation efficiency a less compact calcium rich material is more suitable. Weathering rate and pH can be

engineered by selection of soil mixtures (blending compost with fines, artificial or natural silicates etc.). However, variations in carbonation in this model as a function of pH and weathering rate highlight limitations in the geochemical model and are not necessarily useful for interpretation of site design.

Additional work is required to develop the geochemical modelling of carbonate precipitation in soils using proprietary software such as Geochemists Workbench®, specifically developing a multi phase equilibrium model that investigates secondary mineral formation where pH is allowed to vary. Furthermore, soil chemistry is influenced by complex hydrodynamics which have not been fully investigated in this model. Therefore, additional work is required to model carbonate precipitation in soils over changing saturation.

7.5.2 Silicate mineral transport distance

The maximum transport distance is primarily dependant on the value of carbon against the value of the silicate material. Assuming the value of the silicate material is between the landfill tax £-2.50 t^{-1} (inert waste) and the aggregates levy £2 t^{-1}, soil mineral carbonation is comparable to underground carbon storage (the grey band in Figure 7.10) when the transport distance is approximately 50 km. This approach, while identifying a radius around a point source of silicates, also suggests an application rate. For instance, 600kg ha^{-1} a^{-1} is the application rate of a point source that produces 50 kt of material a^{-1} (assuming 10% of the surrounding land is available).

7.5.3 Implications for engineers

BS 6031:2009 Code of practice for earthworks contains a proviso for ‘carbon critical design’. However, the associated carbon calculator (available from the Environment Agency website) accounts for the emissions from material production and transport, and does not account for changes in carbon due to soil modification. This thesis suggests that soil carbon may be used to offset the emissions associated with construction. For example, the 2012 London Olympic site (600 hectares) is expected to be able to store around 250 MtC (30 % organic, 70% inorganic carbon) , based on the figures in this paper, compared to 1 MtC released during construction (Commission for a Sustainable London 2012, 2009). Clearly this is justification for careful soil management as part of civil engineering procedures for new developments. For net positive carbon

accumulation, anthropogenic soils must contain more carbon than the natural soils they replace. The mean concentration of soil carbon is 4-10 kgC m^{-2} in arable and grassland soils (Hopkins et al., 2009; Ostle et al., 2009; Smith et al., 2000). Therefore, it should be standard practice to measure soil carbon concentration before and after construction, and periodically through the early life cycle of the development, which can be done using relatively inexpensive techniques that are routine in pedology (loss on ignition, thermal analysis, acid digestion etc.).

It may be possible to accumulate organic and inorganic carbon simultaneously in soils. However the application of calcium rich materials derived from demolition in soil (which are required for the precipitation of inorganic carbon and results in increased pore water pH) may exist in mutually exclusive soil horizons to the optimum conditions for organic carbon accumulation (lower bulk densities and pH) (Figure 8.2). Additional research is required to establish appropriate management practices required for carbon accumulation in soils. However, research suggests that carbon turnover in forest soils may be less than that in grassland soils in a similar climate (Raich and Tufekcioglu, 2000), which ‘suggests’ that selection of appropriate vegetation in planning and design of new developments is important. Furthermore, Lal (2003) highlights the importance of management practices on carbon accumulation in agricultural soils, particularly leaving plant residue after harvesting to degrade into the soil and refraining from tilling the soil to limit oxidation. It is probable that soil management practices will have implications for soil carbon accumulation throughout the life cycle of a new development analogous to the implications on planning for environmental impact of a building through its entire life cycle, where the use of a building can far outweigh the environmental impact of the construction process.

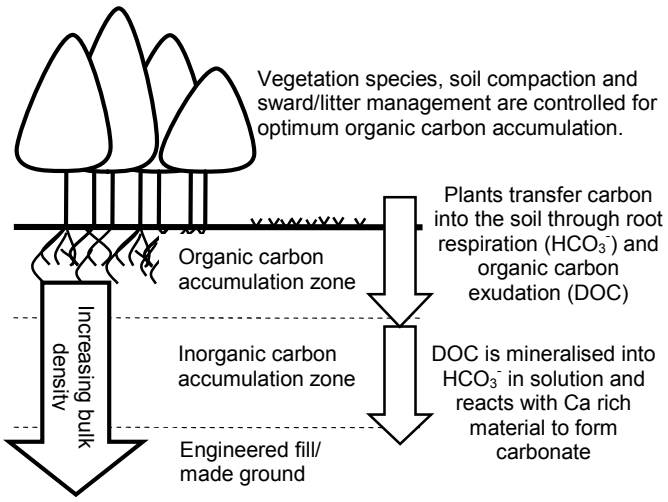

Figure 7.11 – Potential strategy for engineering the soil carbon sink. Source: Renforth et al. (2011a).

Chapter 8

Chapter 8. Discussion

8.1 The efficacy of mineral carbonation

Globally, the total carbonation potential of waste silicate minerals is 192-333 MtC a^{-1}, not including historically produced material that may have a carbonation potential of around 1-2 GtC (Chapter 3). This compares favourably with other carbon mitigation technologies, as part of a 14 GtC a^{-1} portfolio of technologies needed by 2050 to stabilise greenhouse gas concentration in the atmosphere to 500 ppmv (Pacala and Socolow, 2004).

Fieldwork (Chapter 4) has shown the concentration of sequestered inorganic carbon (20-30 kgC m^{-2}) to be equivalent to, if not greater than, organic carbon in natural soils. Existing research on carbon storage in soils is wholly concerned with organic carbon accumulation (e.g. Lal, 2003). However, results here suggest inorganic carbon accumulation warrants the same scrutiny.

Combining the numbers above, it is estimated that around 2 Mha a^{-1} are required to sequester +300 MtC a^{-1}, which is an area equivalent to the size of Wales or ~5 % of global urban land cover (Demographia, 2009). It should be noted that the soils investigated as part of this thesis were not designed for carbon accumulation, and it may be possible to store more carbon than that recorded. It is also possible that multiple carbonation strategies (Chapter 3) will be employed and not all waste silicates will be spread on land. This planetary scale is indicative of the global challenge and comparable to other forms of geoengineering technology (Chapter 2) with the important difference that mineral carbonation on land is more controllable.

The efficiency of carbonation, which is the quantity of carbon captured as a percentage of the maximum carbonation potential, has not been established as part of this thesis. However, weathering trials report up to 76 % of calcium removal from the material, and is equivalent to other carbonation technologies at temperatures greater than 150 °C (Huijgen et al., 2005).

8.2 The rate of mineral carbonation in soils

Table 8.1 summarises carbon accumulation rates measured or estimated in this thesis. Isotopic fractionation mechanisms during the formation of pedogenic carbonates on artificial silicates (Chapter 4) and weathering rates of calcium

from artificial silicates (Chapter 6) suggest that the maximum rates of the underlying chemical processes (x10^6 mgC kg^{-1} (soil) day^{-1}) are rapid and other factors (quantity of available calcium, efficiency of carbonation) will possibly limit the application. They are also several orders of magnitude greater than those calculated from fieldwork experiments and model simulations (2-20 mgC kg^{-1} (soil) day^{-1}), which were estimated between two time points, one of which has an assumed value. Therefore the calculated values from field measurements and modelling are minimum accumulation rates. That withstanding, mineral carbonation in soil is a rapid process that is orders of magnitude greater than organic carbon accumulation in natural soils (mgC kg^{-1} (soil) day^{-1}; Lal, 2003).

*Table 8.1 – Rates of carbon accumulation based on field measurements, modelling and theoretical maximum values from isotopic fractionation mechanisms and weathering experiments. * reported by Lal (2003)*

Investigation		**Rate (mgC kg^{-1}(soil) day^{-1})**
Field measurement – Barrasford quarry after 4 years of operation		2.47
Field measurement –IRD site after 10 years of operation		3.50
Field measurement –Consett Steelworks slag heaps after 25 years of operation		7.62
Field measurement –Science Central after 3 years of operation		18.78
Modelling		18.72
Theoretical maximum based on the supply of Ca and C	Diffusional fractionation – k =$10^{-3.3}$, 10000 cm^2 m^{-3} solution surface area	0.46 x10^6
	Hydroxylation fractionation – k = $10^{-4.1}$ 1000 m^2 kg^{-1} solid surface area	9.15 x10^6
	Weathering experiments – k=10^{-4} and assuming 30% efficiency of Ca to $CaCO_3$	311 x 10^6
Reported organic carbon accumulation in soils*		0.27

8.3 Impact of artificial silicates on the environment

The use of artificial silicates in soils presents a number of challenges to ecosystem development, primarily elevated soil solution pH through the dissolution of hydroxide containing minerals.

Research on naturally high pH groundwaters has discovered large microbial communities existing in this environment. Survival is promoted through

manipulation of the adjacent environment (e.g. by releasing organic compounds).

Microcosm experiments conducted as part of this research and presented in Chapter 7 suggest high pH environments inhibit some microbial activity as a function of nutrient acquisition. Additional nutrients supplied to the solution catalyzed microbial activity and reduced pH.

Field observations of sites modified with artificial silicates demonstrate recovery of plant activity within decades of perturbation analogous to primary succession in natural environments. However, plant growth trials highlight the immediate reduced primary production when soils are mixed with artificial silicates, suggesting that a range of species over a several growing seasons are required to mitigate the effects. Furth more, the addition of organic material (e.g. compost) could be used to mitigate high pH solutions.

Artificial silicate may contain numerous potentially harmful metals. The concentration of which varies between sources, the environmental impact of which has received substantial attention from other researchers. A environmental risk assessment should be conducted before silicates are used in soil.

Chapter 9

Chapter 9. Conclusions and additional work

9.1 Conclusions

Soil is an important part of the global carbon cycle that contains approximately 2800 Gt C, which is 3-4 times more carbon than that contained in the atmosphere. The flux between the atmosphere and soil is estimated to be 75 Gt C a^{-1}, which is an order of magnitude greater than anthropogenic greenhouse gas emissions. Humans release 40 Gt $CO_{2(equivalent)}$ a^{-1}, primarily through fossil fuel combustion, the atmospheric concentration of which is correlated to mean atmospheric temperatures. Projected emission scenarios predict the atmospheric concentration of CO_2 to increase from 350 up to 790 ppmv in the next 100 years, which will increase atmospheric temperatures by 2.0-6.1°C. The political, social, economic and technical barriers that prevent rapid transition to a low carbon economy have led to the concept of 'geoengineering', which is activity that is designed to purposefully alter the Earth's climate.

Historic manipulation of soil through agricultural practices has released 256 Gt C, primarily through the oxidation of soil organic matter. The preponderance of soil in the global carbon cycle and the relative ease at which it can be modified (agriculture/urban environments), suggests that this sink may be engineered to sequester carbon as an emissions mitigation technology. Conventional research has focused on restoring organic carbon concentrations, whereas this thesis of is the first to suggest that inorganic carbon can be engineered through the introduction of silicates into the soil. This is one of a broad portfolio of emergent geoengineering technologies.

A review of waste silicate production statistics suggests that around 15 Gt are created annually, which may be able to sequester up to 332 Mt C a^{-1}. Historically produced material may have a carbon capture potential around 1 Gt C. The study highlights that additional work is required to more accurately quantify the production and carbon capture potential of these materials. Extracting silicates specifically for carbon capture by quarrying igneous rock outcrops may be able to capture around 10^2-10^3 Gt C, this also requires additional research to substantiate.

Using field investigations, this thesis has demonstrated that soils already amended with silicates (brownfield sites, slag heaps) sequester inorganic

carbon (20-30 KgC m^{-2}) to an equivalent, if not greater, extent to natural carbon accumulation. Applying an carbon-oxygen isotopic mixing line hypothesis between hydroxylation/diffusional and lithogenic end members suggests that a large proportion (up to 50 %) of the carbon in the carbonate (with isotope ratios of -3.1 to -27.5 ‰ for $\delta^{13}C$ and -3.9 ‰ to -20.9 ‰ for $\delta^{18}O$) have been sequestered from the atmosphere. Assuming that this carbon has accumulated since demolition, then it is estimated that the rate of carbon capture is 2.1 to 25.8 kgC m^{-2} a^{-1}. To further investigate the rate controlling mechanisms weathering trials, microcosm experiments and geochemical modelling were undertaken.

Batch weathering experiments have shown that up to 75-80% of the calcium in a cement gel is leached out of the material within 5 hours. The measured log weathering rate was between -6.9 and -10.7 mol Ca cm^{-2} sec^{-1}, the more rapid of which are several orders of magnitude greater than that recorded for natural minerals. This suggests that the supply of calcium may not be rate limiting to the precipitation of carbonate or the rate of carbon capture.

Microcosm experiments were undertaken to investigate the contribution of low molecular weight organic compounds to the dissolved inorganic carbon content of soil solutions at elevated pH. The results demonstrate that citrate is stable in high pH solutions whereas acetate is relatively labile, which is a function of nutrient inhibited enzymatic activity. Where organic carbon was successfully mineralised the log rates (-3.4 mmol g^{-1}(field moist soil) sec^{-1}) were equivalent to that found in previous studies.

Geochemical modelling was used to investigate the interaction between soil physical properties and the rate/efficiency of carbon accumulation. The rates of accumulation are equivalent to that found in field investigations.

Weathering trials, fieldwork and modelling suggest that the rate of accumulation (~20 mgC kg^{-1}(soil) day^{-1}) is an order of magnitude greater than rates of accumulation estimated in previous studies for organic carbon. The isotopic interpretation of the carbonates suggests that the maximum chemical controls on the reaction (dissolution of gaseous CO_2, hydroxylation of CO_2, and thin film mechanistic carbonate precipitation) are several orders of magnitude greater than this, and may not limit the rate of carbon capture.

The impact of silicates on resident ecosystems has been qualitatively investigated as part of this thesis. Field observations of soils developed on artificial silicates highlight rapid (10-30 years; in comparison to natural primary/secondary succession on natural silicates, 100+ years) colonisation from specialised plant communities. However, a plant growth trial and microcosm experiments suggest that high pH solutions (buffered by the dissolution of hydroxide bearing minerals associated with artificial silicates) will disrupt ecosystem function. A risk appraisal should be undertaken (similar in scope to those performed for contaminated land) before silicates are applied to land.

The aim of this project was to investigate mineral carbonation in soils as a possible geoengineering technology. It is clear from the results presented in this thesis and summarised above, that mineral carbonation in soils has potential to sequester carbon emissions at the same global scale as other mitigation strategies and may form part of a broad portfolio of measures to this end. This project provides the foundations for additional research on this topic and should be used to inform future studies.

9.2 Additional work and specific recommendations

9.2.1 Material quantification

In Chapter 3 the global production of waste silicates was estimated to be of the order of 190-332 Mt a^{-1}. While some products are globally quantified (slag, cement) there has never been a precedent for measuring others. Therefore, additional work is required in collaboration with material producers to create monitoring and reporting systems to understand the full carbonation potential. Furthermore, the fate of the historically produced material is unknown and it is likely that some if this remains un-carbonated in the environment. Therefore, a global mapping exercise is needed to fully quantify these materials and investigate their carbonation potential.

9.2.2 Field investigation and fieldscale trials

Field investigations have demonstrated inorganic carbon accumulation in soils, and the development of plant communities on sites less than a decade after the material was deposited (Chapters 4 and 7). Additional work is required to understand the ecosystem dynamics of primary succession on artificial silicates,

which is currently being developed on Science Central, a 10 ha brownfield site in the centre of Newcastle upon Tyne, as part of an EPSRC impact award in collaboration with staff in the Schools of Biology and Agriculture at Newcastle University.

Furthermore, the importance of plants in mineral weathering and carbonate precipitation is highlighted in Chapter 6 and 4 respectively. However, a detailed investigation (in the laboratory and at field sites) is required to investigate carbonate precipitation during microbial and plant activity in high pH environments.

9.2.3 Modelling

Chapter 5 presents a model developed as part of this PhD to simulate carbonate precipitation at field scale as a function of soil physical properties. Additional work is required to expand this model to include multiple phases under dynamic pH conditions. Geochemists Workbench® would be suitable for this task.

9.2.4 Isotope fractionation studies

The interpretation of isotopic data of pedogenic carbonates developed on artificial silicates is consistent with other research. However, additional laboratory trials are required to unambiguously determine isotopic fractionation in high pH solutions as a function of precipitation rate, pH and lithogenic carbonate mixing. It is particularly important to determine the influence of lithogenic carbonate with varying isotopic signatures and the isotopic fractionation due to organic carbon inclusion. Finally, an experiment should be undertaken to investigate the influence of temperature on isotopic fractionation (e.g. Dietzel et al., 2009).

An investigation of isotopic signatures across a grain and overgrowth using an ion probe or laser ablation to interrogate a thin section to μm resolution would demonstrate the fractionation processes as a function of time, and simultaneously identify the isotopic end members (Figure 8.3).

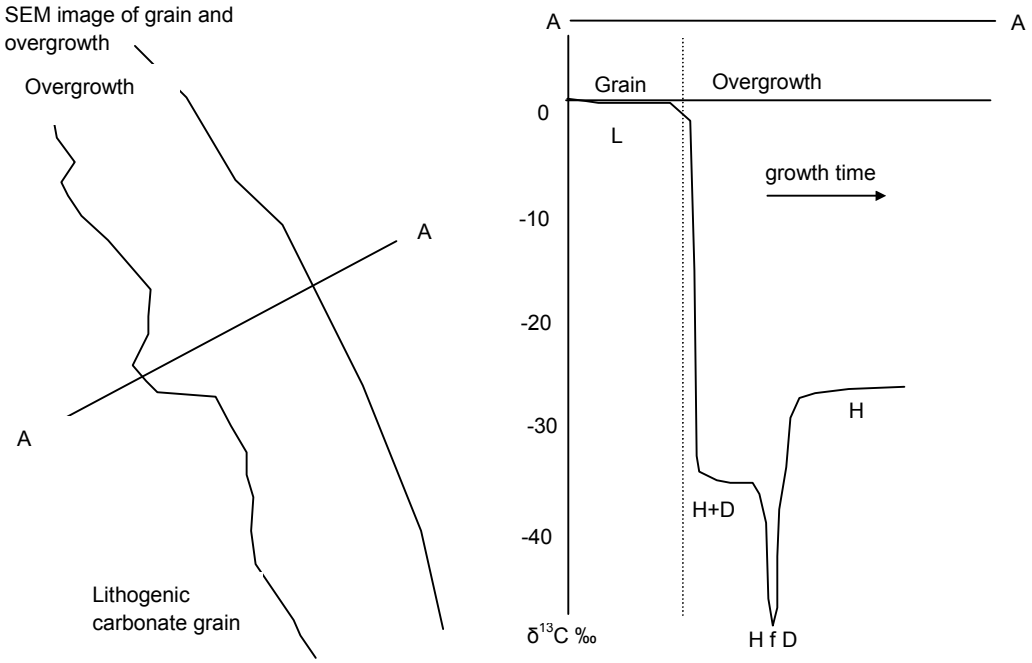

Figure 8.3 – Hypothetical interrogation of isotopic signatures at a μm resolution across a grain and overgrowth. L – Lithogenic carbonate, H – hydroxylation fractionation, D – diffusional fractionation, H f D – Hydroxylation following diffusional fractionation.

9.2.5 Mineral weathering in the laboratory

The experiments in Chapter 6 investigate the weathering of cement under controlled conditions, which simulated cement dissolution as a multiphase material. While this is useful for investigating how hydrated cement behaves in the environment, additional work is required to investigate the weathering of individual phases in cement in similarly controlled conditions.

9.2.6 Organic carbon degradation

The use of artificial silicates in soils presents a number of challenges to ecosystems which should be understood before wide scale implementation.

The microcosm experiments in Chapter 7 should be expanded to evaluate a range of organic acid buffer solutions (malate, oxalate, lactate, succinate etc.) where the organic carbon has been radiolabelled to facilitate detection of reactants and products at soil pore waters concentrations. Long term field scale growth trials are required for a range of plant species to understand the

weathering dynamics of the material, the organic and inorganic carbon accumulation in the soil, and the biological response to extreme growing conditions. This type of study can be used to optimise the soil carbon capture technology and application site design.

Using detailed (flora and fauna species, soil and solution chemistry etc.) chronosequences of plant communities developed on artificial silicates (brownfield sites), stages of plant succession can be used to further understand how silicate environmental impact changes over times.

References

References

Abanades, J. C., M. Akai, S. Benson, K. Caldeira, P. Cook, O. Davidson, R. Doctor, J. Dooley, P. Freund, J. Gale, W. Heidug, H. Herzog, D. Keith, M. Mazzotti, B. Metz, B. Osman-Elasha, A. Palmer, R. Pipatti, K. Smekens, M. Soltanieh, Kelly, Thambimuthu and B. van der Zwaan. (2005) *Special report: Carbon dioxide capture and storage.* IPCC. ISBN-13 978-0-521-68551-1

ACAA. (2008) *Coal combustion product (CCP) production & use survey report.* The American Coal Ash Association Available at http://acaa.affiniscape.com/associations/8003/files/2008_ACAA_CCP_Survey_Report_FINAL_100509.pdf (Accessed: 18/07/2010)

Amrhein, C. and Suarez, D. L. (1992) 'Some factors affecting the dissolution kinetics of anorthite at 25°C', *Geochimica et Cosmochimica Acta,* 56, (5), pp. 1815-1826.

Anand, R. R., Phang, C., Wildman, J. E. and Lintern, M. J. (1997) 'Genesis of some calcretes in the southern Yilgarn Craton, Western Australia: Implications for mineral exploration', *Australian Journal of Earth Sciences,* 44, (1), pp. 87-103.

Anders, E. and Owen, T. (1977) 'Mars and Earth: Origin and abundance of volatiles', *Science,* 198, (4316), pp. 453-465.

Andrews, J. E. (2006) 'Palaeoclimatic records from stable isotopes in riverine tufas: Synthesis and review', *Earth-Science Reviews,* 75, (1-4), pp. 85-104.

Andrews, J. E., Gare, S. G. and Dennis, P. F. (1997) 'Unusual isotopic phenomena in Welsh quarry water and carbonate crusts', *Terra Nova,* 9, (2), pp. 67-70.

Aplet, G. H., Hughes, R. F. and Vitousek, P. M. (1998) 'Ecosystem development on Hawaiian lava flows: biomass and species composition', *Journal of Vegetation Science,* 9, (1), pp. 17-26.

Appelo, C. A. J. and Postma, D. (2005) *Geochemistry, groundwater and pollution.*2nd ed London: Taylor & Francis. ISBN 04 1536 421 3

Archer, D. E., Takahashi, T., Sutherland, S., Goddard, J., Chipman, D., Rodgers, K. and Ogura, H. (1996) 'Daily, seasonal and interannual variability of sea-surface carbon and nutrient concentration in the equatorial Pacific Ocean', *Deep Sea Research Part II: Topical Studies in Oceanography,* 43, (4-6), pp. 779-808.

Arvidson, R. S. and Mackenzie, F. T. (1999) 'The dolomite problem; control of precipitation kinetics by temperature and saturation state', *American Journal of Science,* 299, (4), pp. 257-288.

Arya, L. M., Leij, F. J., van Genuchten, M. T. and Shouse, P. J. (1999) 'Scaling parameter to predict the soil water characteristic from particle-size distribution data', *Soil Science Society of America Journal,* 63, (3), pp. 510-519.

Bachmeier, K. L., Williams, A. E., Warmington, J. R. and Bang, S. S. (2002) 'Urease activity in microbiologically-induced calcite precipitation', *Journal of Biotechnology,* 93, pp. 171-181.

Bajnoczi, B., Horvath, Z., Demeny, A. and Mindszenty, A. (2005) *8th Isotope Workshop of the European-Society-for-Isotope-Research.* Leipzig, GERMANY, Jun 25-30.Taylor & Francis Ltd.

Balogh-Brunstad, Z., Keller, C. K., Bormann, B. T., O'Brien, R., Wang, D. and Hawley, G. (2008) 'Chemical weathering and chemical denudation dynamics through ecosystem development and disturbance', *Global Biogeochemical Cycles,* 22, (1), pp. GB1007.

Barlow, S. G. (1996) *The mineralogical, geochemical and experimental evaluation of boulder clay from Adswood, Stockport, as a model brickclay raw material.* PhD thesis. University of Manchester.

Batjes, N. H. (1996) 'Total carbon and nitrogen in the soils of the world', *European Journal of Soil Science,* 47, pp. 151-163.

Batjes, N. H. (2008) *ISRIC - Wise harmonized global soil profile dataset (version 3.1).* Wageningen: ISRIC - World Soil Information

Bayless, E. R. and Schulz, M. S. (2003) 'Mineral precipitation and dissolution at two slag-disposal sites in northwestern Indiana, USA', *Environmental Geology,* 45, (2), pp. 252-261.

Beck, M. B., Jiang, F., Shi, F., Walker, R. V., Osidele, O. O., Lin, Z., Demir, I. and Hall, J. W. (2009) 'Re-engineering cities as forces for good in the environment', *Proceedings of the Institution of Civil Engineers-Engineering Sustainability,* 163, (1), pp. 31-46.

Bellamy, P. H., Loveland, P. J., Bradley, R. I., Lark, R. M. and Kirk, G. J. D. (2005) 'Carbon losses from all soils across England and Wales 1978-2003', *Nature,* 437, (7056), pp. 245-248.

Bennett, P. J., Longstaffe, F. J. and Rowe, R. K. (2000) 'The stability of dolomite in landfill leachate-collection systems', *Canadian Geotechnical Journal,* 37, (2), pp. 371-378.

Berg, A. and Banwart, S. A. (2000) 'Carbon dioxide mediated dissolution of Ca-feldspar: implications for silicate weathering', *Chemical Geology,* 163, (1-4), pp. 25-42.

Bergsdal, H., Bohne, R. A. and Brattebø, H. (2007) 'Projection of Construction and Demolition Waste in Norway', *Journal of Industrial Ecology,* 11, (3), pp. 27-39.

Berner, R. A. (1994) 'Geocarb II; A revised model of atmospheric CO_2 over Phanerozoic time', *American Journal of Science,* 294, (1), pp. 56-91.

Berner, R. A. and Barron, E. J. (1984) 'Factors affecting atmospheric CO_2 and temperature over the past 100 million years', *American Journal of Science,* 284, (10), pp. 1183-1192.

Berner, R. A. and Kothavala, Z. (2001) 'GEOCARB III: A revised model of atmospheric CO_2 over phanerozoic time', *American Journal of Science,* 301, (2), pp. 182-204.

Berner, R. A., Lasaga, A. C. and Garrels, R. M. (1983) 'The carbonate-silicate geochemical cycle and its effect on atmospheric carbon-dioxide over the past 100 million years', *American Journal of Science,* 283, (7), pp. 641-683.

Bertron, A., Duchesne, J. and Escadeillas, G. (2005) 'Attack of cement pastes exposed to organic acids in manure', *Cement and Concrete Composites,* 27, (9-10), pp. 898-909.

BGS. (1927-2008) *World Mineral Production/Statistics*. [Online]. Available at: http://www.bgs.ac.uk/mineralsuk/statistics/worldArchive.html (Accessed: 01/09/2010).

BGS. (2005) *Mineral profile: Cement raw materials. http://www.bgs.ac.uk/mineralsuk/statistics/mineralProfiles.html Accessed 02/09/2010.* British Geological Survey

BGS. (2010) *Mineral Statistics: Cement.* British Geological Survey:

Birch, A. (1967) *Economic history of the British iron and steel industry 1784-1879.* Routledge. ISBN 0-415-38248-3

Birkeland, P. W. and Larson, E. E. (1989) *Putnam's Geology* 5th ed New York, Oxford: Oxford University Press.

Blum, A. E. and Stillings, L. L. (1995) 'Feldspar dissolution kinetics', in White, A. F. and Brantley, S. L.(eds) *Chemical weathering rates of silicate minerals.* Vol. 31 Mineralogical Society of America.

Bobrowsky, P. T. (ed.) (1998) *Aggregate resources: a global perspective.* Rotterdam: A.A. Balkema.

Boden, T. A., Marland, G. and Andres, R. J. (2010) *Global, regional, and national fossil-fuel CO_2 emissions. Carbon Dioxide Information Analysis Center.* Oak Ridge National Laboratory, U.S. Department of Energy

Boer, G. J., McFarlane, N. A. and Lazare, M. (1992) 'Greenhouse gas-induced climate change simulated with the CCS second-generation general circulation model', *Journal of Climate,* 5, (10), pp. 1045-1077.

Boguckyj, A. B., Lanczont, M., Lacka, B., Madeyska, T. and Zawidzki, P. (2006) 'Stable isotopic composition of carbonates in Quaternary sediments of the Skala Podil'ska sequence (Ukraine)', *Quaternary International,* 152-153, pp. 3-13.

Boucot, A. J. and Gray, J. (2001) 'A critique of Phanerozoic climatic models involving changes in the CO_2 content of the atmosphere', *Earth-Science Reviews,* 56, (1-4), pp. 1-159.

Brookes, P. C., Cayuela, M. L., Contin, M., De Nobili, M., Kemmitt, S. J. and Mondini, C. (2008) 'The mineralisation of fresh and humified soil organic matter by the soil microbial biomass', *Waste Management,* 28, (4), pp. 716-722.

Brunauer, S., Emmett, P. H. and Teller, E. (1938) 'Adsorption of gases in multimolecular layers', *Journal of the American Chemical Society,* 60, (2), pp. 309-319.

Business Link (2010) *Environmental tax obligations and breaks*. Available at: http://www.businesslink.gov.uk/bdotg/action/detail?type=RESOURCES&itemId=1074404201 (Accessed: 11/03/10).

Bylund, D., Norström, S. H., Essén, S. A. and Lundström, U. S. (2007) 'Analysis of low molecular mass organic acids in natural waters by ion exclusion chromatography tandem mass spectrometry', *Journal of Chromatography A,* 1176, (1-2), pp. 89-93.

Cailleau, G., Braissant, O. and Verrecchia, E. (2004) 'Biomineralization in plants as a long-term carbon sink', *Naturwissenschaften,* 91, pp. 191-194.

Campbell, G. S. and Norman, J. M. (1977) *An introduction to environmental biophysics* Springer. ISBN 978-0387949376

Cao, M. and Woodward, F. I. (1998) 'Net primary and ecosystem production and carbon stocks of terrestrial ecosystems and their responses to climate change', *Global Change Biology,* 4, pp. 185-198.

Capo, R. C., Whipkey, C. E., Chadwick, O. A. and Stewart, B. W. (2000) 'The importance of sea spray to the cation budget of a coastal Hawaiian soil: a strontium isotope approach', *Chemical Geology,* 168, (1-2), pp. 37-48.

Carr, J. C. and Taplin, W. (1962) *History of the British steel industry.* Harvard University Press. ASIN: B0006D6B9A

Casey, W. H. and Ludwig, C. (1995) 'Silicate mineral dissolution as a ligand-exchange reaction', in White, A. F. and Brantley, S. L.(eds) *Chemical weathering rates of silicate minerals.* Vol. 31 Mineralogical Society of America.

Cerling, T. E. (1984) 'The Stable isotopic composition of modern soil carbonate and Its relationship to climate', *Earth and Planetary Science Letters,* 71, (2), pp. 229-240.

Chadwick, A., Arts, R., Bernstone, C., May, F., Thibeau, S. and Zweigel, P. (2008) *Best practice for the storage of CO_2 in saline aquifers.* British Geological Survey. ISBN: 978-0-85272-610-5.

Chakraborty, D., Chakraborty, A., Santra, P., Tomar, R. K., Garg, R. N., Sahoo, R. N., Choudhury, S. G., Bhavanarayana, M. and Kalra, N. (2006) 'Prediction of hydraulic conductivity of soils from particle-size distribution', *Current Science,* 90, (11), pp. 1526-1531.

Chebotarev, I. I. (1955) 'Metamorphism of natural waters in the crust of weathering 1', *Geochimica et Cosmochimica Acta,* 8, (1-2), pp. 22-32, IN1-IN2, 33-48.

Chen, J. J., Thomas, J. J., Taylor, H. F. W. and Jennings, H. M. (2004) 'Solubility and structure of calcium silicate hydrate', *Cement and Concrete Research,* 34, (9), pp. 1499-1519.

Chung, F. H. (1974) 'Quantitative interpretation of X-ray diffraction patterns of mixtures. I. Matrix-flushing method for quantitative multicomponent analysis', *Journal of Applied Crystallography,* 7, (6), pp. 519-525.

Clark, I. D., Fontes, J.-C. and Fritz, P. (1992) 'Stable isotope disequilibria in travertine from high pH waters: Laboratory investigations and field observations from Oman', *Geochimica et Cosmochimica Acta,* 56, (5), pp. 2041-2050.

Cochran, M. F. and Berner, R. A. (1996) 'Promotion of chemical weathering by higher plants: Field observations on Hawaiian basalts', *Chemical Geology,* 132, (1-4), pp. 71-77.

Commission for a Sustainable London 2012. (2009) *Extinguishing emissions?.* Available at http://www.cslondon.org/wp-content/uploads/downloads/2009/12/2009_Carbon_Review.pdf

Compton, R. G. and Daly, P. J. (1987) 'The dissolution-precipitation kinetics of calcium-carbonate - an assessment of various kinetic equations using a rotating disk method', *Journal of Colloid and Interface Science,* 115, (2), pp. 493-498.

Coyle, M. (2007) *Effects of payload on the fuel consumption of trucks.* Department for Transport

Craig, H. (1953) 'The geochemistry of the stable carbon isotopes', *Geochimica et Cosmochimica Acta,* 3, (2-3), pp. 53-92.

Craig, R. F. (1992) *Soil Mechanics.*5th ed London: Chapman and Hall.

Craighill, A. and Powell, C. (1999) *A lifecycle assessment and evaluation of construction and demolition waste.* CSERG

Crawford, D. L. and Crawford, R. L. (1976) 'Microbial degradation of lignocellulose: the lignin component', *Applied Environmental Microbiology,* 31, (5), pp. 714-717.

Dakora, F. D. and Phillips, D. A. (2002) 'Root exudates as mediators of mineral acquisition in low-nutrient environments', *Plant and Soil,* 245, (1), pp. 35-47.

Dale, V. H. (1997) 'The relationship between land-use change and climate change', *Ecological Applications,* 7, (3), pp. 753-769.

Dart, R. C., Barovich, K. M., Chittleborough, D. J. and Hill, S. M. (2007) 'Calcium in regolith carbonates of central and southern Australia: Its source and implications for the global carbon cycle', *Palaeogeography Palaeoclimatology Palaeoecology,* 249, (3-4), pp. 322-334.

Das, A., Krishnaswami, S. and Bhattacharya, S. K. (2005) 'Carbon isotope ratio of dissolved inorganic carbon (DIC) in rivers draining the Deccan Traps, India: Sources of DIC and their magnitudes', *Earth and Planetary Science Letters,* 236, (1-2), pp. 419-429.

Das, B., Prakash, S., Reddy, P. S. R. and Misra, V. N. (2007) 'An overview of utilization of slag and sludge from steel industries', *Resources, Conservation and Recycling,* 50, (1), pp. 40-57.

Dasgupta, R. and Walker, D. (2008) 'Carbon solubility in core melts in a shallow magma ocean environment and distribution of carbon between the Earth's core and the mantle', *Geochimica et Cosmochimica Acta,* 72, (18), pp. 4627-4641.

DCLG. (2007) *Survey of arisings and use of alternatives to primary aggregates in England, 2005 Construction, demolition and excavation waste.* Crown Copyright

DECC. (2009) *Digest of UK energy statistics'* Department for Energy and Climate Change

DECC. (2010) *Historical coal data: coal production, availability and consumption 1853 to 2007.* Department for Energy and Climate Change

Deer, W. A., Howie, R. A. and Zussman, J. (1996) *An Introduction to the Rock-Forming Minerals.*2nd ed: Prentice Hall. ISBN: 978-0582300941

DEFRA. (2008) *Construction resources and waste roadmap 2008.* Building Research Establishment/ Department for Environment Food and Rural Affairs

DeJong, J. T., Fritzges, M. B. and Nusslein, K. (2006) 'Microbially induced cementation to control sand response to undrained shear', *Journal of Geotechnical and Geoenvironmental Engineering,* 132, (11), pp. 1381-1392.

DeJong, J. T., Soga, K., Banwart, S. A., Whalley, W. R., Ginn, T. R., Nelson, D. C., Mortensen, B. M., Martinez, B. C. and Barkouki, T. (in press) 'Soil engineering in vivo: harnessing natural biogeochemical systems for sustainable, multi-functional engineering solutions', *Journal of The Royal Society Interface*.

del Giorgio, P. A. and Duarte, C. M. (2002) 'Respiration in the open ocean', *Nature,* 420, (6914), pp. 379-384.

Del Grosso, S., Parton, W., Stohlgren, T., Zheng, D., Bachelet, D., Prince, S., Hibbard, K. and Olson, R. (2008) 'Global potential net primary production predicted from vegetation class, precipitation, and temperature.', *Ecology,* 89, (8), pp. 2117–2126.

Demographia. (2009) *Demographia world urban areas (world agglomerations): 2009.* Available at http://www.demographia.com/db-worldua2015.pdf

Denning, A. S., Fung, I. Y. and Randall, D. (1995) 'Latitudinal gradient of atmospheric CO_2 due to seasonal exchange with land biota', *Nature,* 376, (6537), pp. 240-243.

Deshpande, V. P. and Shekdar, A. V. (2005) 'Sustainable waste management in the Indian mining industry', *Waste Management Research,* 23, (4), pp. 343-355.

Dessert, C., Dupre, B., Gaillardet, J., Francois, L. M. and Allegre, C. J. (2003) 'Basalt weathering laws and the impact of basalt weathering on the global carbon cycle', *Chemical Geology,* 202, (3-4), pp. 257-273.

Dietzel, M., Tang, J., Leis, A. and Köhler, S. J. (2009) 'Oxygen isotopic fractionation during inorganic calcite precipitation -- Effects of temperature, precipitation rate and pH', *Chemical Geology,* 268, (1-2), pp. 107-115.

Dietzel, M., Usdowski, E. and Hoefs, J. (1992) 'Chemical and $^{13}C/^{12}C$- and $^{18}O/^{16}O$-isotope evolution of alkaline drainage waters and the precipitation of calcite', *Applied Geochemistry,* 7, (2), pp. 177-184.

Dijkstra, J. J., van der Sloot, H. A. and Comans, R. N. J. (2006) 'The leaching of major and trace elements from MSWI bottom ash as a function of pH and time', *Applied Geochemistry,* 21, (2), pp. 335-351.

Dixon, R., Solomon, A., Brown, S., Houghton, R., Trexier, M. and Wisniewski, J. (1994) 'Carbon pools and flux of global forest ecosystems', *Science,* 263 pp. 185-190.

Donnelly, P., Entry, J., Crawford, D. and Cromack, K. (1990) 'Cellulose and lignin degradation in forest soils: Response to moisture, temperature, and acidity', *Microbial Ecology,* 20, (1), pp. 289-295.

Dotsika, E., Psomiadis, D., Poutoukis, D., Raco, B. and Gamaletsos, P. (2009) 'Isotopic analysis for degradation diagnosis of calcite matrix in mortar', *Analytical and Bioanalytical Chemistry,* 395, (7), pp. 2227-2234.

Downing, T. E., Anthoff, D., Butterfield, B., Ceronsky, M., Grubb, M., Guo, J., Hepburn, C., Hope, C., Hunt, A., Li, A., Markandya, A., Moss, S., Nyong, A., Tol, R. S. J. and Watkiss, P. (2005) *Scoping uncertainty in the social cost of carbon.* London: DEFRA

Drever, J. I. (1997) *The Geochemistry of Natural Waters: Surface and Groundwater.*3rd ed: Prentice-Hall, Inc.

Dreybrodt, W. (1981) 'The kinetics of calcite precipitation from thin-films of calcareous solutions and the grwoth of speleothems - revisited', *Chemical Geology,* 32, (3-4), pp. 237-245.

Duchesne, J. and Reardon, E. J. (1995) 'Measurement and prediction of portlandite solubility in alkali solutions', *Cement and Concrete Research,* 25, (5), pp. 1043-1053.

Ducloux, J., Laouina, A., Chaker, M. and Dinel, H. (1990) 'Carbonate accumulation and weathering of the granitic substratum of Tanecherfi Basin, Northeastern Morocco', *Catena,* 17, (6), pp. 493-508.

Dudka, S. and Adriano, D. C. (1997) 'Environmental impacts of metal ore mining and processing: a review', *Journal of Environmental Quality,* 26, pp. 590-602.

Dupre, B., Dessert, C., Oliva, P., Godderis, Y., Viers, J., Francois, L., Millot, R. and Gaillardet, J. (2003) 'Rivers, chemical weathering and Earth's climate', *Comptes Rendus Geosciences,* 335, (16), pp. 1141-1160.

Durand, N., Gunnell, Y., Curmi, P. and Ahmad, S. M. (2006) 'Pathways of calcrete development on weathered silicate rocks in Tamil Nadu, India: Mineralogy, chemistry and paleoenvironmental implications', *Sedimentary Geology,* 192, (1-2), pp. 1-18.

Durand, N., Gunnell, Y., Curmi, P. and Ahmad, S. M. (2007) 'Pedogenic carbonates on Precambrian silicate rocks in South India: Origin and paleoclimatic significance', *Quaternary International,* 162-163, pp. 35-49.

EA. (2007) *Waste protocols project - Blast furnace slag.* Environment Agency

EIA. (2009) *Annual Energy Review.* U.S. Energy Information Administration

U.S. Energy Information Administration (2010) *International Energy Statistics: Total Coal Consumption* [Online]. Available at: (Accessed: 20/07/2010).

Emerson, S., Quay, P., Karl, D., Winn, C., Tupas, L. and Landry, M. (1997) 'Experimental determination of the organic carbon flux from open-ocean surface waters', *Nature,* 389, (6654), pp. 951-954.

Eppley, R. W. and Peterson, B. J. (1979) 'Particulate organic matter flux and planktonic new production in the deep ocean', *Nature,* 282, (5740), pp. 677-680.

Fang, C. and Moncrieff, J. B. (1998) 'An open-top chamber for measuring soil respiration and the influence of pressure difference on CO_2 efflux measurement', *Functional Ecology,* 12, (2), pp. 319-325.

Fernandez Bertos, M., Simons, S. J. R., Hills, C. D. and Carey, P. J. (2004) 'A review of accelerated carbonation technology in the treatment of cement-based materials and sequestration of CO_2', *Journal of Hazardous Materials,* 112, (3), pp. 193-205.

Ferris, F. G., Wiese, R. G. and Fyfe, W. S. (1994) 'Precipitation of carbonate minerals by microorganisms - implications for silicate weathering and the global carbon-dioxide budget', *Geomicrobiology Journal,* 12, (1), pp. 1-13.

Fischer, H., Meyer, A., Fischer, K. and Kuzyakov, Y. (2007) 'Carbohydrate and amino acid composition of dissolved organic matter leached from soil', *Soil Biology and Biochemistry,* 39, (11), pp. 2926-2935.

Fléhoc, C., Girard, J. P., Piantone, P. and Bodénan, F. (2006) 'Stable isotope evidence for the atmospheric origin of CO_2 involved in carbonation of MSWI bottom ash', *Applied Geochemistry,* 21, (12), pp. 2037-2048.

Fortnagel, P. and Freese, E. (1968) 'Inhibition of aconitase by chelation of transition metals causing inhibition of sporulation in *Bacillus subtilis*', *Journal of Biological Chemistry,* 243, (20), pp. 5289-5295.

Fredericci, C., Zanotto, E. D. and Ziemath, E. C. (2000) 'Crystallization mechanism and properties of a blast furnace slag glass', *Journal of non-crystalline solids* 273, pp. 64-75.

Fredlund, D. G., Xing, A. Q. and Huang, S. Y. (1994) 'Predicting the permeability function for unsaturated soils using the soil-water characteristic curve', *Canadian Geotechnical Journal,* 31, (4), pp. 533-546.

Fritz, P., Fontes, J. C., Frape, S. K., Louvat, D., Michelot, J. L. and Balderer, W. (1989) 'The isotope geochemistry of carbon in groundwater at Stripa', *Geochimica et Cosmochimica Acta,* 53, (8), pp. 1765-1775.

Galle, C., Peycelon, H. and Le Bescop, R. (2004) 'Effect of an accelerated chemical degradation on water permeability and pore structure of cement-based materials', *Advances in Cement Research,* 16, (3), pp. 105-114.

Garlick, G. D. (1969) 'The stable isotopes of oxygen', in Wedepohl, K. H.(ed), *Handbook of geochemistry.* Springer. ISBN: 978-3540065777

Geerlings, J. J. C. (2004) *Process for removal and capture of carbon dioxide from flue gases.* International patient number WO2004/037391 A1

Gibbons, B. H. and Edsall, J. T. (1963) 'Rate of hydration of carbon dioxide and dehydration of carbonic acid at 25°', *Journal of Biological Chemistry,* 238, (10).

Goodarzi, F. (2006) 'Characteristics and composition of fly ash from Canadian coal-fired power plants', *Fuel,* 85, (10-11), pp. 1418-1427.

Gorham, E. (1991) 'Northern Peatlands: Role in the Carbon Cycle and Probable Responses to Climatic Warming', *Ecological Applications,* 1, (2), pp. 182-195.

Goudie, A. S. (1996) 'Organic agency in calcrete development', *Journal of Arid Environments,* 32, pp. 103-110.

Gray, N. F. (2004) *Biology of wastewater treatment.*2nd ed London: Imperial College Press. ISBN: 978-1860943324

Grisafe, D. A., Angino, E. E. and Smith, S. S. (1988) 'Leaching characteristics of a high calcium fly ash as a function of pH: A potential source of selenium toxicity', *Applied Geochemistry,* 3, pp. 601–608.

Groffman, P. M., Pouyat, R. V., Cadenasso, M. L., Zipperer, W. C., Szlavecz, K., Yesilonis, I. D., Band, L. E. and Brush, G. S. (2006) 'Land use context and natural soil controls on plant community composition and soil nitrogen and carbon dynamics in urban and rural forests', *Forest Ecology and Management,* 236, (2-3), pp. 177-192.

Gu, J.-D., Ford, T. E., Berke, N. S. and Mitchell, R. (1998) 'Biodeterioration of concrete by the fungus Fusarium', *International Biodeterioration and Biodegradation,* 41, pp. 101-109.

Guggenberger, G., Zech, W. and Schulten, H.-R. (1994) 'Formation and mobilization pathways of dissolved organic matter: evidence from chemical structural studies of organic matter fractions in acid forest floor solutions', *Organic Geochemistry,* 21, (1), pp. 51-66.

Guimaraes, M. S., Valdes, J. R., Palomino, A. M. and Santamarina, J. C. (2007) 'Aggregate production: Fines generation during rock crushing', *International Journal of Mineral Processing,* 81, (4), pp. 237-247.

Gunning, P. J., Hills, C. D. and Carey, P. J. (2010) 'Accelerated carbonation treatment of industrial wastes', *Waste Management,* 30, (6), pp. 1081-1090.

Hamilton, J. P., Pantano, C. G. and Brantley, S. L. (2000) 'Dissolution of albite glass and crystal', *Geochimica et Cosmochimica Acta,* 64, (15), pp. 2603-2615.

Hansell, D. A. and Carlson, C. A. (1998) 'Deep-ocean gradients in the concentration of dissolved organic carbon', *Nature,* 395, (6699), pp. 263-266.

Harber, A. J. and Forth, R. A. (2001) 'The contamination of former iron and steel works sites', *Environmental Geology,* 40, (3), pp. 324-330.

Hartman, H. L. (1987) *Introductory Mining Engineering.* John Wiley and Sons Ltd. ISBN: 0-471-34851-1.

Head, P. (2008) *Entering the ecological age: the engineers role.* Institution of Civil Engineers Available at http://www.arup.com/~/media/Files/PDF/Publications/Research_and_whitepapers/Ecological_Age/EngineersRole.ashx.

Hicks, L. (2008) *Aggregates supply in England: Issues for planning.* British Geological Survey Open Report OR/08/059. Available at http://nora.nerc.ac.uk/5215/1/OR08059.pdf

Hill, P. W., Farrar, J. F. and Jones, D. L. (2008) 'Decoupling of microbial glucose uptake and mineralization in soil', *Soil Biology & Biochemistry,* 40, (3), pp. 616-624.

HM Government. (1995) *Environment Act 1995*.

HM Government. (2008) *Strategy for sustainable construction.*

Hobbs, G. (2008) *Construction Resources and Waste Roadmap 2008.* Building Research Establishment

Hodgkinson, E. S. and Hughes, C. R. (1999) 'The mineralogy and geochemistry of cement/rock reactions: high-resolution studies of experimental and analogue materials', *Geological Society, London, Special Publications,* 157, (1), pp. 195-211.

Hodson, M. E., Langan, S. J. and Meriau, S. (1998) 'Determination of mineral surface area in relation to the calculation of weathering rates', *Geoderma,* 83, (1-2), pp. 35-54.

Hopkins, D. W., Waite, I. S., McNicol, J. W., Poulton, P. R., Macdonald, A. J. and O'Donnell, A. G. (2009) 'Soil organic carbon contents in long-term experimental grassland plots in the UK (Palace Leas and Park Grass) have not changed consistently in recent decades', *Global Change Biology,* 15, pp. 1739-1754.

Hubbert, K. R., Graham, R. C. and Anderson, M. A. (2001) 'Soil and weathered bedrock', *Soil Science Society of America Journal,* 65, (4), pp. 1255-1262.

Hudson, J. D. (1977) 'Stable isotopes and limestone lithification', *Journal of the Geological Society,* 133, (6), pp. 637-660.

Huijgen, W. J. J. and Comans, R. N. J. (2006) 'Carbonation of steel slag for CO_2 sequestration: leaching of products and reaction mechanisms', *Environmental Science and Technology,* 40, pp. 2790-2796.

Huijgen, W. J. J., Witcamp, G. and Comans, R. (2005) 'Mineral CO_2 sequestration by steel slag carbonation', *Environmental Science and Technology,* 39, (24), pp. 9676-9682.

Huntzinger, D. N., Gierke, J. S., Kawatra, S. K., Eisele, T. C. and Sutter, L. L. (2009) 'Carbon dioxide sequestration in cement kiln dust through mineral carbonation', *Environmental Science & Technology,* 43, (6), pp. 1986-1992.

Huston, M. A. and Marland, G. (2003) 'Carbon management and biodiversity', *Journal of Environmental Management,* 67, (1), pp. 77-86.

IEA. (2009) *CO_2 emissions from fossil fuel combustion: Highlights.* International Energy Agency ISBN: 978-92-64-08027-8

Inglethorpe, S. D. J., Morgan, D. J., Highley, D. E. and Bloodworth, A. J. (1993) *Industrial Minerals Laboratory Manual: Bentonite.* British Geological Survey

Inskeep, W. P. and Bloom, P. R. (1985) 'An evaluation of rate-equations for calcite precipitation kinetics at pCO_2 less than 0.01 atm and pH greater than 8', *Geochimica et Cosmochimica Acta,* 49, (10), pp. 2165-2180.

IPCC. (2000) *Emissions Scenarios.* Intergovernmental Panel on Climate Change

Islander, R. L., Devinny, J. S., Mansfeld, F., Postyn, A. and Shih, H. (1991) 'Microbial ecology of crown corrosion in sewers', *Journal of Environmental Engineering,* 117, (6), pp. 751-770.

ISSF. (2008) *Stainless and heat resisting steel crude steel production.* International Stainless Steel Forum. Available at http://www.worldstainless.org/Statistics/Crude/

Jackson, T. and Voigt, G. (1971) 'Biochemical weathering of calcium-bearing minerals by rhizosphere micro-organisms, and its influence on calcium accumulation in trees', *Plant and Soil,* 35, (1), pp. 655-658.

Jaillard, B., Guyon, A. and Maurin, A. F. (1991) 'Structure and composition of calcified roots, and their identification in calcareous soils', *Geoderma,* 50, pp. 197-210.

James, N. P. (1972) 'Holocene and Pleistocene calcareous crust (caliche) profiles: criteria for subaerial exposure', *Journal of Sedimentary Petrology,* 42, (4), pp. 817-836.

Janssens, I. A., Freibauer, A., Ciais, P., Smith, P., Nabuurs, G.-J., Folberth, G., Schlamadinger, B., Hutjes, R. W. A., Ceulemans, R., Schulze, E. D., Valentini, R. and Dolman, A. J. (2003) 'Europe's terrestrial biosphere absorbs 7 to 12 % of European anthropogenic CO_2 emissions', *Science,* 300, (5625), pp. 1538-1542.

Javoy, M. (1999) 'Chemical Earth models', *Comptes Rendus de l'Académie des Sciences - Series IIA - Earth and Planetary Science,* 329, (8), pp. 537-555.

Javoy, M., Pineau, F. and Allegre, C. J. (1982) 'Carbon geodynamic cycle', *Nature,* 300, (5888), pp. 171-173.

Javoy, M., Pineau, F. and Delorme, H. (1986) 'Carbon and nitrogen isotopes in the mantle', *Chemical Geology,* 57, (1-2), pp. 41-62.

Jenkinson, D. S., Andrew, S. P. S., Lynch, J. M., Goss, M. J. and Tinker, P. B. (1990) 'The Turnover of Organic Carbon and Nitrogen in Soil [and Discussion]', *Philosophical Transactions: Biological Sciences,* 329, (1255), pp. 361-368.

Jennings, H. M. (1986) 'Aqueous solubility relationships for two types of calcium silicate hydrate', *Journal of the American Ceramic Society,* 69, (8), pp. 614-618.

Jenny, H. (1941) *Factors of Soil Formation.* New York, London: McGraw-Hill. ISBN: 0-486-68128-9

Jo, H. K. and McPherson, G. E. (1995) 'Carbon storage and flux in urban residential greenspace', *Journal of Environmental Management,* 45, pp. 109-133.

Jobbagy, E. and Jackson, R. (2000) 'The vertical distribution of soil organic carbon and Its relation to climate and vegetation', *Ecological Applications,* 10, (2), pp. 423-436.

Jones, D. L. (1998) 'Organic acids in the rhizosphere - a critical review', *Plant and Soil,* 205, (1), pp. 25-44.

Jones, D. L., Dennis, P. G., Owen, A. G. and van Hees, P. A. W. (2003) 'Organic acid behavior in soils - misconceptions and knowledge gaps', *Plant and Soil,* 248, (1-2), pp. 31-41.

Kalin, R. M., G. Dardis and J. Lowndes. (1997) 'Secondary carbonates in the Antrim basalts: Geochemical weathering at 35KyBP', *Geofluids II Conference Extended Abstracts*, pp. 22-25.

Kartam, N., Al-Mutairi, N., Al-Ghusain, I. and Al-Humoud, J. (2004) 'Environmental management of construction and demolition waste in Kuwait', *Waste Management,* 24, (10), pp. 1049-1059.

Kasting, J. (1984) 'Comments on the BLAG model; The carbonate-silicate geochemical cycle and its effect on atmospheric carbon dioxide over the past 100 million years', *American Journal of Science,* 284, (10), pp. 1175-1182.

Kaye, J. P., Majumdar, A., Gries, C., Buyantuyev, A., Grimm, N. B., Hope, D., Jenerette, G. D., Zhu, W. X. and Baker, L. (2008) 'Hierarchical bayesian scaling of soil properties across urban, agricultural, and desert ecosystems', *Ecological Applications,* 18, (1), pp. 132-145.

Kaye, J. P., McCulley, R. L. and Burke, I. C. (2005) 'Carbon fluxes, nitrogen cycling, and soil microbial communities in adjacent urban, native and agricultural ecosystems', *Global Change Biology,* 11, pp. 575-587.

Keeling, C. D. and Worf, T. P. (2004) 'Atmospheric CO_2 records from sites in the SIO air sampling network ', *Trends: A Compendium of Data on Global Change*

Kelemen, P. B. and Matter, J. (2009) 'In situ carbonation of peridotite for CO_2 storage', *PNAS,* 105, (45), pp. 17295–17300.

Kendall, C. and Coplen, T. B. (2001) 'Distribution of oxygen-18 and deuterium in river waters across the United States', *Hydrological Processes,* 15, (7), pp. 1363-1393.

Khalaf, F. M. and DeVenny, A. S. (2004) 'Recycling of Demolished Masonry Rubble as Coarse Aggregate in Concrete: Review', *Journal of Materials in Civil Engineering,* 16, (4), pp. 331-340.

Kharaka, Y. K., Gunter, W., Aggarwal, P. K., Perkins, E. H. and De Braal, J. D. (1988) *SOLMINEQ88: A computer programme for geochemical modelling of water-rock interactions.*

Kheshgi, H. S. (1995) 'Sequestering atmospheric carbon dioxide by increasing ocean alkalinity', *Energy,* 20, (9), pp. 915-922.

Knauth, L. P., Brilli, M. and Klonowski, S. (2003) 'Isotope geochemistry of caliche developed on basalt', *Geochimica et Cosmochimica Acta,* 67, (2), pp. 185-195.

Kosednar-Legenstein, B., Dietzel, M., Leis, A. and Stingl, K. (2008) 'Stable carbon and oxygen isotope investigation in historical lime mortar and plaster - Results from field and experimental study', *Applied Geochemistry,* 23, (8), pp. 2425-2437.

Koukouzas, N., Ward, C. R., Papanikolaou, D., Li, Z. and Ketikidis, C. (2009) 'Quantitative evaluation of minerals in fly ashes of biomass, coal and biomass-coal mixture derived from circulating fluidised bed combustion technology', *Journal of Hazardous Materials,* 169, (1-3), pp. 100-107.

Koukouzas, N. K., Zeng, R., Perdikatsis, V., Xu, W. and Kakaras, E. K. (2006) 'Mineralogy and geochemistry of Greek and Chinese coal fly ash', *Fuel,* 85, (16), pp. 2301-2309.

Kourmpanis, B., Papadopoulos, A., Moustakas, K., Stylianou, M., Haralambous, K. J. and Loizidou, M. (2008) 'Preliminary study for the management of construction and demolition waste', *Waste Management Research,* 26, (3), pp. 267-275.

Kovda, I., Mora, C. I. and Wilding, L. P. (2006) 'Stable isotope compositions of pedogenic carbonates and soil organic matter in a temperate climate Vertisol with gilgai, southern Russia', *Geoderma,* 136, (1-2), pp. 423-435.

Krishnamurthy, R. V., Schmitt, D., Atekwana, E. A. and Baskaran, M. (2003) 'Isotopic investigations of carbonate growth on concrete structures', *Applied Geochemistry,* 18, (3), pp. 435-444.

Krulwich, T. A. (1995) 'Alkaliphiles:‘basic’molecular problems of pH tolerance and bioenergetics', *Molecular Microbiology,* 15, (3), pp. 403-410.

Kumada, K. (1987) *Chemistry of soil organic matter.* Tokyo and Amsterdam: Japan Scientific Societies Press and Elsevier Science Publishers. ISBN: 0-444-98936-6

Kutzbach, J., Ruddiman, W., Vavrus, S. and Philippon, G. (2010) 'Climate model simulation of anthropogenic influence on greenhouse-induced climate change (early agriculture to modern): the role of ocean feedbacks', *Climatic Change,* 99, (3), pp. 351-381.

Kuzyakov, Y. (2006) 'Sources of CO_2 efflux from soil and review of partitioning methods', *Soil Biology and Biochemistry,* 38, (3), pp. 425-448.

Kuzyakov, Y. and Domanski, G. (2000) 'Carbon input by plants into the soil - review', *Journal of Plant Nutrition and Soil Science,* 163, pp. 421-431.

Łącka, B., Łanczont, M., Komar, M. and Madeyska, T. (2008) 'Stable isotope composition of carbonates in loess at the carpathian margin (SE Poland) ', *Studia Quaternaria,* 25, pp. 3-21.

Lackner, K. S., Butt, D. P. and Wendt, C. H. (1997) 'Progress on binding CO_2 in mineral substrates', *Energy Conversion and Management,* 38, pp. S259-S264.

Lackner, K. S., Wendt, C. H., Butt, D. P., Joyce, E. L. and Sharp, D. H. (1995) 'Carbon dioxide disposal in carbonate minerals', *Energy,* 20, (11), pp. 1153-1170.

Lal, R. (2003) 'Global potential of soil carbon sequestration to mitigate the greenhouse effect', *Critical Reviews in Plant Sciences,* 22, pp. 151-184.

Lawson, N., Douglas, I., Garvin, S., McGrath, C., Manning, D. A. C. and Vetterlein, J. (2001) 'Recycling construction and demolition wastes – a UK perspective ', *Environmental Management and Health,* 12, (2), pp. 146-157.

Lea, F. M. (1970) *The chemistry of cement and concrete [3rd Edition].* London: Edward Arnold Ltd. ISBN 978-0750662567

Lécuyer, C., Simon, L. and Guyot, F. (2000) 'Comparison of carbon, nitrogen and water budgets on Venus and the Earth', *Earth and Planetary Science Letters,* 181, (1-2), pp. 33-40.

Lee, A. R. (1974) *Blastfurnace and steel slag - Production, properties and uses.* London: Edward Arnold Ltd. ISBN: 978-0713133158

Lee, S. and Spears, D. A. (1997) 'Natural weathering of pulverized fuel ash and porewater evolution', *Applied Geochemisrry,* 12, pp. 367-376.

Lehmann, A. and Stahr, K. (2007) 'Nature and significance of anthropogenic urban soils', *Journal of Soils and Sediments,* 7, (4), pp. 247-260.

Lekakh, S. N., Rawlins, C. H., Robertson, D. G. C., Richards, V. L. and Peaslee, K. D. (2008) 'Kinetics of aqueous leaching and carbonization of steelmaking slag', *Metallurgical and Materials Transactions B,* 39, (1), pp. 125-134.

Lenton, T. M. and Britton, C. (2006) 'Enhanced carbonate and silicate weathering accelerates recovery from fossil fuel CO_2 perturbations', *Global Biogeochemical Cycles,* 20, (3), pp. 12.

Lesley, R. W. (1924) *History of the Portland Cement Industry in the United States.* New York: Arno Press. ISBN: 978-0405047121

Létolle, R., Gégout, P., Moranville-Regourd, M. and Gaveau, B. (1990) 'Carbon-13 and oxygen-18 mass spectrometry as a potential tool for the study of carbonate phases in concretes', *Journal of the American Ceramic Society,* 73, (12), pp. 3617-3625.

Lichtfouse, É. (1997) 'Heterogeneous turnover of molecular organic substances from crop soils as revealed by ^{13}C labeling at natural abundance with Zea mays', *Naturwissenschaften,* 84, (1), pp. 23-25.

Litton, C. M., Raich, J. W. and Ryan, M. G. (2007) 'Carbon allocation in forest ecosystems', *Global Change Biology,* 13, pp. 2089-2109.

Liu, Y., Lin, C. and Wu, Y. (2007) 'Characterization of red mud derived from a combined Bayer Process and Calcining method for alumina refining', *Chinese Journal of Geochemistry,* 25, (0), pp. 40-40.

Lorenz, K., Preston, C. M. and Kandeler, E. (2006) 'Soil organic matter in urban soils: Estimation of elemental carbon by thermal oxidation and characterization of organic matter by solid-state 13C nuclear magnetic resonance (NMR) spectroscopy', *Geoderma,* 130, (3-4), pp. 312-323.

Lothenbach, B., Matschei, T., Möschner, G. and Glasser, F. P. (2008) 'Thermodynamic modelling of the effect of temperature on the hydration and porosity of Portland cement', *Cement and Concrete Research,* 38, (1), pp. 1-18.

Lovelock, J. (2006) *The revenge of Gaia: Why the Earth is fighting back and how we can still save humanity* Allen Lane. ISBN: 978-0141025971

Lowndes, I. and Jeffrey, K. (2009) *Optimising the efficiency of primary aggregate production.* Mineral Industry Research Organisation. Available at http://www.sustainableaggregates.com/docs/revs/t2b_oepap.pdf

Mackenzie, F. T., Lerman, A. and Andersson, A. J. (2004) 'Past and present of sediment and carbon biogeochemical cycling models', *Biogeosciences,* 1, (1), pp. 11-32.

Macleod, G., Fallick, A. E. and Hall, A. J. (1991) 'The mechanism of carbonate growth on concrete structures, as elucidated by carbon and oxygen isotope analyses', *Chemical Geology,* 86, (4), pp. 335-343.

Maggio, G. and Cacciola, G. (2009) 'A variant of the Hubbert curve for world oil production forecasts', *Energy Policy,* 37, (11), pp. 4761-4770.

Mahieux, P. Y., Aubert, J. E. and Escadeillas, G. (2009) 'Utilization of weathered basic oxygen furnace slag in the production of hydraulic road binders', *Construction and Building Materials,* 23, (2), pp. 742-747.

Manning, D. A. C. (1995) *Introduction to industrial minerals.* London: Chapman and Hall.

Manning, D. A. C. (2001) 'Calcite precipitation in landfills: an essential product of waste stabilization', *Mineralogical Magazine,* 65, (5), pp. 603-610.

Manning, D. A. C. (2008) 'Biological enhancement of soil carbonate precipitation: passive removal of atmospheric CO_2', *Mineralogical Magazine,* 72, pp. 639-649.

Manning, D. A. C., Rae, E. I. C. and Small, J. S. (1991) 'An exploratory study of acetate decomposition and dissolution of quartz and Pb-rich potassium feldspar at 150°C, 50 MPa (500 bars)', *Mineralogical Magazine,* 55, pp. 183-195.

Marty, B. and Tolstikhin, I. N. (1998) 'CO_2 fluxes from mid-ocean ridges, arcs and plumes', *Chemical Geology,* 145, (3-4), pp. 233-248.

Matschei, T., Lothenbach, B. and Glasser, F. P. (2007) 'Thermodynamic properties of Portland cement hydrates in the system CaO-Al_2O_3-SiO_2-$CaSO_4$-$CaCO_3$-H_2O', *Cement and Concrete Research,* 37, (10), pp. 1379-1410.

Matter, J. M. and Keleman, P. B. (2009) 'Permanent storage of carbon dioxide in geological reservoirs by mineral carbonation ', *Nature Geoscience,* 2, pp. 837-841.

Mayes, W., Younger, P. and Aumônier, J. (2008) 'Hydrogeochemistry of alkaline steel slag leachates in the UK', *Water, Air, and Soil Pollution,* 195, (1), pp. 35-50.

Mayes, W. M., Batty, L. C., Younger, P. L., Jarvis, A. P., Kõiv, M., Vohla, C. and Mander, U. (2009) 'Wetland treatment at extremes of pH: A review', *Science of The Total Environment,* 407, (13), pp. 3944-3957.

Mayes, W. M., Younger, P. L. and Aumonier, J. (2006) 'Buffering of alkaline steel slag leachate across a natural wetland', *Environmental Science & Technology,* 40, (4), pp. 1237-1243.

Mazzotti, M., J.C., A., Allam, R., K.S., L., Meunier, F., Rubin, E., Sanchez, J. C., Yogo, K. and Zevenhoven, R. (2005) *Chapter 7: Mineral carbonation and industrial uses of carbon dioxide.* IPCC

Meehl, G. A., Arblaster, J. M. and Tebaldi, C. (2005) 'Understanding future patterns of increased precipitation intensity in climate model simulations', *Geophysical Research Letters,* 32, (18), pp. L18719.

Metz, B., Davidson, O. R., Bosch, P. R., Dave, R. and L.A., M. (2007) *Contribution of Working Group III to the Fourth Assessment Report of the Intergovernmental Panel on Climate Change.* Cambridge and New York: Intergovernmental Panel on Climate Change ISBN 978-0-521-70598-1

Mikhailova, E. A., Post, C. J., Magrini-Bair, K. and Castle, J. W. (2006) 'Pedogenic carbonate concretions in the Russian Chernozem', *Soil Science,* 171, (12), pp. 981-991.

Milliman, J. D. and Droxler, A. W. (1995) 'Calcium carbonate sedimentation in the global oceans: lickages between the neritic and pelagic environments', *Oceanography,* 8, (3), pp. 92-94.

Mineral Solutions. (2004) *Combination of basaltic quarry fines with organic process residues for the development of novel growing media.* Mineral industry research organisation MA/1/3/003

Montes-Hernandez, G., Pérez-López, R., Renard, F., Nieto, J. M. and Charlet, L. (2009) 'Mineral sequestration of CO_2 by aqueous carbonation of coal combustion fly-ash', *Journal of Hazardous Materials,* 161, (2-3), pp. 1347-1354.

Mörner, N.-A. and Etiope, G. (2002) 'Carbon degassing from the lithosphere', *Global and Planetary Change,* 33, (1-2), pp. 185-203.

Morse, J. W., Arvidson, R. S. and Luttge, A. (2007) 'Calcium carbonate formation and dissolution', *Chemical Reviews,* 107, (2), pp. 342-381.

Moulton, K. L., West, J. and Berner, R. A. (2000) 'Solute flux and mineral mass balance approaches to the quantification of plant effects on silicate weathering', *American Journal of Science,* 300, (7), pp. 539-570.

Murphy, E. M., Davis, S. N., Long, A., Donahue, D. and Jull, A. J. T. (1989) '^{14}C in fractions of dissolved organic carbon in ground water', *Nature,* 337, (6203), pp. 153-155.

Myneni, R. B., Dong, J., Tucker, C. J., Kaufmann, R. K., Kauppi, P. E., Liski, J., Zhou, L., Alexeyev, V. and Hughes, M. K. (2001) 'A large carbon sink in the woody biomass of Northern forests', *Proceedings of the National Academy of Sciences of the United States of America,* 98, (26), pp. 14784-14789.

Myneni, S. C. B., Traina, S. J. and Logan, T. J. (1998) 'Ettringite solubility and geochemistry of the $Ca(OH)_2$-$Al_2(SO_4)_3$-H_2O system at 1 atm pressure and 298 K', *Chemical Geology,* 148, (1-2), pp. 1-19.

Nambu, K., van Hees, P. A. W., Jones, D. L., Vinogradoff, S. and Lundström, U. S. (2008) 'Composition of organic solutes and respiration in soils derived from alkaline and non-alkaline parent materials', *Geoderma,* 144, (3-4), pp. 468-477.

Nancollas, G. H. and Reddy, M. M. (1971) 'The crystallization of calcium carbonate II. Calcite growth mechanism', *Journal of Colloid and Interface Science,* 37, pp. 824-829.

Neaman, A., Chorover, J. and Brantley, S. L. (2006) 'Effects of organic ligands on granite dissolution in batch experiments at pH 6', *American Journal of Science,* 306, (6), pp. 451-473.

Nesbitt, H. W. and Skinner, W. M. (2001) 'Early development of Al, Ca, and Na compositional gradients in labradorite leached in pH 2 HCl solutions', *Geochimica et Cosmochimica Acta,* 65, (5), pp. 715-727.

Nettleton., W. D. (ed.) (1991) *Occurrence, characteristics, and genesis of carbonate, gypsum, and silica accumulations in soils.* Madison: Soil Science Society of America. ISBN: 0891187944

Nguyen, C. (2003) 'Rhizodeposition of organic C by plants: mechanisms and controls', *Agronomie,* 23, (5-6), pp. 375-396.

Nogami, Y., Maeda, T., Negishi, A. and Sugio, T. (1997) 'Inhibition of sulfur oxidizing activity by nickel ion in *Thiobacillus thiooxidans* NB1-3 isolated from the corroded concrete ', *Bioscience, biotechnology, and biochemistry,* 61, (8), pp. 1373-1375.

Oikonomou, N. D. (2005) 'Recycled concrete aggregates', *Cement and Concrete Composites,* 27, (2), pp. 315-318.

Oliva, P., Viers, J. and Dupré, B. (2003) 'Chemical weathering in granitic environments', *Chemical Geology,* 202, (3-4), pp. 225-256.

O'Neil, J. R. and Barnes, I. (1971) 'C13 and O18 compositions in some fresh-water carbonates associated with ultramafic rocks and serpentinites: western United States', *Geochimica et Cosmochimica Acta,* 35, (7), pp. 687-697.

Ostle, N. J., Levy, P. E., Evans, C. D. and Smith, P. (2009) 'UK land use and soil carbon sequestration', *Land Use Policy,* 26, (Supplement 1), pp. S274-S283.

Pacala, S. and Socolow, R. (2004) 'Stabilization wedges: solving the climate problem for the next 50 years with current technologies', *Science,* 305, (5686), pp. 968-972.

Pachiaudi, C., Marechal, J., Vanstrydonck, M., Dupas, M. and Dauchotdehon, M. (1986) 'Isotopic fractionation of carbon during CO_2 absorption by mortar', *Radiocarbon,* 28, (2A), pp. 691-697.

Parry, M. L., Canziani, O. F., Palutikof, J. P., van der Linden, P. J. and Hanson, C. E. (2007) *Contribution of Working Group II to the Fourth Assessment Report of the Intergovernmental Panel on Climate Change.* Cambridge and New York: Intergovernmental Panel on Climate Change ISBN: 978 0521 88010-7

Paustian, K., Andren, O., Janzen, H. H., Lal, R., Smith, P., Tian, G., Tiessen, H., Van Noordwijk, M. and Woomer, P. L. (1997) 'Agricultural soils as a sink to mitigate CO_2 emissions', *Soil Use and Management,* 13, (4), pp. 230-244.

Pedersen, K., Nilsson, E., Arlinger, J., Hallbeck, L. and O'Neill, A. (2004) 'Distribution, diversity and activity of microorganisms in the hyper-alkaline spring waters of Maqarin in Jordan', *Extremophiles,* 8, (2), pp. 151-164.

Petit, J. R., Jouzel, J., Raynaud, D., Barkov, N. I., Barnola, J. M., Basile, I., Bender, M., Chappellaz, J., Davis, M., Delaygue, G., Delmotte, M., Kotlyakov, V. M., Legrand, M., Lipenkov, V. Y., Lorius, C., Pepin, L., Ritz, C., Saltzman, E. and Stievenard, M. (1999) 'Climate and atmospheric history of the past 420,000 years from the Vostok ice core, Antarctica', *Nature,* 399, (6735), pp. 429-436.

Pichtel, J. (2005) *Waste management practices: Municipal, hazardous, and industrial.* CRC Press. ISBN: 978-0849335259

Pinsent, B. R. W., Pearson, L. and Roughton, F. J. W. (1956) 'The kinetics of combination of carbon dioxide with hydroxide ions', *Transactions of the Faraday Society,* 52, pp. 1596 - 1598.

Plummer, N. and Sprinkle, C. (2001) 'Radiocarbon dating of dissolved inorganic carbon in groundwater from confined parts of the Upper Floridan aquifer, Florida, USA', *Hydrogeology Journal,* 9, (2), pp. 127-150.

Poh, H. Y., Ghataora, G. S. and Ghazireh, N. (2006) 'Soil stabilization using basic oxygen steel slag fines', *Journal of Materials in Civil Engineering,* 18, (2), pp. 229-240.

Poirier, N., Sohi, S. P., Gaunt, J. L., Mahieu, N., Randall, E. W., Powlson, D. S. and Evershed, R. P. (2005) 'The chemical composition of measurable soil organic matter pools', *Organic Geochemistry,* 36, (8), pp. 1174-1189.

Post, W. M. and Kwon, K. C. (2000) 'Soil carbon sequestration and land-use change: processes and potential', *Global Change Biology,* 6, (3), pp. 317-327.

Pouyat, R., Groffman, P., Yesilonis, I. and Hernandez, L. (2002) 'Soil carbon pools and fluxes in urban ecosystems', *Environmental Pollution,* 116, (Supplement 1), pp. S107-S118.

Pouyat, R., Yesilonis, I. and Golubiewski, N. (2009) 'A comparison of soil organic carbon stocks between residential turf grass and native soil', *Urban Ecosystems,* 12, (1), pp. 45-62.

Pouyat, R. V., Yesilonis, I. D. and Nowak, D. J. (2006) 'Carbon storage by urban soils in the United States', *Journal of Environmental Quality,* 35, (4), pp. 1566-1575.

Prentice, I. C., Cramer, W., Harrison, S. P., Leemans, R., Monserud, R. A. and Solomon, A. M. (1992) 'A global biome model based on plant physiology and dominance, soil properties and climate', *Journal of Biogeography,* 19, (2), pp. 117-134.

Proctor, D. M., Fehling, K. A., Shay, E. C., Wittenborn, J. L., Green, J. J., Avent, C., Bigham, R. D., Connolly, M., Lee, B., Shepker, T. O. and Zak, M. A. (2000) 'Physical and Chemical Characteristics of Blast Furnace, Basic Oxygen Furnace, and Electric Arc Furnace Steel Industry Slags', *Environmental Science & Technology,* 34, (8), pp. 1576-1582.

Raich, J. W. and Tufekcioglu, A. (2000) 'Vegetation and soil respiration: Correlations and controls', *Biogeochemistry,* 48, (1), pp. 71-90.

Randall, B. A. O. (1989) 'Dolerite-pegmatites from the Whin Sill near Barrasford, Northumberland', *Proceedings of the Yorkshire Geological and Polytechnic Society,* 47, (3), pp. 249-265.

Randerson, J. T., Iii, F. S. C., Harden, J. W., Neff, J. C. and Harmon, M. E. (2002) 'Net ecosystem production: A comprehensive measure of net carbon accumulation by ecosystems', *Ecological Applications,* 12, (4), pp. 937-947.

Rawlins, B. G., Vane, C. H., Kim, A. W., Tye, A. M., Kemp, S. J. and Bellamy, P. H. (2008) 'Methods for estimating types of soil organic carbon and their application to surveys of UK urban areas', *Soil Use and Management,* 24, (1), pp. 47-59.

Reardon, E. J. and Fagan, R. (2000) 'The calcite/portlandite phase boundary: enhanced calcite solubility at high pH', *Applied Geochemistry,* 15, (3), pp. 327-335.

Reimens, C. and de Caritat, P. (1998) *Chemical elements in the environment: Factsheets for the Geochemist and Environmental Scientist.* Springer. ISBN 978-3540636700

Rendek, E., Ducom, G. and Germain, P. (2006) 'Carbon dioxide sequestration in municipal solid waste incinerator (MSWI) bottom ash ', *Journal of hazardous materials,* 128, pp. 73-79.

Renforth, P., Edmondson, J., Leake, J. R., Gaston, K. J. and Manning, D. A. C. (2011a) 'Designing a carbon capture function into urban soils', *Proceedings of the Institution of Civil Engineers Urban Design and Planning,* 164, (2), pp. in press.

Renforth, P., Washbourne, C-L., Taylder J., Manning, D. A. C. (2011b). Silicate production and availability for mineral carbonation. Environmental Science and Technology, 45, (6) pp 2035-2041

Renforth, P., Manning, D. A. C. and Lopez-Capel, E. (2009) 'Carbonate precipitation in artificial soils as a sink for atmospheric carbon dioxide', *Applied Geochemistry,* 24, pp. 1757-1764.

Roadcap, G. S., Kelly, W. B. and Bethke, C. M. (2005) 'Geochemistry of extremely alkaline (pH>12) ground water in slag fill aquifers ', *Ground Water,* 43, (6), pp. 806-816.

Robie, R. A. and Hemingway, B. S. (1995) *Thermodynamic properties of minerals and related substances at 298.15 K and 1 bar (105 pascals) pressure and at higher temperatures.* Washington: No. 2131

Rochelle, C. A., Bateman, K., MacGregor, R., Pearce, J. M., Savage, D. and Wetton, P. (1998) *The evaluation of chemical mass transfer in the disturbed zone of a deep geological disposal facility for radioactive wastes. IV The kinetics of dissolution of chlorite and carbonates at elevated pH.* British Geological Survey

Rogers, J. R., Bennett, P. C. and Choi, W. J. (1998) 'Feldspars as a source of nutrients for microorganisms', *American Mineralogist,* 83, (11-12_Part_2), pp. 1532-1540.

Rogers, R. P. (2009) *An economic history of the American steel industry* Routledge. ISBN: 0-203-88103-6

Rothschild, L. J. and Mancinelli, R. L. (2001) 'Life in extreme environments', *Nature,* 409, (6823), pp. 1092-1101.

Rothstein, D., Thomas, J. J., Christensen, B. J. and Jennings, H. M. (2002) 'Solubility behavior of Ca-, S-, Al-, and Si-bearing solid phases in Portland cement pore solutions as a function of hydration time', *Cement and Concrete Research,* 32, (10), pp. 1663-1671.

RPS MCOS. (2004) *A guide to construction and demolition waste legislation.* RPS – Ireland. Available at http://www.ncdwc.ie/html/documents/GuidetoConstructionandDemolitionWasteLegislation.pdf

Russell, N. V., Méndez, L. B., Wigley, F. and Williamson, J. (2002) 'Ash deposition of a Spanish anthracite: effects of included and excluded mineral matter', *Fuel,* 81, (5), pp. 657-663.

Ryan, P. R., Delhaize, E. and Jones, D. L. (2001) 'Function and mechanism of organic anion exudation from plant roots', *Annual Review of Plant Physiology and Plant Molecular Biology,* 52, pp. 527-560.

Sabine, C. L., Feely, R. A., Gruber, N., Key, R. M., Lee, K., Bullister, J. L., Wanninkhof, R., Wong, C. S., Wallace, D. W. R., Tilbrook, B., Millero, F. J., Peng, T.-H., Kozyr, A., Ono, T. and Rios, A. F. (2004) 'The oceanic sink for anthropogenic CO_2', *Science,* 305, (5682), pp. 367-371.

Salomons, W. and Mook, W. G. (1976) 'Isotope geochemistry of carbonate dissolution and re-precipitation in soils', *Soil Science,* 122, (1), pp. 15-24.

Sattler, U. T. E., Immenhauser, A., HillgÄRtner, H. and Esteban, M. (2005) 'Characterization, lateral variability and lateral extent of discontinuity surfaces on a Carbonate Platform (Barremian to Lower Aptian, Oman)', *Sedimentology,* 52, (2), pp. 339-361.

Schaeler, B., Offermann, D., Kuell, V. and Jarisch, M. (2009) 'Global water vapour distribution in the upper troposphere and lower stratosphere during CRISTA 2', *Advances in Space Research,* 43, (1), pp. 65-73.

Schiebe, F. R., Welch, N. H. and Cooper, L. R. (1983) 'Measurement of fine silt and clay size distributions', *Transactions of the American Society of Agricultural and Biological Engineers* 26, (2), pp. 491-494.

Schimel, D. S., House, J. I., Hibbard, K. A., Bousquet, P., Ciais, P., Peylin, P., Braswell, B. H., Apps, M. J., Baker, D., Bondeau, A., Canadell, J., Churkina, G., Cramer, W., Denning, A. S., Field, C. B., Friedlingstein, P., Goodale, C., Heimann, M., Houghton, R. A., Melillo, J. M., Moore, B., Murdiyarso, D., Noble, I., Pacala, S. W., Prentice, I. C., Raupach, M. R., Rayner, P. J., Scholes, R. J., Steffen, W. L. and Wirth, C. (2001) 'Recent patterns and mechanisms of carbon exchange by terrestrial ecosystems', *Nature,* 414, (6860), pp. 169-172.

Schlesinger, W. H. (1977) 'Carbon balance in terrestrial detritus', *Annual Review of Ecology and Systematics,* 8, (1), pp. 51-81.

Schnitzer, M. and Khan, S. U. (1978) *Soil organic matter.* Amsterdam: Elsevier Scientific Publishers B.V. ISBN: 0-444-41610-2

Schuur, H. M. L. (2000) 'Calcium silicate products with crushed building and demolition waste', *Journal of Materials in Civil Engineering,* 12, (4), pp. 282-287.

Schweda, P. (1990) *Kinetics and mechanisms of alkali feldspar dissolution at low temperatures.* PhD thesis. Stockholm University.

Scrivener, K. L., Füllmann, T., Gallucci, E., Walenta, G. and Bermejo, E. (2004) 'Quantitative study of Portland cement hydration by X-ray diffraction/Rietveld analysis and independent methods', *Cement and Concrete Research,* 34, (9), pp. 1541-1547.

Seifritz, W. (1990) 'CO_2 disposal by means of silicates ', *Nature,* 345, pp. 486-486.

Senwo, Z. N. and Tabatabai, M. A. (1998) 'Amino acid composition of soil organic matter', *Biology and Fertility of Soils,* 26, (3), pp. 235-242.

Severinghaus, J. P., Broecker, W. S., Dempster, W. F., MacCallum, T. and Wahlen, M. (1994) 'Oxygen loss in Biosphere 2', *Eos, Transactions of the American Geophysical Union,* 75, (3), pp. 33.

Shaw, S., Clark, S. M. and Henderson, C. M. B. (2000a) 'Hydrothermal formation of the calcium silicate hydrates, tobermorite ($Ca_5Si_6O_{16}(OH)_2 \cdot 4H_2O$) and xonotlite ($Ca_6Si_6O_{17}(OH)_2$): an in situ synchrotron study', *Chemical Geology,* 167, (1-2), pp. 129-140.

Shaw, S., Henderson, C. M. B. and Komanschek, B. U. (2000b) 'Dehydration/recrystallization mechanisms, energetics, and kinetics of hydrated calcium silicate minerals: an in situ TGA/DSC and synchrotron radiation SAXS/WAXS study', *Chemical Geology,* 167, (1-2), pp. 141-159.

Shen, H. and Forssberg, E. (2003) 'An overview of recovery of metals from slags', *Waste Management,* 23, (10), pp. 933-949.

Siegenthaler, U. and Sarmiento, J. L. (1993) 'Atmospheric carbon dioxide and the ocean', *Nature,* 365, (6442), pp. 119-125.

Sikes, N. E. and Ashley, G. M. (2007) 'Stable isotopes of pedogenic carbonates as indicators of paleoecology in the Plio-Pleistocene (upper Bed I), western margin of the Olduvai Basin, Tanzania', *Journal of Human Evolution,* 53, (5), pp. 574-594.

Sing, K. (2001) 'The use of nitrogen adsorption for the characterisation of porous materials', *Colloids and Surfaces a-Physicochemical and Engineering Aspects,* 187, pp. 3-9.

Singh, B. P., Il Lee, Y., Pawar, J. S. and Charak, R. S. (2007) 'Biogenic features in calcretes developed on mudstone: Examples from Paleogene sequences of the Himalaya, India', *Sedimentary Geology,* 201, (1-2), pp. 149-156.

Skidmore, M., Sharp, M. and Tranter, M. (2004) 'Kinetic isotopic fractionation during carbonate dissolution in laboratory experiments: Implications for detection of microbial CO_2 signatures using δ^{13}C-DIC', *Geochimica et Cosmochimica Acta,* 68, (21), pp. 4309-4317.

Smetak, K. M., Johnson-Maynard, J. L. and Lloyd, J. E. (2007) 'Earthworm population density and diversity in different-aged urban systems', *Applied Soil Ecology,* 37, (1-2), pp. 161-168.

Smith, P., Goulding, K. W. T., Smith, K. A., Powlson, D. S., Smith, J. U., Falloon, P. and Coleman, K. (2000) 'Including trace gas fluxes in estimates of the carbon mitigation potential of UK agricultural land', *Soil Use and Management,* 16, (4), pp. 251-259.

Sohi, S. P., Mahieu, N., Arah, J. R. M., Powlson, D. S., Madari, B. and Gaunt, J. L. (2001) 'A procedure for isolating soil organic matter fractions suitable for modeling', *Soil Science Society of Americal Journal,* 65, (4), pp. 1121-1128.

Sollins, P., Homann, P. and Caldwell, B. A. (1996) 'Stabilization and destabilization of soil organic matter: mechanisms and controls', *Geoderma,* 74, (1-2), pp. 65-105.

Solomon, S., Qin, D., Manning, M., Chen, Z., Marquis, M., Averyt, K. B., Tignor, M. and Miller, H. L. (2007) *Contribution of Working Group I to the Fourth Assessment Report of the Intergovernmental Panel on Climate Change.* Cambridge and New York: Intergovernmental Panel on Climate Change ISBN: 978 0521 88009-1

Stanton, T. E. (1940) 'Expansion of concrete through reaction between cement and aggregate', *Proceedings of the American Society of Civil Engineers,* 66, (10), pp. 1781-1811.

Stern, N. (2006). "Stern Review on The Economics of Climate Change. Executive

Summary". HM Treasury, London. (http://webarchive.nationalarchives.gov.uk/+/http://www.hm-treasury.gov.uk/sternreview_index.htm Accessed 29/03/11).

Stevens, T. O., McKinley, J. P. and Fredrickson, J. K. (1993) 'Bacteria associated with deep, alkaline, anaerobic groundwaters in Southeast Washington', *Microbial Ecology,* 25, (1), pp. 35-50.

Stevenson, B. A., Kelly, E. F., McDonald, E. V. and Busacca, A. J. (2005) 'The stable carbon isotope composition of soil organic carbon and pedogenic carbonates along a bioclimatic gradient in the Palouse region, Washington State, USA', *Geoderma,* 124, (1-2), pp. 37-47.

Stillings, L. L. and Brantley, S. L. (1995) 'Feldspar dissolution at 25-degrees-c and pH3 - reaction stoichiometry and the effect of cations', *Geochimica et Cosmochimica Acta,* 59, (8), pp. 1483-1496.

Stocks-Fischer, S., Galinat, J. K. and Bang, S. S. (1999) 'Microbiological precipitation of $CaCO_3$', *Soil Biology and Biochemistry,* 31, (11), pp. 1563-1571.

Stott, P. A., Tett, S. F. B., Jones, G. S., Allen, M. R., Mitchell, J. F. B. and Jenkins, G. J. (2000) 'External control of 20th century temperature by natural and anthropogenic forcings', *Science,* 290, (5499), pp. 2133-2137.

Strom, L., Owen, A. G., Godbold, D. L. and Jones, D. L. (2001) 'Organic acid behaviour in a calcareous soil: sorption reactions and biodegradation rates', *Soil Biology and Biochemistry,* 33, (15), pp. 2125-2133.

Strom, L., Owen, A. G., Godbold, D. L. and Jones, D. L. (2005) 'Organic acid behaviour in a calcareous soil implications for rhizosphere nutrient cycling', *Soil Biology and Biochemistry,* 37, (11), pp. 2046-2054.

Strycharz, S. and Newman, L. (2009) 'Use of native plants for remediation of trichloroethylene: I. deciduous trees', *International Journal of Phytoremediation,* 11, (2), pp. 150 - 170.

Sverdrup, H. and Warfvinge, P. (1988) 'Weathering of primary silicate minerals in the natural soil environment in relation to a chemical-weathering model', *Water Air and Soil Pollution,* 38, (3-4), pp. 387-408.

Tack, F. M., Callewaert, O. W. J. J. and Verloo, M. G. (1996) 'Metal solubility as a function of pH in a contaminated, dredged sediment affected by oxidation', *Environmental Pollution,* 91, (2), pp. 199-208.

Tailings.info. (2009) tailings.info message: Tailing Quantities, 09/12/2009.

Takahashi, T., Amano, Y., Kuchimura, K. and Kobayashi, T. (2008) 'Carbon content of soil in urban parks in Tokyo, Japan', *Landscape and Ecological Engineering,* 4, (2), pp. 139-142.

Takahashi, T., Sutherland, S. C., Sweeney, C., Poisson, A., Metzl, N., Tilbrook, B., Bates, N., Wanninkhof, R., Feely, R. A., Sabine, C., Olafsson, J. and Nojiri, Y. (2002) 'Global sea-air CO_2 flux based on climatological surface ocean pCO_2, and seasonal biological and temperature effects', *Deep Sea Research Part II: Topical Studies in Oceanography,* 49, (9-10), pp. 1601-1622.

Tallent-Halsell, N. and Watt, M. (2009) 'The invasive *Buddleja davidii* (Butterfly Bush)', *The Botanical Review,* 75, (3), pp. 292-325.

Tans, P. P., Fung, I. Y. and Takahashi, T. (1990) 'Observational constraints on the global atmospheric CO_2 budget', *Science,* 247, (4949), pp. 1431-1438.

Taylor, B. J., Burgess, I. C., Land, D. H., Mills, D. A. C., Smith, D. B. and Warren, P. T. (1971) *British Regional Geology- Northern England* 4th ed: ISBN 978-0118840644

The British Cement Association (2010) *Industry Profile*. Available at: http://www.cementindustry.co.uk (Accessed: 18/03/2010).

The Royal Society. (2009) *Geoengineering the climate: Science governance and uncertainty.* Available at http://royalsociety.org/WorkArea/DownloadAsset.aspx?id=10768

Thomas, L. (1992) *Handbook of practical coal geology.* John Wiley and Sons. ISBN: 978-0471935575

Tiago, I., Chung, A. P. and Verissimo, A. (2004) 'Bacterial diversity in a nonsaline alkaline environment: heterotrophic aerobic populations', *Applied Environmental Microbiology,* 70, (12), pp. 7378-7387.

Townsend, T. G., Jang, Y. and Thurn, L. G. (1999) 'Simulation of construction and demolition waste leachate', *Journal of Environmental Engineering,* 125, (11), pp. 1071-1081.

Trevors, J. T. (1996) 'Sterilization and inhibition of microbial activity in soil', *Journal of Microbiological Methods,* 26, (1-2), pp. 53-59.

Turner, J. V. (1982) 'Kinetic fractionation of carbon-13 during calcium carbonate precipitation', *Geochimica et Cosmochimica Acta,* 46, (7), pp. 1183-1191.

Tyler, J. J., Leng, M. J. and Arrowsmith, C. (2007) 'Seasonality and the isotope hydrology of Lochnagar, a Scottish mountain lake: implications for palaeoclimate research', *The Holocene,* 17, (6), pp. 717-727.

UKQAA. (2007) *Technical Datasheet 8.1 - Environment and Sustainability.* UK Quality Ash Association. Available at http://www.ukqaa.org.uk/Datasheets_PDF/Datasheet_8-1_July_2007.pdf

Usdowski, E. and Hoefs, J. (1986) '$^{13}C/^{12}C$ partitioning and kinetics of CO_2 absorption by hydroxide buffer solutions', *Earth and Planetary Science Letters,* 80, (1-2), pp. 130-134.

U.S. Department of the Interior and U.S. Geological Survey (1990-2007) *Minerals Yearbook* [Online]. Available at: http://minerals.usgs.gov/minerals/pubs/country/index.html#pubs (Accessed: 14/01/09).

U.S. Department of the Interior and U.S. Geological Survey (2004) *Minerals Yearbook* [Online]. Available at: http://minerals.usgs.gov/minerals/pubs/country/index.html#pubs (Accessed: 14/01/09).

U.S. Department of the Interior and U.S. Geological Survey (2006) *Coal combustion products statistics* [Online]. Available at: http://minerals.usgs.gov/minerals/pubs/commodity/coal/ (Accessed: 25/07/2010).

USGS. (2008) *USGS Minerals Yearbook.* U.S. Department of the Interior and U.S. Geological Survey

U.S. Department of the Interior and U.S. Geological Survey (2009) *Iron and steel slag statistics* [Online]. Available at: http://minerals.usgs.gov/minerals/pubs/commodity/iron_&_steel_slag/ (Accessed: 05/08/2010).

USGS. (2010a) *Historical statistics for mineral and material commodities in the United States.* United States Geological Survey

USGS. (2010b) *USGS Minerals Yearbook.* U.S. Department of the Interior and U.S. Geological Survey

van Breemen, N., Finlay, R., Lundström, U., Jongmans, A. G., Giesler, R. and Olsson, M. (2000) 'Mycorrhizal weathering: A true case of mineral plant nutrition?', *Biogeochemistry,* 49, (1), pp. 53-67.

van Grinsven, J. J. M. and van Riemsdijk, W. H. (1992) 'Evaluation of batch and column techniques to measure weathering rates in soils', *Geoderma,* 52, (1-2), pp. 41-57.

van Hees, P. A. W., Lundström, U. S. and Morth, C. M. (2002) 'Dissolution of microcline and labradorite in a forest O horizon extract: the effect of naturally occurring organic acids', *Chemical Geology,* 189, (3-4), pp. 199-211.

van Oss, H. G. (2009) *Iron and steel slag.* United States Geological Survey. Available at http://minerals.usgs.gov/minerals/pubs/commodity/iron_&_steel_slag/mcs-2009-fesla.pdf

van Oss, H. G. and Padovani, A. C. (2003) 'Cement manufacture and the environment', *Journal of Industrial Ecology,* 7, (1), pp. 93-126.

van Strydonck, M. J. Y., Dupas, M. and Keppens, E. (1989) 'Isotopic fractionation of oxygen and carbon in lime mortar under natural environmental conditions', *Radiocarbon* 31, pp. 610-618.

VanGulck, J. F., Rowe, R. K., Rittmann, B. E. and Cooke, A. J. (2003) 'Predicting biogeochemical calcium precipitation in landfill leachate collection systems', *Biodegradation,* 14, (5), pp. 331-346.

Vassilev, S. V. and Vassileva, C. G. (1997) 'Geochemistry of coals, coal ashes and combustion wastes from coal-fired power stations', *Fuel Processing Technology,* 51, (1-2), pp. 19-45.

Velbel, M. A. and Losiak, A. I. (2008) 'Influence of surface-area estimation on rates of plagioclase weathering determined from naturally weathered 3400 y old Hawaiian basalt', *Mineralogical Magazine,* 72, (1), pp. 91-94.

Verrecchia, E. P. and Verrecchia, K. E. (1994) 'Needle-fibre calcite: a critical review and a proposed classification', *Journal of Sedimentary Research,* 64, (3), pp. 650-664.

Vestin, J. L. K., Norström, S. H., Bylund, D. and Lundström, U. S. (2008) 'Soil solution and stream water chemistry in a forested catchment II: Influence of organic matter', *Geoderma,* 144, (1-2), pp. 271-278.

Vetterlein, J. P. (2003) *Availability of trace metals from potentially contaminated demolition materials - implications for risk evaluation.* PhD thesis. Newcastle University.

Walker, J. C. G., Hays, P. B. and Kasting, J. F. (1981) 'A negative feedback mechanism for the long-term stabilization of Earth's surface-temperature', *Journal of Geophysical Research-Oceans and Atmospheres,* 86, (NC10), pp. 9776-9782.

Wall, D. H. and Virginia, R. A. (1999) 'Controls on soil biodiversity: insights from extreme environments', *Applied Soil Ecology,* 13, (2), pp. 137-150.

Wang, H. and Greenberg, S. E. (2007) 'Reconstructing the response of C_{-3} and C_{-4} plants to decadal-scale climate change during the late Pleistocene in southern Illinois using isotopic analyses of calcified rootlets', *Quaternary Research,* 67, (1), pp. 136-142.

Wayne, R. P. (2000) *Chemistry of atmospheres: An introduction to the chemistry of the atmospheres of Earth, the planets, and their satellites* Oxford University Press. ISBN: 978-0198503750

WCI. (2008) *The coal resource: a comprehensive overview of coal.* World Coal Institute Available at http://www.worldcoal.org/bin/pdf/original_pdf_file/coal_resource_overview_of_coal_report(03_06_2009).pdf

Weber, C. L. and Matthews, H. S. (2008) 'Quantifying the global and distributional aspects of American household carbon footprint', *Ecological Economics,* 66, (2-3), pp. 379-391.

Wedepohl, K. H. (1995) 'The composition of the continental crust', *Geochimica et Cosmochimica Acta*, 59, (7), pp. 1217-1232

Weil, M., Jeske, U. and Schebek, L. (2006) 'Closed-loop recycling of construction and demolition waste in Germany in view of stricter environmental threshold values', *Waste Management Research,* 24, (3), pp. 197-206.

White, A. F. (1995) 'Chemical weathering rates of silicate minerals in soils', in White, A. F. and Brantley, S. L.(eds) *Chemical weathering rates of silicate minerals.* Vol. 31 Mineralogical Society of America. ISBN: 978-0939950386

White, A. F. and Brantley, S. L. (eds.) (1995) *Chemical weathering rates of silicate minerals.* Mineralogical Society of America.

Wilburn, D. R. and Goonan, T. G. (1998) *Aggregates from natural and recycled sources - Economic assessments for construction applications: a materials flow analysis.* US Geological Survey

Willet, J. C. (2007) *Crushed Stone.* US Geological Survey

Wilson, E. O. (2000) 'A global biodiversity map', *Science,* 289, (5488), pp. 2279.

Wilson, S. A., Barker, S. L. L., Dipple, G. M. and Atudorei, V. (in press) 'Isotopic disequilibrium during uptake of atmospheric CO_2 into mine process waters: Implications for CO_2 sequestration', *Environmental Science & Technology*, pp. null-null.

Wilson, S. A., Dipple, G. M., Power, I. A., Thom, J. M., Anderson, R. G., Raudsepp, M., Gabites, J. E. and Southam, G. (2009a) 'Carbon dioxide fixation within mine wastes of ultramafic-hosted ore deposits: examples from the Clinton Creek and Cassiar Chrysotile deposits, Canada', *Economic Geology,* 104, (1), pp. 95-112.

Wilson, S. A., Raudsepp, M. and Dipple, G. M. (2009b) 'Quantifying carbon fixation in trace minerals from processed kimberlite: A comparative study of quantitative methods using X-ray powder diffraction data with applications to the Diavik Diamond Mine, Northwest Territories, Canada', *Applied Geochemistry,* 24, (12), pp. 2312-2331.

Woods, S., Mitchell, C. J., Harrison, D. J., Ghazireh, N. and Manning, D. A. C. (2004) 'Exploitation and use of quarry fines: a preliminary report', *International Journal of Pavement Engineering and Asphalt Technology,* 5, pp. 54-62.

Worrell, E., Price, L., Martin, N., Hendriks, C. and Meida, L. O. (2001) 'Carbon dioxide emissions from the global cement industry', *Annual Review of Energy and the Environment,* 26, (1), pp. 303-329.

Yadav, V. S., Prasad, M., Khan, J., Amritphale, S. S., Singh, M. and Raju, C. B. (2010) 'Sequestration of carbon dioxide (CO_2) using red mud', *Journal of Hazardous Materials,* 176, (1-3), pp. 1044-1050.

Yanes, Y., Delgado, A., Castillo, C., Alonso, M. R., Ibáñez, M., De la Nuez, J. and Kowalewski, M. (2008) 'Stable isotope ($\delta^{18}O$, $\delta^{13}C$, and δD) signatures of recent terrestrial communities from a low-latitude, oceanic setting: Endemic land snails, plants, rain, and carbonate sediments from the eastern Canary Islands', *Chemical Geology,* 249, (3-4), pp. 377-392.

Zanchetta, G., Vito, M. D., Fallick, A. E. and Sulpizio, R. (2000) 'Stable isotopes of pedogenic carbonates from the Somma-Vesuvius area, southern Italy, over the past 18 kyr: palaeoclimatic implications', *Journal of Quaternary Science,* 15, (8), pp. 813-824.

Zevenhoven, R., Eloneva, S. and Teir, S. (2006) 'Chemical fixation of CO_2 in carbonates: Routes to valuable products and long-term storage', *Catalysis Today,* 115, pp. 73-79.

Zhang, J., Quay, P. D. and Wilbur, D. O. (1995) 'Carbon isotope fractionation during gas-water exchange and dissolution of CO_2', *Geochimica et Cosmochimica Acta,* 59, (1), pp. 107-114.

Appendix A

Appendix A. Analytical methods

A.1 Calcimeter carbonate determination

Carbonate (inorganic carbon) content was determined using an Eijkelkamp calcimeter and the method described in BS 7755-3.10:1995. Between 0.5 and 5 g of sample were weighed onto 200 ml conical flasks containing 20 ml of deionised water. 7 ml of 4 mol l^{-1} hydrochloric acid was measured into 10 ml glass vials, which were placed upright in the conical flasks. A rubber stopper was inserted into each flask neck, which contained a tube connecting the calcimeter to the atmosphere inside the flask. The calcimeter reservoirs were realigned and the burette was disconnected from the atmosphere. The acid containing vials were over turned and the calcimeter reservoirs were re adjusted to compensate for any pressure increase (Plate A.1).

The technique was calibrated against analytical grade calcium carbonate, and checked using WEPAL standard reference material ISE 930 2004:1 and NCS DC 73307 carbonate standards. The results are presented in Table A.1.

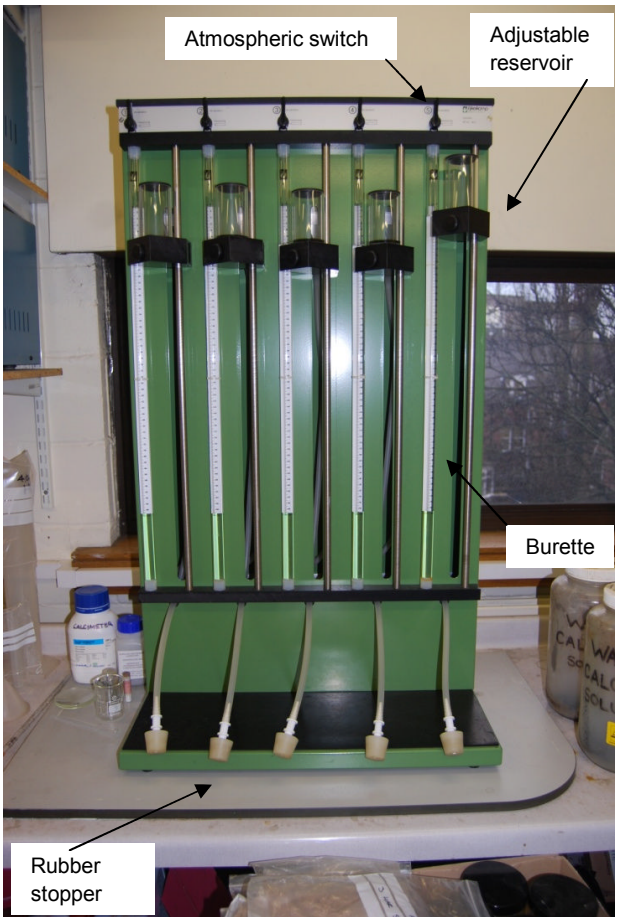

Plate A.1 – Eijkelkamp calcimeter, School of Civil Engineering and Geosciences, Newcastle University

Table A.1 – Calcimeter standards.			
	ISE 930 2004:1 Clay soil, Ivory Coast	**NCS DC 73307** Stream Sediment, Beijing, China	**Pure $CaCO_3$**
Actual value	8.06	9.55	99.97
Mean determined	7.88	9.21	99.12
Standard deviation	0.11	0.13	1.51

A.2 pH determination for soils and solutions

pH was analysed using a Jenway 3020 pH meter (Plate A.2), which was calibrated using calibration solutions at pH 4 7 and 10. Soil pH was analysed according to ISO 10390 1994, where 5 ml of soil was immersed in 20 ml of solution, shaken for 15 minutes and left to settle overnight. The solution pH was measured as above. Repeatability was < ±0.03.

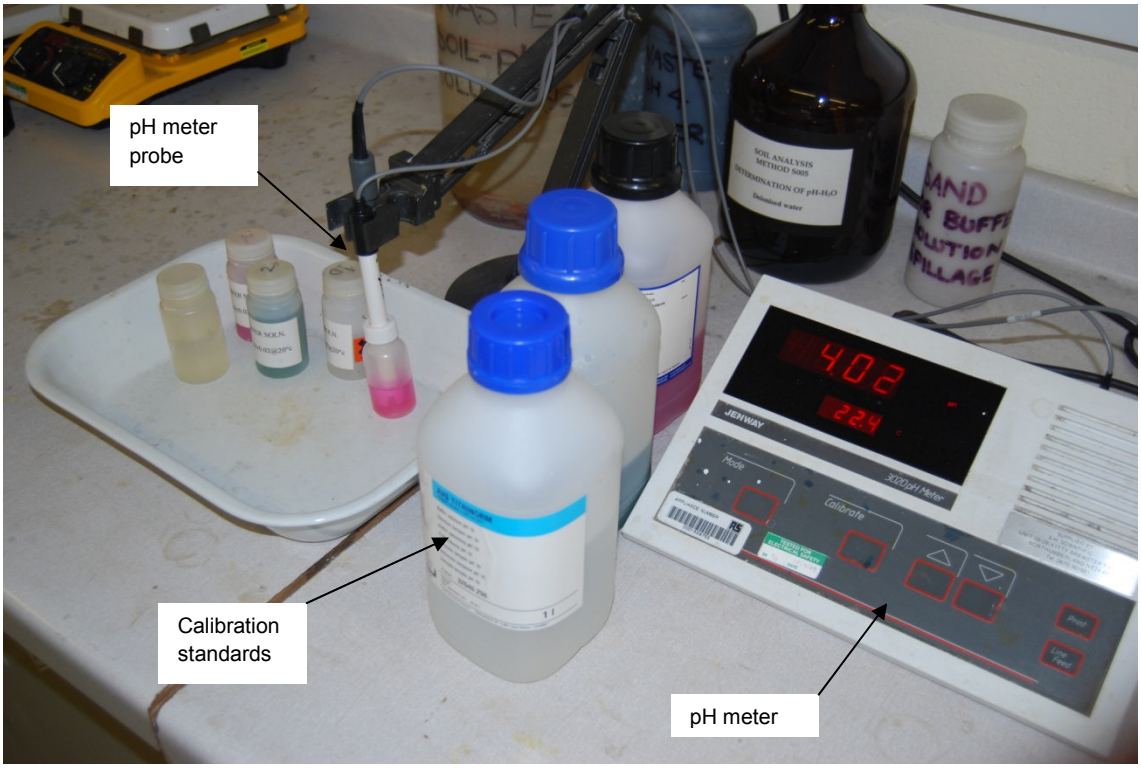

Plate A.2 – Jenway 3020 pH meter School of Civil Engineering and Geosciences, Newcastle University

A.3 Isotope Ratio Mass Spectrometry (IRMS)

Iso-Analytical carbonate stable isotopes

Samples were shipped to Iso-Analytical (Iso-Analytical Ltd, The Quantum, Phase 3, Marshfield Bank, Crewe, Cheshire, CW2 8UY) and analysis was undertaken by laboratory staff. The following description of analysis was supplied with the data.

For analysis, sample powder was placed in clean glass septum capped vials. The vials were then placed in a drying oven for 4 hours prior to the caps being fitted to ensure no moisture is present. The vials then had their headspaces flushed with pure helium (99.995%). After flushing, pure phosphoric acid* was injected into the vials and mixed with the sample powder. The samples were left to react with the acid for 24 hours at ambient temperatures then heated for 2 hours at 60 °C to ensure complete conversion to carbon dioxide.

*Phosphoric acid suitable for isotopic analysis of carbonate samples is prepared according to the procedure published by Coplen et al. (1983) Nature, vol. 302, pp. 236-238.

The CO_2 gas was then analysed by continuous flow isotope ratio mass spectrometry. In brief, the CO_2 is flushed from the septum vial using a double holed needle and resolved on a packed column gas chromatograph. The carbon dioxide then enters the ion source of a Europa Scientific 20-20 IRMS and is ionised and accelerated. Here, gas species of different mass are separated in a magnetic field then simultaneously measured using a Faraday cup collector array at m/z 44, 45, and 46.

The reference material used for this analysis was calcium carbonate standard IA-R022 ($\delta\,^{13}C_{V\text{-}PDB}$ -28.63 ‰ and $\delta\,^{18}O_{V\text{-}PDB}$ -22.69 ‰), which is traceable to NBS-19 (Limestone, $\delta\,^{13}C_{V\text{-}PDB}$ +1.95 ‰ and $\delta\,^{18}O_{V\text{-}PDB}$ -2.2 ‰). During analysis NBS-19, IA-R022 and NBS-18 ($\delta\,^{13}C_{V\text{-}PDB}$ -5.01 ‰ and $\delta\,^{18}O_{V\text{-}PDB}$ -23.20 ‰) were analysed as check samples. The results of these analyses are included in the Table A.2. The International Atomic Energy Agency, Vienna distributes NBS-18 and NBS-19 as international reference standards.

Table A.2 – Stable isotope ratios of standards for carbonate analysis.					
IA-R022 (uncertified)		**NBS-18**		**NBS-19**	
Calcium Carbonate		**Calcite** (Fen, Norway)		**Calcium Carbonate**	
$\delta^{13}C_{V\text{-}PBD}$ (‰)	$\delta^{18}O_{V\text{-}PBD}$ (‰)	$\delta^{13}C_{V\text{-}PBD}$ (‰)	$\delta^{18}O_{V\text{-}PBD}$ (‰)	$\delta^{13}C_{V\text{-}PBD}$ (‰)	$\delta^{18}O_{V\text{-}PBD}$ (‰)
-28.64	-22.58	-5.03	-23.33	1.94	-2.25
-28.59	-22.64	-5.01	-23.04	1.87	-2.24
-28.60	-22.62	-5.03	-23.14	1.87	-2.16
-28.54	-22.73	-5.12	-23.20		
-28.69	-22.57	-5.16	-23.09		
-28.63	-22.68	-5.06	-23.12		
-28.68	-22.60				
-28.72	-22.62				
-28.60	-22.76				
-28.63	-22.69				
-28.67	-22.85				
Accepted = -28.63	Accepted = -22.69	Accepted = -5.01	Accepted = -23.20	Accepted = 1.95	Accepted = -2.20
Repeatability for $\delta^{13}C_{V\text{-}PBD}$ = 0.05 ‰ and $\delta^{18}O_{V\text{-}PBD}$ = 0.07 ‰					

Iso Analytical organic carbon stable isotopes

The technique used for analysis was EA-IRMS (elemental analyser isotope ratio mass spectrometry). In brief, in this technique samples and reference materials are weighed into tin capsules, sealed, and then loaded into an automatic sampler on a Europa Scientific elemental analyser. From where they are dropped in sequence into a furnace held at 1000 °C and combusted in the presence of oxygen. The tin capsules flash combust, raising the temperature in the region of the sample to ~ 1700 °C. The combusted gases are swept in a helium stream over combustion catalyst (Cr_2O_3), copper oxide wires (to oxidize hydrocarbons), and silver wool to remove sulphur and halides. The resultant gases, N_2, NO_x, H_2O, O_2, and CO_2 are swept through a reduction stage of pure copper wires held at 600° C. This step removes any oxygen and converts NO_x species to N_2. A magnesium perchlorate chemical trap is used to remove water. Nitrogen and carbon dioxide are separated using a packed column gas chromatograph held at an isothermal temperature of 110 °C. The resultant carbon dioxide peak enters the ion source of the Europa Scientific 20-20 IRMS where it is ionised and accelerated. Gas species of different mass are separated in a magnetic field then simultaneously measured using a Faraday cup collector array to measure the isotopomers of CO_2 at m/z 44, 45, and 46.

Both references and samples are converted to CO_2 and analysed using this method. The analysis proceeds in a batch process by which a reference is analysed followed by a number of samples and then another reference.

The reference material used during analysis was Iso-Analytical Ltd. working reference standard IA-R001, wheat flour, with a $\delta^{13}C$ value of -26.43 ‰ vs. V-PDB. IA-R001 is traceable to IAEA-CH-6 (sucrose) with an accepted $\delta^{13}C$ value of –10.43 ‰ vs. V-PDB. IA-R001 was chosen as reference material as it has a similar organic matrix to the samples. Reference standards IA-R001, IA-R005 (Iso-Analytical working standard, beet sugar, $\delta^{13}C$ = -26.03 ‰ vs. V-PDB) and IA-R006 (Iso-Analytical working standard, cane sugar, $\delta^{13}C$ = -11.64 ‰ vs. V-PDB) were measured for quality control during analysis of the samples. The results of the quality control samples are included in Table A.3. The International Atomic Energy Agency, Vienna, distributes IAEA-CH-6 as an isotope reference standard.

Table A.3 – Organic carbon stable isotope standards.

IA-R001	**IA-R005**	**IA-R006**
Flour	**Beet Sugar**	**Cane Sugar**
$\delta^{13}C_{V\text{-}PDB}$ (‰)	**$\delta^{13}C_{V\text{-}PDB}$ (‰)**	**$\delta^{13}C_{V\text{-}PDB}$ (‰)**
-26.39	-25.95	-11.80
-26.41	-25.91	-11.80
-26.51	-26.00	-11.71
-26.50		
-26.37		
-26.40		
Expected = -26.43	Expected =-26.03	Expected =-11.64
Repeatability for $\delta^{13}C_{V\text{-}PDB}$ = 0.05 ‰		

Scottish Universities Environmental Research Centre (SUERC) - carbonate stable isotopes

Samples were powdered at Newcastle University and analysed by the author at SUERC during a short visit in 2010.

Stable isotope ratio of carbon and oxygen was determined using a similar setup to that of Iso-Analytical. The variation being that the samples were digested at 70 °C overnight in phosphoric acid and organic carbon was removed using a Emitech K1050X Plasma Ash at 80 W. Stable isotopes in the evolved gas were

measured using a Prism 3 stable isotope mass spectrometer (Plate A.3), calibrated using an internal standard which relates to PDB by $\delta^{13}C$ = -35.12 ‰ and $\delta^{18}O$ -32.03 ‰. Repeatability was 0.07 and 0.19 for $\delta^{13}C$ and $\delta^{18}O$ respectively.

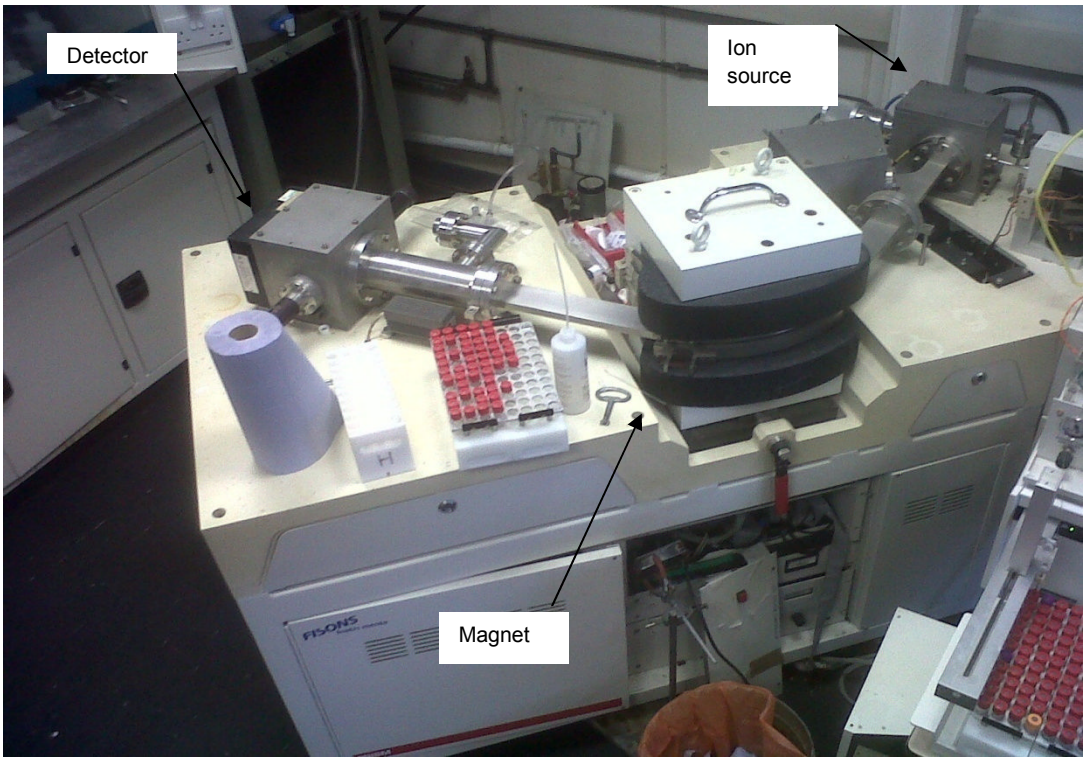

Plate A.3 – Prism 3 mass spectrometer, SUERC, East Kilbride.

A.4 Powder X-ray Diffraction (XRD)

X-ray diffraction analysis was conducted using a PANalytical X'Pert Pro Multipurpose Diffractometer (PW3040/60) fitted with an X'Celerator and a secondary monochromator (Plate A.4). For data acquisition, the Cu anode was supplied with 40 kV and a current of 40 mA to generate Cu K-alpha radiation (lambda = 1.54180 angstroms) or Cu K-alpha1 (lambda = 1.54060 angstroms). The spectra was acquired over 2-70 °2θ with a nominal step size of 0.0167 °2θ and time per step of 100 or 150 seconds. All scans were carried out in 'continuous' mode using the X'Celerator RTMS detector.

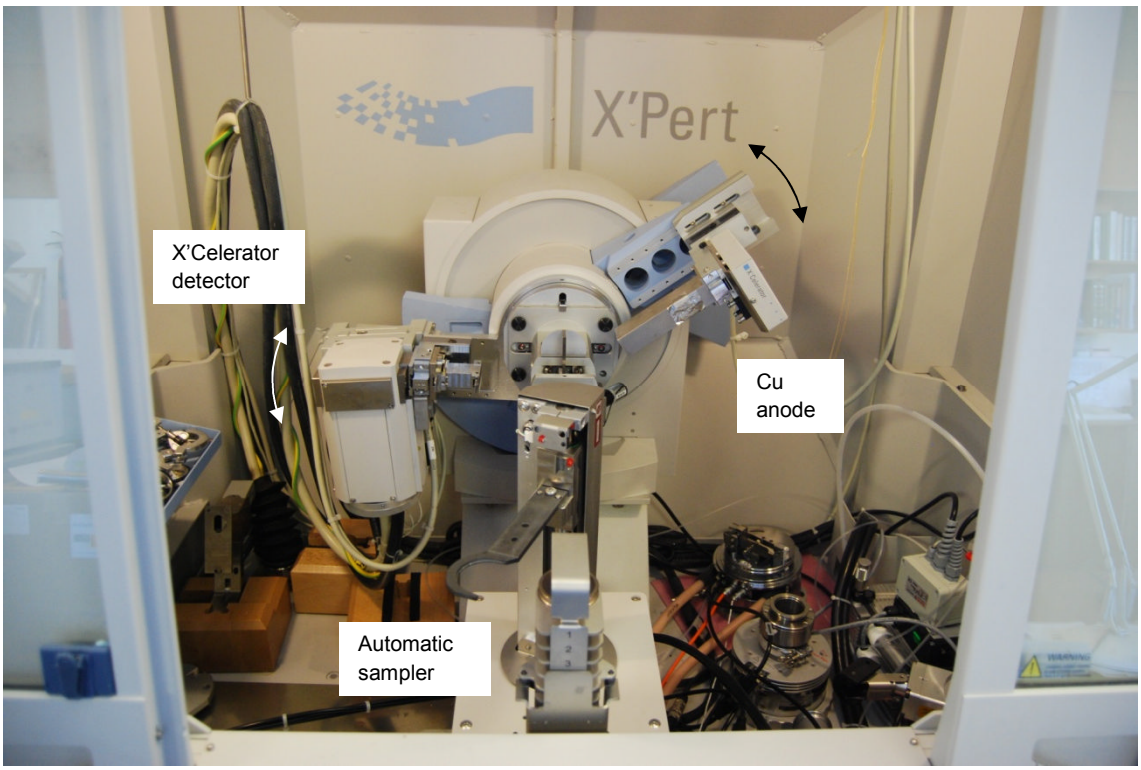

Plate A.4 – PANalytical X'Pert Pro Multipurpose Diffractometer, School of Chemical Engineering and Advanced Materials, Newcastle University.

A.5 Total Organic Carbon (TOC) determination

Approximately 0.1 g of sample, in a porous crucible, was treated with sufficient hydrochloric acid (4 mol l^{-1}) to remove carbonates and left to stand in a fume cupboard for 6-8 hours prior to being dried overnight at 65 °C. The organic carbon was determined using a Leco CS244 Carbon/Sulphur analyser in the School of Civil Engineering and Geosciences, Newcastle University (Plate A.5). The samples were oxidised in an induction furnace (using a tungsten accelerator - SL266 Sci-lab Analytical Ltd.) which was flushed with high purity oxygen at 2.0 atm. The evolved gas is passed through a series of cleaning columns and CO_2 concentration is analysed using an infrared detector. The machine is calibrated using a Leco 501-506 Carbon and Sulphur in Steel standard, and checked using WEPAL standard reference material ISE 999 2005:3 (a moist clay soil from the Ivory Coast).

Plate A.5 – Leco CS244 Carbon/Sulphur carbon analyser, School of Civil Engineering and Geosciences, Newcastle University.

TOC values for the standard ISE 999 2005:3 were 0.49, 0.54, 0.49, 0.53 and 0.45 ($\bar{x}$ = 0.50, s = 0.04) which is within the range of acceptable values (0.46 ± 0.05). 5 successive measurements of TOC for a sample from the microcosm experiments were used to measure the repeatability (= 0.40).

A.6 X-ray florescence (XRF) Analysis

XRF analysis was conducted by staff at the University of Leicester, department of Geology using a PANalytical Axios Advanced XRF spectrometer. Samples were powdered and mixed with 1:5 ratio of flux (80% lithium metaborate, 20% lithium tetraborate). The samples and flux were ignited at 1100 °C and cast into glass beads. The machine was calibrated using certified British Chemical Standards (BCS) BCS375 (sodium feldspar), BCS376 (potassium feldspar) and BCS372/1 (hydrated cement).

A.7 Free lime determination

Free lime was determined in accordance with the methods in Swenson and Throvaldson (1950) and Lerch and Bogue (1930)[†]. Approximately 1 g of sample was weighed into a 100 ml Erlenmeyer flask containing 60 ml of neutralised glycerol-ethanol solution*, anti-bumping granules, and an anhydrous strontium

chloride accelerant. A reflux condenser was inserted into the neck of the beaker (Plate A.6) and the solution was boiled for 20 minute time intervals.

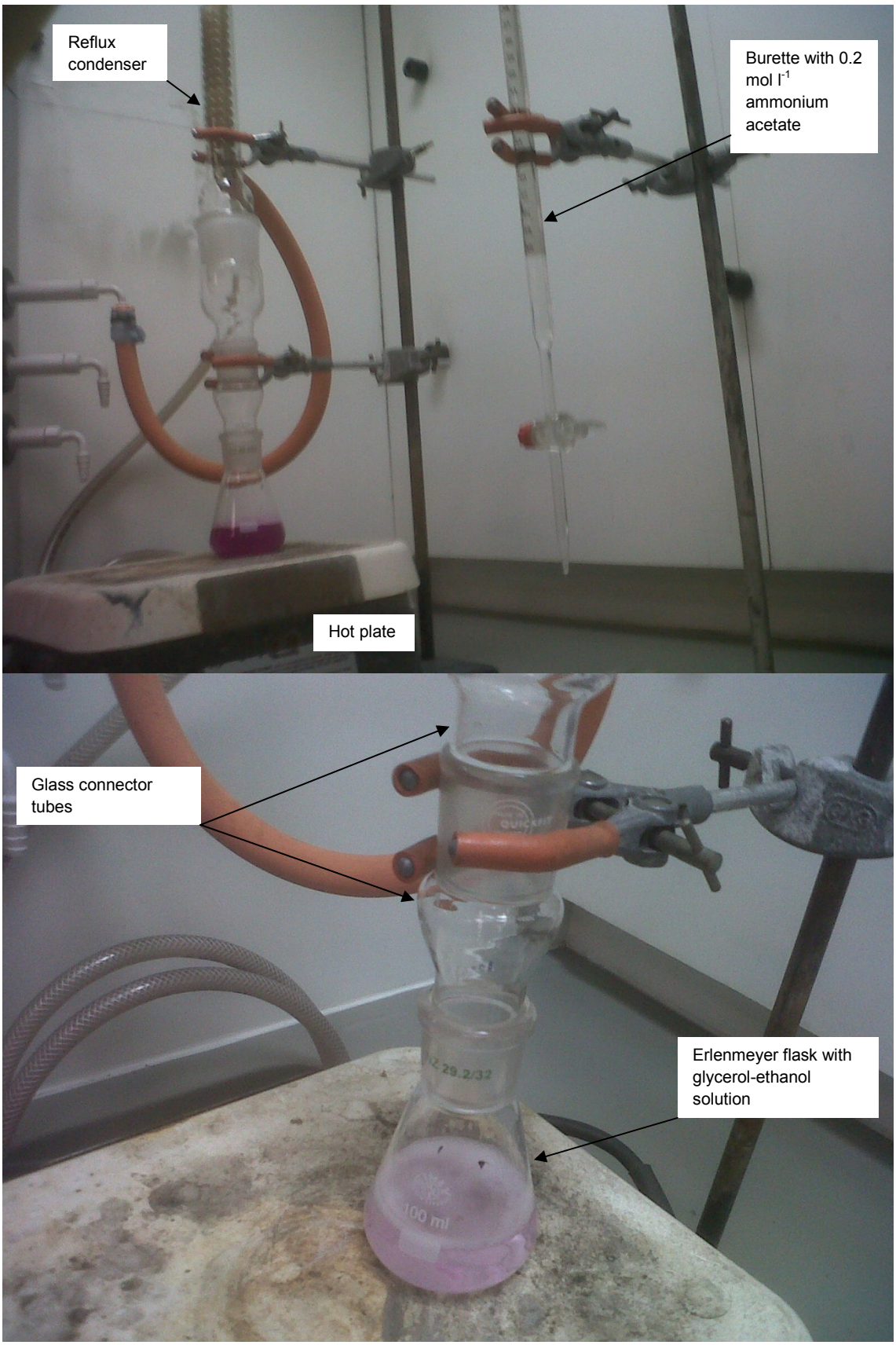

Plate A.6 – Apparatus setup for determination of free lime

If a colour change was noticed, the mixture was titrated to colourless with ammonium acetate solution**. This procedure was repeated until no colour change was detected in a 1 hour time interval.

†Swendon E.G. and Throvaldson T. (1950) The alcohol-glycerol method for the determination of free lime. *Canadian Journal of Chemistry*, 29 140-153. Lerch W. and Bogue R.H. (1930) Revised procedure for the determination of uncombined lime in Portland cement. *Industrial and Engineering Chemistry*, 2(3) 296-298.

*1 part glycerol to 5 parts ethanol, spiked with 2 ml l^{-1} of phenolphthalein indicator (made up with ethanol). Neutrality was maintained by addition of dilute NaOH ethanol solution or ammonium acetate solution**

**0.2 mol l^{-1} of ammonium acetate was made up with ethanol.

The method was calibrated using 0.1 grams of CaO made from analytical grade $CaCO_3$ that was decarbonated at 950C over 8 hours in a platinum crucible and muffle furnace.

A.8 Scanning electron microscopy (SEM)

Images were taken using an FEI XL series environmental scanning electron microscope at Newcastle University. The pressure inside the chamber was controlled at 1.4 Torr, flushed with nitrogen gas, and the incident electron energy was 20 kV. Characteristic X-ray spectra were determined using X-ray photoelectron spectroscopy.

A.9 Thermogravimetric – Differential Scanning Calometry - Quadrupole Mass Spectrometry (TG-DSC-QMS)

Thermogravimetric analysis measures the mass changes of a sample under a heating regime. At Newcastle University the thermogravimetric system (Netzsch TG209) requires between 30 and 60 mg of powdered sample, which was weighed into a platinum crucible and placed onto a balance (10^{-3} mg sensitivity) inside a heating chamber. The atmosphere inside the furnace was continually purged with HeO while the sample was heated to between 900-1000°C with a linear heating rate of 10°C $minute^{-1}$. The machine records the weight loss as a function of time. Newcastle University's TG-DSC (Netzsch STA449C Jupiter)

operates in the same way, but simultaneously measures energy flux inside the heating chamber. The system is coupled to a quadrupole mass spectrometer (Netzsch QMS403C Aëolos), which continually speciates the evolved gas during thermal decomposition, providing a qualitative indicator of sample chemistry (Plate A.7).

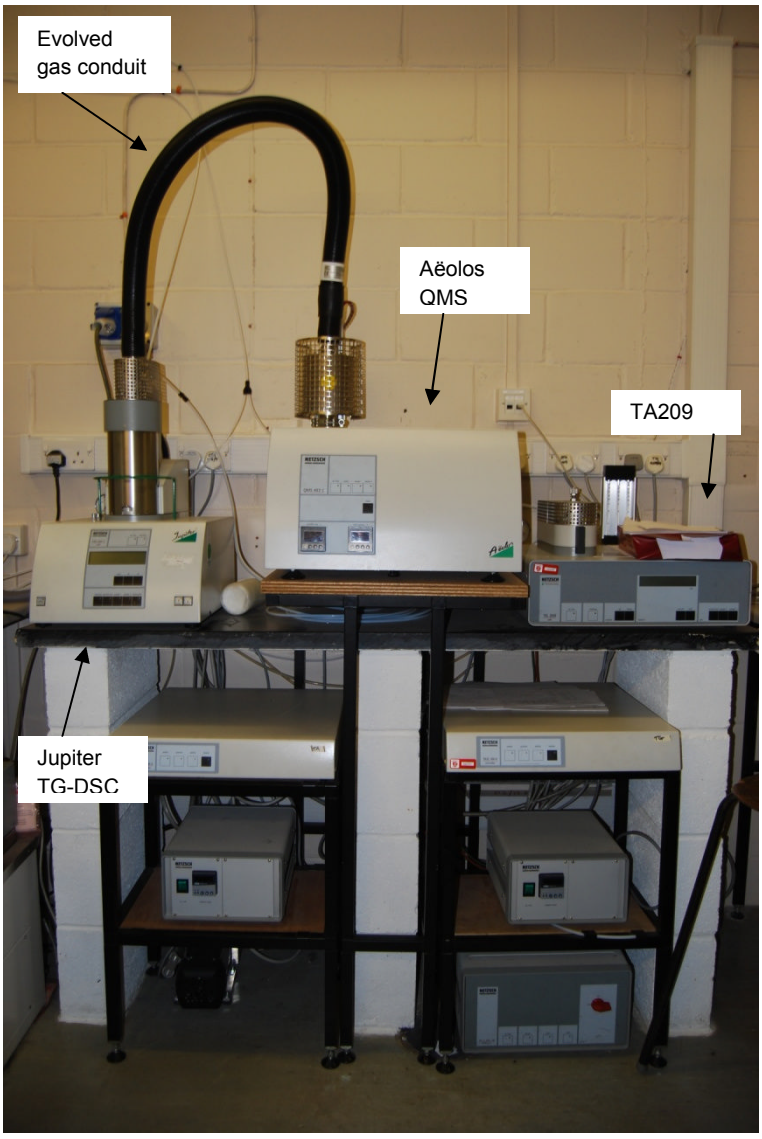

Plate A.7 – TG-DSC-QMS, Civil Engineering and Geosciences, Newcastle University

A.10 Atomic Absorption Spectroscopy (AAS)

The AAS analyses referred to in this thesis were undertaken at Newcastle University using a bench-top Varian SpectrAA 400 (Plate A.8). The machine is programmed with the settings in Table A.4, using an air and acetylene. Samples are introduced into the machine through a nebulizer and ionised in an air

acetylene flame (2200-2400 °C). Absorbance through the flame is calibrated against standards (0-25 mg l^{-1}) and absorbance is manually reduced if necessary by rotating the burner.

Table A.4 – programme settings for determination of calcium using AAS.

Parameter	**Value**
Lamp current	10 mA
Slit width	0.5 nm
Wavelength	422.7
Fuel	Air-acetylene

Samples were acidified using concentrated nitric acid spiked with 0.1 % lanthanum (as $LaCl_2$ Spectrosol stock solutions) and diluted using volumetric flasks to within the calibration range. Standards were similarly diluted from 1000 mg l^{-1} stock solutions, matching background matrix where appropriate.

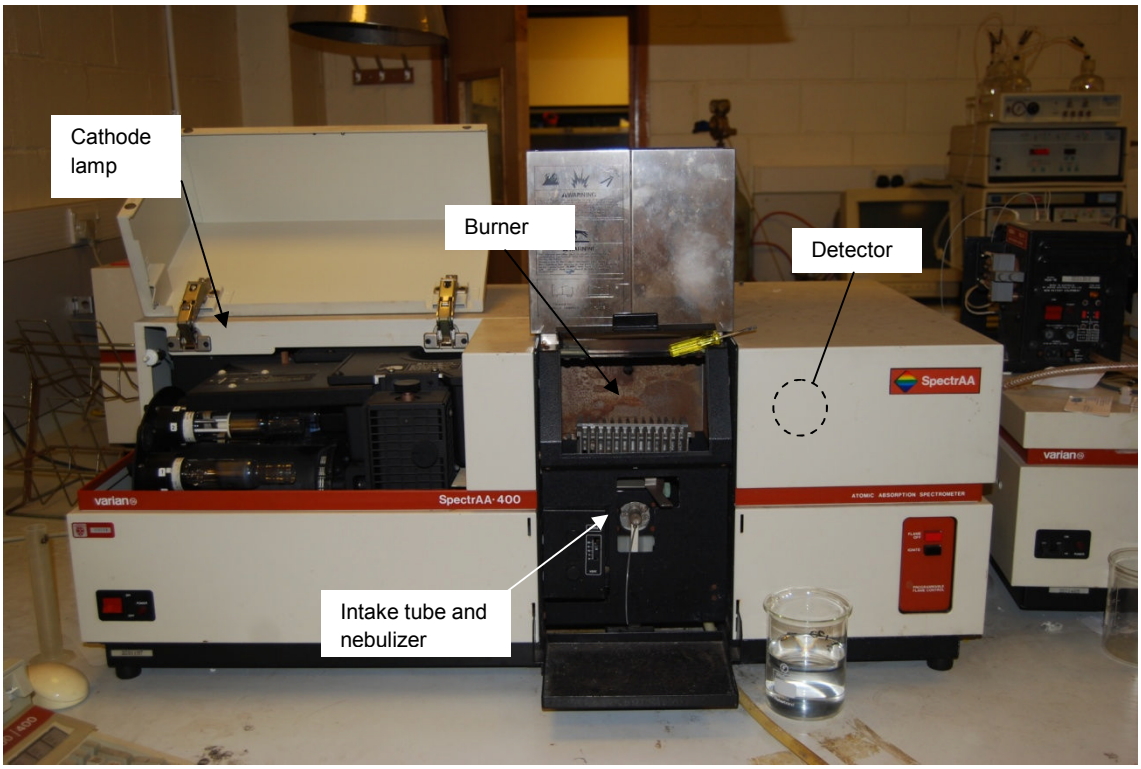

Plate A.8 – Varian SpectrAA 400 *Atomic Absorption Spectrometer, Civil Engineering and Geosciences, Newcastle University*

A.11 Determination of organic and inorganic carbon content of solutions

Organic and inorganic carbon concentration in solutions was measured using a Shimadzu TOC 5050A Total Carbon Analyser (Plate A.9). Solution samples, pre filtered through a 0.2 µm aperture cellulose nitrate filter, were decanted into 5 ml glass vials and placed onto an auto sampler. The liquid was drawn into one of two inlet valves via a peristaltic pump. Through the first inlet, the sample was oxidised in a furnace at 800 °C converting the carbon in the sample to CO_2 which was measured using an infrared detector. Through the second inlet valve, the solution sample was dosed with concentrated phosphoric acid and the CO_2 was stripped and measured as above. The first measurement is the total carbon in the solution; the second is inorganic carbon (organic carbon is calculated through subtraction).

Plate A.9 – Shimadzu TOC 5050A Total Carbon Analyser, School of Civil Engineering and Geosciences, Newcastle University

The accuracy and repeatability of the total carbon analyser was determined using sodium citrate (for organic carbon 100 mg C l^{-1} pH 5) standards made by dissolving analytical grade solids separately into 18 Ω deionised water. Measurements of 94.0, 109.5, 100.2, 112.9 and 96.3 mg l^{-1} were made ($\bar{x}$ = 102.6 % s = 8.3). Sample 4, microcosm B in Chapter 4 had the largest inorganic carbon content (~100 mg l^{-1}) and was rerun an additional 4 times ($\bar{x}$ = 99.9 %, s = 5.0).

Appendix B

Appendix B. Data Tables

B.1 Chapter 4 Data Tables

B.1.1 Barrasford quarry, Northumberland

Table B.1 – Carbonate concentration of soils at Barrasford quarry.

Plot	Depth (cm)	%CaCO3	%C
P1	0-10	6.54	0.78
	10-20	5.85	0.70
	20-30	5.54	0.66
P2	0-10	3.39	0.41
	10-20	5.3	0.64
	20-30	7.32	0.88
P3	0-10	2.38	0.29
	10-20	0.48	0.06
	20-25	1.68	0.20
P4	0-10	2.26	0.27
	10-20	1.36	0.16
	20-23	1.12	0.13
P5	0-10	0.05	0.01
	10-20	0.06	0.01
	20-24	0.27	0.03

Table B.2 – Stable isotope ratios of carbonates at Barrasford quarry.

Sample	$d^{13}C_{V\text{-}PDB}$ (‰)	$d^{18}O_{V\text{-}PDB}$ (‰)
PIC3(1)	-1.49	-11.90
PIC3(2)	-1.61	-12.00
PIC3(3)	-2.49	-12.46
P2C3(1)	-3.46	-13.12
P2C3(2)	-3.50	-12.27
P2C3(2)D	-3.38	-12.43
P2C3(3)	-2.55	-11.90
P3C3(1)	-2.64	-12.26
P4C3(1)	-1.51	-12.11
P1OLD(1)	-1.62	-12.49
P1OLD(2)	-1.50	-12.38
P1OLD(2)D	-1.67	-12.26
P1OLD(3)	0.09	-11.29
P5OLD(1)	-0.69	-11.42
Local limestone 1	0.59	-11.10
Local limestone 1D	0.61	-11.03
Local limestone 2	1.63	-10.64
Local limestone 2D	1.59	-10.55

Table B.3 – Strontium isotope ratios at Barrasford quarry.		
Sample	**^{87}Sr / ^{86}Sr**	**±2SE**
P1C3(3)	0.708958	0.000016
P2C3(1)	0.709650	0.000017
P2C3(2)	0.709023	0.000014
Local limestone	0.710677	0.000018
Raw Dol	0.706172	0.000016

B.1.2 Other sites on the Whin Sill, Northumberland

Samples were taken from the soil developed on the Whin Sill over a 6 week period between June and August 2008. Whin sill derived soils at Rugley farm, Northumberland (NU163606) predominately supported arable crops (wheat and barley), whereas, soil south and around the grounds of Dunstanbugh Castle (NU257227) supported pastoral farming.

Table B.4 – Carbonate content of soils at Dunstanburgh Castle.			
Sample		**Depth (cm)**	**% $CaCO_3$**
Dun 01 (2-10 cm)		-6	<0.01
Dun 01 (10-20 cm)		-15	0.08
Dun 01 (20-30cm)		-25	0.02
Dun 01 (30-40 cm)		-35	<0.01
Dun 02 (2-10 cm)		-6.0	<0.01
Dun 02 (10-20 cm)		-15	0.03
Dun 02 (20-30cm)		-25	<0.01
Dun 02 (30-40 cm)		-35	0.03
Dun 03 (2-20cm)		-11	<0.01
Dun 04 (2-10cm)		-6	<0.01
Dun 04 (10-20cm)		-15	<0.01
Dun 05 (2-10cm)		-6	<0.01
Dun 05 (10-30 cm)		-20	<0.01
Dun 06 (2-10cm)		-6	<0.01
Inside the grounds at Dunstanbugh Castle	MH1	Surface	1.3488
	MH2	Surface	-0.0564
	MH3	Surface	-0.0152
	MH4	Surface	-0.0511

Table B.5 – Carbonate content of soils at Rugley Farm.		
Sample	**Depth (cm)**	**% $CaCO_3$**
Rug 01 (0-15cm)	-8	<0.01
Rug 01 (15-30cm)	-23	0.03
Rug 01 (30-45cm)	-38	<0.01
Rug 01 (45-60cm)	-53	<0.01
Rug 01 (60-70cm)	-65	<0.01
Rug 02 (0-15cm)	-8	0.05
Rug 02 (15-30cm)	-23	<0.01
Rug 02 (30-45cm)	-38	2.93
Rug 02 (45-60cm)	-53	0.34
Rug 03 (0-15cm)	-8	<0.01
Rug 03 (15-30cm)	-23	0.03
Rug 03 (30-45cm)	-28	<0.01
Rug 03 (45-60)	-53	<0.01
Rug 4 (0-15cm)	-8	<0.01
Rug 04 (15-30cm)	-23	<0.01
Rug 4 (30-45)	-38	<0.01
Rug 04 (45-60cm)	-53	<0.01
Rug 05 (0-15cm)	-8	0.02
Rug 05 (15-30cm)	-23	0.44
Rug 5 (30+)	-30	<0.01

B.1.3 IRD site, Byker, Newcastle upon Tyne

Table B.6 – Carbonate content of soil at the IRD site, Byker.					
Sample	**%$CaCO_3$**	**%C**	**Sample**	**%$CaCO_3$**	**%C**
A2TP1 0-20	19.91	2.39	A2TP3 20-40	6.99	0.84
A2TP1 20-40	19.35	2.32	A2TP3 40-60	6.54	0.78
A2TP1 40-60	19.59	2.35	A2TP3 60-100	6.07	0.73
A2TP1 100-170	11.39	1.37	A2TP3 120-190	8.38	1.01
A2TP1 170-200	11.86	1.42	A2TP3 190-230	6.06	0.73
A2TP1 200-230	12.57	1.51	A2TP3 230-290	6.19	0.74
A2TP1 200-230 Clay	4.25	0.51	A2TP4 0-20	11.61	1.39
A2TP1 230-290	12.54	1.50	A2TP4 20-40	7.97	0.96
A2TP2 0-20	8.91	1.07	A2TP4 40-60	4.51	0.54
A2TP2 20-40 Black	5.63	0.68	A2TP5 0-20	13.57	1.63
A2TP2 20-40 Mixed	3.94	0.47	A2TP5 20-40	17.15	2.06
A2TP2 40-60	7.33	0.88	A2TP5 40-60	17.07	2.05
A2TP2 60-100	3.26	0.39	A2TP5 60-100 Black	2.17	0.26
A2TP2 100-190 Brown	6.82	0.82	A2TP5 60-100 Brown	17.69	2.12
A2TP2 100-190 Black	3.49	0.42	A2TP5 100-150	10.91	1.31
A2TP2 200-250	4.16	0.50	A2TP5 150-170	9.29	1.11
A2TP3 0-20	6.02	0.72			

Table B.7 – Stable isotope ratios of carbonates at the IRD site.		
Sample	**$d^{13}C_{V\text{-}PDB}$ (‰)**	**$d^{18}O_{V\text{-}PDB}$ (‰)**
A2TP1 0-20	-7.70	-8.65
A2TP1 0-20 D	-7.66	-8.57
A2TP1 40-60	-20.18	-13.05
A2TP1 200-230	-18.63	-11.74
A2TP2 0-20	-15.11	-11.96
A2TP2 40-60	-10.69	-10.09
A2TP2 40-60D	-10.77	-10.11
A2TP2 200-250	-7.78	-8.52
A2TP2 200-250D	-8.03	-8.56
A2TP3 0-20	-6.66	-8.45
A2TP3 40-60	-6.35	-9.13
A2TP3 190-230	-7.36	-8.62
A2TP4 0-20	-8.52	-7.87
A2TP4 40-60	-14.96	-9.48
A2TP5 0-20	-16.20	-10.84
A2TP5 40-60	-20.11	-12.32
A2TP5 150-170	-17.15	-11.16
A2TP5 150-170D	-17.01	-11.02
A2TP1 RS 100-170	-27.50	-20.89
A2TP1 RS 170-200	-22.97	-14.15
A2TP2 RS 200-250	-21.02	-12.79
A2TP2 RS 100-190	-13.33	-3.92
A2TP5 RS 40-60	-18.87	-13.87
A2TP5 RS 40-60D	-18.91	-13.94

Table B.8 – Isotope ratio of organic carbon at the IRD site.	
Sample	**$\delta^{13}C_{V\text{-}PDB}$ (‰)**
TP1 0-20	-19.80
TP1 40-60	-23.01
TP1 230	-23.30
TP2 0-20	-23.77
TP2 40-60	-22.17
TP2 40-60D	-22.10
TP2 200-250	-23.66
TP3 0-20	-22.47
TP3 40-60	-23.05
TP3 190-230	-22.53
TP4 0-20	-23.41
TP4 0-20D	-23.27
TP4 40-60	-23.09
TP5 0-20	-23.77
TP5 40-60	-23.83
TP5 150-170	-23.29

B.1.4 Former steelworks at Consett, County Durham

Table B.9 – Carbonate content of soil at the former steelworks in Consett.

Sample	%$CaCO_3$	%C
Con 01 (0-35cm)	6.05	0.73
Con 02 (0-22cm)	<0.01	<0.01
Con 02 (20-34cm)	<0.01	<0.01
Con 3 (0-22cm)	38.26	4.59
Con 3 (15-30)	0.03	<0.01
Con 4 (0-19cm)	4.60	0.55
Con 05 (0-15cm)	0.34	0.04
Con Hp (0-8cm)	86.66	10.40
Con Hp (8-15cm)	48.67	5.84
Con HP2	58.11	6.97
Con Hp2 (bottom)	78.45	9.41
Con MH1	<0.01	<0.01
Con Mh1	<0.01	<0.01
Con 01 (surface sediment)	93.43	11.21

Table B.10 – Stable isotope ratios of carbonates at the former steelworks, Consett.

Sample	$d^{13}C_{V\text{-}PDB}$ (‰)	$d^{18}O_{V\text{-}PDB}$ (‰)
CON 01 (0-35)	-22.11	-14.20
CON 01 (Surface Sediment)	-22.71	-16.09
CON 03 (0-22)	-	-
CON 04 (0-19)	-17.62	-11.29
CON HP (0-8)	-22.14	-15.47
CON HP (8-15)	-18.18	-11.78
CON HP (8-15)D	-18.27	-11.88
CON HP2 (bottom)	-20.29	-13.31
CON HP2	-21.82	-15.49

B.1.5 Science Central, Newcastle upon Tyne

Table B.11 – Data for Science Central.

ID	Easting (m)	Northing (m)	%$CaCO_3$	%TOC	%TIC	%MOIST	%CaO	%MgO	%Fe_2O_3	$\delta^{13}C$ (‰)	$\delta^{18}O$ (‰)
B12	423921.43	564286.96	23.03	1.32	2.76	12.78					
B13	423921.43	564266.96	44.38	1.02	5.33	20.13	22.03	6.17	3.55	-3.65	-8.10
B14	423921.43	564246.96	42.95	0.99	5.15	24.85					
B15	423921.43	564226.96	50.17	0.27	6.02	12.08	22.01	5.25	3.24	-3.13	-8.69
C3	423941.43	564466.96	26.21	1.72	3.15	14.69					
C4	423941.43	564446.96	27.27	1.54	3.27	11.60					
C5	423941.43	564426.96	24.14	2.03	2.90	17.53					
C6	423941.43	564406.96	25.08	1.60	3.01	16.82					
C7	423941.43	564386.96	26.73	1.59	3.21	17.30					
C8	423941.43	564366.96	25.46	1.59	3.05	17.39					
C9	423941.43	564346.96	22.75	2.00	2.73	17.53					
C10	423941.43	564326.96	26.39	1.49	3.17	14.97					
C11	423941.43	564306.96	25.67	1.40	3.08	16.48					
C12	423941.43	564286.96	25.54	1.52	3.06	17.60					
C13	423941.43	564266.96	22.04	0.93	2.64	18.55					
C14	423941.43	564246.96	20.47	1.12	2.46	16.59					
C15	423941.43	564226.96	32.02	1.22	3.84	13.37					
D3	423961.43	564466.96	23.92	1.27	2.87	14.28	13.90	2.09	3.85	-8.72	-10.46
D4	423961.43	564446.96	19.36	1.37	2.32	11.96					
D5	423961.43	564426.96	32.12	1.27	3.85	19.69	17.93	2.08	3.50	-7.79	-11.18
D6	423961.43	564406.96	25.64	1.51	3.08	16.80					
D7	423961.43	564386.96	21.06	1.77	2.53	17.79	13.06	2.05	4.06	-9.11	-9.40
D8	423961.43	564366.96	26.67	1.71	3.20	16.80					
D9	423961.43	564346.96	19.15	2.88	2.30	17.03	11.45	1.53	4.13	-10.78	-10.62
D10	423961.43	564326.96	25.72	1.68	3.09	15.12					
D11	423961.43	564306.96	21.87	2.15	2.62	17.51	13.21	1.90	4.12	-9.78	-9.79
D12	423961.43	564286.96	30.50	1.76	3.66	18.42					
D13	423961.43	564266.96	24.46	1.74	2.94	18.85	14.04	1.54	3.83	-11.20	-11.93
D14	423961.43	564246.96	20.32	0.87	2.44	17.53					
D15	423961.43	564226.96	21.98	1.99	2.64	17.83	13.34	1.97	3.57	-10.70	-10.77
E3	423981.43	564466.96	25.47	1.64	3.06	15.03					
E4	423981.43	564446.96	27.57	1.98	3.31	14.20					
E5	423981.43	564426.96	28.98	1.50	3.48	13.98					
E6	423981.43	564406.96	26.61	1.61	3.19	16.93					
E7	423981.43	564386.96	19.80	1.64	2.38	15.12					
E8	423981.43	564366.96	20.84	2.33	2.50	17.56					
E9	423981.43	564346.96	23.29	2.06	2.79	15.72					
E10	423981.43	564326.96	18.88	2.67	2.27	16.70					
E11	423981.43	564306.96	20.35	1.34	2.44	15.94					
E12	423981.43	564286.96	26.45	1.62	3.17	16.94					
E13	423981.43	564266.96	20.46	1.46	2.45	15.89					
E14	423981.43	564246.96	22.98	2.04	2.76	18.06					
E15	423981.43	564226.96	28.02	1.32	3.36	12.28					
F3	424001.43	564466.96	22.91	1.41	2.75	14.89	13.93	1.57	3.83	-9.12	-10.46
F4	424001.43	564446.96	24.79	1.38	2.98	10.18					
F5	424001.43	564426.96	20.30	2.33	2.44	15.17	16.76	2.00	3.70	-8.89	-10.19
F6	424001.43	564406.96	24.92	1.59	2.99	17.95					
F7	424001.43	564386.96	21.67	1.52	2.60	20.59	13.39	1.65	3.88	-10.01	-11.39
F8	424001.43	564366.96	29.24	1.82	3.51	14.16					
F9	424001.43	564346.96	30.07	1.72	3.61	13.63	15.83	2.24	4.08	-8.44	-10.09
F10	424001.43	564326.96	27.96	1.45	3.36	15.85					
F11	424001.43	564306.96	27.46	1.55	3.30	18.68	15.91	2.09	3.51	-9.39	-10.78
F12	424001.43	564286.96	27.52	1.78	3.30	19.46					
F13	424001.43	564266.96	24.06	1.34	2.89	17.99	14.60	1.88	3.69	-13.38	-11.51
F14	424001.43	564246.96	25.91	3.26	3.11	16.63					
F15	424001.43	564226.96	26.17	2.26	3.14	17.69	13.65	2.47	3.83	-7.42	-10.07
G3	424021.43	564466.96	21.06	1.60	2.53	14.78					
G4	424021.43	564446.96	25.08	1.47	3.01	15.61					
G5	424021.43	564426.96	23.07	2.06	2.77	17.14					
G6	424021.43	564406.96	19.96	1.72	2.40	13.74					

Table B.11 – Data for Science Central.

ID	Easting (m)	Northing (m)	%$CaCO_3$	%TOC	%TIC	%MOIST	%CaO	%MgO	%Fe_2O_3	$\delta^{13}C$ (‰)	$\delta^{18}O$ (‰)
G7	424021.43	564386.96	22.24	1.84	2.67	17.27					
G8	424021.43	564366.96	27.21	1.66	3.27	16.45					
G9	424021.43	564346.96	28.34	1.48	3.40	16.32					
G10	424021.43	564326.96	26.52	1.72	3.18	15.73					
G11	424021.43	564306.96	23.07	1.31	2.77	16.71					
G12	424021.43	564286.96	25.59	1.37	3.07	16.51					
G13	424021.43	564266.96	24.12	1.40	2.89	13.33					
G14	424021.43	564246.96	32.58	1.50	3.91	18.25					
G15	424021.43	564226.96	29.59	1.48	3.55	15.09					
H3	424041.43	564466.96	21.70	1.44	2.60	14.80	14.35	1.29	3.85	-10.66	-10.98
H4	424041.43	564446.96	25.37	1.58	3.04	19.04					
H5	424041.43	564426.96	21.08	2.08	2.53	31.39	12.42	1.39	3.55	-10.67	-11.79
H6	424041.43	564406.96	16.89	2.42	2.03	14.10					
H7	424041.43	564386.96	21.08	2.01	2.53	14.19	13.43	1.62	3.83	-10.30	-11.15
H8	424041.43	564366.96	25.11	1.64	3.01	18.42					
H9	424041.43	564346.96	25.72	1.89	3.09	19.18	16.49	1.86	3.65	-9.26	-9.53
H10	424041.43	564326.96	24.77	1.48	2.97	12.20					
H11	424041.43	564306.96	25.63	1.61	3.08	14.47	16.59	2.00	3.61	-9.51	-10.42
H12	424041.43	564286.96	27.45	1.40	3.29	13.35					
H13	424041.43	564266.96	21.06	3.20	2.53	19.24	12.78	1.48	3.45	-10.93	-10.66
H14	424041.43	564246.96	17.27	1.21	2.07	15.25					
H15	424041.43	564226.96	18.57	1.21	2.23	14.65	11.78	1.70	3.43	-10.12	-10.83
I3	424061.43	564466.96	20.53	1.62	2.46	19.38					
I4	424061.43	564446.96	18.10	2.19	2.17	16.61					
I5	424061.43	564426.96	17.18	2.11	2.06	16.86					
I6	424061.43	564406.96	22.27	1.69	2.67	15.26					
I7	424061.43	564386.96	17.54	1.96	2.10	13.46					
I8	424061.43	564366.96	20.04	1.81	2.40	14.35					
I9	424061.43	564346.96	23.07	1.45	2.77	13.04					
I10	424061.43	564326.96	29.00	1.78	3.48	15.73					
I11	424061.43	564306.96	25.21	1.50	3.02	18.14					
I12	424061.43	564286.96	19.09	1.63	2.29	12.05					
I13	424061.43	564266.96	20.59	1.18	2.47	15.94					
I14	424061.43	564246.96	19.07	1.07	2.29	15.16					
I15	424061.43	564226.96	22.77	1.05	2.73	17.63					
J3	424081.43	564466.96	19.71	1.90	2.37	19.38	12.87	1.15	4.08	-11.34	-10.74
J4	424081.43	564446.96	24.98	1.45	3.00	17.39					
J5	424081.43	564426.96	22.38	1.81	2.69	16.33	13.76	1.62	4.10	-10.06	-11.51
J6	424081.43	564406.96	19.00	1.71	2.28	16.60					
J7	424081.43	564386.96	19.80	1.88	2.38	14.83	12.56	1.57	3.98	-11.05	-11.10
J8	424081.43	564366.96	17.42	1.66	2.09	13.13					
J9	424081.43	564346.96	17.19	1.87	2.06	14.20	11.05	1.13	4.11	-13.29	-10.86
J10	424081.43	564326.96	21.79	1.64	2.61	12.30					
J11	424081.43	564306.96	17.07	1.61	2.05	16.47	10.90	0.92	4.22	-13.55	-11.43
J12	424081.43	564286.96	17.78	2.17	2.13	31.72					
J13	424081.43	564266.96	21.91	1.42	2.63	12.43	12.39	1.78	3.73	-10.81	-11.27
J14	424081.43	564246.96	22.08	1.37	2.65	16.76					
J15	424081.43	564226.96	21.63	1.52	2.60	15.58	12.77	1.70	3.50	-9.89	-11.08
K4	424101.43	564446.96	22.65	1.93	2.72	13.22					
K5	424101.43	564426.96	20.37	1.82	2.44	16.39					
K6	424101.43	564406.96	19.01	1.71	2.28	14.37					
K7	424101.43	564386.96	10.51	2.73	1.26	9.97					
K10	424101.43	564326.96	19.01	1.72	2.28	13.20					
K11	424101.43	564306.96	16.43	1.86	1.97	16.66					
K12	424101.43	564286.96	14.75	1.61	1.77	15.31					
K13	424101.43	564266.96	22.64	1.93	2.72	12.04					
K14	424101.43	564246.96	5.27	4.30	0.63	8.78					
K15	424101.43	564226.96	17.31	3.26	2.08	15.94					
L6	424121.43	564406.96	18.43	1.48	2.21	12.21	12.53	1.81	3.96	-8.07	-10.18
L10	424121.43	564326.96	17.35	1.64	2.08	12.05	10.85	0.95	4.04	-12.68	-11.88
L14	424121.43	564246.96	15.14	2.33	1.82	10.72					
L15	424121.43	564226.96	13.85	2.32	1.66	11.79	9.09	1.05	4.15	-11.67	-10.96

Table B.11 – Data for Science Central.											
ID	**Easting (m)**	**Northing (m)**	**%$CaCO_3$**	**%TOC**	**%TIC**	**%MOIST**	**%CaO**	**%MgO**	**%Fe_2O_3**	**$\delta^{13}C$ (‰)**	**$\delta^{18}O$ (‰)**
M10	424141.43	564326.96	15.63	1.77	1.88	11.99					
M14	424141.43	564246.96	25.19	1.69	3.02	8.95					
M15	424141.43	564226.96	10.42	5.67	1.25	12.57					
N10	424161.43	564326.96	16.36	3.17	1.96	10.89	10.51	0.91	4.06	-13.19	-11.64
N12	424161.43	564286.96	22.76	1.78	2.73	15.56	13.51	1.93	3.85	-7.81	-10.05
N13	424161.43	564266.96	15.43	2.43	1.85	10.94					
N14	424161.43	564246.96	18.99	2.75	2.28	12.47	12.39	1.58	4.04	-9.58	-11.36
N15	424161.43	564226.96	7.34	1.88	0.88	13.00					
O12	424181.43	564286.96	17.61	2.18	2.11	11.25					
O13	424181.43	564266.96	14.17	2.67	1.70	9.42					
O14	424181.43	564246.96	10.91	3.23	1.31	15.19					
P12	424201.43	564286.96	12.00	1.69	1.44	8.61	8.01	1.23	4.28	-10.29	-9.83
P13	424201.43	564266.96	17.35		2.08	7.82					
P14	424201.43	564246.96	21.88	2.37	2.63	22.05	13.95	1.04	4.33	-12.43	-11.41
Q13	424221.43	564266.96	18.61	2.28	2.23	14.42					

B.1.6 California

Table B.12 – Carbonate content of soils in California.					
Sample	**%$CaCO_3$**	**%C**	**Sample**	**%$CaCO_3$**	**%C**
UCM 2 B	1.75	0.21	SLA 2 Surf	3.97	0.48
UCM 2	3.57	0.43	SLA 3 0-3	3.05	0.37
UCM 3	0.28	0.03	SLA 3	1.43	0.17
UCM 3 0-10	0.18	0.02	SLA 4 0-3	4.49	0.54
UCM 4 6-9	0.21	0.03	SLA 4 3-6	1.68	0.20
UCM 4 3-6	12.05	1.45	SLA 5 0-9	1.44	0.17
UCM 4 0-3	0.26	0.03	SLA 6 0-3	2.13	0.26
UCSC 2	0.11	0.01	SLA 6 3-6	1.79	0.21
UCSC 1	0.12	0.01	SLA Surf	2.53	0.30
UCSB (Conc)	0.19	0.02	CMP 1 A	5.19	0.62
UCSB Pot	6.28	0.75	CMP 1 B	5.31	0.64
UCSB 3	0.74	0.09	CMP 1 D	6.05	0.73
UCSB 3 B	1.86	0.22	CMP 1 E	6.13	0.74
UCSB Soil	2.80	0.34	CMP 1 F	7.28	0.87
UCSB 6-9	2.21	0.27	CMP 1 G	7.94	0.95
SAC 1	2.22	0.27	CMP 2 Surf	4.83	0.58
SAC 2	0.57	0.07	CMP Hard	10.40	1.25
SAC 3	2.65	0.32	UCD 3 Surf	0.58	0.07
SAC 4 6-9	2.07	0.25	UCD 1	0.22	0.03
SLA MRF	3.20	0.38	UCD 3 Surf	0.64	0.08

Table B.13 – Stable isotopes of carbonate in soils in California.		
Sample	**$d^{13}C_{V\text{-}PDB}$ (‰)**	**$d^{18}O_{V\text{-}PDB}$ (‰)**
*+Calif UCSB6-9	-15.96	-8.25
*+Calif cmp 1D	-17.49	-9.77
*+Calif cmp 1E	-18.22	-9.92
*+Calif Sac 3	-18.59	-13.42
*+Calif SLA 2	-13.68	-12.24
*+Calif CMP HP	-17.21	-13.57
*+Calif CMP 1B	-17.18	-9.56
*+Calif SLA 4 0-3	-11.22	-14.53
*+Calif SLA MRF	-12.32	-11.89
*+Calif CMP 1G	-18.36	-12.54
*+Calif CMP 1F	-18.57	-10.44
*+Calif UCSB Pot	-7.95	-6.77
*+Calif CMP 1A	-16.30	-9.41
*+Calif UCM 2	-18.84	-11.47
*+Calif UCM 2B	-21.57	-12.26
*+Calif SLA3 surf	-16.68	-26.08
*+Calif ucsb 3b	-17.49	-12.89
*+Calif ucm4 3-6	-18.33	-29.85
*+Calif SLA 6 0-3	-10.89	-13.55
*+Calif UCSB Soil	-15.11	-8.32
*+Calif SAC 1	-18.03	-14.79
*+Calif SAC 1 (2)	-16.94	-12.72

B.2 Chapter 5 Data Tables

B.2.1 Untreated material XRF

Table B.14 – XRF analysis of the untreated materials.

Sample	**XRF Analysis wt%**												
	SiO_2	TiO_2	Al_2O_3	Fe_2O_3	MnO	MgO	CaO	Na_2O	K_2O	P_2O_5	SO_3	LOI	Total
OPC	26.91	0.31	7.60	3.92	0.094	2.62	53.23	0.31	0.837	0.204	2.041	1.85	99.93
Silica Fume	94.23	0.00	0.90	0.21	0.044	0.68	0.35	0.38	1.131	0.063	0.078	1.58	99.65

B.2.2 Batch weathering of Concrete

Table B.15 – Calcium content of solutions during batch weathering of concrete.

Non cumulative calcium content Na citrate sol		**Time interval (day)**								
		1	3	5	10	20	40	60	80	100
Sample	Description	mg/l	mg/l	mg/l	mg/l	mg/l	mg/l	mg/l	mg/l	mg/l
1	Dolerite + Na Cit	331	322	322.75	313.5	303.75	398.5	319.25	331	367
2	Concrete + Na Cit	745.5	826	758	572.5	289	243	293.75	323.75	375.5
3	Dolerite + Deionised	10.1	13.75	20.5	16.25	27.2	15.27	9.02	15.61	9.76
4	Concrete + Deionised	702	667.5	535.5	334.5	228.25	260	221.75	200.75	230
5	Dolerite + Na Cit	346	326.25	346.25	359.25	316.25	367.25	378	378.25	377
6	Concrete + Na Cit	703	696	671.5	654.5	356.5	315.75	329.75	321	314.5
7	Dolerite + Deionised	11.45	20.5	33	11.6	23.9	0	9.01	18.15	14.56
8	Concrete + Deionised	746.5	651.5	368.75	270.25	186	220.75	190.75	171.25	158.75
Reproducibility error		4.55	4.55	4.55	4.55	4.55	4.55	4.55	4.55	4.55

Table B.16 – pH of solution during concrete batch weathering.

Day	**0**	**1**	**3**	**5**	**10**	**20**	**40**	**60**	**80**	**100**
Average pH	11.96	12.19	12.29	12.04	11.88	11.47	11.60	11.74	11.82	11.30

Table B.17 – Carbonate content of solid during the weathering of concrete.

Sample	Substrate	t	%CaCO3
un treated	Concrete	0	0.01
T1	Concrete	1	0.32
T2	Concrete	3	0.52
T3	Concrete	5	0.84
T4	Concrete	10	5.16
T5	Concrete	20	4.80
T6	Concrete	40	5.16

Table B.18 – Calcium content of solutions during batch weathering of concrete of variable grain size.

Non cumulative calcium content Na citrate sol			**Time interval (day)**					
			1	3	7	10	15	30
Sample	Size (µm)	Description	mg/l	mg/l	mg/l	mg/l	mg/l	mg/l
1	300-600	10g Sample pH 3	664	453	351	329.5	326.5	276.5
2	63-212		397	761	518	387.5	322	254.5
3	300-600	10g Sample pH 6	966	421	275	279.5	262	226.5
4	63-212		552	544	289	297	243	248
5	300-600	10g Sample pH 7	268	434	278	192	158.5	138.5
6	63-212		670	524	333	216.5	162.5	130.5
7	300-600	10g Sample pH 3	561	417	499	334	319.5	255
8	63-212		492	476	352	365.5	343	260.5
9	300-600	10g Sample pH 6	302	417	273	264.5	245	226
10	63-212		317	396	369	272.5	259.5	236.5
11	300-600	10g Sample pH 7	603	436	240	200	157.5	136
12	63-212		631	333	286	223.5	160	148
13	Silica sand control		32.7	7.1	11.3	43.5	50.5	18.5
14			36.8	28.3	14	24.5	38.5	24
15			34.1	14.2	6	10.5	25	7.5
Reproducibility error 1-12			87.56	87.56	87.56	43.78	43.78	43.78
Reproducibility error 13-15			8.76	8.76	8.76	43.78	43.78	43.78

Table B.19 – pH of solutions during batch weathering of concrete of variable grain size.

pH	8	15	30
1	12.11	11.92	12.17
2	12.09	12.23	12.20
3	12.29	12.39	12.31
4	12.41	12.42	12.39
5	12.12	12.00	11.85
6	12.18	12.18	12.05
7	12.11	12.12	12.10
8	12.14	12.20	12.13
9	12.32	12.24	12.24
10	12.36	12.05	12.49
11	12.11	12.04	11.83
12	12.22	12.11	12.02
13	2.99	2.99	2.95
14	6.20	6.30	6.250
15	6.03	6.24	6.01

B.2.3 Batch weathering of calcium silicate hydrate gels

Table B.20 – XRF analysis of the hydrated cement pastes (untreated).

Sample	XRF Analysis wt%												
	SiO_2	TiO_2	Al_2O_3	Fe_2O_3	MnO	MgO	CaO	Na_2O	K_2O	P_2O_5	SO_3	LOI	Total
Ca/Si 0.54	60.41	0.15	4.12	1.92	0.067	1.53	21.39	0.33	0.863	0.124	1.158	8.24	100.31
Ca/Si 0.66	56.41	0.15	4.42	2.02	0.067	1.55	24.46	0.32	0.816	0.129	1.316	8.50	100.17
Ca/Si 1.03	46.64	0.19	5.33	2.48	0.072	1.82	31.45	0.28	0.676	0.144	1.539	9.45	100.06

Table B.21 – Free lime concentration of OPC and hydrated cement pastes.

Sample	WT (g)	WT Boat (g)	Total mass (g)	Initial titer (ml)	Final titer (ml)	Total titer (ml)	% Free CaO
CaO Standard	0.0501	0.0012	0.0489	6.2	16.5	10.3	100.00
OPC	0.9995	0.0039	0.9956	0.5	2.3	1.8	0.86
Ca/Si 0.54	1.0659	0.0054	1.0605	2.0	2.1	0.1	0.04
Ca/Si 0.66	1.0718	0.0019	1.0699	2.1	2.2	0.1	0.04
Ca/Si 1.03	1.0306	0.0001	1.0305	2.2	2.4	0.2	0.09

Table B.22 – Change in carbonate concentration during the weathering trials.

Sample	$\%CaCO_3$	%C
Un-weathered 0.54	2.31	0.28
Un-weathered 0.66	2.66	0.32
Un-weathered 1.03	2.88	0.35
Weathered 0.54	3.22	0.39
Weathered 0.54 D	4.33	0.52
Weathered 0.66	3.64	0.44
Weathered 0.66 D	3.46	0.42
Weathered 1.03	4.33	0.52
Weathered 1.03 D	6.27	0.75

Table B.23 – Calcium content of solutions during batch weathering of hydrated cement pastes.

calcium content in sodium citrate solution		**Time interval (h)**				
		1	2	3	4	5
Sample	Ca/Si	mg/l	mg/l	mg/l	mg/l	mg/l
1	0.54	105.00	28.00	11.50	7.95	3.2
2	0.54	98.45	25.10	12.95	8.1	4.8
3	0.66	79.90	35.75	17.00	12.00	6.8
4	0.66	94.85	24.85	16.10	10.20	6.2
5	1.03	129.60	33.20	15.85	21.65	6
6	1.03	121.50	32.35	19.70	12.75	7.15
reproducibility error		1.74	1.74	1.74	1.74	1.74

calcium content in deionised water control		**Time interval (h)**				
		1	2	3	4	5
Sample	Ca/Si	mg/l	mg/l	mg/l	mg/l	mg/l
7	0.54	10.25	10.35	9.65	7.50	7.15
8	0.54	11.85	10.25	9.70	8.50	6.40
9	0.66	13.05	10.80	10.00	9.85	7.25
10	0.66	11.55	10.45	8.15	9.55	7.75
11	1.03	17.80	9.95	12.05	10.30	8.65
12	1.03	16.60	13.60	10.90	10.05	8.40
reproducibility error		1.74	1.74	1.74	1.74	1.74

Table B.24 – pH of solutions during batch weathering of hydrated cement pastes.

For Na citrate solution

	0	**1**	**2**	**3**	**4**	**5**
1	5.07	5.53	5.07	5.14	5.07	5.00
2	5.13	5.66	5.10	5.13	5.02	5.01
3	5.11	5.56	5.18	5.17	5.10	5.09
4	5.05	5.57	5.13	5.15	5.09	5.03
5	5.06	5.59	5.18	5.17	5.09	5.00
6	5.00	5.59	5.19	5.18	5.05	5.05

For Deionised water

	0	**1**	**2**	**3**	**4**	**5**
7		10.02	9.65	9.7	9.7	9.79
8		9.95	9.92	9.71	9.83	9.77
9		10.15	9.99	9.88	9.94	9.88
10		10.03	9.97	9.82	9.88	9.83
11		10.51	10.18	10.3	10.31	9.95
12		10.41	10.28	10.24	10.24	9.94

Table B.25 – Calcium content of solutions during 33 minute batch weathering of hydrated cement paste.					
Non cumulative calcium content		**Time interval (min)**			
		8	16	24	33
Sample	Ca/Si	mg/l	mg/l	mg/l	mg/l
1	0.54	120.35	54.70	32.30	40.90
2	0.54	113.75	55.40	36.50	35.30
3	0.66	133.40	73.50	24.55	53.75
4	0.66	93.50	41.45	38.40	37.60
5	1.03	63.60	47.25	42.95	45.90
6	1.03	64.20	40.65	39.95	38.00
reproducibility error		6.75	6.75	6.75	6.75

Table B.26 – pH of solution during 33 minute batch weathering of hydrated cement pastes.				
	8	**16**	**24**	**33**
1	5.59	5.25	5.24	5.2
2	5.36	5.23	5.15	5.19
3	5.71	5.33	5.23	5.27
4	5.46	5.24	5.25	5.18
5	5.33	5.3	5.23	5.27
6	5.28	5.26	5.26	5.23

B.3 Chapter 6 Data Tables

B.3.1 Solid organic and inorganic carbon content

Table B.27 – Carbonate concentration in untreated soil and post microcosm experiments			
	Experiment A %$CaCO_3$	**Experiment B %$CaCO_3$**	**Average %$CaCO_3$**
Untreated soil	-	-	72.30
1	72.98	65.87	69.43
2	71.77	64.90	68.34
4	73.46	63.38	68.42
5	69.21	64.63	66.92
7	68.48	70.97	69.72
8	69.40	63.31	66.36
10	67.31	64.13	65.72
11	64.14	62.58	63.36

Table B.28 – Total organic carbon concentrations in un-treated and treated solids.			
Sample ID	**TOC wt%**	**Sample ID**	**TOC wt%**
untreated	5.01	C1	4.03
A1	2.33	C2	3.37
A2	2.05	D1	5.22
A4	7.85	D2	5.20
A5	2.60	D3	4.77
A7	2.68	D4	5.45
A8	3.38	D5	4.47
A10	2.60	D6	4.53
A11	3.58	D7	4.69
B1	3.74	D8	5.41
B2	3.56	GardenTS1	9.87
B4	3.73	GardenTS 2	10.39
B5	5.15	GardenTS 4	9.14
B7	4.80	GardenTS 5	9.42
B8	2.37	GardenTS 7	12.14
B10	0.39	GardenTS 8	10.38
B11	2.86	GardenTS 10	10.01
		GardenTS 11	8.5

B.3.2 Microcosm trials

Table B.29 – Carbon concentration of solution in microcosm trial A.						
	Time (h) TOC mg l^{-1}			**Time (h) TIC mg l^{-1}**		
	24	48	168	24	48	168
1	238.70	245.10	273.50	5.75	4.80	5.05
2	226.20	241.20	250.90	4.29	13.03	3.70
3	224.70	227.60	225.40	11.78	5.40	8.24
4	232.50	206.10	112.80	34.15	49.83	115.40
5	234.30	245.50	256.20	23.27	25.08	26.33
6	233.30	236.90	240.90	1.81	0.00	0.93
7	37.48	52.79	50.54	14.79	11.79	10.56
8	23.96	35.00	59.37	1.12	1.40	4.15
9	8.67	7.97	7.11	1.79	2.88	2.22
10	23.34	25.43	33.20	8.60	13.41	22.69
11	19.88	21.81	33.50	9.73	10.44	10.96
12	7.51	6.36	5.50	0.89	2.53	1.09

Table B.30 – Carbon concentration of solution in microcosm trial B.						
	Time (h) TOC mg l^{-1}			**Time (h) TIC mg l^{-1}**		
	24	48	168	24	48	168
1	227.10	252.00	279.40	19.79	16.50	7.37
2	231.10	237.50	258.40	23.04	14.33	7.74
3	232.20	238.20	237.60	19.00	12.49	10.51
4	160.70	140.10	77.90	25.69	42.24	99.90
5	159.20	167.20	173.30	17.69	18.21	21.31
6	153.20	151.60	156.80	0.00	0.00	11.61
7	37.62	50.17	70.46	5.33	4.49	6.47
8	19.71	22.98	34.70	7.55	5.32	5.71
9	10.54	9.75	8.31	3.22	2.54	3.24
10	22.32	30.96	36.29	10.66	15.66	26.17
11	17.33	23.05	32.99	12.35	13.70	16.01
12	8.88	7.85	7.46	0.00	0.00	0.00

Table B.31 – Carbon concentration of solution in microcosm trial C in mg l^{-1}.						
	Time (h)					
TOC	0	24	96	168	240	336
1	240.00	153.50	95.62	46.40	46.60	49.90
2	240.00	153.20	109.60	43.10	44.40	45.30
TIC		24.00	48.00	168.00	240.00	336.00
1		34.35	78.48	112.90	103.50	102.50
2		34.74	70.27	109.10	96.50	104.50

Table B.32 – Carbon concentration of solution in microcosm trial D.						
	Time (h) TOC mg l^{-1}			**Time (h) TIC mg l^{-1}**		
	24	48	168	24	48	168
1	214.60	199.51	118.85	0.00	7.09	64.05
2	210.45	198.30	114.08	2.36	6.60	66.92
3	338.55	344.44	236.67	11.95	16.36	88.43
4	366.17	380.95	273.99	13.83	16.95	77.91
5	193.16	215.09	180.53	12.34	18.61	35.97
6	258.39	305.30	180.53	8.62	18.10	35.97
7	139.46	108.10	86.37	18.34	24.40	70.63
8	145.74	110.83	82.62	19.36	33.17	83.28

Table B.33 – pH of microcosm experiments.

		Time (h)						Time (h)			
		0	24	48	168			0	24	48	168
Experiment A	1	11.47	11.01	11.49	11.16	**Garden Topsoil**	1	11.41	11.00	10.41	9.36
	2	11.60	11.01	10.77	10.46		2	11.67	11.05	10.18	9.33
	3	11.69	11.62	11.60	11.61		3	11.34	11.54	11.57	11.69
	4	6.13	7.24	7.44	7.03		4	5.01	6.36	6.77	6.88
	5	6.00	7.34	7.95	7.86		5	4.85	4.90	5.20	5.44
	6	5.11	5.29	5.29	5.31		6	4.78	5.17	5.17	5.24
	7	11.40	11.07	10.70	9.60		7	11.44	11.08	10.56	9.51
	8	11.88	11.68	11.63	11.63		8	11.36	9.82	8.54	8.07
	9	11.51	11.52	11.47	11.52		9	11.51	11.59	11.65	11.08
	10	8.08	7.97	8.04	7.60		10	5.75	7.06	6.98	7.00
	11	7.03	7.59	7.94	7.84		11	5.25	5.62	5.60	5.44
	12	5.82	5.90	4.25	6.31		12	4.92	5.12	5.37	5.87
Experiment B	1	11.61	12.13	12.09	11.99	**Experiment D**	1	4.71	5.30	6.13	6.65
	2	11.55	11.87	11.53	11.63		2	4.76	5.31	6.15	6.71
	3	11.96	12.15	11.95	12.13		3	11.51	10.36	8.24	7.30
	4	5.88	7.40	7.40	7.20		4	11.54	10.35	8.53	7.35
	5	5.63	7.35	7.83	7.94		5	11.53	10.68	8.77	7.25
	6	4.85	5.15	5.16	5.16		6	11.66	11.25	10.21	7.40
	7	11.82	11.60	11.41	11.26		7	4.77	6.36	6.64	6.82
	8	11.46	11.90	9.73	9.32		8	4.78	6.39	6.65	6.82
	9	11.65	10.49	11.83	11.87						
	10	8.15	8.00	7.94	7.69						
	11	6.80	7.55	7.69	7.93						
	12	5.01	5.93	5.43	5.21						

Table B.34 – Carbon concentration of solution in microcosm trial using garden topsoil.

	Time (h) TOC mg l^{-1}			Time (h) TIC mg l^{-1}		
	24	48	168	24	48	168
1	230.35	252.13	286.07	10.25	11.87	12.63
2	185.54	194.64	213.51	13.06	10.66	7.99
3	206.80	207.13	205.81	5.30	15.47	4.59
4	137.77	99.21	43.10	7.03	28.49	66.60
5	141.43	144.70	147.10	3.37	0.00	0.00
6	167.60	151.40	151.09	4.70	0.00	1.01
7	52.97	79.61	99.33	4.18	13.96	18.57
8	23.68	24.08	31.77	13.85	8.13	8.82
9	10.16	12.09	8.68	5.62	3.63	1.19
10	14.32	18.08	23.74	6.03	7.87	18.6
11	13.53	17.06	21.04	0.00	0.09	0.78
12	9.85	6.57	7.07	0.00	0.00	2.52

B.3.2 Growth experiment

Table B.35 – Chlorophyll content of willow growth trials.									
	2009					**2010**			
	26 August	09 September	17 September	25 September	12 November	26 May	24 June	07 July	19 July
Concrete treated	22.80	13.00	14.20	11.30	10.40	11.60	9.40	7.50	7.80
	18.80	13.90	23.30	12.70	2.00	9.50	8.30	5.80	11.30
	17.40	17.80	20.30	13.50	9.30	10.20	10.40	14.50	8.40
	22.30	19.60	21.20	22.10	9.30	9.80	10.10	10.00	9.40
	17.60	12.90	21.30	20.10	6.30	9.90	13.70	9.60	7.90
Average	19.78	15.44	20.06	15.94	7.46	10.20	10.38	9.48	8.96
sd	2.59	3.07	3.45	4.83	3.41	0.82	2.02	3.28	1.45
Control	8.30	13.00	18.70	15.10	13.30	17.30	16.10	18.70	16.00
	7.80	17.50	15.60	8.80	6.50	17.50	15.40	19.20	19.90
	14.10	11.60	9.80	26.20	2.70	22.20	17.40	12.00	26.50
	17.40	8.10	23.00	10.50	14.10	16.00	12.60	26.60	21.00
	16.90	17.60	17.40	8.20	5.80	24.90	18.10	25.70	21.90
Average	12.90	13.56	16.90	13.76	8.48	19.58	15.92	20.44	21.06
sd	4.61	4.06	4.82	7.46	4.98	3.79	2.14	5.95	3.78

Appendix C

Appendix C – Chapter 6 calculations

C.1 Chemical flux data from field sites

Using chemical flux data (Tables C.1 – C.3) from a number of field investigations (Moulton et al., 2000; Oliva et al., 2003; Dessert et al., 2003)* the weathering rate (r), expressed as mol m^{-2} sec^{-1}, can be calculated using Equation C.1.

*Moulton, K. L., West, J. and Berner, R. A. (2000) 'Solute flux and mineral mass balance approaches to the quantification of plant effects on silicate weathering', *American Journal of Science,* 300, (7), pp. 539-570.
Oliva, P., Viers, J. and Dupré, B. (2003) 'Chemical weathering in granitic environments', *Chemical Geology,* 202, (3-4), pp. 225-256.
Dessert, C., Dupré, B., Gaillardet, J., Francois, L. M. and Allegre, C. J. (2003) 'Basalt weathering laws and the impact of basalt weathering on the global carbon cycle', *Chemical Geology,* 202, (3-4), pp. 257-273.

Equation C.1: $$r = Log\left(\frac{M}{3.1536\times10^{6}\cdot S}\right)$$

where M is the solute flux in mol ha^{-1} a^{-1}, and S is the surface area in m^2 ha^{-1}.

Table C.1 – Chemical flux data from Moulton et al. (2000), assuming 1000-10000 cm^2 g^{-1} mineral surface area and 1800-2500 kg m^{-3} soil density.

	Weathering rate (mol ha^{-1} a^{-1})						**Log rate (mol m^{-2} sec^{-1})**			
Vegetation	HCO_3^-	Na^+	Mg^{2+}	Ca^{2+}	ΣCations	Si	Cations upper estimate	Cations lower estimate	Si upper estimate	Si lower estimate
Bare soil	353	138	49	127	314	320	-14.26	-15.88	-15.87	-15.87
Bare, no soil	362	109	39	96	244	287	-14.37	-15.99	-15.92	-15.92
S. Birch	911	109	158	268	535	646	-14.03	-15.65	-15.56	-15.56
N. Birch	985	158	162	231	551	679	-14.01	-15.63	-15.54	-15.54
Conifer	999	217	157	242	616	756	-13.96	-15.58	-15.50	-15.50

Table C.2 – Chemical flux data from Oliva et al. (2003) assuming 1000-10000 cm^2 g^{-1} mineral surface area and 1800-2500 kg m^{-3} soil density.					
Weathering rate (mol ha^{-1} a^{-1})		**Log rate (mol m^{-2} sec^{-1})**			
Cations	Si	Cations upper estimate	Cations lower estimate	Si upper estimate	Si lower estimate
7552	8066	-12.88	-15.50	-12.85	-15.47
6021	3875	-12.97	-15.59	-13.17	-15.79
5544	3175	-13.01	-15.63	-13.25	-15.87
3681	1384	-13.19	-15.81	-13.61	-16.23
3554	2433	-13.20	-15.82	-13.37	-15.99
2773	2019	-13.31	-15.93	-13.45	-16.07
2631	1683	-13.33	-15.95	-13.53	-16.15
2568	1411	-13.34	-15.96	-13.60	-16.22
2563	1284	-13.35	-15.97	-13.65	-16.27
2437	960	-13.37	-15.99	-13.77	-16.39
2110	2580	-13.43	-16.05	-13.34	-15.96
2079	1403	-13.44	-16.06	-13.61	-16.23
1992	1617	-13.45	-16.07	-13.55	-16.17
1942		-13.47	-16.09		
1800	1139	-13.50	-16.12	-13.70	-16.32
1787	380	-13.50	-16.12	-14.17	-16.79
1714	1534	-13.52	-16.14	-13.57	-16.19
1674	1489	-13.53	-16.15	-13.58	-16.20
1512	1004	-13.57	-16.19	-13.75	-16.37
1469	1539	-13.59	-16.21	-13.57	-16.19
1404	816	-13.61	-16.23	-13.84	-16.46
1354	1255	-13.62	-16.24	-13.66	-16.28
1233	217	-13.66	-16.28	-14.42	-17.04
1230		-13.66	-16.28		
1174	1189	-13.68	-16.30	-13.68	-16.30
1146	1624	-13.69	-16.31	-13.54	-16.16
1091	171	-13.72	-16.34	-14.52	-17.14
1089	930	-13.72	-16.34	-13.79	-16.41
1049		-13.73	-16.35		
1018		-13.75	-16.37		
958		-13.77	-16.39		
945		-13.78	-16.40		
922	665	-13.79	-16.41	-13.93	-16.55
907	728	-13.80	-16.42	-13.89	-16.51
877	763	-13.81	-16.43	-13.87	-16.49
863		-13.82	-16.44		
831	515	-13.83	-16.45	-14.04	-16.66

Table C.2 – Chemical flux data from Oliva et al. (2003) assuming 1000-10000 cm^2 g^{-1} mineral surface area and 1800-2500 kg m^{-3} soil density.					
Weathering rate (mol ha^{-1} a^{-1})		**Log rate (mol m^{-2} sec^{-1})**			
815	989	-13.84	-16.46	-13.76	-16.38
793	820	-13.85	-16.47	-13.84	-16.46
780		-13.86	-16.48		
772	486	-13.87	-16.49	-14.07	-16.69
754	700	-13.88	-16.50	-13.91	-16.53
730	485	-13.89	-16.51	-14.07	-16.69
700	909	-13.91	-16.53	-13.80	-16.42
669	1330	-13.93	-16.55	-13.63	-16.25
635	590	-13.95	-16.57	-13.98	-16.60
635	401	-13.95	-16.57	-14.15	-16.77
630	730	-13.95	-16.57	-13.89	-16.51
629		-13.96	-16.58		
625	208	-13.96	-16.58	-14.44	-17.06
613		-13.97	-16.59		
596		-13.98	-16.60		
580	659	-13.99	-16.61	-13.94	-16.55
574	1287	-14.00	-16.61	-13.64	-16.26
565	942	-14.00	-16.62	-13.78	-16.40
546	387	-14.02	-16.64	-14.17	-16.79
511		-14.05	-16.67		
505	199	-14.05	-16.67	-14.46	-17.08
477	557	-14.08	-16.70	-14.01	-16.63
471		-14.08	-16.70		
464	849	-14.09	-16.71	-13.83	-16.44
425	676	-14.13	-16.75	-13.92	-16.54
423		-14.13	-16.75		
397		-14.16	-16.78		
377	24	-14.18	-16.80	-15.37	-17.99
376	837	-14.18	-16.80	-13.83	-16.45
365		-14.19	-16.81		
340	552	-14.22	-16.84	-14.01	-16.63
334		-14.23	-16.85		
317	4	-14.25	-16.87	-16.15	-18.77
314	668	-14.26	-16.88	-13.93	-16.55
292	530	-14.29	-16.91	-14.03	-16.65
286		-14.30	-16.92		
283	233	-14.30	-16.92	-14.39	-17.01
277	313	-14.31	-16.93	-14.26	-16.88
274	409	-14.32	-16.94	-14.14	-16.76
271		-14.32	-16.94		

Table C.2 – Chemical flux data from Oliva et al. (2003) assuming 1000-10000 cm^2 g^{-1} mineral surface area and 1800-2500 kg m^{-3} soil density.					
Weathering rate (mol ha^{-1} a^{-1})		**Log rate (mol m^{-2} sec^{-1})**			
268	479	-14.33	-16.95	-14.07	-16.69
268		-14.33	-16.95		
267		-14.33	-16.95		
263		-14.33	-16.95		
258		-14.34	-16.96		
258	615	-14.34	-16.96	-13.97	-16.58
257	154	-14.34	-16.96	-14.57	-17.19
253	392	-14.35	-16.97	-14.16	-16.78
224	506	-14.40	-17.02	-14.05	-16.67
218	222	-14.42	-17.04	-14.41	-17.03
216	201	-14.42	-17.04	-14.45	-17.07
174		-14.51	-17.13		
166	632	-14.53	-17.15	-13.95	-16.57
145	141	-14.59	-17.21	-14.60	-17.22
120	411	-14.67	-17.29	-14.14	-16.76
111	321	-14.71	-17.33	-14.25	-16.87
101		-14.75	-17.37		
84	177	-14.83	-17.45	-14.51	-17.13
34	243	-15.22	-17.84	-14.37	-16.99
	1270			-13.65	-16.27

Table C.3 – Chemical flux data from Dessert et al. (2003) assuming 1000-10000 cm^2 g^{-1} mineral surface area and 1800-2500 kg m^{-3} soil density.

	Weathering rate (t km^{-2} a^{-1})	**Log rate (mol m^{-2} sec^{-1})**	
	Cations	Cations upper estimate	Cations lower estimate
Columbian Plateau	7.7	-13.81	-15.43
Deccan Traps	25.1	-13.29	-14.91
Hawii	11.9	-13.62	-15.24
Iceland	17.7	-13.45	-15.07
Iceland 2	20.9	-13.37	-14.99
Java	152	-12.51	-14.13
M Central	5.6	-13.95	-15.57
M Central 2	5.9	-13.92	-15.54
Parana Traps	20.6	-13.38	-15.00
Le Reunion	48.4	-13.01	-14.63
Sao Miguel	13.3	-13.57	-15.19

C.2 Percentage of calcium weathered into solution

To estimate the percentage of calcium leached from the material, the cumulative calcium concentration (mg l^{-1}) is calculated through summation of calcium concentrations taken at each sample interval (t; Equation C.2).

Equation C.2: $$[Ca^{2+}]_c = [Ca^{2+}]_0 + [Ca^{2+}]_{0+t} + [Ca^{2+}]_{0+2t} + \cdots + [Ca^{2+}]_{jt}$$

where 0 is time = 0, and j is the total length of the experiment. Using this, the calcium leached out of the material as a % of the calcium in the material can be calculated (Equation C.3).

Equation C.3: $$\%Ca\ leached = \frac{100 \cdot [Ca^{2+}]_c \cdot V_l}{7.14 \cdot M_s \cdot \%CaO}$$

where V_l is the volume of solution in l, M_s is the mass of the solid in mg and %CaO is the is the quantity of calcium in the material expressed as lime.

C.3 Weathered layer depth

If y is the depth of the weathered layer for a particle with Φ diameter, and an un-weathered inner core of x diameter, then:

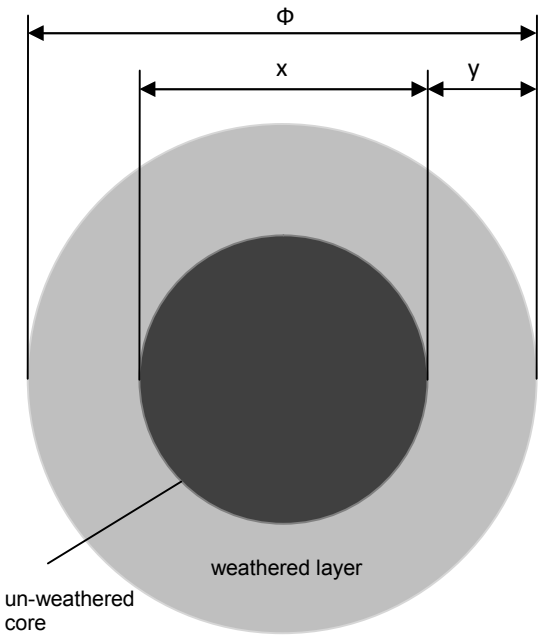

Figure C.1 – Conceptual diagram of a weathered layer

Equation C.4: $\emptyset = x + 2y$

Equation C.5: $V_t = 4\pi\left(\frac{\emptyset}{2}\right)^3$

Equation C.6: $V_x = 4\pi\left(\frac{x}{2}\right)^3$

Equation C.7: $V_y = 4\pi\left(\left(\frac{\emptyset}{2}\right)^3 - \left(\frac{x}{2}\right)^3\right)$

Where V_t, V_x and V_y are the total volume, core and weathered layer volumes respectively.

Assuming that the calcium content recorded in solution [Ca] is the product of the weathered layer:

Equation C.8: $[Ca] = Vy \cdot \rho_s \cdot Ca_p$

Where ρ_s is the density of the solid and Ca_p is the proportion of calcium in the material. The weathering layer (y) can be calculated by combining Equations C.4, C.7 and C.8 (Equation C.9)

Equation C.9: $$y = \frac{\emptyset - 2\cdot\sqrt[3]{\left(\frac{\emptyset}{2}\right)^3 - \frac{[Ca]}{\rho_s \cdot Ca_p \cdot 4\pi}}}{2}$$

If the particle diameter is normally distributed between the two sieve aperture size (i, j), then y can be calculated for each size fraction to estimate an average weathered layer depth (y_a; Equation C.10).

Equation C.10: $$y_a = \sum_{i<\emptyset<j}\left[\frac{f(y)_i}{n}\right]\left[\frac{f(y)_{i+1}}{n}\right]\left[\frac{f(y)_{i+2}}{n}\right]\ldots\left[\frac{f(y)_j}{n}\right]$$

where n is the number of size fractions.

For the experiment in section 6.5.3, using a size fraction of 150 μm < Φ <212 μm, assuming a solid density of 1800 kg m^{-3} and the values in Table C.4, the maximum and minimum weathered layer depths were 11.96 μm and 16.68 μm respectively and y_a = 14.32 μm.

Table C.4 – Variables from experiment.					
Sample	**Ca/Si**	**Weathered Ca (kg)**	**Ca Ratio**	**Total (g)**	**Total Vy (m3)**
1	0.54	3.09E-05	0.21	0.2025	$8.04x10^{-8}$
2	0.54	3.19E-05	0.21	0.2085	$8.27x10^{-8}$
3	0.66	3.57E-05	0.24	0.2045	$8.12x10^{-8}$
4	0.66	3.53E-05	0.24	0.2020	$8.02x10^{-8}$
5	1.03	4.51E-05	0.31	0.2010	$7.98x10^{-8}$
6	1.03	4.63E-05	0.31	0.2060	$8.17x10^{-8}$

Appendix D

Appendix D. Organic acid speciation

D.1 Introduction

There are multiple pathways for carbon transfer from plant to soil (root respiration, decaying biomass, sloughing off cells etc). However, the exudation of low molecular weight organic acid from plant roots is considered an important mechanism in this system (Kuzyakov and Domanski, 2000; Chapter 7). Organic acids are oxidised chemically or by microorganisms through the Krebs cycle producing a range of low molecular weight organic compounds (citrate, malate, fumerate etc), water and CO_2. Quantification and turnover rate of organic acids in the environment is an emergent field of study, which has direct implications for global carbon cycle modelling and nutrient plant dynamics (Jones et al., 2003; Ryan et al., 2001).

Exudation of organic acids (and protons) into the soil is a nutrient acquisition mechanism used by plants particularly on poor or high pH soils, by lowing pH and forming organic complexes with metals (Ca, Mn, Zn etc; Jones et al., 2003). Research has investigated the dynamics of organic acids on calcareous soils (pH <8.5; Strom et al., 2005; Strom et al., 2001). Understandably, research has yet to investigate breakdown in high pH soils (pH >10.5) given the usual range of natural soils (pH 6-8). However, recent research at Newcastle University has justified the case for high pH organic acid degradation research as part of work investigating how soils can be engineered to capture carbon.

Recent results (discussed in Chapter 4) suggest that brownfield soils in urban environments act as substantial carbon sinks storing more carbon than most natural soils (20-30 kgC m^{-2}; Renforth et al., 2009). Dissolution of calcium hydroxide in solution buffers the pH to >11 which favours the precipitation of calcium carbonate provided the components of calcium carbonate (calcium and dissolved carbon dioxide) are available. With this in mind, it is important to investigate the contribution of degraded organic acids to the dissolved carbon dioxide pool, as a consequence of their decomposition (see Chapter 7).

Results in Chapter 7 suggest that bulk dissolved organic carbon pool is relatively stable in high pH solutions. Repeat microcosm experiments were conducted to investigate whether there is any detectable molecular

transformation of the dissolved organic carbon content. The experimental matrix used in this study is identical to the high pH trials presented in Chapter 7, Section 7.5.1, but the initial citrate concentration (10 mmol l^{-1}) was increased to facilitate detection of proportionately small transformations (Table D.1). Aliquots were taken after 0, 12 and 24 hours for organic acid speciation. The bulk solution was analysed for organic carbon after 24 hours.

Table D.1 – Experimental matrix for organic acid speciation microcosm trial. Note the missing numbers represent various trials where the data is not presented below or used for interpretation.

Material	Sodium citrate+ Calcium hydroxide	Deionised water + Calcium hydroxide	Sodium citrate	Deionised water
Un-treated soil	1	8	15	22
Sterilised soil	3	10	17	24
No material control	7	14	21	28

D.3 Analysis method

Organic carbon and inorganic carbon was analysed using a Shimadzu TOC5050A Total Carbon Analyser (Appendix A.11). 1 ml splits of the aliquots were diluted with 0.5 mol l^{-1} octane sulphonic acid, sonicated for 40 minutes and analysed for acetate using a Dionex ISC-1000 at (Newcastle University) fitted with an IonPac® ICE-AS1 column. Organic acids were measured using liquid chromatography couple with quadrapole mass spectrometry (LC-MS/MS; Mid Sweden University, Sweden- Plate D.1) as described in Bylund et al. (2007).

Plate D.1 – LC/MS system at Mid Sweden University (A) Liquid chromatographer - Shimadzu LC-10AD pump and Agilent 1100 autoinjector (B) Supelcogel C610-H column (C) API3000 mass spectrometer

D.4 Results and discussion

D.4.1 Total dissolved organic and inorganic carbon

Dissolved organic carbon varied between 0 and 872 mg l^{-1} (Table D.2). Both control experiments with deionised water have relatively low organic carbon concentrations suggesting that pre-existing organic carbon in the soil did not dissolve into solution. The sodium citrate solution dosed with calcium hydroxide had an organic carbon concentration approximately 300 mg l^{-1} less than the un-treated solution (Figure D.1). This is possibly an artefact of calcium citrate solubility (precipitation of calcium citrate buffered the organic carbon content to ~500 mg l^{-1}).

Table D.2 – Total dissolved organic and inorganic carbon from microcosm trial at 24 hours.		
	TIC (mg l^{-1})	**TOC (mg l^{-1})**
1	7.748	565.1
3	6.849	508.3
7	4.559	338.3
8	4.804	115.6
10	2.374	72.31
14	1.332	0
15	5.509	855.6
17	8.321	808.2
21	3.789	872.6
22	16.52	28.81
24	16.5	13.56
28	0	9.634

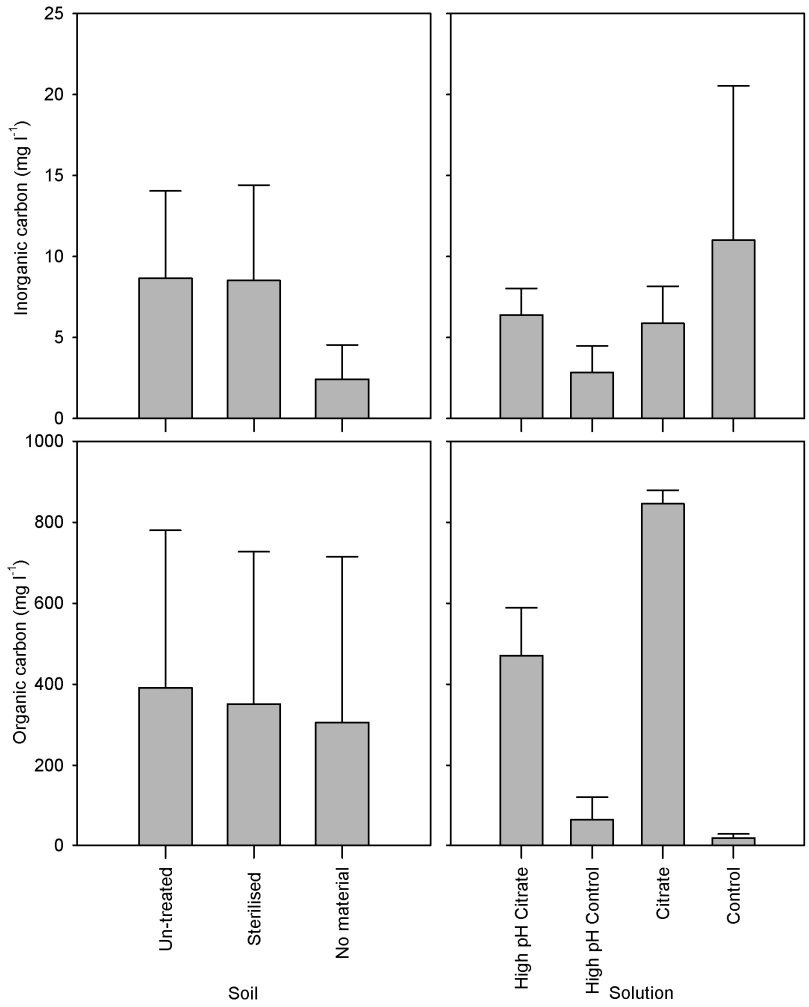

Figure D.1 – Total dissolved organic and inorganic carbon in microcosm trial. Note the error bars represent the standard deviation of values (the effect of varying solution treatment on each substrate).

D.4.2 Acetate concentration

Acetate concentration ranged from 0 – 27.1 mg l^{-1} with no systematic variation between treatments.

D.4.3 Low molecular weight organic acids

Besides the expected large citrate concentration, organic acid concentration was low (Table D.3). The consistently high citrate concentration in all of the trials and the potential of calcium citrate precipitation (above) suggests that citrate was buffered to approximately ~600-3000 µmol l^{-1} (although there is an apparent discontinuity between the total dissolved organic carbon content and the sum of carbon content of the organic acids). All solutions mix with soil demonstrated small increases in pyruvate, lactate, oxalate and succinate concentration, which was possibly leached from the soil.

*Table D.3 – Data from LC-MS/MS analysis (concentrations are in µmol l^{-1})*Acetate was determined from liquid chromatography at Newcastle University.*

Sample Name	Acetate*	pyruvate	lactate	oxalate	malonate	maleate	succinate	citraconate	glutarate	malate	ketoglutarate	tartrate	c-aconitate	shikimate	citrate	isocitrate	fumarate	trans-aconitate
PBR61 T0	-	0.53	2.39	0.74	0.00	0.08	0.83	0.02	0.07	0.61	0.04	0.00	0.06	0.00	604.4	0.23	0.00	0.03
PRB61 T12	-	2.98	4.40	4.25	0.00	0.07	1.96	0.02	0.14	1.22	0.09	0.00	0.06	0.07	529.4	0.48	0.18	0.05
PRB61 T24	20.4	4.12	8.11	1.19	0.00	0.13	2.44	0.03	0.17	2.22	0.17	0.00	0.11	0.07	486.5	0.75	0.23	0.07
PBR63 T0	-	0.95	2.97	0.72	0.00	0.06	0.76	0.02	0.07	0.54	0.04	0.00	0.02	0.00	647.3	0.16	0.00	0.02
PRB63 T12	-	3.97	3.80	11.66	0.00	0.09	1.73	0.01	0.12	1.37	0.12	0.00	0.05	0.06	621.9	0.43	0.16	0.05
PRB63 T24	-	5.11	5.17	36.47	0.00	0.10	2.05	0.02	0.14	1.81	0.17	0.00	0.08	0.06	572.3	0.56	0.21	0.06
PRB67 T0	-	2.03	2.20	9.88	0.00	0.14	1.24	0.09	0.63	0.78	0.09	0.00	0.05	0.00	627.5	0.45	0.06	0.05
PRB67 T12	-	0.00	1.62	0.98	0.00	0.04	0.17	0.01	0.03	0.40	0.03	0.00	0.01	0.00	605.2	0.14	0.00	0.01
PRB67 T24	26.8	0.68	1.48	0.13	0.00	0.06	0.18	0.01	0.03	0.51	0.03	0.06	0.01	0.00	535.5	0.11	0.00	0.01
PRB68 T0	-	0.80	1.53	0.18	0.24	0.06	0.63	0.02	0.06	0.07	0.04	0.02	0.05	0.00	2.23	0.00	0.02	0.01
PBR68 T12	1.6	1.75	5.09	6.24	1.69	0.07	1.80	0.02	0.12	0.43	0.06	0.00	0.04	0.05	1.25	0.00	0.15	0.02
PRB68 T24	19.2	5.09	6.84	97.07	3.64	0.10	2.35	0.03	0.17	1.08	0.15	0.04	0.07	0.06	2.23	0.07	0.27	0.03
PRB610 T0	-	0.63	1.27	0.12	0.15	0.05	0.56	0.01	0.04	0.08	0.04	0.00	0.01	0.00	0.11	0.00	0.04	0.00
PRB610 T12	-	4.32	3.54	12.23	1.55	0.07	1.77	0.02	0.13	0.47	0.11	0.02	0.03	0.05	0.58	0.05	0.18	0.02
PBR610 T24	24.7	3.57	6.49	10.01	2.11	0.09	1.95	0.03	0.14	0.73	0.10	0.01	0.03	0.00	3.12	0.03	0.25	0.03
PRB614 T0	-	0.79	1.54	0.69	0.09	0.09	0.22	0.02	0.05	0.10	0.03	0.02	0.03	0.00	1.70	0.01	0.00	0.01
PRB614 T12	-	0.72	2.26	0.47	0.06	0.03	0.12	0.01	0.03	0.04	0.02	0.01	0.01	0.00	0.62	0.00	0.00	0.00
PRB614 T24	-	0.97	1.76	0.25	0.14	0.14	0.25	0.01	0.05	0.15	0.03	0.05	0.01	0.00	3.74	0.00	0.00	0.00
PRB615 T0	-	2.94	0.79	0.22	0.00	0.09	0.16	0.00	0.01	0.33	0.05	0.00	0.03	0.00	3223.24	0.09	0.56	0.00
PRB615 T12	-	99.86	1.08	1.50	0.00	0.06	1.05	0.00	0.27	0.51	153.54	0.00	2.04	0.00	2131.29	0.18	0.12	1.63
PRB615 T24	-	51.39	2.20	38.76	0.00	0.05	1.33	0.00	0.08	0.76	0.32	0.00	0.77	0.00	3065.37	0.86	6.88	0.00
PRB617 T0	-	2.90	1.08	1.55	0.00	0.10	0.51	0.00	0.19	0.61	0.06	0.00	0.02	0.00	2854.87	0.14	0.00	0.00
PRB617 T12	-	17.75	1.15	0.00	0.00	0.04	0.28	0.00	0.01	0.63	0.15	0.00	0.07	0.00	2539.13	0.22	0.08	0.00
PBR617 T24	-	27.51	1.91	3.33	0.00	0.06	0.38	0.00	0.02	0.41	0.31	0.00	0.13	0.00	2604.91	0.19	0.13	0.00
PRB621 T0	-	0.63	1.12	0.40	0.00	0.03	0.08	0.00	0.02	0.39	0.01	0.00	0.00	0.00	3094.07	0.10	0.00	0.00
PRB621 T12	-	1.33	0.96	0.26	0.00	0.03	0.07	0.00	0.01	0.27	0.03	0.00	0.01	0.00	3108.13	0.00	0.00	0.00
PRB621 T24	-	1.83	1.26	0.39	0.00	0.06	0.11	0.00	0.01	0.49	0.01	0.00	0.01	0.00	3515.99	0.14	0.00	0.00
PRB622 T0	-	0.00	0.50	0.29	0.06	0.04	0.08	0.01	0.02	0.06	0.06	0.03	0.02	0.00	12.64	0.00	0.00	0.00
PRB622 T12	-	0.05	0.38	1.39	0.03	0.07	0.01	0.01	0.02	0.01	0.03	0.02	0.02	0.00	0.00	0.00	0.00	0.00
PRB622 T24	-	0.00	0.00	0.12	0.00	0.01	0.00	0.00	0.00	0.00	0.00	0.00	0.02	0.00	0.00	0.00	0.00	0.00
PRB624 T0	-	3.40	1.27	24.24	0.54	0.06	0.19	0.02	0.03	0.54	0.09	0.00	0.03	0.00	274.66	0.35	0.00	0.01
PRB624 T12	-	5.35	2.16	16.65	0.83	0.07	0.43	0.02	0.04	0.64	0.16	0.05	0.05	0.00	4.03	0.18	0.00	0.02
PRB624 T24	-	9.97	3.81	9.32	1.44	0.09	0.76	0.03	0.07	0.67	0.24	0.04	0.07	0.00	1.01	0.18	0.14	0.03
PRB628 T0	-	0.47	0.77	1.14	0.08	0.05	0.12	0.01	0.02	0.08	0.02	0.05	0.01	0.00	13.55	0.00	0.00	0.00
PRB628 T12	-	0.29	0.99	0.07	0.12	0.04	0.08	0.01	0.01	0.06	0.00	0.05	0.00	0.00	20.70	0.00	0.00	0.00
PRB628 T24	-	0.26	0.57	1.75	0.19	0.04	0.03	0.00	0.01	0.06	0.00	0.10	0.02	0.00	132.78	0.00	0.00	0.01

D.5 Conclusion

In Chapter 7 the stability of bulk organic carbon in high pH solutions was demonstrated. The experiment presented here confirms that there is no molecular transformation of this organic carbon, which remains primarily citrate. Small concentrations of other organic acids were detected, which are primarily leached from the substrate.

Discrepancies were detected between the bulk organic carbon content of the solutions dosed with calcium hydroxide and the control. This is possibly an artefact of calcium-citrate solubility, and not organic carbon degradation.

Additional work in this area is discussed in Chapter 7 and 8.

D.6 Appendix D references

Bylund, D., Norström, S. H., Essén, S. A. and Lundström, U. S. (2007) 'Analysis of low molecular mass organic acids in natural waters by ion exclusion chromatography tandem mass spectrometry', *Journal of Chromatography A,* 1176, (1-2), pp. 89-93.

Jones, D. L., Dennis, P. G., Owen, A. G. and van Hees, P. A. W. (2003) 'Organic acid behavior in soils - misconceptions and knowledge gaps', *Plant and Soil,* 248, (1-2), pp. 31-41.

Kuzyakov, Y. and Domanski, G. (2000) 'Carbon input by plants into the soil - review', *Journal of Plant Nutrition and Soil Science,* 163, pp. 421-431.

Renforth, P., Manning, D. A. C. and Lopez-Capel, E. (2009) 'Carbonate precipitation in artificial soils as a sink for atmospheric carbon dioxide', *Applied Geochemistry,* 24, pp. 1757-1764.

Ryan, P. R., Delhaize, E. and Jones, D. L. (2001) 'Function and mechanism of organic anion exudation from plant roots', *Annual Review of Plant Physiology and Plant Molecular Biology,* 52, pp. 527-560.

Strom, L., Owen, A. G., Godbold, D. L. and Jones, D. L. (2001) 'Organic acid behaviour in a calcareous soil: sorption reactions and biodegradation rates', *Soil Biology and Biochemistry,* 33, (15), pp. 2125-2133.

Strom, L., Owen, A. G., Godbold, D. L. and Jones, D. L. (2005) 'Organic acid behaviour in a calcareous soil implications for rhizosphere nutrient cycling', *Soil Biology and Biochemistry,* 37, (11), pp. 2046-2054.